THE UNIVERSITY OF CHICAGO

DRIVERS AND CONSEQUENCES OF INTRASPECIFIC TRAIT VARIATION: ECOLOGY OF A FOREST-STREAM COMMUNITY

A DISSERTATION SUBMITTED TO

THE FACULTY OF THE DIVISION OF THE BIOLOGICAL SCIENCES

AND THE PRITZKER SCHOOL OF MEDICINE

IN CANDIDACY FOR THE DEGREE OF

DOCTOR OF PHILOSOPHY

DEPARTMENT OF ECOLOGY AND EVOLUTION

BY

SARA LINDSAY JACKREL

CHICAGO, ILLINOIS

AUGUST 2016

DEDICATION

To ISH, RMJ, MEJ, SPS, PB^2, and TAJ.

TABLE OF CONTENTS

LIST OF TABLES

LIST OF FIGURES

ACKNOWLEDGMENTS

My dissertation would not have been possible without the guidance and encouragement from countless students, faculty, and staff at University of Chicago. My committee members, Cathy Pfister, Trevor Price, Joy Bergelson and Greg Dwyer, provided invaluable guidance throughout all stages of my dissertation. I was fortunate to have an exceptional advisor, Tim Wootton, who provided incredible patience, insight, and dedication to developing my abilities as a scientist. Tim was invaluable in all facets of my dissertation, including direct advising, encouraging me to dive into challenging and new directions, and promoting independence as a researcher. I also want to thank Cathy Pfister for her supportive mentorship and engagement, particularly during field seasons. Trevor Price has also been an outstanding mentor by challenging me to think about broader questions, providing detailed and provocative feedback on my dissertation chapters, and being exceptionally encouraging and supportive throughout my tenure as a graduate student.

I want to thank several labs that welcomed me to work in their labs to learn new techniques and analyses. The Colman Isotope Lab, including Albert Colman, Gerry Olack, and Aric Mine provided invaluable assistance in developing nutrient analysis protocols. The Gilbert Lab, including Jack Gilbert, Jarrad Hampton-Marcell, Sarah Owens, Simon Lax, and Sean Gibbons, provided technical and analytical support for microbiome analyses. I am particularly indebted to the Bergelson Lab and Tim Morton for enthusiastically teaming up to tackle the secondary metabolite chemistry of red alder trees.

Lastly, my fellow graduate students have provided an outstanding academic community and home during my time in Chicago that has provided essential support in many facets of my dissertation. I want to particularly thank Rob Arthur, Misha Blizard, Allison Johnson, Sophie McCoy, Jon Mitchell, John Park, Courtney Stepien, the Pfister-Wootton Lab group, and the individuals noted on page 18 for inspiring discussions, supportive field seasons, and making Chicago a home.

CHAPTER I

DRIVERS AND CONSEQUENCES OF INTRASPECIFIC TRAIT VARIATION: ECOLOGY OF A FOREST-STREAM COMMUNITY

INTRODUCTION

Understanding adaptation in nature is a fundamental goal in biology. In its broadest sense, adaptation is any change in the community that results in members that are more suited to their environment. Adaptive change could arise from physiological shifts within individuals, shifts within populations of a species, or changes in species composition within communities. Adaptation is a major driver of the biological diversity on Earth and preserving this diversity has immediate applications for maintaining ecosystem services, buffering against climate change, and protecting vital ecosystem functions, such as nutrient cycling and energy flow through food webs. The mechanisms explaining *why* diversity maintains ecosystems are less known. Diversity includes both within and among species variation. The potential for diversity *within* species to have broad consequences on community ecology has only recently been discovered, with the magnitudes rivaling that of species diversity (Crutsinger et al. 2006, Crutsinger et al. 2008, Bassar et al. 2010, Bolnick et al. 2011, Violle et al. 2012). While the field of community ecology has traditionally viewed within-species variation as noise in a dataset to be controlled with replication, experimental design and statistics, we are now discovering that individual differences can result in broad ecosystem changes.

As examples of the ecosystem-level effects of species and within-species diversity, in this dissertation, I explore the drivers and consequences of among and within-species differences in riparian trees across a forest-stream ecosystem boundary. In *Chapter II: Diversity of Riparian Plants Among and Within Species Shapes River Communities*, I first aimed to test whether organismal diversity among and within species effects ecosystem function with effects transmitting across ecosystem boundaries. I tested whether recipient communities adjust, in turn, to maximize their function in response to changes in donor composition at these two scales of diversity. I found that recipient communities decomposed leaves from local species rapidly: leaves from early successional plants decomposed rapidly in stream reaches surrounded by early successional forest and leaves from later successional plants decomposed rapidly adjacent to later successional forest. Further, leaves from locally sourced alder tree decomposed more rapidly than leaves sourced from alder growing in other areas on the Olympic Peninsula, Washington. I conclude that plant biodiversity at the within and across species scale has strong effects on aquatic ecosystems. This finding highlights the potential for natural change and anthropogenic activities in terrestrial systems to alter the ecology and evolution of aquatic systems (Jackrel and Wootton 2015b).

In *Chapter III: Local Adaptation of Stream Communities to Intraspecific Variation in a Terrestrial Ecosystem Subsidy*, I extended the finding that aquatic communities adjust to plants at the species scale to now test for local adaptation to within-species plant diversity. Cross-ecosystem fluxes such as leaf litter can intertwine otherwise disparate food webs, but the effects of biodiversity at the genotypic level on fluxes across ecosystems boundaries was not yet known. I found that aquatic communities showed accelerated function in decomposing leaves of individual trees to which they were regularly exposed. Aquatic decomposer communities rapidly process leaves only from trees the community could have realistically adapted to over time both at large (across-river) and smaller (within-river) scales. Thus I concluded that genetic diversity and the effects of selection in one ecosystem can indirectly shape the structure of other ecosystems through ecological fluxes (i.e. leaf litter) across boundaries. Preserving localized within-species variation can therefore have large-scale consequences for maintaining productive communities and essential ecosystem functions both within and across ecosystem boundaries (Jackrel and Wootton 2014).

In *Chapter IV: Cascading Effects of Induced Terrestrial Plant Defenses on Aquatic and Terrestrial Ecosystem Function*, I tested whether terrestrial herbivory can have cascading implications on energy capture by small stream communities. Herbivores induce plants to undergo diverse processes that minimize costs to the plant, such as producing defenses to deter herbivory or reallocating limited resources to inaccessible portions of the plant. Yet most plant tissue is consumed by decomposers, not herbivores, and these defensive processes aimed to deter herbivores may alter plant tissue even after detachment from the plant. All consumers value nutrients, but plants also require these nutrients for basic cellular and defensive processes. I therefore experimentally simulated herbivory with and without nutrient additions on red alder. I found that the induced defenses inhibit both terrestrial herbivores and aquatic decomposers. This decline in decomposition was particularly strong among fertilized trees receiving the herbivory treatment, suggesting plants funneled a nutritionally valuable resource into enhanced defense. This study illustrated how terrestrial herbivory can have important cross-ecosystem implications, and demonstrates how changes in terrestrial herbivory patterns (due to climate change and invasive species) may have cascading consequences on aquatic ecosystems (Jackrel and Wootton 2015a).

Having documented that plant defenses targeting terrestrial herbivores impede aquatic consumers, in *Chapter V: Intraspecific Leaf Chemistry Drives Locally Accelerated Ecosystem Function in Aquatic and Terrestrial Communities*, I tested whether these defenses drive ecosystem functioning and local adaptation in streams and riparian soils. I found that alder leaves have extensive geographic structuring in two understudied classes of secondary metabolites that have been attracting recent attention in the ecological and medical literature – ellagitannins and diarylheptanoids. Ellagitannins are one of the strongest drivers of aquatic leaf decomposition, superseding nitrogen and phosphorus, and thus bringing to question the assumption that nutrients drive aquatic ecosystem functions. I found that geographically neighboring trees share similar chemistry, and that this chemistry variation among individual trees was by itself sufficient to drive the same local adaptation patterns in streams that I originally documented with intact leaves. This local adaption pattern was evident at both the across and within river scales and in both streams and riparian soil. Ultimately, I connected the long-neglected ellagitannins to a key ecosystem function and probable driver of adaptive processes in multiple ecosystems. Further, as the first comprehensive study of diarylheptanoid function in a natural ecosystem, documenting their diversity and toxicity in nature is of particular relevance to medical research. I concluded that within-species variation in leaf defensive chemistry drives local adaptation in terrestrial and aquatic ecosystems. This finding demonstrates that selective forces driving divergence and creating diversity in terrestrial environments ultimately drive locally adaptive changes in recipient aquatic ecosystems (Jackrel et al. 2016).

In *Chapter VI: Herbivore Stress and Nutrient Additions Alter Secondary Metabolite Chemistry*, I extend the experiment detailed in *Chapter III* with high-resolution chemistry data of a red alder tree's response to an herbivory treatment with and without supplemental nutrients. While we had shown in *Chapter III* that much of the reduction in decomposition of leaves from the herbivory treatment could be explained by the sharp decline in leaf nitrogen, I found that secondary metabolites also shift by experimental treatment. Both this altered phenolic profile combined with nutrient reduction evidently leads to reduced consumption by aquatic decomposers.

The network of stream microorganisms, the microbiome, is an often over-looked aspect of stream function and likely contributes to the locally adaptive ecosystem responses that I have documented. In *Chapter VII:* Identifying *the Plant Associated Microbiome across Aquatic and Terrestrial Environments*, I determine the appropriate methods for studying the colonization and succession of riverine microbial communities on red alder leaves through the decomposition process using a reciprocal transplant leaf pack experiment and 16S rRNA sequencing. I evaluated whether molecular methods that limit contamination from host plant chloroplast and mitochondria during amplicon sequencing may or may not yield biased characterizations for a diversity of aquatic and terrestrial microbiota. The method used to block amplification of plant chloroplast DNA caused a particular bias against many Alphaproteobacteria taxa. These methods have informed continued study of microbial communities from a reciprocal transplant experiment, in which preliminary data not shown here suggests that local versus non-local leaves are colonized by substantially different microbial communities. These sequencing data will clarify how within-species diversity in leaf traits in one ecosystem may structure aquatic microbe communities through ecological fluxes across boundaries, as well as aid the development of a complete, cohesive story of the food web interactions connecting aquatic and terrestrial communities. Overall, these findings unravel how within-species variation in terrestrial herbivore defense drives adaptation of local consumers that perform ecosystem functions that are essential for maintaining the health of both local and nearby ecosystems.

CONCLUSIONS

Forest-stream systems may be ideal models for further study of eco-evolutionary dynamics of adaptation in ecosystem function. Potential avenues for investigation include untangling environmental versus genetic drivers of plant metabolomics driving local adaptation. Determining the driving factors of diversity within a plant species is a critical step towards understanding *why* and *how* decomposers are adapting. This could potentially provide insight into the evolutionary paths of such processes, and perhaps their generality throughout nature. Whether in this system or a similar system, a donor/recipient model should be developed to test the generality, mechanisms, and tempo of adaptive processes. Decomposition in donor versus recipient systems is a natural experimental contrast. Efficient consumption by terrestrial decomposers likely generates feedbacks for the parent plant, creating a tradeoff situation for the parent tree that must defend leaves during the growing season but also relies on efficient nutrient recycling by decomposers residing on the forest floor that are inhibited by these defense compounds. The efficiency of aquatic decomposition, in contrast, should be of no consequence to the parent tree. By contrasting these two scenarios, one could determine what factors change the trajectory and rate of these adaptive processes. Specific objectives of such studies could investigate the underlying mechanisms of these adaptive processes, i.e., do we see consistent differences in the soil or aquatic microbiome across plant genotypes and species receiving long-term subsidies of that type of leaf litter? Do parent plant feedbacks change the trajectory or rate of this adaptive process? Does similarity between plant species, either in defensive chemistry or phylogenetically, predict similarity between the adapted decomposer communities for each species? Do plant stressors, such as leaf herbivory, root herbivory, and pathogen exposure, that alter defensive chemistry change the trajectory or rate of this adaptive process?

By pairing in depth studies of natural systems with controlled experiments, we may be able to determine the trajectory and rate of local adaptive processes. This information may elucidate the generality of such processes in systems throughout nature, and potentially clarify the ecosystem-wide consequences of environmental changes, including shifting land-use, species diversity, and genetic diversity. Data from such surveys and experiments could ultimately be used to generate mathematical models to predict how adaptation of ecosystem functions alters energy flow and nutrient cycling. Further, by measuring how adaptation to plant diversity alters rates of ecosystem functions, carbon storage, and carbon flux, these data can be used to predict how global changes disrupting these adaptive interactions will alter carbon cycling through landscapes and ultimately affect climate. Such research could provide transition rate data – the time required for a community that is poorly efficient at consuming non-local leaves to adapt to the new leaf source under different scenarios. These data could then be used to predict carbon allocation differences in adapted versus non-adapted habitats, and changes over time as the non-adapted state transitions towards efficiency. These predictions could then be tested by measuring carbon storage and flux at sites experiencing shifting species range limits and other disturbances in the source of leaf litter (i.e., logging and reforestation).

Understanding local adaptation processes in aquatic systems could aid conservation of these ecosystems balanced with land use – including fisheries, logging, and agriculture. Defensive chemistry of leaves entering decomposer communities will change as a consequence of altered genetic structure due to logging practices and agricultural land use, shifting species ranges, changes in annual insect abundance (due to climate change and non-native species), increased global nitrogen availability, and forestry fertilization practices (Vitousek et al. 1997, Tylianakis et al. 2008). A number of studies could directly investigate the consequences of such landscape changes on local adaptation driving key ecosystem processes. For example, logging and agriculture are two of the dominant forces shaping landscapes worldwide. How does this broader landscape matrix of agricultural land use and logging activity that surrounds conserved habitats alter plant chemistry, plant genetics, and local adaptation of ecosystem processes? Landscape disturbances may facilitate gene flow of wind-pollinated plants,(Foré et al. 1992, Young et al. 1993, Berge et al. 1998) but often inhibits movement of consumers (Rothermel and Semlitsch 2002). As plant landscapes change over time, movement of aquatic consumers among aquatic habitats may affect the ability of consumers to adapt to these changes. For these reasons, the composition of the landscape matrix through which plant gene flow and consumer movement occurs likely plays a critical role in the development of local adaptation, rates of carbon cycling, and efficient ecosystem function. Disruption of these delicate local adaptation processes may alter rates of nutrient cycling, carbon storage and energy capture in freshwater systems and in turn limit growth among aquatic microbes, invertebrates and vertebrates. Changes in assemblages of the aquatic insect larvae that feed on leaf litter and eventually emerge as terrestrial adults, further affects their consumers (including amphibians, fish, spiders, birds, and bats) (Sabo and Power 2002, Murakami and Nakano 2002 , Kato et al. 2003, Fukui et al. 2006).

Testing the effects of landscape disturbances on within-species plant diversity and fine-scale adaptation patterns in ecosystem processes could result in further applied applications. For example, aquatic systems are often hotspots of biodiversity. Do changes in adaptation in ecosystem processes alter fitness and evolutionary trajectories in microbial, invertebrate, and vertebrate communities inhabiting aquatic systems? Do such changes in biodiversity have further implications for ecosystem services such as preserving water quality or sequestering carbon? Rates of leaf decomposition dictated by presence or absence of adaptation may alter nutrient cycling, potentially resulting in eutrophication and overgrowth of cyanobacteria. The cytotoxins produced by these bacteria, deteriorate water quality and are a primary management concern for maintaining safe drinking water (Dai et al. 2012, Posch et al. 2012). Applications may also arise for mitigating climate change. Aquatic habitats, despite occupying a relatively small amount of land area, sequester nearly as much carbon as terrestrial systems (Kayranli et al. 2009). The majority of carbon entering forested streams and wetlands occurs via leaf litter fall, and the microbial consumers of this leaf litter play vital roles in the cycling of carbon through these wetlands. Ultimately, understanding the mechanisms and circumstances of local adaptation in these ecosystem processes may elucidate potential feedback effects on global carbon cycling and climate.

CHAPTER II

DIVERSITY OF RIPARIAN PLANTS AMONG AND WITHIN SPECIES SHAPES RIVER COMMUNITIES[1]

ABSTRACT

Organismal diversity among and within species may affect ecosystem function with effects transmitting across ecosystem boundaries. Whether recipient communities adjust their composition, in turn, to maximize their function in response to changes in donor composition at these two scales of diversity is unknown. We use small stream communities that rely on riparian subsidies as a model system. We used leaf pack experiments to ask how variation in plants growing beside streams in the Olympic Peninsula of Washington State, USA affects stream communities via leaf subsidies. Leaves from red alder (*Alnus rubra*), vine maple (*Acer cinereus*), bigleaf maple (*Acer macrophyllum*) and western hemlock (*Tsuga heterophylla*) were assembled in leaf packs to contrast low versus high diversity, and deployed in streams to compare local versus non-local leaf sources at the among and within species scales. Leaves from individuals within species decomposed at varying rates; most notably thin leaves decomposed rapidly. Among deciduous species, vine maple decomposed most rapidly, harbored the least algal abundance, and supported the greatest diversity of aquatic invertebrates, while bigleaf maple was at the opposite extreme for these three metrics. Recipient communities decomposed leaves from local species rapidly: leaves from early successional plants decomposed rapidly in stream reaches surrounded by early successional forest and leaves from later successional plants decomposed rapidly adjacent to later successional forest. The species diversity of leaves inconsistently affected decomposition, algal abundance and invertebrate metrics. Intraspecific diversity of leaf packs also did not affect decomposition or invertebrate diversity. However,

[1] This manuscript is reprinted with permission: S.L. Jackrel and J.T. Wootton. 2015. PLOS ONE e0142362.

locally sourced alder leaves decomposed more rapidly and harbored greater levels of algae than leaves sourced from conspecifics growing in other areas on the Olympic Peninsula, but did not harbor greater aquatic invertebrate diversity. In contrast to alder, local intraspecific differences via decomposition, algal or invertebrate metrics were not observed consistently among maples. These results emphasize that biodiversity of riparian subsidies at the within and across species scale have the potential to affect aquatic ecosystems, although there are complex species-specific effects.

INTRODUCTION

Community composition of donor habitats can have large-scale consequences for ecosystem function and community structure in recipient systems. Leaf litter falls from terrestrial plants in riparian zones and provides critical food resources to aquatic invertebrates and microbes residing in small streams. We evaluate how composition of riparian plants at the within and among species scales affects adjacent stream communities and function.

Preservation of biodiversity has been noted as a key means of maintaining ecosystem function (Cardinale et al. 2006a, Gessner et al. 2010). Most studies have focused on species diversity, without considering phenotypic and/or genetic diversity within species. Recent studies have found that population genetic diversity in plants can increase consumer diversity and rates of ecosystem function (Crutsinger et al. 2006). Many prior studies have found that rates of leaf litter decomposition in streams are affected by species diversity (Swan et al. 2009, Gessner et al. 2010), but few have studied within species variation (Lecerf and Chauvet 2008). Here, we compare the effects of diversity at these two scales, asking whether diversity of terrestrial plants among and within species increases aquatic ecosystem function and effects primary producers and consumers by measuring leaf decomposition, algal abundance, and invertebrate richness and abundance (Fig 2.1).

Additionally, we ask whether recipient aquatic communities locally adjust to changes in subsidies received from the donor community of riparian plants (both at the among and within species scales) and thereby increase ecosystem function. Leaf litter fuels small stream communities during autumnal leaf senesce, but riparian subsidies are also sizable during summer (Jackrel and Wootton 2014) when food resources are vital for the growing season of many aquatic decomposers (Ward and Cummins 1979). Consequently, aquatic organisms should be efficient consumers of locally available riparian subsidies. Shifting aquatic invertebrate communities with stream size is a well-known example of this local matching: small, narrow stream channels are dominated by leaf-shredding species because these waters receive less sunlight and more leaves per unit of water, while in contrast, the turbid waters of larger streams are instead dominated by collector/filtering species that extract the fine particulate organic matter that is abundant in these channels (Vannote et al. 1980). Aquatic community matching at finer scales is also possible because the generation time of decomposers is minor relative to the timespan of forest succession and the lifespan of a tree. Indeed, a recent study found that the successional stage of riparian forest affects aquatic decomposition: leaf litter breakdown of certain tree species is higher in stream reaches surrounded by those same riparian tree species (Kominoski et al. 2011). Here, we test whether aquatic decomposer communities locally adjust to leaf litter subsides at these two scales: among tree species (as a comparison with this previous result) and within tree species.

Matching of an aquatic decomposer community could be in any form (such as intraspecific genetic or phenotypically plastic change, or species sorting) that leads to more efficient decomposition of leaf litter. At the interspecific scale, we compare rates of decomposition of red alder (*Alnus rubra*) and western hemlock (*Tsuga heterophylla*) in early versus later successional stretches of river, respectively. We compare our results to a previously documented pattern of more efficient processing of alder leaves in early successional forest in British Columbia (Kominoski et al. 2011). At the intraspecific scale, we compared rates of decomposition of local versus non-locally sourced leaves from three deciduous species (red alder, vine maple and bigleaf maple).

Finally, we test how a well-known driver of intraspecific leaf variation, plant-herbivore interactions, affects aquatic leaf decomposition. We investigated whether plant traits correlated with mechanical and chemical defense to terrestrial herbivory may affect aquatic decomposer communities. We tested whether aquatic decomposition was influenced by the following traits: tree age (because defense often varies with ontogeny (Boege and Marquis)), leaf thickness (a frequent means of mechanical defense (Coley 1983)), and leaf damage due to terrestrial herbivory (as an indicator of past stress and probable induction of a defensive response).

MATERIALS AND METHODS

Study Site

We studied aquatic decomposition at 4 sites on the South Fork Pysht River (48.09 °N, 124.12 °W) in the Olympic Peninsula of Washington State from June – August, 2011. Riparian forest communities varied from early successional forest dominated by red alder to later successional forest dominated by a mix of red alder, bigleaf maple (*Acer macrophyllum*), western hemlock (*Tsuga heterophylla*) and other conifers. We chose four of our river sites to contrast riparian forest communities: we chose sites with similar stream morphology and paired two sites adjacent to early successional forest against two sites adjacent to later successional forest. The early successional sites are along reaches where fire and logging during the 1930's-1970's removed most trees from the area, and alder subsequently recolonized and maintained dominance, resisting invasion of conifers. Later successional sites were intervening river reaches with adjacent pockets of forest in which conifers were not completely removed by harvest and fire, although riparian disturbance and wind throw allowed some alders to establish at these sites too. Previous studies show that reaches throughout this river share similar water chemistry (including $SiOH_4$, DOC, PO_4, NO_3, NO_2, NH_4, N:P), stream composition (% riffle, % pool, water depth variance, % coarse woody debris, % cobble, %silt/sand) and temperature (Wootton 2012b).

We added two additional sites on the Pysht River adjacent to early successional forest for our second experimental run. All six sites were between 0.2 – 3.5 km apart. Common understory vegetation at all sites included salmonberry (*Rubus spectabilis*), vine maple (*Acer cinereus*), thimbleberry (*Rubus parviflorus*), salal (*Gautheria shallon*) and sword fern (*Polystichum munitum*). Additional stream morphology and environmental characteristics of these sites are described elsewhere (Wootton 2012a, b, Jackrel and Wootton 2014).

Leaf Pack Experiment

Fresh green leaves are generally more nutrient rich and decompose more rapidly than senescent leaves (Fonte and Schowalter 2004). In the Pysht River, green leaves fall in large quantities during the summer growing season, decompose quickly, and support high aquatic invertebrate diversity (Jackrel and Wootton 2014). We hand-picked fresh, green leaves with little or no visible herbivore or pathogen damage from alder, hemlock and maple trees and sealed them in plastic bags. Leaves were collected from the riparian zone of the Pysht river, riparian zones of the Hoko river (26 km away, 48.15 °N, 124.21 °W) and non-riparian forest in Sekiu (48.15°N, 124.19 °W), Clallam Bay (48.16 °N, 124.22 °W) and Pysht (48.18 °N, 124.16 °W), WA. We constructed leaf packs containing 12 leaves each using 19 cm x 15.25 cm bags made of 4.75 mm nylon seine netting, this netting size allows colonization by most stream invertebrates (Jackrel, personal observation). We recorded initial weights of leaf packs and deployed packs at each site by attaching them with a cable to a steel reinforcing bar secured on the stream bottom perpendicular to the flow. Seventeen or 18 days after deployment, depending on experimental run, we removed packs and sealed them inside plastic bags. We removed leaves from mesh bags, gently washed them with water to dislodge invertebrates and silt, blotted them dry with paper towels and weighed them to the nearest centigram. We preserved all invertebrates from each leaf pack in 70% ethanol, enumerated and identified all to the lowest possible taxonomic unit using a dissecting scope (Merritt et al. 2008), and calculated diversity using Shannon's diversity metric (Magurran 1988).

In the first of our two experimental runs, we worked in four riparian sites (two adjacent to early successional forest and two adjacent to later successional forest, as described above) from June 23 – July 10, 2011. We constructed 48 single-individual alder packs (two leaf packs for each of 12 local alder genotypes and each of 12 non-local alder genotypes), 8 mixed-individual alder packs (each containing two leaves from each of six trees: three local and three non-local genotypes), 8 mixed-individual hemlock packs, 8 alder-hemlock mixed-species packs, and 4 alder-maple mixed-species packs (each containing 4 alder, 4 vine maple, and 4 bigleaf leaves). From each individual tree, we constructed duplicate leaf packs and deployed one leaf pack from each duplicate at a site adjacent to early successional forest and the second leaf pack from each duplicate at a site adjacent to later successional forest. In the second run from July 25 – August 10, 2011 we asked whether aquatic communities were more efficient decomposers of low versus high species diversity and local versus non-local riparian subsidies at the intraspecific scale in three deciduous plants: red alder, vine maple and bigleaf maple. At the six riparian study sites described above, we deployed 24 single-individual alder packs (two leaf packs for each of six local alders and each of six non-local alders), 24 single-individual vine maple packs, 24 single-individual bigleaf maple packs, and an additional 12 mixed-species packs (each containing 4 alder, 4 vine maple and 4 bigleaf maple leaves).

Chlorophyll Measurements

We asked if leaf pack composition affects algal abundance in the second experimental run. We hypothesized that algal colonization and growth may be affected by leaf traits such as nutrients and/or defense compounds that could leach out of the leaves and that vary within and among species. We have found that alder genotypes vary substantially in leaf Nitrogen and Phosphorus content, and additionally, that the Pysht river may be Nitrogen and Phosphorus co-limited (Wootton 2012b, Jackrel and Wootton 2015a). We quantified algal accrual from each leaf pack by brushing accumulation from each nylon mesh net bag into 100 ml water, homogenizing the sample with a hand blender, and extracting chlorophyll *a* from a 1 ml subsample mixed with 9 ml ethanol in a black vial. Quantity of extracted chlorophyll *a* was measured using a Turner fluorometer with a 440 nm excitation filter and a 665 nm emission filter, calibrated against pure chlorophyll *a* standards derived from spinach (Sigma Aldrich). Note that this procedure measures algae from a standardized surface and area, and that the

Table 2.1: Explanation of experimental design used in the first experimental run. Numbers in the contrast columns indicate the contrast coefficients (0, 1, -1, etc.), which were assigned to sum to zero. Colors indicate the levels within each contrast comparison as described in the contrast key.

Leaf Pack Contents	Treatment Code	Source	Successional Stage of Riparian Zone	Contrasts 1	2	3	4	5	6
Alder Genotype 1	2	Away	Alder (Site 1)	-1	1	0	0	0	1
Alder Genotype 1	4	Away	Conifer (Site 1)	-1	1	0	0	0	-1
Alder Genotype 2	2	Away	Alder (Site 1)	-1	1	0	0	0	1
Alder Genotype 2	4	Away	Conifer (Site 1)	-1	1	0	0	0	-1
Alder Genotype 3	2	Away	Alder (Site 1)	-1	1	0	0	0	1
Alder Genotype 3	4	Away	Conifer (Site 1)	-1	1	0	0	0	-1
Alder Genotype 4	2	Away	Alder (Site 1)	-1	1	0	0	0	1
Alder Genotype 4	4	Away	Conifer (Site 1)	-1	1	0	0	0	-1
Alder Genotype 5	2	Away	Alder (Site 1)	-1	1	0	0	0	1
Alder Genotype 5	4	Away	Conifer (Site 1)	-1	1	0	0	0	-1
Alder Genotype 6	2	Away	Alder (Site 1)	-1	1	0	0	0	1
Alder Genotype 6	4	Away	Conifer (Site 1)	-1	1	0	0	0	-1
Alder Genotype 7	1	Home	Alder (Site 1)	1	1	0	0	0	1
Alder Genotype 7	3	Home	Conifer (Site 1)	1	1	0	0	0	-1
Alder Genotype 8	1	Home	Alder (Site 1)	1	1	0	0	0	1
Alder Genotype 8	3	Home	Conifer (Site 1)	1	1	0	0	0	-1
Alder Genotype 9	1	Home	Alder (Site 1)	1	1	0	0	0	1
Alder Genotype 9	3	Home	Conifer (Site 1)	1	1	0	0	0	-1
Alder Genotype 10	1	Home	Alder (Site 1)	1	1	0	0	0	1
Alder Genotype 10	3	Home	Conifer (Site 1)	1	1	0	0	0	-1
Alder Genotype 11	1	Home	Alder (Site 1)	1	1	0	0	0	1
Alder Genotype 11	3	Home	Conifer (Site 1)	1	1	0	0	0	-1
Alder Genotype 12	1	Home	Alder (Site 1)	1	1	0	0	0	1
Alder Genotype 12	3	Home	Conifer (Site 1)	1	1	0	0	0	-1
Hemlock-Alder Mix 1	9	mixed	Alder (Site 1)	0	0	-2	0	1	-1
Hemlock-Alder Mix 1	10	mixed	Conifer (Site 1)	0	0	-2	0	1	1
Hemlock-Alder Mix 2	9	mixed	Alder (Site 1)	0	0	-2	0	1	-1
Hemlock-Alder Mix 2	10	mixed	Conifer (Site 1)	0	0	-2	0	1	1
Alder Mix 1	5	mixed	Alder (Site 1)	0	-6	1	1	0	1
Alder Mix 1	6	mixed	Conifer (Site 1)	0	-6	1	1	0	-1
Alder Mix 2	5	mixed	Alder (Site 1)	0	-6	1	1	0	1
Alder Mix 2	6	mixed	Conifer (Site 1)	0	-6	1	1	0	-1
Hemlock Mix 1	7	mixed	Alder (Site 1)	0	0	1	-1	0	-1
Hemlock Mix 1	8	mixed	Conifer (Site 1)	0	0	1	-1	0	1
Hemlock Mix 2	7	mixed	Alder 1 (Site 1)	0	0	1	-1	0	-1
Hemlock Mix 2	8	mixed	Conifer 1 (Site 1)	0	0	1	-1	0	1
Alder Genotype 13	4	Away	Conifer (Site 2)	-1	1	0	0	0	-1
Alder Genotype 13	2	Away	Alder (Site 2)	-1	1	0	0	0	1
Alder Genotype 14	4	Away	Conifer (Site 2)	-1	1	0	0	0	-1
Alder Genotype 14	2	Away	Alder (Site 2)	-1	1	0	0	0	1
Alder Genotype 15	4	Away	Conifer (Site 2)	-1	1	0	0	0	-1
Alder Genotype 15	2	Away	Alder (Site 2)	-1	1	0	0	0	1
Alder Genotype 16	4	Away	Conifer (Site 2)	-1	1	0	0	0	-1
Alder Genotype 16	2	Away	Alder (Site 2)	-1	1	0	0	0	1
Alder Genotype 17	4	Away	Conifer (Site 2)	-1	1	0	0	0	-1
Alder Genotype 17	2	Away	Alder (Site 2)	-1	1	0	0	0	1
Alder Genotype 18	4	Away	Conifer (Site 2)	-1	1	0	0	0	-1
Alder Genotype 18	2	Away	Alder (Site 2)	-1	1	0	0	0	1
Alder Genotype 19	3	Home	Conifer (Site 2)	1	1	0	0	0	-1
Alder Genotype 19	1	Home	Alder (Site 2)	1	1	0	0	0	1
Alder Genotype 20	3	Home	Conifer (Site 2)	1	1	0	0	0	-1
Alder Genotype 20	1	Home	Alder (Site 2)	1	1	0	0	0	1
Alder Genotype 21	3	Home	Conifer (Site 2)	1	1	0	0	0	-1
Alder Genotype 21	1	Home	Alder (Site 2)	1	1	0	0	0	1
Alder Genotype 22	3	Home	Conifer (Site 2)	1	1	0	0	0	-1
Alder Genotype 22	1	Home	Alder (Site 2)	1	1	0	0	0	1
Alder Genotype 23	3	Home	Conifer (Site 2)	1	1	0	0	0	-1
Alder Genotype 23	1	Home	Alder (Site 2)	1	1	0	0	0	1
Alder Genotype 24	3	Home	Conifer (Site 2)	1	1	0	0	0	-1
Alder Genotype 24	1	Home	Alder (Site 2)	1	1	0	0	0	1
Alder Mix 3	6	mixed	Conifer (Site 2)	0	-6	1	1	0	-1
Alder Mix 3	5	mixed	Alder (Site 2)	0	-6	1	1	0	1
Alder Mix 4	6	mixed	Conifer (Site 2)	0	-6	1	1	0	-1
Alder Mix 4	5	mixed	Alder (Site 2)	0	-6	1	1	0	1
Hemlock Mix 3	8	mixed	Conifer (Site 2)	0	0	1	-1	0	1
Hemlock Mix 3	7	mixed	Alder (Site 2)	0	0	1	-1	0	-1
Hemlock Mix 4	8	mixed	Conifer (Site 2)	0	0	1	-1	0	1
Hemlock Mix 4	7	mixed	Alder (Site 2)	0	0	1	-1	0	-1
Hemlock-Alder Mix 3	10	mixed	Conifer (Site 2)	0	0	-2	0	1	1
Hemlock-Alder Mix3	9	mixed	Alder (Site 2)	0	0	-2	0	1	-1
Hemlock-Alder Mix 4	10	mixed	Conifer (Site 2)	0	0	-2	0	1	1
Hemlock-Alder Mix 4	9	mixed	Alder (Site 2)	0	0	-2	0	1	-1
Alder-Maple Mix	12	mixed	Conifer (Site 2)	0	0	0	0	-4	-1
Alder-Maple Mix	11	mixed	Alder (Site 2)	0	0	0	0	-4	1
			Sum	0	0	0	0	0	0

Contrast Key: (1) Local matching at within-species scale: leaf packs containing leaves from one local vs. non-locally growing red alder tree. (2) High vs. low diversity within species: leaf packs containing 12 leaves from 1 red alder tree vs. 2 leaves from each of 6 red alder trees. (3) High vs. low species diversity: leaf packs containing leaves from either multiple alder or multiple hemlock vs. mixtures of alder/ hemlock. (4) Contrasting multiple alder vs. multiple hemlock mixed individual packs. (5) Contrasting hemlock/alder vs. alder/ vine maple/ bigleaf maple mixed species packs. (6) Local matching at between species scale: leaf packs contain species that match vs. mismatch those growing in the adjacent riparian forest.

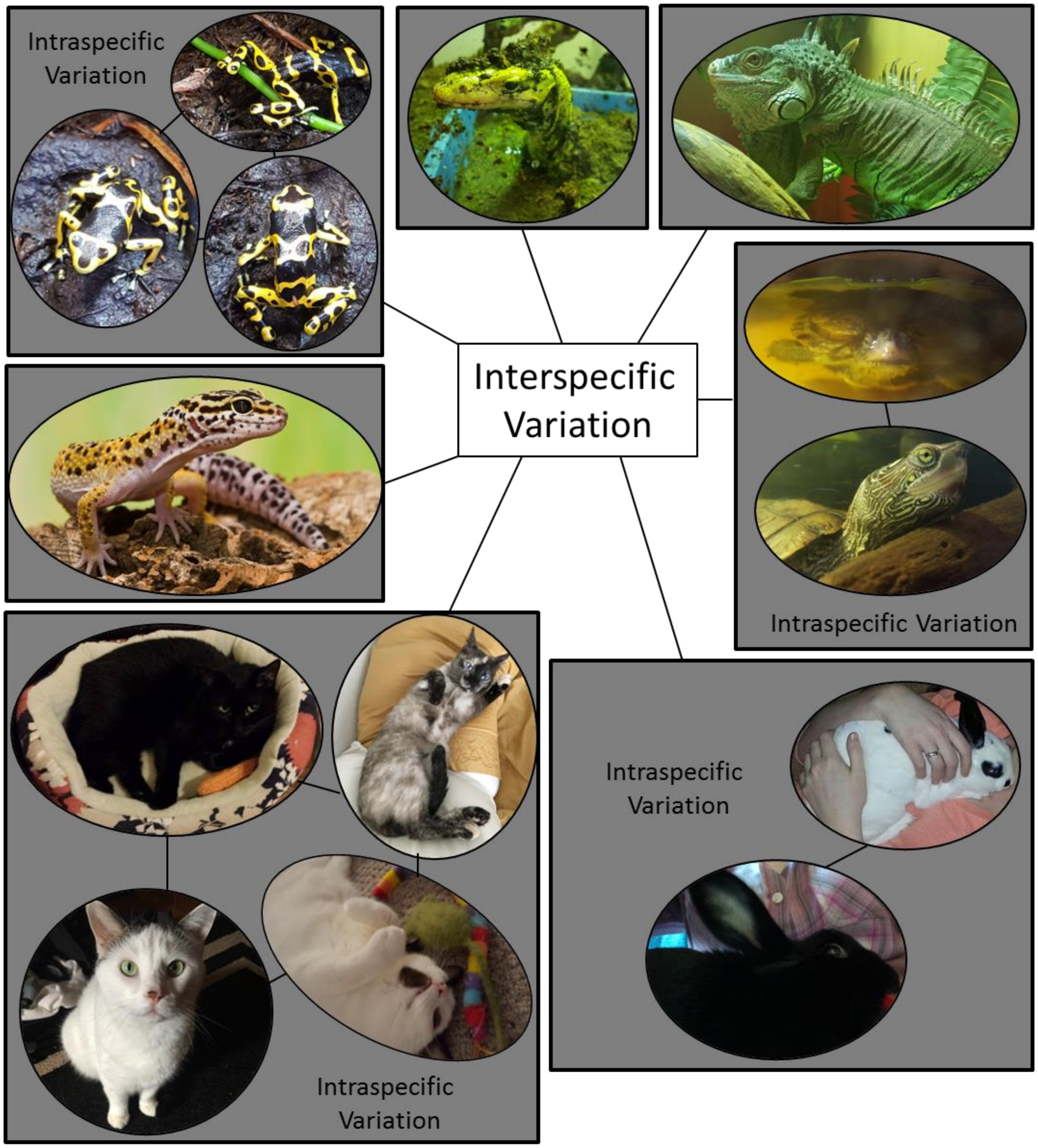

Figure 2.1: Illustration demonstrating interspecific versus intraspecific variation using the Greenwood Palace coinhabitants. Photo rights courtesy of Adama, Boomer, Starbuck (*Dendrobates leucomelas*); Tycho (*Varanus prasinus*); Sam (*Iguana iguana*); Mulder, Scully (*Graptemys geographica*); Ame, Dien Dien (*Oryctolagus cuniculus*); Salem, Alloy, Meeko, Ripley (*Felis catus*); Galileo (*Eublepharis macularius*); and their humans.

analysis is targeted toward probing possible effects of leachates from leaves on algae, not toward measuring total algal standing crop living on the surface of fallen leaves, which would be affected by leaf decomposition differences among treatments and by shading from the mesh bags surrounding the leaves.

Plant Traits

We collected 20 additional leaves per tree in two groups of 10 contiguous leaves starting at the tip of each of two main branches of the tree. We photographed leaves and imported photos into Image J to calculate the fraction of leaf area consumed by terrestrial herbivores. We estimated original leaf area by redrawing the assumed original leaf margin. In cases of very heavy leaf herbivory, we estimated original leaf area using a regression equation relating original leaf area and mid-vein length (original leaf area (cm^2) = 0.939(mid-vein length in cm)$^{1.64}$; R^2 = 0.861). We calculated this regression equation from photographs of intact alder leaves (n = 276). We then took leaf cores 12 mm in diameter from each of the twenty leaves per tree, oven dried the cores, and weighed each core to the nearest milligram as an indicator of leaf thickness, which often plays an important role in rates of herbivory (Coley 1983).

Statistical Analysis

Decomposition rates are reported as percent leaf mass lost over the deployment period (i.e., grams lost over the 17 or 18 days depending on experiment), and data were arcsine-square-root transformed to meet assumptions of normality. For analyses among species, we also measured decomposition as total grams of leaf mass lost. Because the starting weights of leaf packs differed moderately by species due to differences in leaf size (means ± 1 S.D. of alder leaf packs

Table 2.2: Explanation of experimental design used in the second experimental run.

Leaf Pack Contents	Deployment Site	Source
Vine Maple Genotype 1	Site 1	Home
Vine Maple Genotype 1	Site 2	Home
Vine Maple Genotype 2	Site 1	Home
Vine Maple Genotype 2	Site 2	Home
Vine Maple Genotype 3	Site 3	Home
Vine Maple Genotype 3	Site 4	Home
Vine Maple Genotype 4	Site 3	Home
Vine Maple Genotype 4	Site 4	Home
Vine Maple Genotype 5	Site 5	Home
Vine Maple Genotype 5	Site 6	Home
Vine Maple Genotype 6	Site 5	Home
Vine Maple Genotype 6	Site 6	Home
Vine Maple Genotype 7	Site 1	Away
Vine Maple Genotype 7	Site 2	Away
Vine Maple Genotype 8	Site 1	Away
Vine Maple Genotype 8	Site 2	Away
Vine Maple Genotype 9	Site 3	Away
Vine Maple Genotype 9	Site 4	Away
Vine Maple Genotype 10	Site 3	Away
Vine Maple Genotype 10	Site 4	Away
Vine Maple Genotype 11	Site 5	Away
Vine Maple Genotype 11	Site 6	Away
Vine Maple Genotype 12	Site 5	Away
Vine Maple Genotype 12	Site 6	Away
Bigleaf Maple Genotype 1	Site 1	Home
Bigleaf Maple Genotype 1	Site 2	Home
Bigleaf Maple Genotype 2	Site 1	Home
Bigleaf Maple Genotype 2	Site 2	Home
Bigleaf Maple Genotype 3	Site 3	Home
Bigleaf Maple Genotype 3	Site 4	Home
Bigleaf Maple Genotype 4	Site 3	Home
Bigleaf Maple Genotype 4	Site 4	Home
Bigleaf Maple Genotype 5	Site 5	Home
Bigleaf Maple Genotype 5	Site 6	Home
Bigleaf Maple Genotype 6	Site 5	Home
Bigleaf Maple Genotype 6	Site 6	Home
Bigleaf Maple Genotype 7	Site 1	Away
Bigleaf Maple Genotype 7	Site 2	Away
Bigleaf Maple Genotype 8	Site 1	Away
Bigleaf Maple Genotype 8	Site 2	Away
Bigleaf Maple Genotype 9	Site 3	Away
Bigleaf Maple Genotype 9	Site 4	Away
Bigleaf Maple Genotype 10	Site 3	Away
Bigleaf Maple Genotype 10	Site 4	Away
Bigleaf Maple Genotype 11	Site 5	Away
Bigleaf Maple Genotype 11	Site 6	Away
Bigleaf Maple Genotype 12	Site 5	Away
Bigleaf Maple Genotype 12	Site 6	Away
Alder Genotype 1	Site 1	Home
Alder Genotype 1	Site 2	Home
Alder Genotype 2	Site 1	Home
Alder Genotype 2	Site 2	Home
Alder Genotype 3	Site 3	Home
Alder Genotype 3	Site 4	Home
Alder Genotype 4	Site 3	Home
Alder Genotype 4	Site 4	Home
Alder Genotype 5	Site 5	Home
Alder Genotype 5	Site 6	Home
Alder Genotype 6	Site 5	Home
Alder Genotype 6	Site 6	Home
Alder Genotype 7	Site 1	Away
Alder Genotype 7	Site 2	Away
Alder Genotype 8	Site 1	Away

Table 2.2, continued.

Alder Genotype 8	Site 2	Away
Alder Genotype 9	Site 3	Away
Alder Genotype 9	Site 4	Away
Alder Genotype 10	Site 3	Away
Alder Genotype 10	Site 4	Away
Alder Genotype 11	Site 5	Away
Alder Genotype 11	Site 6	Away
Alder Genotype 12	Site 5	Away
Alder Genotype 12	Site 6	Away
Alder-Maple Mix 1	Site 1	Home
Alder-Maple Mix 1	Site 2	Home
Alder-Maple Mix 2	Site 3	Home
Alder-Maple Mix 2	Site 4	Home
Alder-Maple Mix 3	Site 5	Home
Alder-Maple Mix 3	Site 6	Home
Alder-Maple Mix 4	Site 1	Away
Alder-Maple Mix 4	Site 2	Away
Alder-Maple Mix 5	Site 3	Away
Alder-Maple Mix 5	Site 4	Away
Alder-Maple Mix 6	Site 5	Away
Alder-Maple Mix 6	Site 6	Away

= 17.3g ± 2.15, hemlock leaf packs = 12.9g ± 2.73, vine maple leaf packs = 14.2g ± 2.40, bigleaf maple leaf packs = 22.9g ± 4.08), this measure may more accurately indicate the overall quantity of leaf mass consumed compared to a percentage measure. Except where noted, all analyses using decomposition percentage rate and total grams lost (which are tightly correlated, R^2 = 0.995) yielded the same biological conclusions. Unless otherwise stated, the unit of replication is the leaf pack. All one-way analysis of variance, multivariate analysis of variance, regression, t-test, and Tukey post-hoc analyses were performed in R (R Development Core Team 2013). The first round of experiments was analyzed with an analysis of variance with six a priori contrast comparisons and was performed in SPSS (IBM Corp. 2013). There were twelve categories of leaf packs for the first experimental round resulting from the combinations of variables, including species identity in a leaf pack, number of species in a leaf pack, the successional stage of the riparian zone adjacent to the deployment location, and the home/away source of the leaves. We provide a detailed explanation of the experimental design and contrast comparisons in Tables 2.1 and 2.2. Each of our dependent variables (i.e., leaf decomposition rate, invertebrate diversity, and invertebrate abundance) was analyzed independently using an analysis of variance, and if significant across the twelve treatment groups, the a priori contrast comparisons were analyzed, adjusting contrast coefficients as necessary to maintain balance among treatments when estimating group means (as shown in Tables 2.1 and 2.2). For the second round of experiments, we performed one-way analysis of variance tests without predefined contrasts (this experimental design is explained in detail in the appendices). Where indicated, data presented in figures were controlled statistically for deployment location by using residuals to standardize results across multiple sites.

RESULTS

Effects of Interspecific Leaf Variation

Differences between tree species

We saw strong species effects on decomposition: in our first experiment mixed-individual alder packs decomposed proportionately more rapidly than mixed-individual hemlock packs ($F_{1,73} = 4.10$, $p = 0.047$, Tables 2.1 and 2.3) although the difference in total mass loss was statistically weaker ($p = 0.09$). Leaves showed extensive skeletonization and distinct bite marks by invertebrates, but our metrics of invertebrate abundance and richness explained few of the differences we observed in decomposition rates. Leaf packs across treatment groups, including this mixed-alder versus mixed-hemlock comparison, were colonized by a similar abundance ($F_{11,73} = 1.1$, $p = 0.39$) and diversity ($F_{11,73} = 0.56$, $p = 0.86$) of stream invertebrates. Additionally, all treatment groups were colonized by similar numbers of families belonging to different functional feeding groups (including: shredders, scrapers, predators, collector-gathers, and collector-filterers, MANOVA: $F_{11,73} = 0.95$, $p = 0.58$), however the abundance of individuals belonging to each of these functional groups differed across treatment groups (MANOVA: $F_{11,73} = 1.68$, $p < 0.01$). Specifically, predators, but not other functional feeding groups, differed across treatments ($F_{11,73} = 3.8$, $p < 0.001$, Table 2.4): there was a significant species effect, where predators were more abundant among mixed-alder packs than hemlock packs ($F_{1,73} = 5.44$, $p = 0.022$).

In the second experiment, bigleaf maple proportionately decomposed most slowly and vine maple decomposed most rapidly (one-way ANOVA: $F_{3,38} = 4.04$, $p = 0.014$, Tukey HSD: vine maple/bigleaf maple comparison, $p < 0.01$), although the total amount of weight loss was

Table 2.3: Summary of leaf decomposition results from first experimental run of leaf packs.

	df	SS	MS	F	P
Leaf pack Treatments	11	1.203	0.109	6.55	< 0.0001
Within-species matching[1]	1	0.707	0.707	42.38	< 0.0001
Within-species diversity[2]	1	0.032	0.032	1.94	0.168
Species diversity[3]	1	0.041	0.041	2.41	0.122
Species comparison[4]	1	0.068	0.068	4.10	0.047
Mixed species comparison[5]	1	0.096	0.096	5.74	0.020
Species matching[6]	1	0.130	0.130	7.81	0.007
Error	62	1.035	0.017		
Total	73	2.238			

A priori contrasts: (1) Local matching at within-species scale: leaf packs containing leaves from one local vs. non-locally growing red alder tree; (2) High vs. low diversity within species: leaf packs containing 12 leaves from 1 red alder tree vs. 2 leaves from each of 6 red alder trees; (3) High vs. low species diversity: leaf packs containing leaves from either multiple alder or multiple hemlock vs. mixtures of alder/ hemlock; (4) contrasting multiple alder vs. multiple hemlock mixed individual packs (5) contrasting hemlock/alder vs. alder/ vine maple/ bigleaf maple mixed species packs; (6) local matching at between species scale: leaf packs contain species that match vs. mismatch those growing in the adjacent riparian forest.

not different between species, owing to the larger leaves of bigleaf maple (Tukey HSD for the vine maple/bigleaf maple comparison, p = 0.108) (Fig 2.2a). Aligned with this pattern, bigleaf maple supported lower invertebrate diversity than vine maple (one-way ANOVA: $F_{3,38} = 3.95$, p = 0.015, Tukey HSD: vine maple/bigleaf maple comparison, p = 0.017) (Fig 2.2c.), but harbored greater algal accrual than vine maple (one-way ANOVA: $F_{3,38} = 3.56$, p = 0.023, Tukey HSD: p = 0.039) and slightly greater algal accrual than alder (Tukey HSD: p = 0.090).

Effects of diversity among tree species

In the first experiment, multi-species leaf packs (mixed alder/hemlock) and single-species leaf packs (mixed individuals of alder or mixed hemlock) decomposed at similar rates ($F_{1,73} = 2.41$, p = 0.12). However, among multi-species packs, alder/vine maple/bigleaf maple mixed-species packs tended to decompose more rapidly than alder/hemlock mixed packs ($F_{1,73} = 5.74$, p = 0.020, Table 2.3), and these mixed-species deciduous packs also harbored a greater abundance of invertebrate predators than alder/hemlock packs deployed at the same time ($F_{1,73} = 18.2$, $p < 0.001$, Table 2.4).

These diversity comparisons could have been affected by proportional differences in mass contributions of alder versus hemlock to the mixed-species leaf packs, given that decomposition rates varied among species. Therefore, we completed a more targeted comparison of high versus low species diversity using decomposition rates measured in both single and mixed-species leaf packs. We calculated expected decomposition rates for mixed alder-hemlock packs using decomposition data for mixed-individual alder packs and mixed-individual hemlock packs that were deployed at the same location and time as the mixed-species packs. We weighted averages by the starting biomass composition of alder and hemlock in each

Table 2.4: Abundance of predatory aquatic invertebrates among leaf pack treatments from first experimental run.

	df	SS	MS	F	P
Leaf pack Treatments	11	156.2	14.2	3.81	< 0.001
Within-species matching[1]	1	6.02	6.02	1.62	0.21
Within-species diversity[2]	1	0.03	0.03	0.01	0.92
Species diversity[3]	1	0.33	0.33	0.09	0.77
Species comparison[4]	1	20.25	20.25	5.44	0.022
Mixed species comparison[5]	1	67.6	67.6	18.2	< 0.001
Species matching[6]	1	1.64	1.64	2.27	0.14
Error	62	230.9	3.724		
Total	73	387.1			

The a priori contrasts are the same as those reported in Table 3: (1) Local matching at within-species scale: leaf packs containing leaves from one local vs. non-locally growing red alder tree; (2) High vs. low diversity within species: leaf packs containing 12 leaves from 1 red alder tree vs. 2 leaves from each of 6 red alder trees; (3) High vs. low species diversity: leaf packs containing leaves from either multiple alder or multiple hemlock vs. mixtures of alder/ hemlock; (4) contrasting multiple alder vs. multiple hemlock mixed individual packs (5) contrasting hemlock/alder vs. alder/ vine maple/ bigleaf maple mixed species packs; (6) local matching at between species scale: leaf packs contain species that match vs. mismatch those growing in the adjacent riparian forest.

mixed-species pack. Mixed-species packs lost twice as much leaf mass as expected (paired t-test of expected vs. observed decomposition rate, $t_7 = 3.4$, $p = 0.011$), but expected and observed invertebrate diversity and abundance were similar (paired t-tests, $p > 0.1$).

In the second experimental run, we observed similar decomposition rates among high and low species diversity packs (either compared to each species individually: alder, vine, or bigleaf maple, all Tukey HSD $p > 0.01$, or as a group: $F_{1,40} = 0.12$, $p = 0.73$), but in contrast to the first experiment, we found invertebrate abundances were lower among single-species (alder, vine maple or bigleaf maple) compared to mixed-species packs (enumeration $F_{1,40} = 5.106$, $p = 0.030$). The diversity of invertebrates did not differ between low and high tree-species diversity packs (Shannon diversity $F_{1,40} = 1.131$, $p = 0.29$, Fig 2.2c). Algal accrual was also similar between high tree-species diversity packs and single tree species packs (either compared to each species individually: alder, vine or bigleaf maple, all Tukey HSD $p > 0.1$, or as a group: $F_{1,40} = 1.218$, $p = 0.28$) (Fig 2.2b).

We also did a more targeted diversity comparison of single-species versus alder-maple packs. We estimated starting composition of each species in the mixed-species packs using average weight data from single-species packs. Expected decomposition rates were calculated using data from single-species packs that were deployed at the same location and time as the mixed alder-maple packs. In contrast to the first round, we found no evidence of accelerated decomposition in high diversity packs (paired t-test $t_{11} = 0.34$, $p = 0.77$). Observed and expected values of algal abundance, invertebrate diversity and invertebrate abundance were all similar (paired t-tests, all $p > 0.1$).

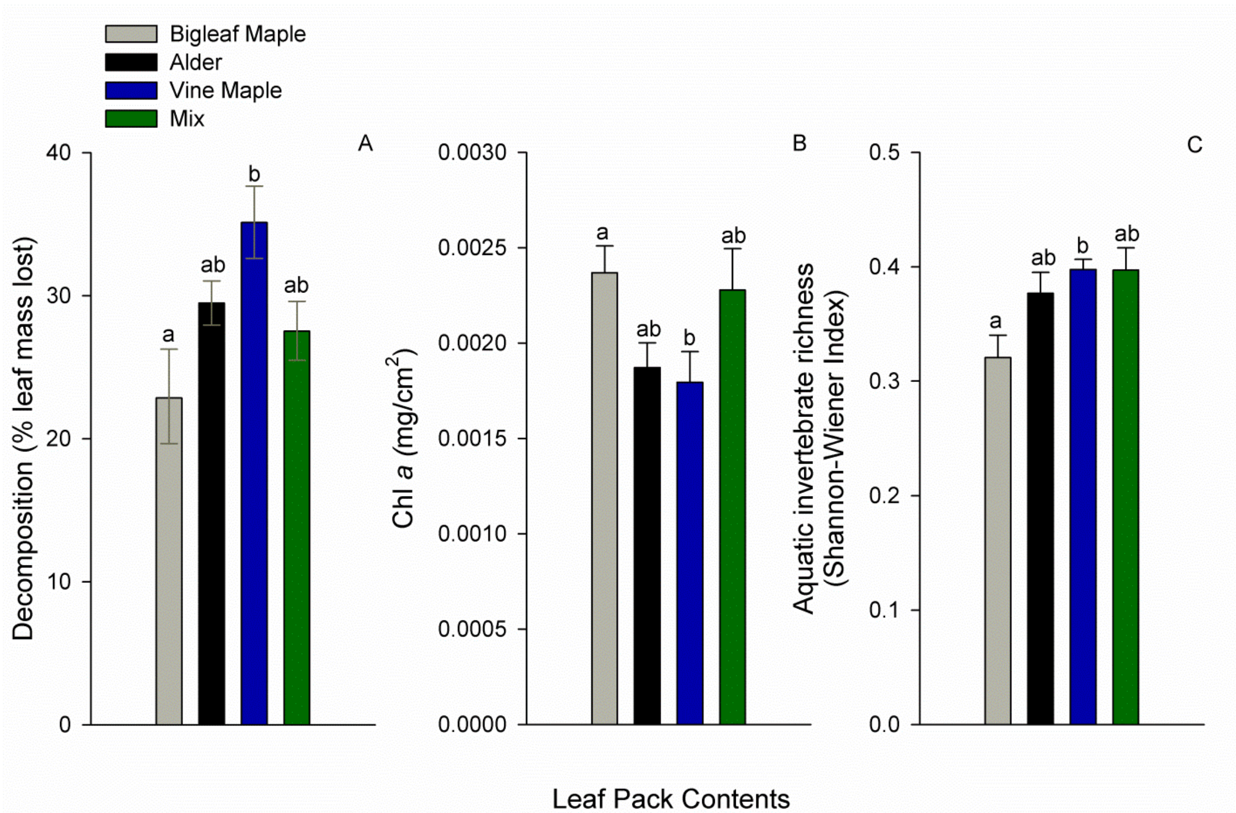

Figure 2.2: Biological responses to among species variation of leaf packs (mean ± 1 se). (*a*) Decomposition rates, (*b*) algal accrual and (*c*) aquatic invertebrate richness (Shannon's diversity index) of alder (n = 24), vine maple (n = 24) and bigleaf maple (n = 24) in single and mixed species leaf packs (n = 12). Significant comparisons (P < 0.05) indicated by a star.

Effects of Intraspecific Leaf Variation

Individual differences

In the first and second experiments, we found that different aquatic communities responded consistently to different alder genotypes: 24 replicate leaf packs constructed from 12 trees and deployed at two different sites exhibited highly correlated decomposition rates (R^2 = 0.75, $p < 0.001$). Bigleaf maple, but not vine maple, also showed consistent results across sites for a given individual (BLM: $R^2 = 0.57$, $p < 0.01$, $n = 12$; VM: $R^2 = 0.19$, $p = 0.16$, $n = 12$). Although genotypes showed varying decomposition rates, this variation within species was not correlated with either algal abundance (second experiment) or invertebrate abundance or diversity (either experiment) (alder, bigleaf maple and vine maple all $p > 0.05$).

Plant traits affecting individual differences

Alder, vine maple and bigleaf maple with thinner leaves tended to show greater decomposition (either as a Pearson correlation between decomposition and leaf thickness, R^2 = 0.216, $p < 0.001$, or as a model term of decomposition as a function of leaf thickness ($F_{1,36}$ = 7.46, $p < 0.01$), tree diameter and species) (Fig 2.5a). There was no common relationship across species between tree diameter and leaf thickness: larger alder trees tended to have thinner leaves (alder experiment 1: $R^2 = 0.27$, $p = 0.027$; alder experiment 2: $R^2 = 0.24$, $p = 0.10$), larger vine maples tended to have thicker leaves ($R^2 = 0.278$, $p = 0.095$) and bigleaf maple showed no pattern ($R^2 = 0.00$, $p = 0.96$) (Fig 2.5b). Possibly as a consequence of this inconsistent relationship between tree diameter and leaf thickness, we found trunk diameter, as a proxy of age, was a significant but inconsistent predictor of decomposition rate ($F_{1,36} = 21.88$, $p < 0.001$;

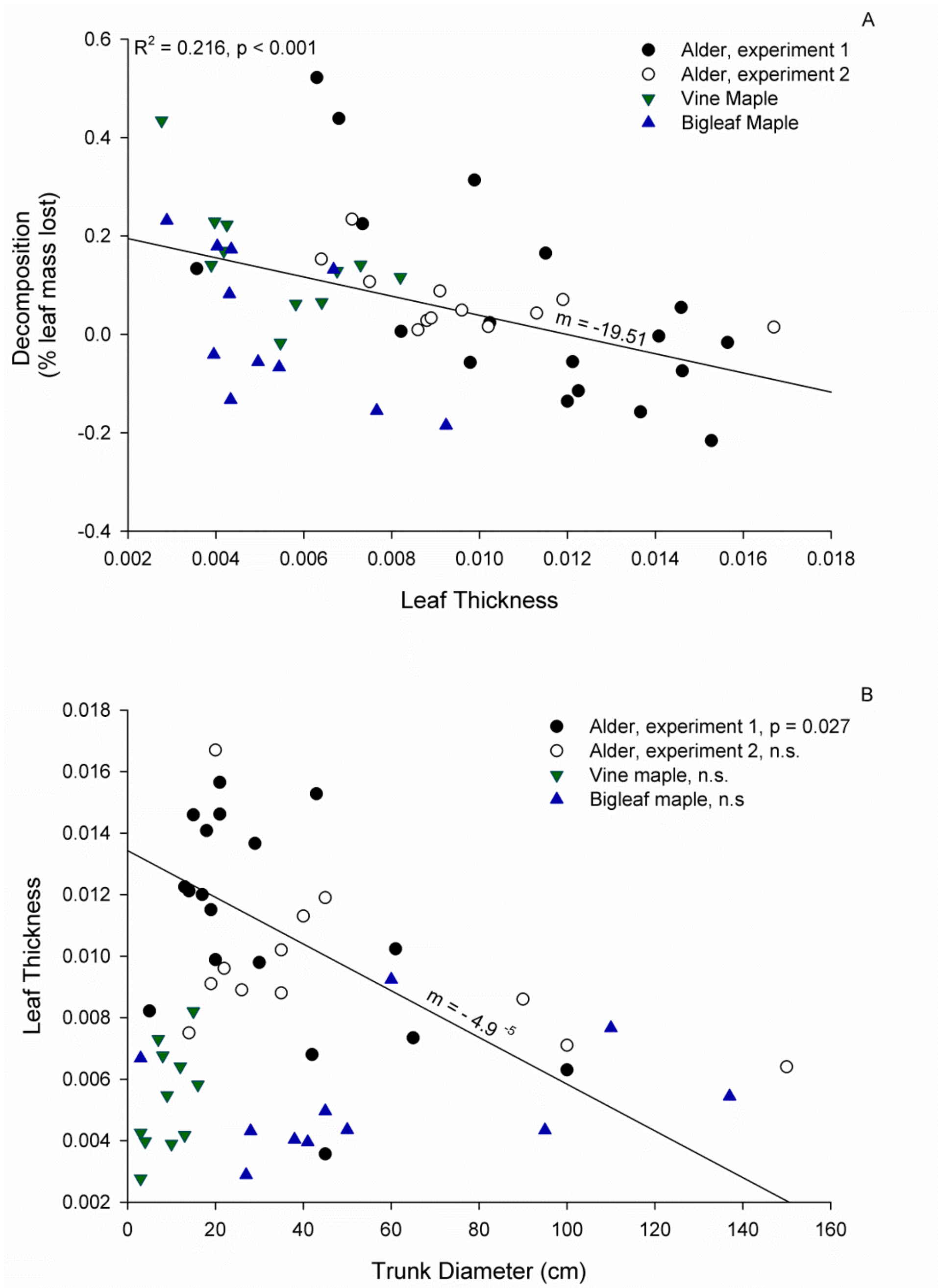

Figure 2.3: Plant traits influencing the degree of aquatic decomposition of deciduous leaves over the experimental period. (a) Correlation between decomposition and leaf thickness are shown for each species independently and combined (note negative decomposition rates indicate mass gained), and (*b*) correlation between trees size and leaf thickness are shown for each species independently to illustrate species differences.

tree diameter*species interaction = $F_{1,36}$= 2.56 p = 0.07). Leaves from larger alder tended to decompose more rapidly than smaller alder, while leaves from smaller vine maple decomposed more rapidly than larger vine maples (alder: R^2 = 0.177, p = 0.021; maple: R^2 = 0.504, p = 0.015). Smaller individuals of bigleaf maple also decomposed more rapidly than larger individuals(R^2 = 0.425, p = 0.030), however given the lack of relationship between tree diameter and leaf thickness, this result seems to be driven by some other ontogenetic factor.

Terrestrial herbivory was not correlated with alder decomposition rate in either run of experiments (experiment 1, *n* = 18, R^2 = 0.006, p = 0.76; experiment 2, *n* = 12, R^2 = 0.011, p = 0.74). We did not estimate terrestrial herbivory for maples.

Intraspecific diversity

In the first experiment, we found that despite alder genotypes showing a range of decomposition rates, single and multi-individual alder leaf packs did not exhibit significantly different decomposition rates ($F_{1,73}$ = 1.94, p = 0.17, Table 2.3). Single versus mixed-individual alder packs also harbored similar invertebrate abundance ($F_{1,26}$ = 1.801, p = 0.19) and diversity ($F_{1,26}$ = 0.517, p = 0.48). Additionally, we calculated expected decomposition rates and invertebrate metrics for each mixed-individual alder pack using data from single-individual alder packs deployed at the same deployment location and time as the mixed packs. We found no evidence of accelerated decomposition in mixed-individual alder packs (paired t-test: t_7 = 0.99, p = 0.36), and observed versus expected values for invertebrate diversity and abundance were similar (paired t-tests, $p > 0.1$)

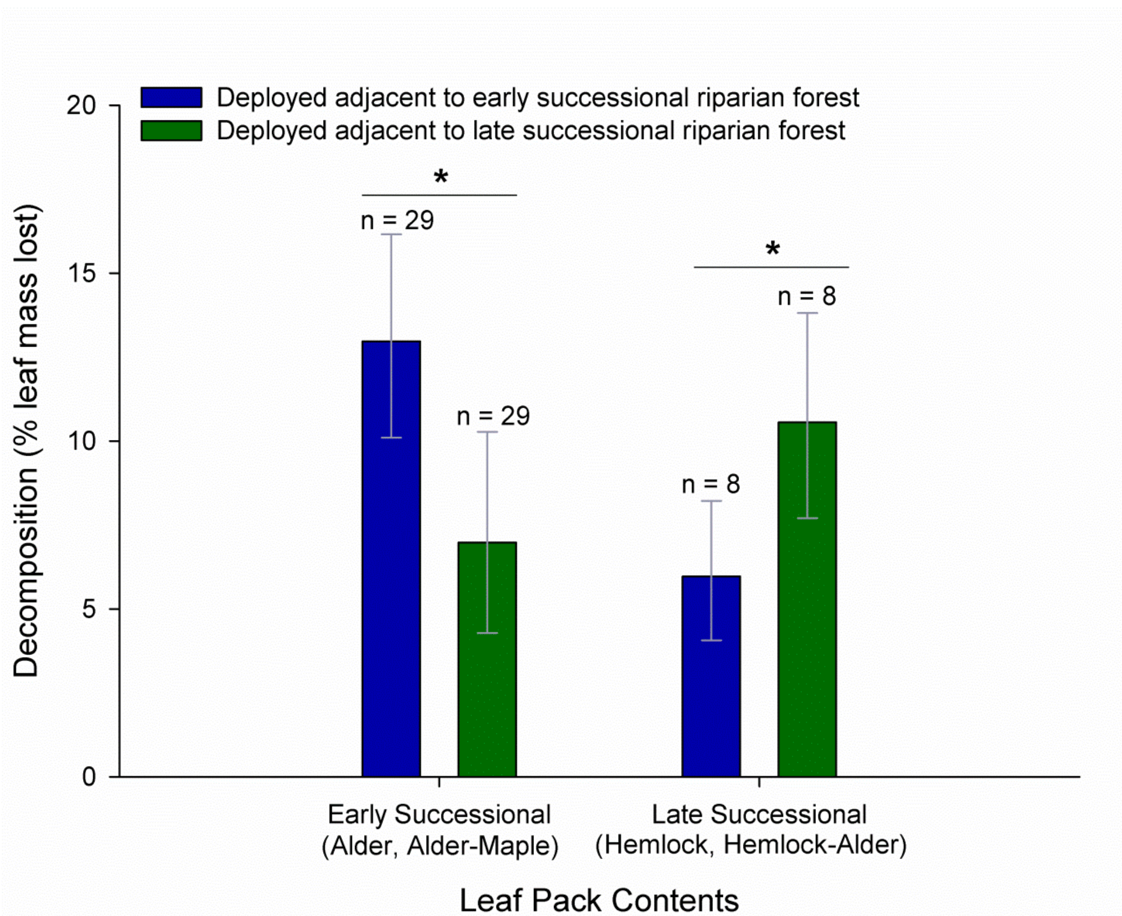

Figure 2.4: Leaf decomposition rate when leaf contents match the successional stage of adjacent riparian forest. Comparative decomposition (mean ± 1 se) of leaf packs containing early (alder or a mix of alder, vine maple and bigleaf maple) versus later successional species (hemlock or a mix of hemlock and alder) deployed at sites adjacent to early versus later successional riparian forest. Significant comparisons (paired t-tests $P < 0.05$) indicated by a star.

Recipient Community Matching to Donor Subsidies

Species scale

Aquatic communities more efficiently processed leaf litter when the species composition matched the local successional stage of the adjacent forest: leaf packs including both local and non-local genotypes for each species decomposed more rapidly when deployed at sites surrounded by riparian forest of matching composition to that of the pack contents ($F_{1,73} = 7.82$, $p = 0.007$, Table 2.3). Specifically, alder packs and alder-maple packs decomposed more rapidly at sites surrounded by early successional forests while hemlock packs and alder-hemlock packs exhibited the opposite trend of more rapid decomposition at sites surrounded by later successional forest (Fig 2.3).

Within species scale

This local preference pattern was also found at the intraspecific scale, but only for alder, the most abundant deciduous tree. Alder leaves sourced from local trees growing along the banks of the Pysht river decomposed significantly more than immigrant alder leaves (Run 1: $F_{1,73} = 42.38$, $p < 0.001$, Table 2.3; Run 2: $F_{1,10} = 7.08$, $p = 0.024$). Interestingly, local alder packs that generally showed accelerated decomposition rates also harbored greater algal abundances than immigrant packs (alder: $F_{1,10} = 6.25$, $p = 0.031$) (Fig 2.4b). Despite rapid decomposition of local alder leaves, neither invertebrate abundance nor diversity differed between local and immigrant leaf packs of alder ($p > 0.1$, Fig 2.4c).

Leaves from immigrant vine maple tended to decompose more quickly than leaves from local vine maple ($F_{1,10} = 5.77$, $p = 0.037$). Local versus immigrant packs showed similar rates of decomposition for bigleaf maple ($F_{1,10} = 1.18$, $p = 0.3$) and mixed-species packs ($F_{1,4} = 0.10$, p =

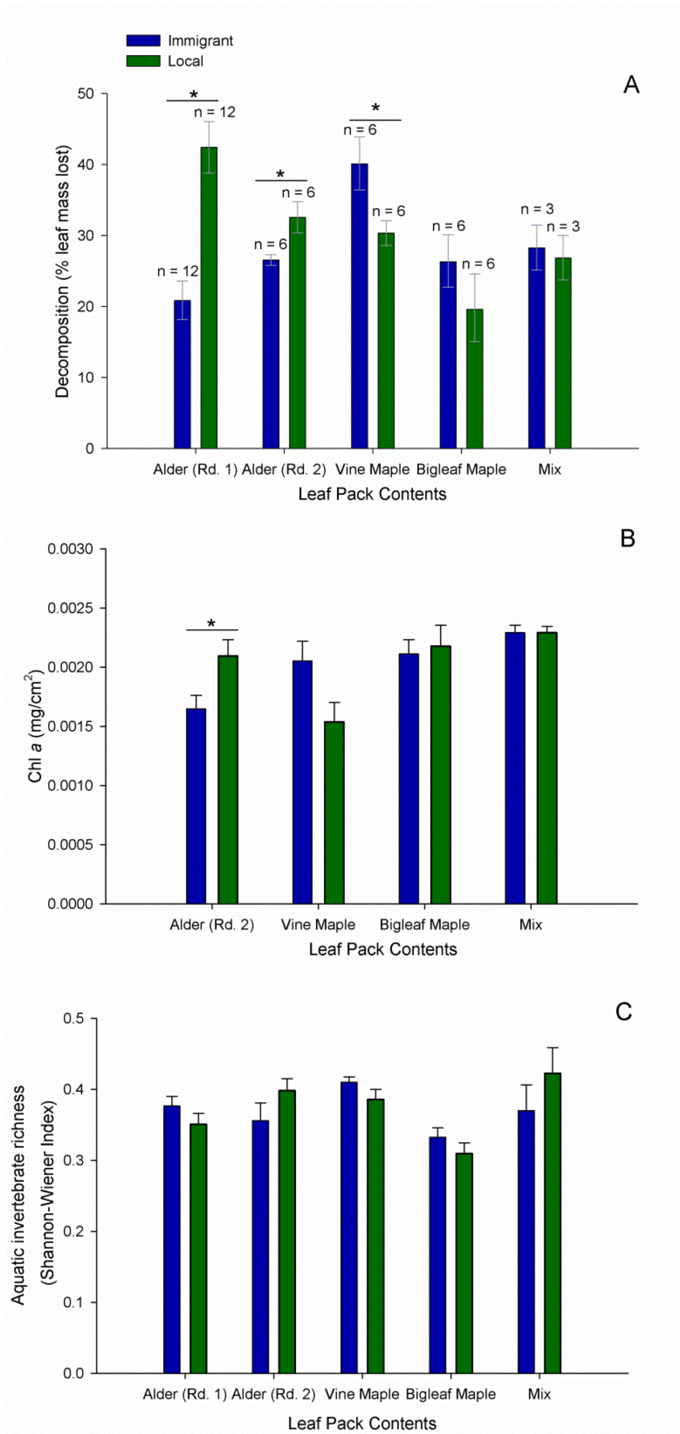

Figure 2.5: Biological responses to variation at the within-species scale (mean ± 1 se). (*a*) decomposition rates, (*b*) algal accrual and (*c*) aquatic invertebrate Shannon diversity richness of local versus immigrant alder (from two experimental runs), vine maple, bigleaf maple and mix packs containing all three species. Significant comparisons (P < 0.05) indicated by a star.

0.76). Matching the similar decomposition rates we observed for these comparisons, algal accrual on local and immigrant packs of vine maple, bigleaf maple, and mixed packs was similar (all $p > 0.05$). There were also no differences in invertebrate abundance or diversity between local and immigrant vine maple, bigleaf maple or mixed-species packs (all $p > 0.1$, Fig 2.4c). These invertebrate results statistically control for deployment site because we found general differences in the aquatic communities inhabiting early versus later successional sites: aquatic invertebrate diversity was greater on leaf packs adjacent to later successional riparian forest than early successional forest (paired t-tests (means ± se): later 0.43 ± 0.022 se, early 0.37 ± 0.017, $t_{13} = 2.22$, $p = 0.045$), however abundance was greater on leaf packs adjacent to early successional riparian forest (early riparian 46 ± 4.6 se individuals, later riparian 74 ± 9.0, $t_{13} = 2.89$, $p = 0.013$).

Local, riparian alder tended to have thinner leaves than immigrant alders growing in non-riparian forests ($F_{1,16} = 17.2$, $p < 0.001$). Therefore in our second experiment we included several riparian alder collected along the Hoko River, some of which had leaves as thin as alder on the Pysht. Although the immigrant group as a whole had slightly thicker leaves, $F_{1,10} = 5.67$, $p = 0.039$, when comparing six immigrant and local individuals with equally thin leaves ($t_3 = 0.58$, $p = 0.59$), immigrant leaves still tended to decompose less ($t_3 = 3.54$, $p = 0.023$).

DISCUSSION

Effects of Interspecific Leaf Variation

Species ordering of decomposition rates (most rapid: vine maple, alder, bigleaf maple: least rapid) in the Pysht river appears to be general (Triska and Sedell 1976). Aligned with this pattern of interspecific decomposition, vine maple tended to support higher invertebrate diversity

Table 3.1: Analysis of variance comparing aquatic decomposition rates of replicate red alder leaf packs from individual riparian trees that were deployed in the immediately adjacent river (home sites), the same river at a different site (away site, home river) and a different river (away river). Indented lines are planned orthogonal contrasts decomposing the main effects. Upstream and downstream: relative position of incubation sites within the home or away river. Variance arising from mean decomposition rates of individual trees across all treatments partitioned into effects of experimental run (variation in individuals used, river sites used and time of year) and residual effects due purely to individual differences.

Source	Df	SS	MS	*F*	P (*F* = 1)
Leaf Source	3	0.169	0.056	4.41	**0.006**
River: Home vs. Away	1	0.119	0.119	9.36	**0.003**
Home vs. Away Sites within Home River	1	0.046	0.046	3.58	0.061
Upstream vs. Downstream within Away	1	0.006	0.006	0.43	0.51
Individual Tree	39	4.780	0.123	9.62	< **0.001**
Experimental Run Effects	1	1.856	1.856	15.34	**0.008**
Source Location within Experimental Run	6	0.728	0.121	1.78	0.13
Individual Tree within Source Location	32	2.176	0.068	5.34	<**0.001**
Error	105	1.338	0.013		

than bigleaf maple. We found species diversity had inconsistent effects on decomposition. Alder-hemlock packs decomposed substantially more than expected based on decomposition rates of either species alone. In contrast, we found high diversity packs of deciduous species decomposed additively, and there was no significant increase in invertebrate diversity with increasing interspecific tree diversity. This lack of synergistic decomposition among the mixed deciduous species packs matches some previous studies (Schindler and Gessner 2009), but is in contrast to literature reviews that find non-additive effects in up to 80% of studies (Gartner and Cardon 2004, Lecerf et al. 2011). A possible explanation for why diversity did not affect decomposition or invertebrates is that while our mixed species packs increased richness, the larger size of bigleaf maple leaves likely led to lower evenness than intended.

Effects of Intraspecific Leaf Variation

At the intraspecific scale, we found substantial individual variation in decomposition rate of alder leaves, but leaf packs with high intraspecific diversity decomposed additively compared to single-individual packs. There was also no significant change in invertebrate diversity with increasing intraspecific tree diversity. We tested whether intraspecific variation was due to varying degrees of terrestrial herbivory damage, but we found that our estimates of terrestrial herbivory did not scale with aquatic decomposition. We hypothesized that herbivores and decomposers may have similar feeding preferences if both favor high nutrient quality. Alternatively, herbivore preferences could be negatively correlated with decomposer preferences if feeding by herbivores induces plant defenses that deter decomposers. To detect whether terrestrial herbivory indirectly affects aquatic decomposition, more directed experiments are necessary to untangle how constitutive and induced properties of leaves drive feeding preferences. Previous studies have demonstrated mammalian browsing (Irons Iii et al. 1991) and insect defoliation (Hutchens and Benfield 2000) are positively associated with rapid stream decomposition of leaves, however, these studies did not disentangle correlation from causation. In a more targeted study of experimentally inducing defenses in isolation and in tandem with nutrient additions to red alder trees (Jackrel and Wootton 2015a), we show that a red alder tree's response to herbivory stress does in fact strongly deter aquatic decomposition of leaf litter. In our previous study, we found this reduction in decomposition was due in part to a sharp reduction in leaf nitrogen content that was a consequence of the herbivory stress(Jackrel and Wootton 2015a).

Recipient Community Matching to Donor Subsidies

We found evidence of recipient aquatic communities matching to donor subsidies from riparian forest at the species and within-species scales. Aquatic decomposers more efficiently processed leaf litter that matched the successional stage of immediate riparian forest: alder decomposed more rapidly in stream reaches surrounded by alder dominated forest and hemlock decomposed more rapidly adjacent to later successional forest. This result is similar to a previous study by Kominoski et al., which found alder decomposed more quickly adjacent to deciduous forest (Kominoski et al. 2011). In our study we found a reciprocal pattern with hemlock, while Kominoski et al. found hemlock decomposed independently of forest composition. Whether this discrepancy arises from sample size differences or from geographic differences in leaves and decomposers requires further study. One possible explanation for this difference would be if the British Columbia study sites experienced less severe disturbance (such as logging or scouring floods) than the Washington sites, and consequently have had a more persistent conifer forest and therefore stronger selective pressure to retain efficiency for decomposing hemlock.

Leaves from local alder trees along the Pysht River decomposed more than alder leaves from trees growing in more distant areas. Studies of *Alnus glutinosa* have found intraspecific variation in stream decomposition at a continental scale (Lecerf and Chauvet 2008), however our result suggests local population differences among trees within a single region. Generally individuals with thinner leaves tended to have faster leaf decomposition rates, and while we cannot exclude the possibility that differences in leaf thinness may have contributed to the difference between local and immigrant alder leaves in our first experimental run, alder leaves collected from the riparian zone of a distant river often had leaves as thin as local leaves but still decomposed less.

This result spurred a targeted study of local matching of aquatic communities to intraspecific variation in alder leaves (Jackrel and Wootton 2014), in which we showed, using reciprocal transplant experiments across four rivers, that aquatic communities strongly prefer local alder leaves at both the larger across-river scale and the within-river scale. Our experiments in these rivers suggest that aquatic decomposer communities are locally matched to intraspecific variation in riparian subsidies. However, we found no evidence of local matching to variation in either vine maple or bigleaf maple. This inconsistency might be explained by tradeoffs in the aquatic community to efficiently handling different local plant species. Aquatic communities seem to most efficiently process alder, the most abundant deciduous tree, which provides as much as 95-98% of the total summer leaf fall in rivers in the Olympic Peninsula [3], at the expense of efficiently processing leaves of less common species. Additionally, although local alder leaf packs decomposed significantly more than immigrant leaf packs, we saw similar invertebrate communities colonize the two types of leaf packs.

Overall, our metrics of invertebrate abundance and richness explained few of the differences we observed in decomposition rates. Invertebrate communities may have caused a large portion of the variation in leaf decomposition rates observed, but our single sample of the invertebrate community per leaf pack may have been insufficient to detect differences among invertebrate communities. Alternatively, either within-species differences in invertebrates or shifts in microbial decomposer communities may be playing a large role in differentially decomposing leaf packs.

Our algal abundance measures were intended to determine whether leachates from leaves that vary among and within species of trees have implications for adjacent algal communities. Algal abundance did not scale with intraspecific variation in decomposition. Our interspecific results showed bigleaf maple packs harbored the greatest algal abundance and the lowest decomposition rates. In contrast, local alder leaf packs decomposed faster but harbored greater algal abundance than immigrant alder packs. This reversed pattern might be explained by differences in interspecific leaf chemistry affecting decomposition. Elsewhere we show that rapidly-decomposing alder leaves contain high nitrogen concentrations (Jackrel and Wootton 2015a), which might stimulate surrounding algal growth when leached from the leaves. If reduced decomposition in bigleaf maples instead arises from production of defensive compounds, their release into the surrounding water may offer a local algal refuge by repelling algal grazers.

Our results document how biodiversity among and within species can have cascading effects on aquatic organisms receiving significant subsidies. Although we did not measure strong effects of diversity at the leaf pack scale, our finding of local matching suggests biodiversity is a critical component shaping ecosystem functioning. Diversity across reaches evidently facilitates adaptive processes that increase decomposition efficiency at two scales: aquatic communities showed local matching to early versus later successional stages of riparian forest, as well as local matching to within species differences in alder genotypes. This biological variation in plant traits may be the consequence of innumerable terrestrial processes, such as terrestrial herbivory, nutrient and water availability, and frequency and intensity of natural and anthropogenic disturbance. Understanding how these different terrestrial processes shape plant traits will be important in predicting consequences of environmental changes on recipient systems. The effects of diversity from donor communities versus authochtonous diversity within the recipient system may be a worthwhile future comparison due to differences in feedbacks that may alter selection pressures for efficiency. Maintaining maximal ecosystem function may depend on maintaining local diversity at a scale often overlooked in conservation and restoration efforts. Determining the temporal scale of these processes is essential for predicting how rapid anthropogenic changes may disrupt across-ecosystem linkages. To determine the relevant spatial scale and why local preferences are evident in some cases but not others, we need further studies to unravel the mechanisms underlying these apparently adaptive responses of ecological communities.

ACKNOWLEDGMENTS

We thank C. Pfister, T. Price, J. Bergelson, G. Dwyer and several anonymous reviewers for constructive comments and discussion on this work. We thank Merrill & Ring Inc. and J. Murray for facilitating research on their lands and C. Stepien, P. Zaykoski, S. Betcher and A. Weill for field and laboratory assistance.

CHAPTER III

LOCAL ADAPTATION OF STREAM COMMUNITIES TO INTRASPECIFIC VARIATION IN A TERRESTRIAL ECOSYSTEM SUBSIDY[1]

ABSTRACT

Cross-ecosystem fluxes can intertwine otherwise disparate food webs, but the effects of biodiversity at the genotypic level on fluxes across ecosystems boundaries is not known. Fresh leaves, which vary in traits such as defensive compounds against terrestrial herbivores, drop off trees and enter streams, providing a vital resource for riverine organisms. We demonstrate substantial variation in decomposition rates among individual trees in four different rivers in the Olympic Peninsula of Washington State, USA. We show that locally derived red alder leaf litter decomposes on average 24% faster than red alder leaf litter introduced from other riparian zones. Within rivers, leaves downstream of their parent trees decompose nearly as quickly as leaves from local trees. Leaves upstream of the parent tree decomposed as slowly as leaves from trees growing alongside different rivers. Over time, aquatic decomposer communities have locally adapted to the specific trees supplying the riparian subsidies. In energy-limited environments, such as small shaded streams, consumers must be efficient foragers. Our results indicate that this pressure for efficiency has led to adaptation at a particularly fine scale. More broadly, these results illustrate how genetic diversity and the effects of selection in one ecosystem can indirectly shape the structure of other ecosystems through ecological fluxes across boundaries.

INTRODUCTION

Biodiversity is essential for preserving ecosystem function and maintaining ecosystem resistance and resilience to disturbance. Biodiversity includes both intraspecific and interspecific

[1] This manuscript is reprinted with permission: S.L. Jackrel and J.T. Wootton. 2014. *Ecology* **95**: 37-43.

variation, but with few exceptions (Whitham et al. 2006), most attention has focused on diversity at the species level (Tilman et al. 2001, Downing and Leibold 2002, Cardinale et al. 2006). The community-level consequences of variability between individuals within a species are not well known, despite being an essential element in understanding evolution and ecological function (Valen 1965, Lomnicki 1988, Whitham et al. 2006).

Intraspecific biodiversity can affect interspecific interactions. Interspecific trophic interactions are essential energy conduits for the survival of individuals. Therefore, natural selection can direct a consumer species towards different diets in different regions. Even an interaction in which a consumer feeds on a single species throughout its range may still vary spatially due to geographical variation in prey attributes and changing environmental context. Spatial variation in prey and predators can lead to a geographic mosaic of coevolutionary interactions, such as between plants and terrestrial herbivores, that can have cascading effects on other organisms that must also adapt towards an optimal diet (Thompson 2005).

The effects of interspecific interactions can be transmitted across ecosystem boundaries thereby affecting organisms spatially disjunct from where the interactions occurred (Murakami and Nakano 2002 , Knight et al. 2005, Spiller et al. 2010, Wesner 2010). Organism fluxes across ecosystem boundaries are known to be a major factor in determining ecosystem function in recipient systems (Polis and Hurd 1996, Huxel and McCann 1998, Nakano and Murakami 2001). These fluxes from donor habitats may vary across space due to a geographic mosaic of interspecific interactions occurring in the donor habitat. As local consumers should be adapted to the traits of prey transported across boundaries, the coevolutionary processes occurring in the donor ecosystem may dictate ecosystem function in the recipient system. Local adaptation in the recipient system can arise from mechanisms acting through at least two levels of the ecological hierarchy: through phenotypic shifts in the traits of individuals (which may be genetic or plastic), and through altered species composition of communities that are recipients of cross-system fluxes. Indeed, there is evidence in stream-riparian forest environments that community-level variation in riparian tree species composition generates local aquatic community adaptation through leaf fluxes into adjacent rivers (Kominoski et al. 2011).

Stream habitats are tightly interconnected with the terrestrial surroundings (Nakano et al. 1999, Sabo and Power 2002, Fukui et al. 2006). For example, aquatic macroinvertebrate communities of forested streams depend on terrestrial leaf litter, though the relative importance of leaf litter varies depending on stream width. Streams with a narrow channel width receive less sunlight and more leaves per unit of water. As a consequence, leaf shredding species dominate smaller streams while collector/filtering species extract fine particulate organic matter from the turbid waters of larger streams (Vannote et al. 1980). Local macroinvertebrate community composition also depends on the successional stage of the riparian forest. For example, aquatic leaf litter breakdown rates of certain tree species are higher in stream reaches surrounded by those same riparian tree species (Kominoski et al. 2011). These differences in macroinvertebrate composition in association with differences in stream size and differences in riparian vegetation may reflect an adaptive shift in the community that should increase the efficiency of energy utilization (Vannote et al. 1980).

While previous research has shown ecological shifts favoring increased ecosystem efficiency in response to differences in species composition and rates of subsidy inputs, the consequences of individual variation in food resources has not been investigated. Abundant evidence of macroinvertebrate community adaptation to other forms of variation in riparian ecosystems (tree species composition and quantity of leaf input relative to stream width) makes this forest-stream consumer community an ideal system to test for adaptation to intraspecific differences in cross-ecosystem subsidies. Here we use leaf inputs into streams as a model to show that individual variation within riparian tree species generates adaptation of consumer communities across ecosystems. Adaptation of macroinvertebrates to the leaves supplied by trees should be evident because the generation time of trees is multiple orders of magnitude longer than that of decomposers, allowing natural selection to shape decomposer communities to most efficiently decompose leaves growing in the immediate area. Additionally, feedback interactions of aquatic decomposers on their resource providers should be minimal (trees receive no direct fitness impact if their leaves are readily eaten after being shed into the river), and therefore should allow for an assessment of the unidirectional impact of intraspecific trait variation on decomposer communities. Using a reciprocal transplant experiment across four rivers in the Olympic Peninsula of Washington, we show that aquatic decomposer communities have locally adapted to more efficiently feed on the leaves dropping from specific individual trees growing along the banks of their river.

MATERIALS AND METHODS

Study Sites

We studied aquatic decomposition at eight stream reaches in the Olympic Peninsula of Washington State. Two deployment sites were on each of four rivers: the South Fork Pysht, Hoko, Little Hoko, and Sekiu (see Appendix 3A for river descriptions). The riparian zones of all eight sites consisted of early successional forest dominated by red alder with small numbers of bigleaf maple (*Acer macrophyllum*), western hemlock (*Tsuga heterophylla*) and other conifers. Common understory vegetation included salmonberry (*Rubus spectabilis*), vine maple (*Acer* *cinereus*), thimbleberry (*Rubus parviflorus*), salal (*Gautheria shallon*) and sword fern (*Polystichum munitum*).

Methods Background

Compared to dried senescent leaves, fresh green leaves decompose more quickly, support higher macroinvertebrate diversity, and fall into streams in large quantities during the summer growing season (Stout et al. 1985). To measure leaf fall during summer months in rivers of the Olympic Peninsula, we deployed 0.6-m wide pieces of 6.4-mm wire mesh nets in the Hoko and Little Hoko Rivers to catch floating leaf litter over 24h periods in July and August. Trapped leaves were enumerated and categorized by tree species and dominant leaf color (estimated by eye). Grams of leaf litter were calculated using the mean fresh weight of red alder leaf datasets from the Hoko River ($n = 540$, $\mu = 0.658$ g/leaf) and the Little Hoko River ($n = 492$, $\mu = 0.507$ g/leaf).

Field Experiment

To test for the direct and indirect effects of individual variation within red alder on decomposition rates, we carried out a reciprocal transplant design in which leaves from individual trees growing along rivers were enclosed in mesh leaf packs and were either placed in the river they grew adjacent to, or in a different river (4.5 – 26 km away). The experiment was replicated in two different pairs of similar sized rivers (between two 3rd - order streams: South Fork Pysht River and Little Hoko River; and between two 4th - order streams: Sekiu River and Hoko River). We asked whether individual trees exhibited variation in decomposition rates across all rivers to establish whether there was detectable variation in traits among individuals. We also tested whether rates of decomposition of leaves from the same individuals were higher in their ‘home’ river than in the ‘away’ river; such a pattern would indicate adaptation of the decomposer community to the specific genotypes/phenotypes of individual trees living locally along the river banks.

We conducted two rounds of reciprocal transplant experiments: between the South Fork of the Pysht and Little Hoko Rivers from July 9-26, 2012 and between the Hoko and Sekiu Rivers from August 1-17, 2012. Five red alder trees growing in the riparian zone immediately upstream of each of the eight aquatic deployment sites were used. For each experimental run, we used 20 trees (or 40 trees in total). From each of these forty trees, we hand-picked fifty-two fresh, green leaves and sealed them in plastic bags. Leaves with little or no visible damage from herbivores and/or pathogens were used. For each individual tree, we constructed four leaf packs with 12 leaves each using 19 cm x 15.25 cm bags made of 4.75 mm mesh nylon seine netting. Using 4.75 mm mesh netting allowed colonization by most stream macroinvertebrates. Crayfish and larger caddisflies (*Dicosmecus* and *Psycoglypha*) were observed feeding through the mesh openings but were usually too large to enter the bags. We deployed 20 leaf packs at each site (one pack per site for each of 20 trees; Appendix 3B illustrates the experimental design).

Initial weights of leaf packs were recorded and packs were strung with cable ties onto a steel reinforcing bar, which laid on the stream bottom perpendicular to the flow and was pinned at either end by two other bars pounded into the stream bottom at a 45° angle. Leaf packs were deployed for 17 or 18 days at each site. During removal, cable ties were snipped and leaf packs were placed inside sealed plastic bags. Leaves were removed from mesh bags and gently washed with water to dislodge macroinvertebrates and silt. Leaves were blotted dry with paper towels and weighed to the nearest centigram. Several bags were lost from the upper Sekiu River site, which created a slightly unbalanced design.

Statistical analyses

Regression analyses were conducted using SYSTAT and R. Percent leaf mass remaining per leaf pack was calculated and all statistical analyses were completed using the general linear model module of SYSTAT. Breakdown rates were arcsine square root transformed to meet assumptions of normality for statistical analyses and results are reported on the untransformed scale. We used an analysis of variance, controlling for variation arising from individual tree effects (a random effect), to compare mean decomposition rates among experimental treatments (the fixed effect) using planned orthogonal contrasts: 1) home river vs. away river reciprocal transplant treatments, 2) home site vs. away site packs within the home river, and 3) upstream vs. downstream location within the away river. We also partitioned the variance explained by individual tree into components arising from the early versus late season experimental runs, the source population within experimental run, and individuals within source populations to further probe the scale of individual variation. Note that variation between the two experimental runs could be attributed to individual tree differences, environmental differences among experimental rivers, experiment duration, and temporal differences in environmental conditions. Percent leaf mass lost is reported in terms of fresh leaf weight, where the final leaf weights were weighed as blotted dry weights and then converted to fresh weight using the regression equation (fresh weight = 0.941(blotted) -0.00337) generated from the lab experiment (Appendix 3C). Because we suspected there might be asymmetry in adaptation to leaves based on location of a leaf source, we also compared whether upstream and downstream decomposition within the home river varied between individuals depending on whether leaves were derived from an upstream or downstream source, by testing whether the difference in decomposition rate of individual trees differed from zero for trees from upstream and from downstream sources, using paired t-tests.

RESULTS

Measurements of summer leaf litter fall into streams during four 24h leaf collection periods indicated red alder (*Alnus rubra*) comprised 95-98% of all leaf litter entering reaches of the Hoko and Little Hoko Rivers. Of this litter, 23-34% of leaves were entirely green, while 37-53% of leaves were mostly green (Appendix 3D). Entirely green leaves were trapped on average at a rate of 59 grams-meter^{-1}-day^{-1} at the Little Hoko River and 38 g-m^{-1}-d^{-1} at the Hoko River. Mostly green leaves were trapped on average at a rate of 108 g-m^{-1}-d^{-1} at the Little Hoko and 58 g-m^{-1}-d^{-1} at the Hoko River. Because fresh, green leaves from red alder trees enter streams in large quantities during the summer growing season for aquatic decomposers, we used red alder in the reciprocal transplant experiment.

In our reciprocal transplant experiment, we found significant direct and indirect effects of intraspecific trait variation on decomposition rates. Aquatic decomposition rates were highly variable among individual red alder trees within a river (Table 3.1, $F_{32,105} = 5.34$, $p < 0.001$, Appendix 3E). Beyond this individual variability, there was significant across-river local adaptation: leaves decomposed more in their home river location than their away river (Home Sites vs. sites on Away River (Table 3.1, $F_{1,105} = 9.36$, $p = 0.003$)). Seventy-eight percent of trees' leaves decomposed more quickly at their home river than the away river, which differed significantly from the 50% expected by chance (Appendix 3F). Even within the same river, decomposition rates at away sites tended to be lower than at home sites, although the magnitude of difference was not as large as the among river comparison, but approached statistical significance (Table 3.1, $F_{1,105} = 3.58$, $p = 0.061$; Fig. 3.1). Twenty-two of thirty-seven (59%) trees had their leaf packs decompose most rapidly in the home river at the site immediately adjacent to

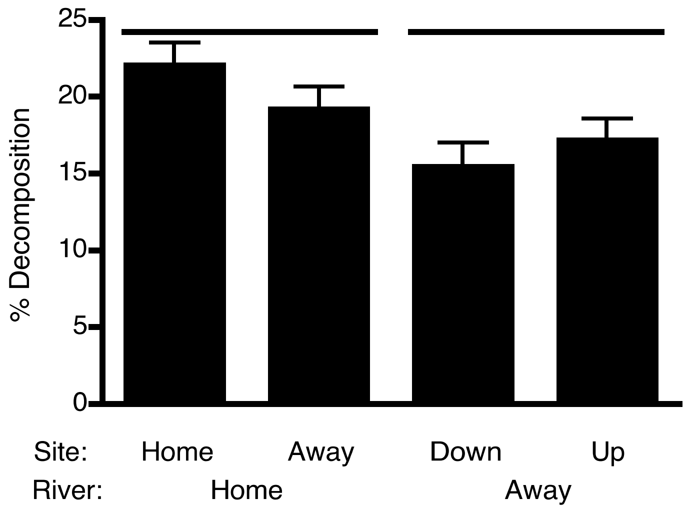

Figure 3.1: Leaf decomposition by river deployment location. Four leaf packs from each of 10 trees at each of 4 rivers were deployed at two sites at the home river and two sites at the away river (n = 160). The x-axis describes home vs. away location at two scales: by river and sites within river. There is one upstream and one downstream site per river (ex. ‘River: Away; Site: Down’ is a leaf pack incubated at the furthest downstream site on the away river where ‘away’ is relative to the source tree that those leaves came from). The y-axis is decomposition (mean ± SE) of percent leaf mass lost from ANOVA after factoring out effects of individual tree identity. Mass lost was calculated using final weights that were adjusted to a fresh leaf weight scale using a regression equation (Appendix 4C). Bars sharing a line are not significantly different from each other.

where the tree was growing compared to 25% expected by chance (Appendix 3F). In light of the near-significance of within-river adaptation and the unidirectional flow of rivers, we more fully investigated the pattern by categorizing each tree by its location relative to the deployment sites: the home site where the tree was located was either upstream or downstream of the away site within the home river. Leaves incubated downstream of their source tree tended to break down at similar rates (Δ decomposition = 0.088 ± 3.68 (s.d.) %, n = 17; paired t-test, p = 0.54) as leaves incubated at the home site of their source tree. In contrast, leaves incubated upstream of their source tree broke down more slowly than leaves at the home site of their tree (Δ decomposition = 1.1 ± 0.77 (s.d.) %, n = 18; paired t-test, $p < 0.001$). This result was not caused by simple differences in decomposition rate in upstream vs. downstream locations: the rates of decomposition of leaves placed at their home sites did not differ between upstream (23.5 ± 2.18 (s.d.) %) and downstream (20.0 ± 2.73 (s.d.) %) locations (t-test, p = 0.45), and no systematic differences existed in decomposition rates for leaves of individual trees placed in upstream compared to downstream sites in away rivers (Table 3.1, p = 0.51)

DISCUSSION

Biodiversity ranges from phenotypic diversity within species to diversity among species, but most ecological studies have been restricted to studying only effects of among-species biodiversity on ecosystem processes. This study shows that differences among individuals in one ecosystem can shape the structure of another ecosystem through fluxes across boundaries. We found significant variation in aquatic leaf decomposition among individual red alders, a pattern also observed in other tree studies (LeRoy et al. 2006, Marks et al. 2009). Here, we extend these findings to show that stream consumer communities are locally adapted to intraspecific variation in subsidies from riparian to riverine ecosystems. Green leaves were a substantial and consistent food resource available in these streams for aquatic decomposers during their growing season, a time when high quality resources are vital. Natural selection should drive community composition to consist of organisms that can efficiently feed on the most commonly available resources. We found that aquatic decomposers do indeed process locally derived leaf litter significantly faster than leaf litter originating from other riparian zones, a pattern consistent in two independent reciprocal transplant experiments using a pair of two small rivers and a pair of two medium-sized rivers.

We also found evidence that aquatic communities more rapidly decomposed leaves of individual trees to which they were regularly exposed within rivers. This was strongly evident at the across-river scale. At the within-river scale, even though the overall analysis was not quite significant ($p= 0.061$), we found a clear and highly significant pattern at the within-river scale once we accounted for each tree's upstream vs. downstream location. In the within-river treatments, leaves from trees growing at away sites that were upstream of the deployment site decomposed as quickly as leaves from trees growing at that deployment site. The leaves from upstream trees could realistically be washed downstream and used by the local community. Downstream leaves never float against the current to fuel upstream communities, hence these communities were less adapted to downstream trees. Thus, the aquatic decomposer community rapidly processed leaves only from trees the community could have realistically adapted to over time both at large (across-river) and smaller (within-river) scales.

A corollary is that upstream decomposer communities might be more strongly adapted to their home leaves. Upstream communities might receive leaves from a smaller number of trees, and might benefit from even stronger adaptation to the less diverse resource pool, if a specialist-generalist tradeoff exists. We found no evidence, however, of more rapid decomposition in upstream compared to downstream home sites. This result could indicate that there is no cost of decomposers adapting to upstream leaves, so decomposers adapt to any resources regularly available. Or, any effects of stronger adaptation in upstream locations could be masked if these stretches of river experience more stressful biotic and abiotic conditions. Alternatively, leaves were floating into upstream sites from even further upstream or other locations outside the riparian zone so that there was no substantial asymmetry in the variety of food resources to which local decomposers would adapt.

We attribute the differences observed in leaf loss to biotic processes (evident by the large number of macroinvertebrates collected from each leaf pack and visible chewing patterns from larger caddisflies). Abiotic conditions such as sunlight, water turbulence and leaching could all cause leaf mass loss. Our laboratory experiment (Appendix 4C) shows that leaching in tap water caused negligible leaf mass loss. Additionally, at each deployment site, home and away leaf packs were intermixed so that there would be no systematic differences in the abiotic conditions affecting each group.

We do not know the basis of the individual leaf variability. There are a number of potential sources of within-species variation including genetic variation in trees, induced plant defenses, and ontogenetic changes in the phenotype of different aged red alder stands. Each of these sources of variation could feasibly create spatial clustering of leaf traits that would explain why we found individuals within populations to decompose at more similar rates than between populations. Limited gene flow could cause nearby trees to be close relatives whereas natural selection could create phenotypic differences between locations where spatial variation exists in terrestrial insect loads or microclimatological conditions. Although we have no information on the red alder genetic structure, plants show substantial phenotypic plasticity, and may express different levels or types of plant defenses when terrestrial herbivore loads and composition vary spatially (Mooney et al. 2009, Ali and Agrawal 2012). Additionally, natural disturbance or logging often creates local gaps that are colonized by a cohort of trees of relatively uniform age. These cohorts could exhibit spatial variation in traits if the genotype of the recruitment pool varies through time because of biased pollen flow or seed dispersal, large-scale temporal variation in environmental conditions, or genetic drift, or if phenotypic effects such as age-related changes in leaf traits vary through time (Donaldson et al. 2006). All of these mechanisms can create spatial variation that can indirectly exert an influence on the function of other ecosystems through cross-system flow.

The result of this variation is direct effects on the quality of leaves available for consumers: certain trees decomposed readily at all locations while others hardly broke down even at their home location. Many environmental variables such as soil nutrients, hydrology, and sunlight intensity affect leaf traits in ways that can directly affect both herbivory and decomposition rates. For example, leaves with high nitrogen concentrations are particularly valuable food sources for terrestrial insects (Mattson 1980). Leaf palatability is also influenced by leaf thickness and toughness which can depend on sunlight intensity, water availability, and leaf age (Coley 1980, Sariyildiz and Anderson 2003). Beyond the direct effects of leaf quality and regardless of the specific drivers of this intraspecific variation, this trait variability provided a medium on which the decomposer community could adapt to individual trees over time. This local adaptation to leaf traits was strong enough to be detectable despite high intraspecific variation in inherent decomposition rates.

The local adaptation pattern observed from our experiment could be caused by a number of factors. First, decomposers may be physiologically or morphologically acclimating to the leaf traits of resources abundant in their lifetimes. Second, species of decomposers might evolve over time to be comprised of individuals with traits that maximize efficient resource use. Third, the community could be adapting via taxon sorting among macroinvertebrate and/or microbial decomposers, as species that more efficiently dealt with local resource traits outcompete less efficient species. The latter two hypotheses predict that varying successional age of the riparian zone will generate differences in decomposition efficiency as the community adapts over time to the growing riparian trees, whereas the first hypothesis predicts a more rapid physiological response. More detailed information on both the macro- and micro- decomposer communities is necessary before these mechanisms can be fully sorted out. Regardless of the mechanism, it is clear that ecosystem decomposition rates adapt to individual variability of resources entering through leaf flux.

Although the exact mechanism of the adaptation process is not known, the key properties of these results correspond to those of geographic mosaics of coevolution. Genetics and/or environmental variation in biotic and abiotic conditions across the geographic range of a tree species appears to have caused local clustering or a mosaic of leaf traits. It follows from our results that effects of coevolutionary dynamics, especially where geographic mosaics exist, are likely to indirectly dictate the functioning of neighboring ecosystems through cross-boundary fluxes

ACKNOWLEDGMENTS

We thank J. Bergelson, G. Dwyer, C.A. Pfister and T.D. Price for constructive comments and discussion on this work. This work was supported by the NSF GRFP, the DOE GAANN, and the University of Chicago Hinds Fund grant to SLJ, and an Olympic Natural Resources Grant and NSF grant DEB 09-19420 to JTW. We thank Merrill & Ring Inc., J. Murray, M. Hurd, D.

Hurd, Hoko River State Park, and the Washington State Department of Natural Resources for providing facilities and facilitating research on their lands.

Appendix 3A: Location, morphology, and environmental characteristics for four rivers used in the local adaptation experiments.

Table 3.A.1: Temperature, photosynthetically active radiation (PAR), flow rate, conductivity, pH and dissolved oxygen for four rivers were collected in July 2013. Temperature and PAR data are mean values over a 7 day period for all except two sites: Sekiu upstream (2 days) and Little Hoko upstream (1 day). Average daytime temperatures were determined from 10 minute interval readings using HOBO data loggers where daytime temperature value corresponded to a non-zero light measurement. Minimum and maximum temperatures include daytime and nighttime measurements. Flow rate was measured during 30 second increments using a Global Water flow probe. Conductivity, pH and dissolved oxygen were measured using a Hach HQ40d multiprobe. Further stream characteristics for the Pysht and Little Hoko can be found in Wootton (2012a, b).

River:	Pysht		Little Hoko		Sekiu		Hoko	
Upstream; Downstream	Up	Down	Up	Down	Up	Down	Up	Down
Stream order	3	3	3	3	4	4	4	4
Latitude (48°N+ °)	0.167	0.173	0.153	0.153	0.165	0.165	0.153	0.154
Longitude (124°W+ °)	0.157	0.169	0.206	0.210	0.245	0.244	0.211	0.211
Average temperature (°C)	14.1	14.8	14.2	14.3	16.1	15.9	16.7	16.2
Minimum temperature (°C)	10.7	12.4	12.8	12.9	14.1	13.9	14.1	13.9
Maximum temperature (°C)	16.3	16.8	15.6	16.4	18.2	18.9	19.8	18.8
PAR (µmol $m^{-2}s^{-1}$)	3255	3342	5257	4592	5677	8478	8304	18567
Width (m)	7.5	8.1	8.3	8.5	24.6	16.5	12.8	23.3
Depth (cm)	37	40	28	31	46	35	36	30
Flow rate (cm s^{-1})	0.75	1.3	3.49	0.76	1.75	1.43	4.14	1.86
pH	5.89	5.84	5.90	5.94	5.82	5.75	5.88	5.90
Conductivity (µS cm^{-1})	112.2	129.2	69.6	68.9	74.2	72.7	80.5	75.3
Dissolved oxygen (mg L^{-1})	9.76	9.99	9.37	9.46	8.48	8.91	9.61	9.39

LITERATURE CITED

Wootton, J. T. 2012a. Effects of timber harvest on river food webs: physical, chemical and biological responses. PLoS ONE 7:e43561.

Wootton, J.T. 2012b. River food web response to large-scale riparian zone manipulations. PLoS ONE 7:e51839.

Appendix 3B: Illustration of experimental design for reciprocal transplant experiments.

Figure 3.B.1: Reciprocal transplant experiments were performed between two medium-sized rivers in each of two experimental runs. Five red alder trees from each of four sites, two from each river, were used in each run. From each of these twenty trees, we made four leaf packs consisting of leaves from a single individual tree; each were constructed identically, but were deployed in each of the four different sites in the experimental run. Therefore, at each aquatic deployment site, there were twenty leaf packs incubated: one per tree. For example, incubating in the water at Site 1 of the Hoko River were 5 leaf packs from 5 trees growing along Site 1 of the Hoko, 5 packs from trees growing along Site 2 of the Hoko, and 10 packs from the 10 trees growing along the Sekiu River. This diagram includes arrows for only one tree of five per site and for only two of the four sites, one per river, as a partial example of the complete design.

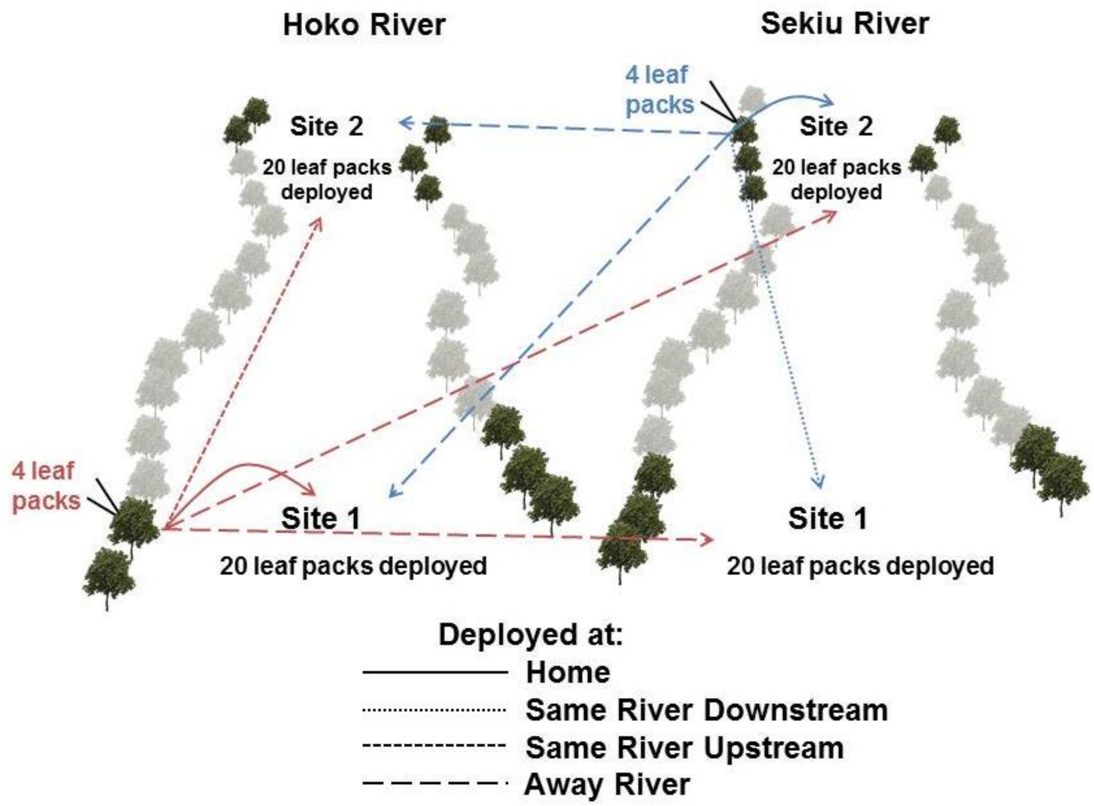

Appendix 3C: Background experiments for determining the methods used for evaluating leaf decomposition measurements.

Leaf decomposition studies in streams necessarily require that leaves are incubated under different conditions (immersed in water) than those in which the leaves were initially collected (exposed to air). To determine how leaf mass changed with immersion and post-immersion handling, we carried out an experiment manipulating leaf handling and comparing post-treatment to pre-treatment leaf weights.

Leaf pack studies often use dried autumnal leaf litter in which senescent leaves are dried to a constant weight for precise measurements (Gessner 1991). To find an accurate method for measuring percent decomposition of fresh green leaves, we collected 12 leaves from 19 red alder trees. Six leaves per tree were weighed as a group at three stages: 1) freshly picked from a tree, 2) submerged in water for 17 days and blotted dry with paper towels, 3) oven dried to a constant weight. The other six leaves per tree were oven dried before and after being submerged to estimate mass loss during handling, leaching into water or due to measurement error. Results from this section informed leaf processing methods in the following field experiment.

Initial leaf mass and final leaf mass showed positive relationships, as expected. The strongest correlation was between pre-oven dried leaves and post-oven dried leaves after submersion ($r^2 = 0.991$). This indicated minimal leaf mass loss due to non-decomposition processes (such as handling, measurement error or leaching) in this experiment. The correlation between freshly picked leaf weight and the weight of leaves blotted dry with paper towels was also strong (Fig. 4.C.1, $r^2 = 0.983$, AIC = -31.4), whereas the correlation between freshly picked leaf weight and oven dried leaf weight was appreciably weaker ($r^2 = 0.875$). Hence, we used the relationship from the analysis of blotted dry leaves to back-calculate fresh weights of leaves following incubation in the rivers.

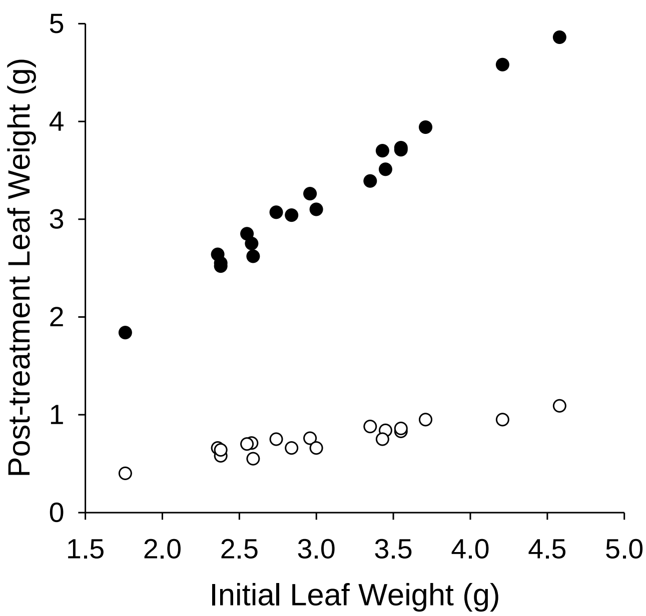

Figure 3.C.1: Regressions of initial fresh red alder leaf weight in groups of six leaves from each of 19 trees against those leaves after submerged in water for 17 days and blotted dry (●) (R^2= 0.983, fresh weight = 0.941(blotted) - 0.00337), and then after being oven dried to a constant weight (○) (R^2=0.875, fresh weight = 4.0627(dry) +0.0105).

Literature Cited

Gessner, M. O. 1991. Differences in processing dynamics of fresh and dried leaf litter in a stream ecosystem. Freshwater Biology **26**:387-398.

APPENDIX 3D: Leaf litter fall into rivers during summer months.

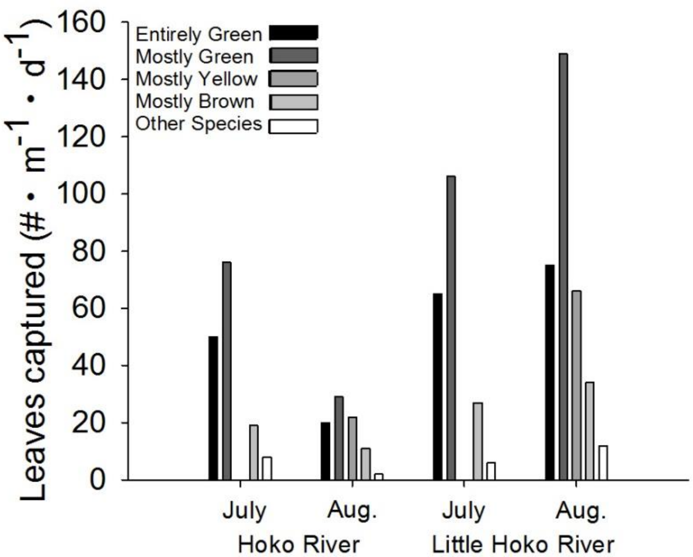

Figure 3.D.1: Type and quantity of leaf litter fall into rivers, July and August 2012. Shaded bars are red alder of different leaf color, open bar is the input of all other tree species.

APPENDIX 3E: Individual tree variation in leaf decomposition rates across four rivers.

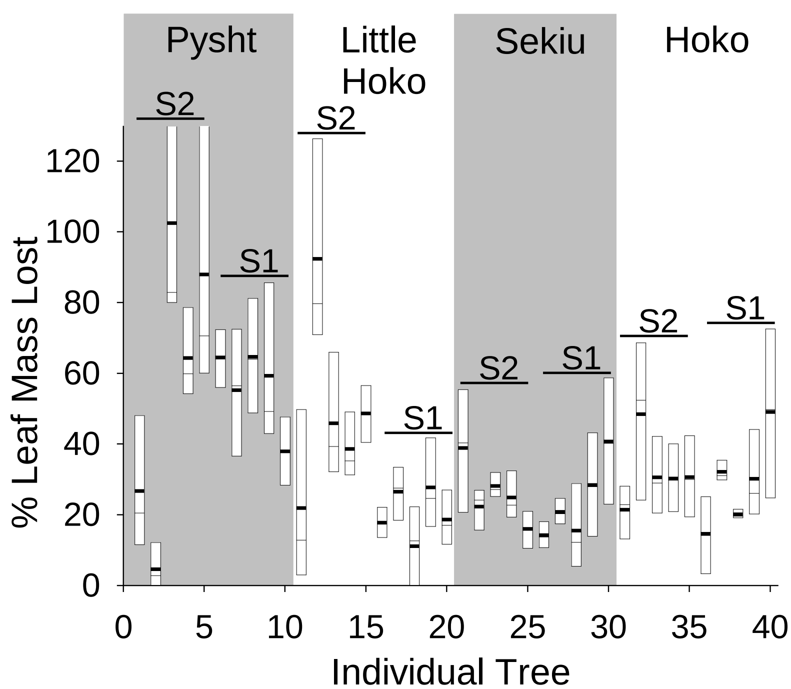

Figure 3.E.1: Box plots of decomposition rates of replicate leaf packs made from individual trees and deployed at four locations across two rivers. Thin line (-) = median, thicker line () = mean, upper box edge = 25th percentile and lower box edge = 75th percentile. Trees are ordered from most upstream to most downstream, from left to right, within each river.

APPENDIX 3F: Non-parametric comparisons of decomposition rates in reciprocal transplant experiments.

Table 3.F.1: Results of non-parametric comparisons among incubation sites. Overall, 22 of 37 (59%) trees had their leaf packs decompose most rapidly at the site immediately adjacent to where the tree was growing compared to 25% expected by chance (decomposition happening most rapidly at any one of the four sites used in the experimental run) (Friedman's Test, Q = 13.2, d.f. = 3, $p = 0.004$, $N = 28$). Sample sizes differ due to the slightly unbalanced design from leaf packs lost at the upstream site of the Sekiu River.

Comparison with Home River/Home Site	Wilcoxon sign-rank pairwise comparisons
Home River/Away Site	$z = -1.456$, $p = 0.145$, $n = 37$
Away River/Away Site #1	$z = -3.870$, $p < 0.001$, $n = 37$
Away River/Away Site #2	$z = -3.325$, $p < 0.001$, $n = 28$

CHAPTER IV

CASCADING EFFECTS OF INDUCED TERRESTRIAL PLANT DEFENSES ON AQUATIC AND TERRESTRIAL ECOSYSTEM FUNCTION[1]

ABSTRACT

Herbivores induce plants to undergo diverse processes that minimize costs to the plant, such as producing defenses to deter herbivory or reallocating limited resources to inaccessible portions of the plant. Yet most plant tissue is consumed by decomposers, not herbivores, and these defensive processes aimed to deter herbivores may alter plant tissue even after detachment from the plant. All consumers value nutrients, but plants also require these nutrients for primary functions and defensive processes. We experimentally simulated herbivory with and without nutrient additions on red alder (*Alnus rubra*), which supplies the majority of leaf litter for many rivers in western North America. Simulated herbivory induced a defense response with cascading effects: terrestrial herbivores and aquatic decomposers fed less on leaves from stressed trees. This effect was context dependent: leaves from fertilized-only trees decomposed most rapidly while leaves from fertilized trees receiving the herbivory treatment decomposed least, suggesting plants funneled a nutritionally valuable resource into enhanced defense. One component of the defense response was a decrease in leaf nitrogen leading to elevated carbon: nitrogen. Aquatic decomposers prefer leaves naturally low in C:N and this altered nutrient profile largely explains the lower rate of aquatic decomposition. Furthermore, terrestrial soil decomposers were unaffected by either treatment, but did show a preference for local and nitrogen-rich leaves. Our study illustrates the ecological implications of terrestrial herbivory and

[1] This manuscript is reprinted with permission: S.L. Jackrel and J.T. Wootton. 2015. *Proceedings of the Royal Society of London B: Biological Sciences* **282**: 20142522.

these findings demonstrate that the effects of selection caused by terrestrial herbivory in one ecosystem can indirectly shape the structure of other ecosystems through ecological fluxes across boundaries.

INTRODUCTION

Plant-herbivore interactions are a well-studied example of antagonistic coevolutionary arms races (Breedlove and Ehrlich 1968, Agrawal 2007). Plant defenses are varied and can include reduction in tissue quality, production of mechanical and chemical defenses, and signals to attract predators of the herbivores to the source of infestation (Agrawal 1998, Allmann and Baldwin 2010). Some of these defenses are produced constitutively and others plastically, in response to herbivory, with the type and quantity of defense often dependent on available resources. These strong plant-herbivore relationships are an ideal system to study cascading trophic linkages (Choudhury 1988, Kotilainen et al. 2009) because of the extensive intraspecific variability in the plant resource, and the obvious effects this variability should have at other trophic levels, such as decomposer communities.

With 80-90% of annual plant production ending up as detritus, understanding the cascading effects of plant-herbivore interactions on decomposition is essential to understanding vital ecosystem processes in both aquatic and terrestrial systems (Cyr and Face 1993, Cebrian 1999). Decomposers play no direct role in the interactions between terrestrial plants and their arboreal herbivores. Yet, decomposers in both aquatic and terrestrial systems are dependent on the mosaic of nutritionally diverse leaf litter whose composition is shaped by herbivores.

Plant defenses that target terrestrial herbivores may have varied effects on decomposers (Hättenschwiler and Vitousek 2000). Decomposers and terrestrial herbivore preferences may be positively correlated if they both favor leaves of high nutrient quality (though nutrient requirements may differ: often nitrogen limits terrestrial systems while phosphorus usually limits freshwater systems (Schindler 1977, Vitousek and Howarth 1991)). Conversely, decomposer and terrestrial herbivore preferences may be negatively correlated if feeding by terrestrial herbivores induces the production of defenses that deter decomposition. If the constitutive properties and the induced properties of leaves drive feeding preferences in different directions, a relationship between herbivore and decomposer feeding may be difficult to detect without manipulating defense production and/or nutrient content.

Here, we ask how aquatic and terrestrial decomposition processes are affected by terrestrial herbivores and nutrients in the streams and forests of the Pacific Northwest. In forested regions, aquatic insect and microbial decomposers residing in small streams rely heavily on fallen organic matter from terrestrial vegetation (Motomori et al. 2001, Lecerf et al. 2005) especially where vegetation in these forests shades the stream, limiting primary production in the stream's water column. Fresh green leaves fall into Pacific Northwest streams in abundance and throughout the season, and are an important food source for aquatic decomposers, particularly during the summer growing season for macroinvertebrates (Jackrel and Wootton 2014). Aquatic leaf decomposition varies substantially depending on the species of the source tree (Kominoski et al. 2011) and even among individuals within a single species of tree (Jackrel and Wootton 2014). Two potential contributors to this within species variation in leaf decomposition rates could be individual tree differences in leaf defensive properties and leaf nutrient content. Herbivory stress and the availability of nutrients both influence the production of plant defenses (Bryant et al. 1987a, Bryant et al. 1987b) and nutrient content often drives diet selection independent of its effect on defense production (Mattson 1980b, Behmer and Joern 1993). Varying nutrient stress may change the trade-off balance for the costs of defense, that is, surplus nutrients may mitigate defense induction (Hunter and Schultz 1995); or conversely, plants with surplus nutrients can afford a greater defense response (Cipollini and Bergelson 2001). We experimentally studied the potential for the cascading effects of terrestrial herbivory, independently and in combination with nutrient additions, across the ecosystem boundary between the terrestrial and stream ecosystem.

Our response variables to these experimental manipulations are measured changes in ecosystem processes. To date, we know of no comprehensive studies of either induced or constitutive defense compounds in red alder. Identifying chemical structures and unraveling the physiology behind induced defense compounds in an extensive task. Instead, we report here the broad-scale ecological consequences of herbivory and nutrients on ecosystem function.

METHODS

Study Sites

We experimentally studied herbivore effects on aquatic and terrestrial decomposition on the Olympic Peninsula of Washington State, USA, using leaves of a numerically and structurally dominant deciduous tree species (red alder, *Alnus rubra*) commonly found in riparian zones and disturbed forests of the Pacific Northwest. Alders have an unusual capacity to fix atmospheric nitrogen due to symbiotic root associations with the *Frankia alni* bacterium. Red alder is thus an abundant pioneer species that enriches soil for further plant succession (Luken and Fonda 1983). Alder trees experience ubiquitous insect damage to leaves with 45 – 100% (mean 74.3% ± 3.1SE) of leaves having visible signs of damage (such as defoliation and skeletonization, rolled and folded leaves, leaf miner scars, and galls), including up to 16% of leaf area consumed by chewing insects (mean 6.2% ± 0.65SE, determined from a regional survey of 30 trees across the study region, with twenty leaves per tree imported into Image J to measure area consumed).

Alder trees used in the experiment were growing at 21 locations along roadsides of the Merrill & Ring Pysht Tree Farm (48.09 °N, 124.12 °W). Leaf packs were deployed in the soil of each of these 21 locations and at 7 locations along the South Fork of the Pysht River, which runs through the tree farm. The riparian zones along the South Fork Pysht are comprised of early successional forest dominated by red alder with occasional bigleaf maple (*Acer macrophyllum*), western hemlock (*Tsuga heterophylla*) and other conifers. Understory vegetation included mostly salmonberry (*Rubus spectabilis*), thimbleberry (*Rubus parviflorus*), vine maple (*Acer cinereus*), sword fern (*Polystichum munitum*) and salal (*Gautheria shallon*). In surveys of collected leaves that fell naturally in the Pysht during the summer season, we found 78% of alder leaves were green as opposed to brown senescent litter. We document a more extensive survey of leaf litter (g/m^2) entering small streams in the Olympic Peninsula elsewhere (Jackrel and Wootton 2014). Location, morphology, nutrient and environmental characteristics for our study sites on the Pysht river have been published previously (Wootton 2012a, Jackrel and Wootton 2014).

Experimental Design

Leaf defensive traits could inhibit leaf decomposers as well as the terrestrial herbivores these components are meant to deter. Nutrients could affect decomposers directly via nutrition or indirectly by providing resources for plants to generate a more complete defense response. Therefore, we implemented a 2 x 2 experimental design to test the independent and interactive effects of herbivory and fertilizer treatments. Our experimental units were 84 young to moderately aged individuals (15.7 ± 1.4 cm SE trunk diameter at 1.5 m above ground, which correlates on average to a 15 year old tree growing on a site of average quality (Worthington et al. 1960)) of red alder, similar in size across treatment groups ($F_{3,82} = 0.31$, $p = 0.82$). In May 2012, we organized the four treatments into 21 blocks, (4 trees per block, see Appendix 4A) with each block at least 100 m apart from each other and each experimental tree within blocks at least 100 m from the next tree to minimize cross contamination of methyl jasmonate, the compound we used to induce plant defenses. Jasmonates are volatile chemicals released during herbivory that may be used by undamaged plants to recognize when neighboring plants have been damaged, and thus constitute an early warning system for plants to manufacture anti-herbivory compounds before they are directly threatened (Bruin et al. 1995). Prior to experimental treatments, we surveyed each tree for insect damage on four branches (ten leaves per branch). Three-quarters of surveyed leaves showed visible signs of insect damage, but damage levels were consistent across treatment group assignments ($F_{3,83} = 1.56$, $p = 0.21$).

In the herbivory treatment, we wounded every third leaf below 2 m in height by punching two 6.35 mm holes using an office hole punch. We brushed each punched leaf with 50 µL of a 100mM methyl jasmonate solution in 10% ethanol and 0.125% Triton-X. We repeated this procedure three times over a 6 day period in June, with the same leaves punched and treated each time. Thus, by the end of the treatment, one-third of alder leaves below 2 m had been given six hole-punches and brushed with methyl jasmonate three times. We left the remaining leaves untouched for use in leaf pack experiments. This treatment was intended to mimic a sustained threat to the plant, rather than a one-time pulse of damage, which often fails to induce strong defense responses in plants (Mithöfer et al. 2005). For the fertilizer treatment, we spread a single addition of 10 g triple superphosphate fertilizer (P_2O_5) beneath two trees per block on May 23, 2012, which was 10 days or 26 days prior to the start of the methyl jasmonate herbivory treatment depending on the block of trees. We chose to fertilize with phosphorus because it often limits nitrogen-fixers such as red alder, and similar phosphorus additions have increased growth in young of the alder species used here in south-coastal British Columbia (Brown et al. 2011) as well as speckled alder (*Alnus incana*) in northeastern North America (Gökkaya et al. 2006).

We removed fresh green leaves from each of the 84 trees for use in caterpillar feeding trials and in leaf packs deployed in aquatic and terrestrial systems. All leaves collected from trees in the herbivory treated group were adjacent to leaves given the herbivory treatment. No leaves directly receiving the hole punches and methyl jasmonate were used in the experiments to avoid inadvertently applying methyl jasmonate residue to streams. We collected leaves with little or no natural herbivore damage and sealed them in plastic bags.

To test whether experimental treatments affected terrestrial herbivory, we collected leaf-rolling caterpillars (*Epinotia albangulana*) from inside rolled-up leaves of alder trees. These herbivores were widespread on red alder and often inflicted heavy damage to individual trees. We placed each caterpillar in a separate arena containing two 12 mm diameter leaf cores from two of the four treatments being studied, for example, one leaf core from a leaf was removed from a tree treated with methyl jasmonate vs. one leaf core from a control tree from the same block. Caterpillars typically spun webs beneath and ate only one of the two leaf cores offered in the arena, therefore showing an unambiguous measure of preference. Experiments lasted until the caterpillars chose a leaf. We discarded trials if caterpillars did not eat either leaf core after 24 hours and these trials were excluded from the analysis.

At the same time as the caterpillar feeding preference experiment, we used green leaves to make leaf packs. From each tree, we made two packs that contained 12 leaves inside 19 cm x 15.25 cm bags made of 4.75 mm mesh nylon seine netting. Using 4.75 mm mesh netting allowed colonization by most stream macroinvertebrates in the Pysht River (unpublished data, S. Jackrel). We observed that larger caddisflies (*Dicosmoecus* and *Psycoglypha*) would feed through the mesh openings but were usually too large to enter the bags. We recorded initial weights of leaf packs and placed the packs in either the aquatic environment or terrestrial environment.

We strung leaf packs designated for the aquatic environment with cable ties onto a steel reinforcing bar, and laid the bar on the stream bottom perpendicular to the flow, pinned at each end by two other bars pounded into the stream bottom at a 45° angle. We deployed leaf packs for 17-21 days at 7 locations in the Pysht River. Leaf packs deployed at two locations were not usable, because they were left in the river too long and excessive decomposition made comparisons across packs inaccurate, so we report results only from the remaining 5 locations. During removal, we placed each leaf pack inside a sealed plastic bag. We removed leaves from mesh bags and gently washed the leaves with tap water to dislodge macroinvertebrates and silt. We blotted the leaves dry with paper towels and weighed leaves to the nearest centigram.

We strung leaf packs designated for the terrestrial environment onto a steel reinforcing bar using cable ties and pounded the bar into the soil. We covered leaf packs with approximately 1.25 cm of debris from the immediate area and deployed packs for either 56 or 67 days at 21 locations (each deployment site was located next to one tree, selected at random, per block of four trees). We periodically watered leaf packs to accelerate decomposition. At the end of the deployment, we removed leaf packs from each mesh bag and gently washed the leaves to dislodge macroinvertebrates and silt. We oven dried and weighed leaves to the nearest centigram.

Either 43 or 56 days after the herbivory treatment, we collected 20 additional leaves per tree in two groups of 10 contiguous leaves starting at the branch tip from two different main branches of the tree. We took leaf cores 12mm in diameter from each of the twenty leaves per tree, oven dried, and weighed each core to the nearest milligram as an indicator of leaf thickness, which often plays an important role in deterring herbivory (Coley 1983).

CNP measurements

From each tree, we collected 3-5 extra leaves immediately before and after the experiment. We oven dried leaves immediately after collection and then ground leaves into a fine powder. We packed 3mg of leaf powder into 3.5 x 5 mm tin capsules prior to analysis and measured percent nitrogen, percent carbon, and $^{15}N/^{14}N$ and $^{13}C/^{12}C$ ratios using a Costech 4010 Elemental Analyzer combustion system coupled to a Thermo DeltaV Plus IRMS via a Thermo Conflo IV interface at the University of Chicago Stable Isotope Ratio facility. The reproducibility was 0.11‰ for ^{13}C and 0.17‰ for ^{15}N, and cocoa powder and glutamic acid were used as isotopic controls. To measure phosphorus we modified an ashing, acid-hydrolysis, and phosphomolybdate-blue spectrophotometric protocol of Monaghan and Ruttenberg 1999 (see Appendix 4B for details of modifications).

Statistical Analyses

We completed all statistical analyses using SPSS (IBM Corp. 2013) and R (R Development Core Team 2013). We report aquatic percent leaf mass lost in terms of fresh leaf weight, where the final leaf weights were measured as blotted weights and then converted to fresh weight using the regression equation (fresh weight = 0.9412 × blotted weight − 0.0034; R^2 = 0.983) generated from a lab experiment (Jackrel and Wootton 2014). Decomposition rate data were arcsine square-root transformed to meet assumptions of normality and controlled statistically by deployment location to standardize results across multiple rounds of experiments.

Analysis of variance was used to test the effects of the fertilizer and herbivory treatments on aquatic and terrestrial decomposition. For the aquatic decomposition results, stepwise multiple regression analysis was used to identify potentially important covariates, some of which varied with experimental treatment, and the analysis of variance was expanded to include these additional covariates. Where treatment effects or covariates were not significant, we removed these terms from the model to maximize statistical power and identify a more parsimonious model.

RESULTS

Effect of Experimental Treatments on Leaf Traits

The % N and P values at the start of the experimental treatments were high relative to reported literature values (2.78 ± 0.048 se % N vs. 1.65 – 2.45% N; and 0.22 ± 0.0049 % P vs. 0.13 – 0.17%) (DeBell and Radwan 1984). Natural % N content varied substantially among individuals before the start of the experiment (range: 1.83 - 4.43% N), and N levels decreased (range: 1.06 – 3.58%) during the experiment for 80% of trees (n = 80). At the beginning of the experiment, leaves from trees destined to be given the herbivory treatment were similar in % N concentration ($\%N_0 = 2.72 \pm 0.056$, n = 41) to control trees ($\%N_0 = 2.84 \pm 0.079$, n = 40) (Table C1, p = 0.30), and leaves from trees destined to be given the phosphorus fertilizer were similar in %N concentration ($\%N_0 = 2.85 \pm 0.07$, n = 41) to control trees ($\%N_0 = 2.71 \pm 0.06$, n = 40; Table C1, p = 0.11).

By the completion of the herbivory treatment, leaf composition changed considerably (Table 4.C.4, p = 0.00235). Leaf C:N content increased 2.5 times faster among trees given the terrestrial herbivory treatment compared to trees in the control group (Fig. 4.1, p = 0.0026), leading C:N content of leaves from the herbivory treated group to be 12.7% higher when experimental leaves were deployed (herbivory treated: $\bar{x} = 21.11 \pm 0.45$, n = 36; control trees: $\bar{x}$

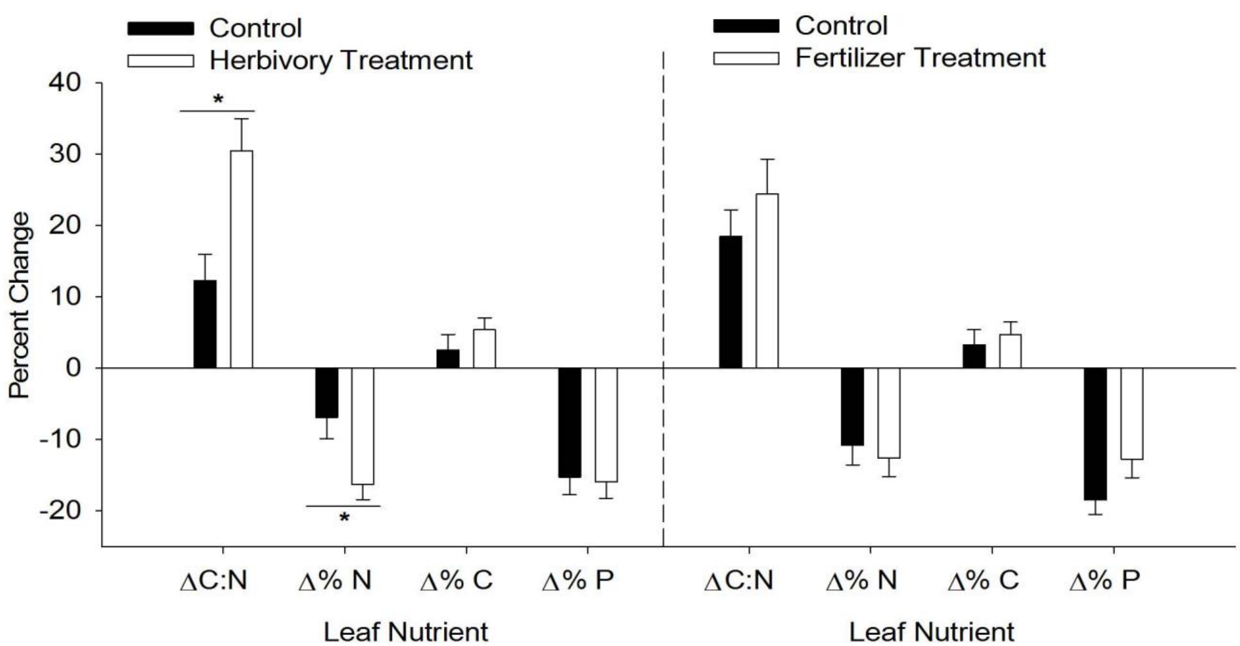

Figure 4.1: Change in C:N, % C, % N and % P content of red alder leaves from trees given an herbivory treatment versus control trees (left-hand side), and trees given a fertilizer treatment versus control trees (right-hand side). Significant comparisons (t-tests $p < 0.05$) between herbivory treated and control trees indicated by a star.

18.73 ± 0.74, n = 36; Table 4.C.4). This C:N pattern was caused by both a 2 fold greater decline in % N and a tendency for % C to increase among trees given the herbivory treatment (Fig. 4.1; Table 4.C.4, p = 0.0061 and p = 0.40, respectively).

In contrast, trees given the fertilizer did not have significantly different leaf traits (Table 4.C.4, p = 0.532). Fertilized trees changed similarly in % N concentration compared to control trees (Fig. 4.1, p = 0.64). Fertilized trees retained 44% more phosphorus content (control group declined 18.4%, while fertilized group declined 12.8%, (Fig. 4.1, Table 4.C.2, p = 0.0594), however this effect of the fertilizer treatment did not lead to a significant difference in % P content of leaves between the treatment groups (control trees: $\bar{x}$ = 0.177 ± 0.0041, n = 42; fertilized trees: $\bar{x}$ = 0.215 ± 0.0074, n = 42; Table 4.C.4, p = 0.680). Leaves from fertilized trees were 6.5% thicker (Table 4.C.4, p = 0.047).

Terrestrial Herbivory

Epinotia albangulana leaf-rollers fed less frequently on trees given the herbivory treatment than on untreated control trees (χ_1^2 = 4.34, p = 0.037, Fig. 4.2a). The two tree treatment groups (either with or without fertilizer) given the herbivory treatment (eaten in 33.3-37.9% of trials) were eaten half as often as the two treatment groups not given the herbivory treatment (eaten in 63.3-65.5% of trials). Leaf-rollers also fed more frequently on the leaf option lower in C:N content (in 62.2% of trials, χ_1^2 = 3.9, p = 0.048, n = 74).

Aquatic Decomposition

Of the leaf packs deployed in the Pysht River, leaves from the control trees decomposed 42% faster than leaves from herbivory treated trees (Fig 4.2b, Table 4.D.1, p = 0.0056). Leaf decomposition did not vary overall with P addition, but there was a significant interaction (p = 0.028) between herbivory and nutrient treatments on aquatic decomposition: simulated herbivory

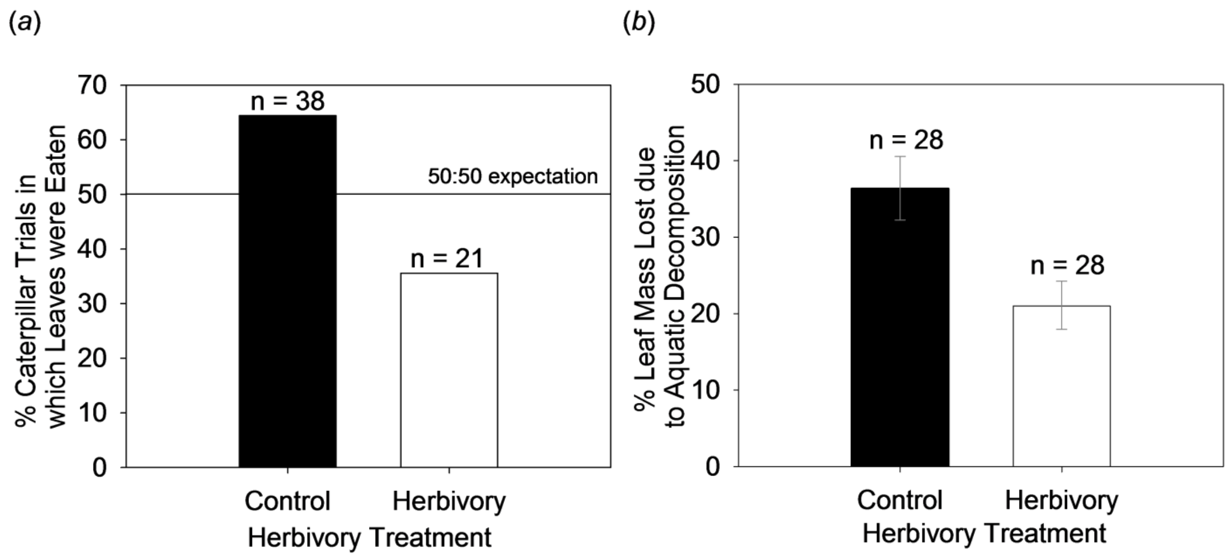

Figure 4.2: Effects of a jasmonate herbivory treatment applied to foliage of red alder trees on (*a*) caterpillar feeding trials and (*b*) average (± se) aquatic decomposition rate of red alder leaf litter. Aquatic results are from analysis of variance after factoring out deployment location.

had a strong inhibitory effect under P addition (60% reduction), but a weak effect without P addition (13% reduction). When evaluating the effect of the P addition independent of the herbivore treatment, among only the subset of trees not given the herbivory treatment, leaf decomposition was 75% greater with the P addition (Fig. 4.3, paired t-test $t_{13} = 2.63$, $p = 0.021$).

We determined whether other traits not intentionally directly manipulated in our experiment were associated with aquatic decomposition. In particular, aquatic decomposition declined significantly as C:N content increased, either when considering all trees ($R^2 = 0.232$, $p < 0.001$, Fig. 4.4a), which included trees that shifted C:N in response to simulated herbivory (Fig. 4.1), or when considering only control trees that naturally varied in C:N ($R^2 = 0.542$, $p < 0.003$). When including all measured leaf traits in a stepwise multiple regression, the best model (indicated by the lowest AIC score) of aquatic decomposition included C:N and $^{15}N/^{14}N$ ($R^2 = 0.31$, $p < 0.001$; Fig. 4.5; Table 4.D.3; Fig 4.D.1). To test the degree to which these covariates could explain observed treatment differences, we conducted a follow-up ANCOVA, including a leaf C:N term in addition to both treatment effects. Leaf C:N exhibited a negative effect on aquatic decomposition in the analysis ($p < 0.001$), but the N-isotope term was not significant and did not vary by experimental treatments (Table 4.C.4), so was removed. After factoring out variation in C:N, the residual effect of simulated herbivory was much weaker (13% decline) and not statistically significant ($p = 0.27$, Table 4.D.2), but a positive effect of adding P on average was revealed (39% increase, $p = 0.044$, Table 4.D.2). The interactive effect of simulated herbivory and P addition remained ($p = 0.06$; Table 4.D.2, Fig. 4.3): herbivory reduced aquatic decomposition by 32% under P addition, but tended to elevate aquatic decomposition by 19% without P addition. These results suggest that the fertilizer treatment had a qualitative effect on leaf traits that we could not detect from our measurements of quantitative nutrient levels.

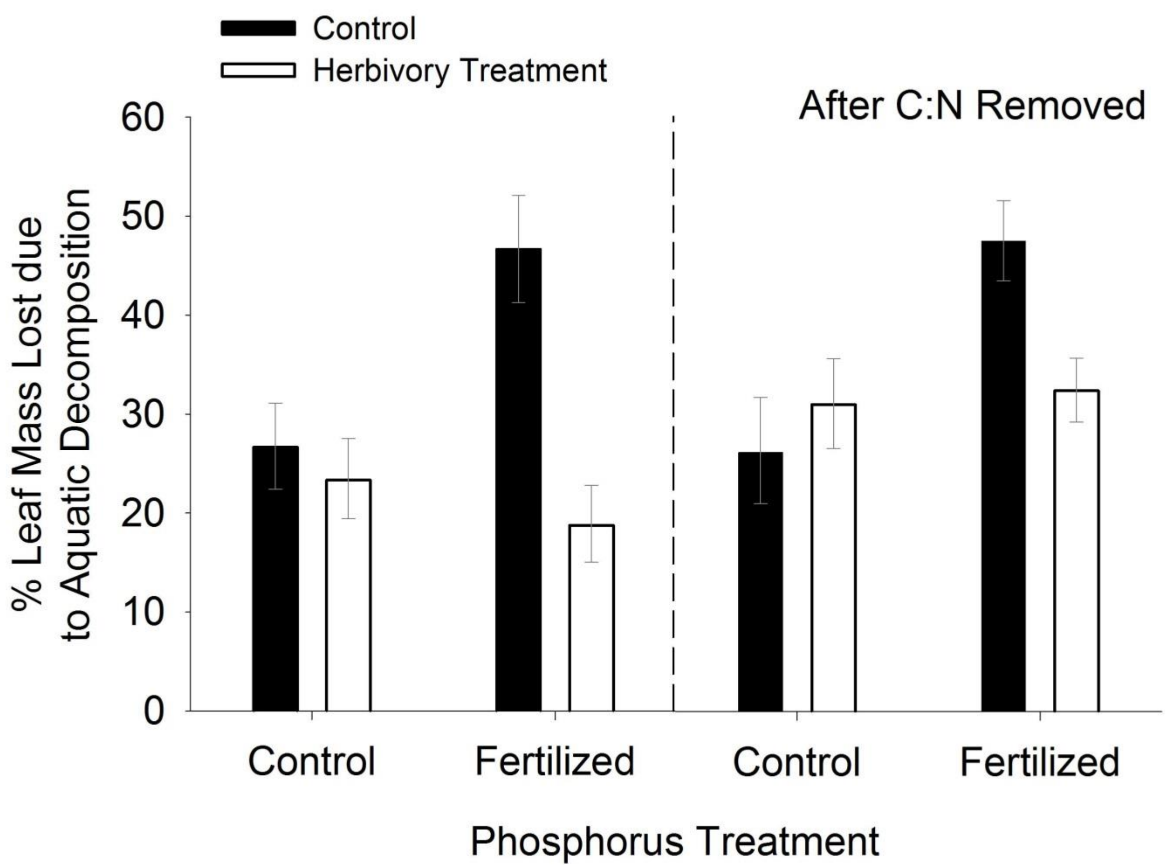

Figure 4.3: Residual effects (mean ± se) of herbivory and fertilizer treatments on aquatic decomposition of red alder from analysis of variance after factoring out deployment location (Table 4.D.1) and both deployment location and C:N in leaves at the time of leaf pack assembly, immediately after the herbivory treatment (Table 4.D.2).

Terrestrial Decomposers

Leaf packs from the herbivory treated trees decomposed at a similar rate ($\bar{x}$ = 1.188 ± 0.025 se % leaf mass lost per day, n = 42) to leaves from control trees ($\bar{x}$ = 1.194 ± 0.020% leaf mass lost per day, n = 41) (Table 4.E.1). However, decomposition increased by 1% for every 5% percentage decrease in leaf C:N content (Fig. 4.4b). For terrestrial soil decomposition, the best model (indicated by the lowest AIC score) included leaf thickness, C:N, tree diameter, N:P and $^{13}C/^{12}C$ (R^2 = 0.424) (Fig. 4.D.1, Table 4.E.2). Interestingly, decomposers showed a local preference for leaves from the nearest tree. Each deployment location was next to one of the four trees per block, and at 52% of these sites, highest decomposition occurred for leaf packs from the tree growing immediately above (Table 4.E.1, p = 0.00857). Repeating analyses without these home leaf packs did not change conclusions for the herbivory or fertilizer treatments.

DISCUSSION

Aquatic decomposition rate of red alder leaves varies substantially across individual source trees (Jackrel and Wootton 2014). Two mechanisms that may contribute to these individual tree differences include varying leaf nutrient quality and leaf defense traits (Driebe and Whitham 2000, LeRoy et al. 2007). Here we have shown that a terrestrial herbivory treatment that induced a systemic defense response in red alder trees decreased terrestrial insect feeding as expected and had a cascading effect into aquatic ecosystems by significantly inhibiting aquatic decomposition. Leaf C:N content varied widely among our study trees and we found that terrestrial herbivores, aquatic decomposers and terrestrial decomposers all strongly preferred leaves with low C:N levels. Our analysis of leaf traits indicated that the herbivory treatment caused a decrease in nitrogen levels and this resulting change in C:N played a large

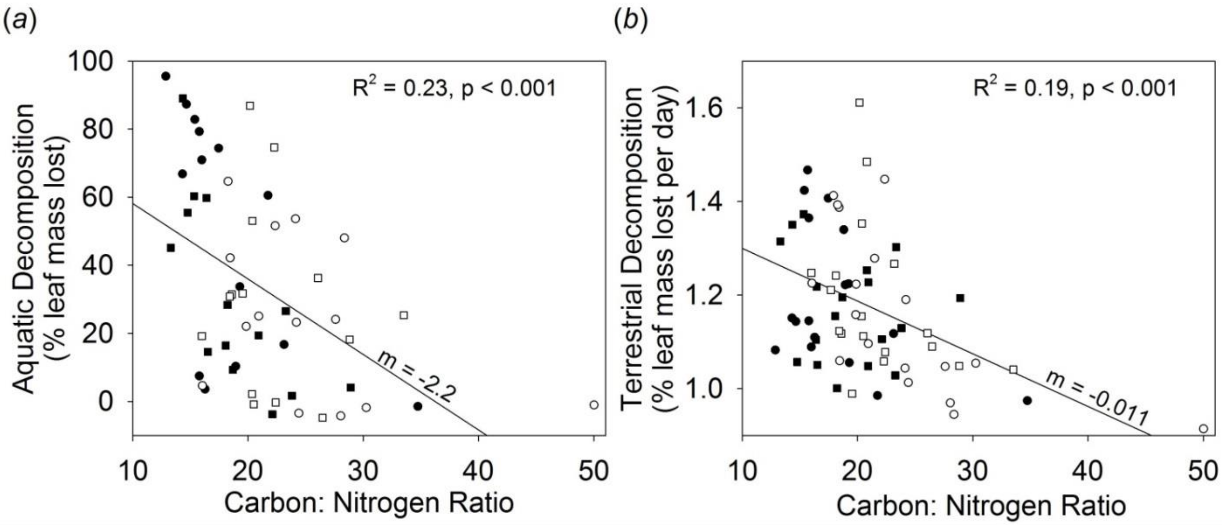

Figure 4.4: Effects of innate and experimentally induced variation in C:N of red alder leaves on the leaf decomposition rates in streams (*a*) and forest soil (*b*). Carbon: Nitrogen ratios of leaves at time of leaf pack deployment after the implementation of an herbivory treatment (hollow) versus control (filled), and a phosphorus fertilizer treatment (○) versus control (□). Coefficients of determination and two-tailed p-values are reported for entire data set.

role in why the terrestrial herbivory treatment negatively affected aquatic decomposition.

Induced defenses are costly to plants (Baldwin 1998) and we aimed to contrast plant defense to herbivory both in isolation and in combination with a nutrient rich environment. The effect of the herbivory treatment on aquatic decomposition was strongly context dependent on nutrient availability. Phosphorus fertilizer treatment on red alder has reportedly caused extensive foliar changes including increased foliar N, P, Ca, S, Mg and Fe and decreased K, Cu, Zn (Brown and Courtin 2003). In contrast to other studies (Gökkaya et al. 2006, Brown et al. 2011), our fertilization treatment failed to show quantitative changes in leaf traits (including % N, C, P, $^{15}N/^{14}N$ and $^{13}C/^{12}C$). This discrepancy may be due to the duration between fertilization and sampling. Our fertilization treatment occurred in May (similar to cited studies fertilizing between May and July) and our leaf sampling was within 6-8 weeks of fertilization, which was similar to a seedling study (8 weeks (Brown and Courtin 2003)) but far shorter than other studies on trees (15 months (Gökkaya et al. 2006) and 20 months (Bryant et al. 1987a)). Fertilized trees retained slightly more of their starting P content than control trees, but due to variation in initial P levels, there was no significant difference in P levels between treatment groups. However, the significant interaction between the fertilizer and herbivory treatments suggests that this retention of P among the fertilized trees (or some other leaf trait change) when paired with the herbivory treatment did have a qualitative effect, perhaps by spurring a different physiological response that resulted in qualitative trait shifts and a stronger defense.

We found that low C:N, which was largely determined by variation in N content, was an important diet consideration for two communities that are not typically regarded as N-limited. Freshwater ecosystems are typically limited by P and there is evidence that P is more limiting than N in many Olympic Peninsula rivers (Wootton 2012a, b). Although terrestrial ecosystems are most often limited by N, the forests in our study area are largely dominated by *Alnus rubra,* an N-fixer, and thus are typically less limited by N (Bormann and DeBell 1981). Finding a strong C:N effect is not surprising, however, given recent meta-analyses that have shown many terrestrial and freshwater ecosystems are co-limited by N and P rather than by a single limiting resource (Elser et al. 2007).

The physiological mechanism that caused the elevated C:N among our herbivory treatments is not known. There are many scenarios that could explain the decrease in N, some of which directly involve plant defense, while others are more indirect consequences of herbivory stress. Several possible explanations include: alders released N-containing volatile emissions in response to herbivory (such as methyl anthranilate and indole) (Tscharntke et al. 2001), methyl jasmonate or the herbivory stress as a whole interfered with or deprioritized nitrogen fixation (Sun et al. 2006), or N was shunted out of the leaves into other parts of the plant (such as the roots) as a means of resource protection and/or to dissuade further herbivory (Gómez et al. 2010). The physiological responses resulting in the increased C:N among the herbivory treated trees are quite possibly different among the fertilized versus unfertilized trees (plants growing on N-poor soils often use C-based defenses and vice versa) (Bryant et al. 1983). A study simulating herbivory only using mechanical damage in *Alnus incana* and *A. glutinosa* found no change in %N content (Oleksyn et al. 1998). This may indicate this response is unique to *A. rubra* or that by using methyl jasmonate, our study invoked a more complex defense response. Reduced N foliage in response to mechanical defoliation was documented in black oak (*Quercus velutina*) but not gray birch (*Betula populifolia*) (Valentine et al. 1983). Research evaluating the physiology behind this response would be an interesting future direction.

Determining underlying physiology may explain why the herbivory treatment impeded consumption by terrestrial herbivores and aquatic decomposers, but not terrestrial decomposers. Plants benefit from the action of decomposers breaking down organic material on the forest floor (Horner et al. 1988). These decomposers can be negatively affected by the plant defensive properties produced to deter herbivores (Horner et al. 1988, Kuiters 1990, Hättenschwiler and Vitousek 2000), thus impeding nutrient recycling, and presenting a tradeoff for the host tree that produced those defenses and now relies on nutrient recycling for future growth. A host tree would presumably benefit if terrestrial decomposers were insensitive to plant defense responses aimed to deter terrestrial herbivores. In light of these results, further experiments testing the effects of herbivore defense on terrestrial decomposers are warranted.

For our herbivory treatment, we aimed to mimic a natural herbivory threat by using both mechanical and chemical stressors. Mechanical defoliation has been shown to trigger production of anti-herbivory compounds in a European species of alder (Dolch and Tscharntke 2000), but mechanical damage alone probably only triggers a partial defensive response (Reymond et al. 2000). In order to further induce plant defenses we applied jasmonates because a chemical treatment is a more controlled and reliable method than introducing herbivores. There have been extensive laboratory studies on the role that jasmonates play in inducing plant defenses (Farmer and Ryan 1990, Gundlach et al. 1992) but there are far fewer studies that have successfully used jasmonates to induce defense production in the foliage of trees in nature (Martin et al. 2003, Zeneli et al. 2006, Elderd et al. 2013).

Our herbivory treatment provided a very generalized form of terrestrial herbivory. Different species of terrestrial herbivores may induce separate defense pathways that in turn differentially affect aquatic decomposers. Plants often defend themselves differently depending on how damage is inflicted and sometimes by the composition of insect saliva (Howe and Jander

2008). Natural complexes of herbivores that feed on a single tree may produce varied defense responses that could affect aquatic ecosystems in complex ways, and warrants further study.

Complex responses to herbivore stress may cause red alder tree individuals to have very different leaf traits across space. Herbivore loads and nutrient availability are patchily distributed across landscapes, and varying genetic makeup can also affect how an individual tree responds to herbivore stresses and nutrient availability. Spatial variation in leaf traits could explain the pattern of local adaptation in rivers to different alder populations that we have previously documented in this ecosystem (Jackrel and Wootton 2014). These aquatic decomposer communities are well-matched to the specific red alder trees growing in the immediate area that drop their leaves regularly into that local stretch of river. Here we show that a heavy herbivory treatment lowered aquatic decomposition rates, which supports the idea that spatially variable leaf traits such as leaf defense traits could be driving the previously documented pattern of local adaptation in aquatic ecosystems to their local leaf subsidies. We did not aim to explicitly test local adaptation among terrestrial decomposition, but our results suggest soil communities show similar local preferences. A reciprocal transplant design, as in Jackrel and Wootton (Jackrel and Wootton 2014), would be necessary to conclusively demonstrate local preference by soil organisms. Hence these results warrant further study of how leaf defense traits influences aquatic and terrestrial ecosystems.

Our findings have broad conservation implications for the functioning of these ecosystems. Nutrient availability and terrestrial herbivory pressures are both affected by anthropogenic activities. Logging practices frequently include fertilization of trees to boost growth rates, locally elevating N. Further, global N availability has been increasing due to fossil fuel combustion and synthetic nitrogen fixation (Vitousek et al. 1997). The intensity of terrestrial insect herbivory would be predicted to increase due in part to this addition of nitrogen, as well as an increase in global temperature (Tylianakis et al. 2008). Density patterns of herbivores may also change over time due to the individual or interactive effects of climate change and nitrogen deposition. Our findings suggest that the consequences of these environmental changes may have far reaching implications. Increased terrestrial herbivory has the potential to affect a key ecosystem process that may decrease the abundance of insect decomposers and may lead to a food shortage at higher trophic levels.

ACKNOWLEDGMENTS

We thank C. Pfister, T. Price, J. Bergelson and G. Dwyer for constructive comments and discussion on this work and L. Harris for assistance in the field. We thank Merrill & Ring Inc. and J. Murray for facilitating research on their lands, A. Colman, A. Mine, G. Olack and the Colman Isotope Lab at University of Chicago for nitrogen, carbon and phosphorus analyses, and D. Hurd and M. Hurd for providing work facilities.

Appendix 4A: Illustration of experimental design.

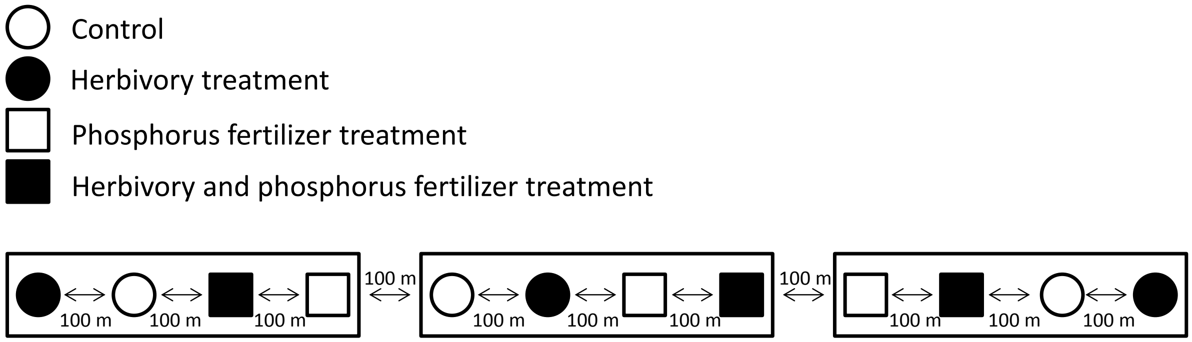

Appendix 4B: Modified protocol for measuring phosphate.

We boiled down 50mg of leaf powder with 0.4mL 20% $Mg(NO_3)^2$ w/v in 95% EtOH and 10mL 1.0M HCL on a 120°C hot plate to 50% of the starting volume. We allowed samples to dry for 48 hours, covered vials with pin pricked aluminum foil caps, and ashed at 550°C in a muffle furnace for 24 hours. Ash was dissolved in 10mL of 0.1M HCL and heated in an 80°C water bath for 30 minutes. We mixed 10µL aliquots of sample with 990µL DI water and 100µL of mixed reagent (containing 5mL 24nM ammonium molybdate, 12.5mL 5N sulfuric acid, 5.0mL 0.31M ascorbic acid and 2.5mL 2.0mM antimony potassium tartrate) in cuvettes to measure total phosphate on a Shimadzu UV-1800 spectrophotometer at 883nm. Reference phosphate compounds returned high yields: 98.6% ± 0.78SE of 10µM glycerophosphate, 102.8% ± 1.33SE of 10µM pyrophosphate, and 93.9% ± 0.50SE of 10µM 5'adenosine monophosphate. We chose 50mg of leaf material per sample after trials of 10, 25, 50 and 100mg. We ran each batch of samples against a five point standard curve of KH_2PO_4 from 0 – 10.0µM. To control for across batch variation, we ran controls of 10µM 5'adenosine monophosphate, which was chosen because it was the most difficult reference compound to obtain high yields. All batches yielded 90.5 - 99.8% of the expectation for 10µM 5'adenosine monophosphate, and correcting for these slight differences did not change conclusions.

Appendix 4C: Effect of herbivory and fertilizer treatments on leaf traits.

Table 4.C.1: Percent nitrogen of red alder leaves before an herbivory and fertilizer treatment.

Source	df	SS	MS	*F*	P (*F* = 1)
Herbivory treatment	1	0.183	0.183	1.110	0.297
Fertilizer treatment	1	0.438	0.438	2.650	0.109
Herbivory x Fertilizer	1	0.327	0.327	1.976	0.165
Block	20	4.238	0.212	1.282	0.229
Error	57	9.424	0.165		

Table 4.C.2: Change in percent phosphorus of red alder leaves following an herbivory and fertilizer treatment.

Source	df	SS	MS	*F*	P (*F* = 1)
Herbivory treatment	1	11	11.1	0.060	0.807
Fertilizer treatment	1	680	680.2	3.698	0.0594
Herbivory x Fertilizer	1	15	14.7	0.080	0.7784
Block	20	7400	370.0	2.011	0.0203
Error	58	10669	183.9		

Table 4.C.3: Change in percent carbon of red alder leaves following an herbivory and fertilizer treatment.

Source	df	SS	MS	*F*	P (*F* = 1)
Herbivory treatment	1	126	125.77	1.055	0.310
Fertilizer treatment	1	33	32.58	0.273	0.604
Herbivory x Fertilizer	1	103	102.68	0.861	0.358
Block	17	2732	160.72	1.348	0.205
Error	48	5723	119.22		

Table 4.C.4: Effects of herbivory and fertilizer treatments on several leaf trait variables via multiple analysis of variance.

Source	df	Wilk's λ	SS	MS	*F*	P (*F* = 1)
Herbivory treatment	1	0.529			3.661	0.00235
Leaf Thickness			4.460^{-6}	4.460^{-6}	2.0367	0.160
% Nitrogen final			2.256	2.256	8.290	0.00608
% Carbon final			18.58	18.581	0.710	0.404
% Phosphorus final			8.8^{-5}	8.8^{-5}	0.115	0.737
Carbon: Nitrogen final			229.13	229.125	9.739	0.00315
Carbon: Phosphorus final			1	0.6	0.0002	0.990
Nitrogen: Phosphorus final			97.77	97.767	13.414	0.00065
$^{13}C/^{12}C$			1.939	1.939	1.707	0.198
$^{15}N/^{14}N$			0.0096	0.00956	0.102	0.751
Fertilizer treatment	1	0.863			0.651	0.746
Leaf Thickness			9.167^{-6}	9.167^{-6}	4.187	0.0466
% Nitrogen final			0.0496	0.0496	0.182	0.671
% Carbon final			25.97	25.970	0.992	0.325
% Phosphorus final			1.32^{-4}	1.32^{-4}	0.172	0.680
Carbon: Nitrogen final			53.70	53.704	2.283	0.138
Carbon: Phosphorus final			5534	5533.9	1.566	0.217
Nitrogen: Phosphorus final			0.41	0.408	0.0560	0.814
$^{13}C/^{12}C$			2.089	2.089	1.839	0.182
$^{15}N/^{14}N$			0.0472	0.0472	0.505	0.481
Herbivory x Fertilizer	1	0.937			0.276	0.977
Leaf Thickness			2.210^{-7}	2.215^{-7}	0.101	0.752
% Nitrogen final			0.0072	0.00718	0.0264	0.872
% Carbon final			15.01	15.014	0.574	0.453
% Phosphorus final			7.6^{-5}	7.614^{-5}	0.0993	0.754
Carbon: Nitrogen final			11.89	11.887	0.0505	0.481
Carbon: Phosphorus final			842	842.5	0.238	0.628
Nitrogen: Phosphorus final			0.00	0.00	0.00	0.999
$^{13}C/^{12}C$			0.115	0.115	0.102	0.752
$^{15}N/^{14}N$			0.0293	0.0293	0.313	0.579
Block	17	0.0238			1.216	0.0763
Leaf Thickness			7.512^{-5}	4.419^{-6}	2.0182	0.0308
% Nitrogen final			5.167	0.304	1.117	0.369
% Carbon final			515.64	30.332	1.159	0.335
% Phosphorus final			0.0262	0.00154	2.0067	0.0319
Carbon: Nitrogen final			904.43	53.202	2.261	0.0149
Carbon: Phosphorus final			130761	7691.8	2.176	0.0192
Nitrogen: Phosphorus final			94.46	5.556	0.762	0.723
$^{13}C/^{12}C$			23.098	1.359	1.196	0.306
$^{15}N/^{14}N$			1.544	0.0908	0.971	0.505
Error	45					
Leaf Thickness			9.853^{-5}	2.190^{-6}		
% Nitrogen final			12.245	0.272		
% Carbon final			1178.1	26.180		
% Phosphorus final			0.0345	7.667^{-4}		
Carbon: Nitrogen final			1058.65	23.526		
Carbon: Phosphorus final			159041	3534.2		
Nitrogen: Phosphorus final			327.98	7.288		
$^{13}C/^{12}C$			51.118	1.136		
$^{15}N/^{14}N$			4.209	0.0935		

Appendix 4D: Treatments and covariates affecting aquatic decomposition rates in streams.

Table 4.D.1: Effects of an herbivory treatment and fertilizer treatment on eventual decomposition in stream environments.

Source	df	SS	MS	*F*	P (*F* = 1)
Herbivory treatment	1	0.410	0.410	8.605	0.00559
Fertilizer treatment	1	0.082	0.0820	1.723	0.197
Herbivory x Fertilizer	1	0.247	0.247	5.179	0.0284
Block	13	5.484	0.422	8.863	<0.001
Deployment Location	4	5.119	1.280	26.888	<0.001
Land Source	9	0.365	0.0405	0.851	0.575
Error	39	1.856	0.0476		

Table 4.D.2: Effects of fertilizer and herbivory treatments on eventual decomposition in stream environments after adjusting for river location and C:N. Testing the herbivory treatment after removing nutrient differences indicates the herbivory treatment was largely a result of nutrient changes, and after removing effects of C:N, the phosphorus fertilizer treatment was significant.

Source	df	SS	MS	*F*	P (*F* = 1)
Herbivory Treatment	1	0.0410	0.0410	1.245	0.272
Fertilizer Treatment	1	0.143	0.143	4.329	0.0443
Herbivory x Fertilizer	1	0.124	0.124	3.769	0.0597
Carbon: Nitrogen	1	1.157	1.157	35.107	<0.001
Block	13	5.484	0.422	12.805	<0.001
Deployment Location	4	5.119	1.280	38.849	<0.001
Land Source	9	0.243	0.0270	0.819	0.602
Error	38	1.252	0.0329		

Table 4.D.3: Standardized coefficients from type III stepwise regression ($F_{2,53} = 13.3$, $p < 0.001$) showing the effects of various leaf traits on aquatic decomposition. Variables excluded from the model were tree trunk diameter, nitrogen: phosphorus, carbon: phosphorus, $^{13}C/^{12}C$, and leaf thickness.

Source	Estimated	t value	Pr(>|t|)
Carbon: Nitrogen	-0.203	-4.725	0.000133
$^{15}N/^{14}N$	0.100	2.330	0.00711

Figure 4.D.1: Illustration of herbivory and fertilizer treatments on leaf traits and covariates influencing aquatic and terrestrial soil decomposition. Thick lines are significant ($p < 0.05$) and thin lines are non-significant variables included in stepwise multiple regressions (Table 3.D.3, Table 3.E.2). Standardized coefficients are reported for effect size comparisons. Significance values of herbivory treatment on leaf traits obtained from paired t-tests (thick lines, $p < 0.01$; thin lines, $p < 0.05$). Significance of residual effect of fertilizer treatment on aquatic decomposition obtained from Table 3.C.2.

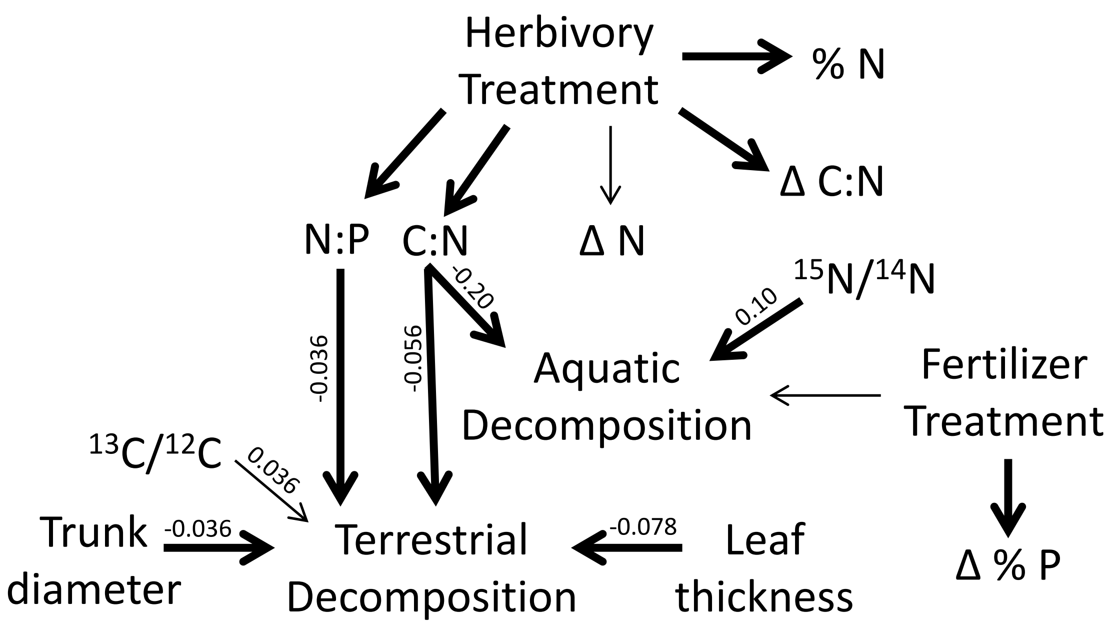

Appendix 4E: Treatments and covariates affecting terrestrial decomposition rates in soil.

Table 4.E.1: Effects of an herbivory treatment, fertilizer treatment and leaf source on eventual decomposition in terrestrial soil environments.

Source	df	SS	MS	*F*	P (*F* = 1)
Leaf source	1	0.0607	0.0607	7.406	0.00857
Herbivory treatment	1	0.0056	0.00562	0.686	0.411
Fertilizer treatment	1	0.0020	0.00202	0.246	0.622
Herbivory x Fertilizer	1	0.0089	0.0089	1.089	0.301
Block	20	1.151	0.0575	7.024	<0.001
Error	58	0.475	0.00819		

Table 4.E.2: Standardized coefficients from type III stepwise regression ($F_{5,56} = 9.967$, $p < 0.001$), showing the association of various leaf traits on terrestrial soil decomposition. Variables excluded from the model were $^{15}N/^{14}N$, carbon: phosphorus.

Source	Estimated	t value	Pr(>|t|)
Leaf thickness	-0.0779	-4.007	0.000183
Carbon: Nitrogen	-0.0563	-3.123	0.00283
Trunk diameter	-0.03589	-2.395	0.0200
Nitrogen: Phosphorus	-0.0362	-2.035	0.0466
$^{13}C/^{12}C$	0.0358	1.862	0.0678

CHAPTER V

INTRASPECIFIC LEAF CHEMISTRY DRIVES LOCALLY ACCELERATED ECOSYSTEM FUNCTION IN AQUATIC AND TERRESTRIAL COMMUNITIES[1]

ABSTRACT

Resource patchiness influences consumer foraging, movement, and physiology. Fluxes across ecosystem boundaries can extend these effects to otherwise distinct food webs. Intraspecific diversity of these cross-ecosystem subsidies can have large consequences for recipient systems. Here, we show intraspecific variation in leaf defensive chemistry of riparian trees drives local adaptation among terrestrial and riverine decomposers that consume shed leaf litter. We found extensive geographic structuring of ellagitannins, diarylheptanoids and flavonoids in red alder trees. Ellagitannins, particularly those with strong oxidative activity, drive aquatic leaf decomposition. Further, spatial variation in these leaf components drives local ecological matching: in experiments using artificial food sources distinguished only by the chemical content of individual trees, we found decomposers both on land and in rivers more quickly consumed locally derived food sources. These results illustrate that terrestrial processes can change the chemistry of cross-ecosystem subsidies in ways that ultimately alter ecosystem function in donor and recipient systems.

INTRODUCTION

Organisms are tightly interconnected in tangled webs of interactions. Variation in organismal diversity across space and time can have cascading effects across multiple trophic levels (Bruno and O'Connor 2005), and even across-ecosystem boundaries. There are many

[1] This manuscript is reprinted with permission: S.L. Jackrel, T.C. Morton, and J.T. Wootton. 2016. *Ecology* In Press.

examples of the tight interconnection between terrestrial and aquatic systems, particularly forest-river systems (Nakano and Murakami 2001, Knight et al. 2005). Preservation of biodiversity is a well-accepted means of preserving many key ecosystem functions by maintaining ecosystem resistance and resilience to disturbance (Cardinale et al. 2006b, Ives and Carpenter 2007), but the mechanisms explaining why diversity maintains ecosystem stability are less known (Ives and Carpenter 2007). Understanding the effects diversity may have on adjacent ecosystems is critical for predicting and mitigating consequences of declining diversity. Species diversity remains the focus of biodiversity studies, but recent work has expanded this field into how biodiversity at the within-species scale affects community structure and ecosystem processes (Crutsinger et al. 2006, Whitham et al. 2006). Studying intraspecific diversity also illuminates the development of linkages at temporal and geographic scales, and points to possible experiments in nature.

Our study examines how selective forces driving divergence and creating diversity ultimately affect adjacent ecosystems receiving subsidies. For example, a major component of plant diversity often arises from plastic and genetic responses to herbivore stress. Plant defenses against herbivores are varied and include production of mechanical and chemical defenses, reduction in tissue quality, and volatile signals to attract predators of the herbivores to sources of infestation (Agrawal 1998, Allmann and Baldwin 2010). Defenses employed by plants often depend on the availability of environmental resources and genetics. Neighboring individuals may share common abiotic resources such as nutrients, have closer genetic relatedness, and experience similar biotic pressures such as herbivory than individuals growing a distance apart (Coley et al. 1985, Schweitzer et al. 2008). Together, these spatial factors can cause a geographic mosaic of interactions (Thompson 2005) resulting in sustained spatial variation in plant diversity with potential consequences for other dependent organisms, such as the terrestrial and aquatic decomposers that consume 80-90% of carbon fixed by plants (Cebrian 1999). Assuming then that consumers should benefit from being adapted to efficiently consume available resources, in a scenario where we see spatial structuring in leaf traits of a plant species (such as defensive chemistry), do communities of consumers in recipient systems vary to efficiently match the plants in adjacent donor communities with different chemical signatures?

We address this question using riparian red alder trees (*Alnus rubra*), a dominant deciduous tree in the Pacific Northwest, as the model system where intraspecific variation in leaves has strong effects on herbivory rates, decomposition in soils, and decomposition in streams (Jackrel and Wootton 2014, 2015a). Previously, we showed that induced defense responses of red alder trees to terrestrial herbivory stress slow leaf decomposition in streams (Jackrel and Wootton 2015a). Additionally, intraspecific variation in red alder leaves causes local matching that enhances rates of aquatic and terrestrial ecosystem function at small scales (< 1.0 km) (Jackrel and Wootton 2014, 2015a). We used reciprocal transplant experiments to show that local communities decomposed leaves from red alder trees growing in the immediate area more quickly than leaves from trees growing at further distances. These opportune systems with trophic effects crossing the aquatic-terrestrial boundary enable us to study the implications of intraspecific diversity on aquatic decomposers largely decoupled from the terrestrial herbivory processes shaping spatial patterns of diversity among trees. Leaf decomposition results from complex interactions among invertebrates, microbes, and hyphomycetes (Wright and Covich 2005). In this study, we demonstrate a chemical basis for the significant ecological variation we observed.

Here, we document presence and relative abundance differences in 10 diarylheptanoids (including two with mass spectra consistent with novel structures) and 13 ellagitannins in leaves from a population of 40 red alder trees growing along the banks of four rivers. Diarylheptanoids are notable in the biomedical literature for their toxicity (Sati et al. 2011) and promise for cancer treatments (Farrand et al. 2014); some evidence also suggests diarylheptanoids inhibit digestion in herbivores (Sunnerheim and Bratt 2004). We took advantage of technical developments to characterize these compounds and explore their ecological importance (González-Hernández et al. 2000, Muilenburg et al. 2011). Recent reviews stress that ellagitannins are an underappreciated class of secondary metabolites (Salminen and Karonen 2011), and plants are known to suppress ellagitannin production in response to reduced insect pressures (Agrawal et al. 2012). Ellagitannins may function as an herbivory defense via their oxidation activity, which can damage essential nutrients (Barbehenn et al. 2006). Because the relative magnitude of oxidation activity in ellagitannins differs from other tannins, which are less easily oxidized but rather are much more effective at binding and inhibiting digestion of plant proteins, traditional functional metrics (such as assays measuring protein-precipitation capacity) that are still frequently used for measuring secondary metabolites are inadequate to fully characterize plant defensive compounds (Stevens et al. 2014, Mason et al. 2015). We use high-resolution (i.e., accurate mass) mass spectrometry that enabled precise separation within classes of compounds (e.g. different ellagitannins) and allowed us to characterize specific compounds that may play important roles in ecology and ecosystem function. Here, we show how secondary metabolites, nutrients, and mechanical defense vary in a natural population of trees and regulate local stream decomposition rates. Further, our results show that aquatic and terrestrial decomposer communities are locally matched to leaf defensive chemistry differences in the local red alder individuals that frequently supply abundant leaf litter to these communities.

METHODS

To determine the driving factor behind local adaptation to intraspecific plant variation in decomposer communities, we first measure intraspecific leaf and tree traits: including secondary metabolites (ellagitannins and diarylheptanoids), nutrients (C, N, and P and the isotopes of C and N), leaf thickness, and trunk diameter. We ask which traits best predict aquatic ecosystem function using data from leaf pack experiments. After finding that ellagitannins are one of the strongest predictors of aquatic decomposition, we use the structure of each ellagitannin to predict the strength of their function (oxidation) against consumers. We then determine whether strength of oxidative function is predictive of aquatic decomposition. Next, we test whether secondary metabolite composition can be predicted by other leaf traits, and whether these metabolites vary geographically. After finding geographic structuring, we completed a diet field experiment to determine whether this geographic variation in chemical components drives adaptation in streams and soils.

Study Sites

Red alder is an abundant deciduous tree in riparian zones of the Pacific Northwest. We chose 40 trees growing along four rivers in the Olympic Peninsula of Washington State: the South Fork Pysht (48.167 °N, 124.157 °W), Hoko (48.261 °N, 124.354 °W), Little Hoko (48.255 °N, 124.343 °W), and Sekiu (48.282 °N, 124.409 °W) (for river descriptions, see (Jackrel and Wootton 2014). Riparian zones at each river consisted of early successional forest dominated by red alder with small numbers of bigleaf maple (*Acer macrophyllum*), western hemlock (*Tsuga heterophylla*) and other conifers.

Leaf Field Experiment and Leaf Preparation

To test how individual variation in alder leaf traits affects aquatic ecosystem function, we used data on leaf decomposition rates in streams from our previous experiment (Jackrel and Wootton 2014). This experiment was replicated in two different pairs of similar sized rivers (between two fourth-order streams, Sekiu River and Hoko River, and between two third-order streams, South Fork Pysht River and Little Hoko River). In brief, green leaves were collected from five red alder trees growing in the riparian zone immediately upstream of each of the eight aquatic deployment sites (2 sites per river and 40 trees in total) and used to construct four leaf packs per tree to measure decomposition rate at four locations: two sites in the adjacent river and two sites in the paired river (see Appendix 5C for an illustration of the reciprocal transplant experimental design). Green leaves are a substantial and consistent energy resource available in these streams for aquatic decomposers during their summer growing season, a time when high quality resources are essential (Stout et al. 1985, Jackrel and Wootton 2014). Initial and final leaf weights were recorded for each leaf pack, yielding four decomposition rates per tree. These data were collected from the Pysht and Little Hoko rivers in July 2012 and the Hoko and Sekiu Rivers in August 2012 (Jackrel and Wootton 2014). Our linear mixed-effects models use individual tree identity as our random effect for our four repeated decomposition measurements, and due to the experimental design, tree identity also incorporates temporal differences between the two experimental rounds.

As an indicator of leaf thickness, we took leaf cores 12mm in diameter from an additional 20 leaves per tree, then oven dried for 48 hours and weighed each core to the nearest milligram. As a proxy for tree age, we measured tree trunk diameter at 1.5 m above ground. Additional leaves were oven dried ground in a mortar, and stored at room temperature until further analyses.

CNP measurements

We packed 3 mg of leaf powder into 3.5x5 mm tin capsules and measured percent nitrogen, percent carbon, and $^{15}N/^{14}N$ and $^{13}C/^{12}C$ ratios using a Costech 4010 Elemental Analyzer combustion system coupled to a Thermo DeltaV Plus IRMS via a Thermo Conflo IV interface at the University of Chicago Stable Isotope Ratio facility. The reproducibility was 0.11 ‰ for ^{13}C and 0.17 ‰ for ^{15}N, and cocoa powder and glutamic acid were used as isotopic controls. To measure phosphorus we used an ashing, acid-hydrolysis, and phosphomolybdate-blue spectrophotometric protocol (Jackrel and Wootton 2015a). In addition to %C and %N, total C and N isotopic ratios were measured as proxy indicators for different leaf components (e.g., ^{13}C-depleted leaves may contain more lignin, while ^{13}C-rich may contain more polysaccharides (Benner et al. 1987, Teece and Fogel 2007)).

Mass Spectrometry Analyses

We extracted 100 mg of leaf powder in 10 mL 70% methanol at ambient temperature, and auto injected 5 µL aliquots of each sample through a Zorbax SB-C18 2.1x150 mm, 3.5 µm column on an Agilent Q-TOF LC-MS with dual ESI (Agilent 6520). We ran each sample separately in negative mode and positive mode using the Auto MS/MS mode with the following parameters: 35 eV fixed collision energy, 325 °C gas temperature, 9 ml/min drying gas, 40 psig nebulizer, 170 V fragmentor, 120 V skimmer voltage, 750 V OCT 1 RF Vpp, and 4500 V capillary voltage. We eluted the samples with 0.1% formic acid in water (A) and 0.1% formic acid in 100% methanol (B). The separation was carried out with the following program: 5 min of 100% A at a rate of 0.2 ml/min, followed by a gradient from 100% to 60% A (0% to 40% B) over 20 min at a rate of 0.1 ml/min. Flow was then held for 5 min at 60% A (40% B) at a rate of 0.3 ml/min. Then a gradient from 60% to 0% A (40% to 100% B) was carried out over 15 min at 0.3 ml/min, and then held for 10 min at 0% A (100% B) at 0.3 ml/min. Additionally, we did targeted Q-TOF runs in High Resolution mode at varied collision energies in precursor and product ion modes to further aid compound characterization (data not shown).

We characterized compounds using retention times and fragmentation patterns of chromatograms with automatic agile integration using Agilent Mass Hunter Software (Qualitative Analysis B6 2012). Additional software was used for heuristic filtering of the obtained molecular formulas (Kind and Fiehn 2007). Commercial standards including oregonin (Sigma-Aldrich, CAS #55303-93-0) and curcumin (Sigma-Aldrich, CAS #458-37-7) were used to aid in characterization. We recorded base peak chromatogram (BPC) abundance for each peak, standardized abundance as BPC per milligram of leaf material extracted to account for slight deviations from 100 mg of leaf powder extractions, and log transformed BPC data to consider relative compound abundances. Samples from all forty trees were run on the machine in a randomized order to control for any potential deviations over time in mass spectrometer performance.

Diet Field Experiment

In a second field experiment, we measured potential responses to individual variation in leaf chemistry by offering to decomposers extracted leaf compounds in an agar matrix. We completed these experiments using the same river pairings as in previous reciprocal transplant experiments (see Appendix 5C for an illustration of the experiment). We collected leaves from the 40 alder trees in June, 2013 and used the same protocol for extracting secondary metabolites as described for mass spectrometry analyses. We allowed the methanol fractions to evaporate and then re-suspended the remaining residue in 10 mL of water. We prepared a general purpose Lepidoptera diet (BioServe, Product #F9772) according to package instructions except for doubling the gelling agent to avoid disintegration of the diet underwater (10.5% supplied agar, 10.5% agarose (Sigma-Aldrich) and 79% dry diet). We chose this proportion of agar, agarose, diet, and water because we found this formula resulted in no visible fragmentation or substantial mass loss after submerging in tap water for seven days. We added 10 g of prepared diet into glass vials, warmed the vials to melt, added 3.3 mL of tree-specific extract, and mixed thoroughly. We immediately loaded liquid diets using 10 cc syringes into randomly selected well locations in 96-well microplates in batches of four plates (e.g. one plate for each of four sites in the Pysht and Little Hoko Rivers). Each of these plates contained 20 different types of diets, one for each of the 20 trees growing along one set of the paired rivers.

For aquatic plates, we surrounded diet options by empty wells and used the middle of each plate to avoid edge effects. We repeated the experiment twice for a total of 16 plates across four rivers. We recorded starting mass of each well filled with diet by taring the balance between diet additions. We placed each plate in bags made of 4.75 mm mesh nylon seine netting fixed across the plate surface with mini-binder clips. This arrangement permitted feeding while proving a gripping surface for macroinvertebrates, and enabled attachment to the stream bed via cable ties attached to steel reinforcing bars pounded into the stream bed (Appendix 5C). We secured plates to the stream bed immediately downstream of the five study trees at each deployment site along the four rivers. We retrieved plates after 2–6 days, depending on general feeding rate, with the goal of removing plates once $\approx$ 50% of the diet had been consumed. We weighed each well of diet to the nearest centigram and calculated percent mass lost. We observed caddisflies, which are known to consume alder litter, actively feeding on the diets. However, we note that in situ feeding experiments cannot preclude other consumers that may not typically feed on intact leaf litter (such as algivores). Any mass loss due to algivore feeding or abiotic processes was controlled by our randomized intermixing of home and away diets that minimized any systematic differences in biotic and abiotic conditions affecting each group.

In riparian soil, instead of duplicate rounds, we assigned each specific diet to two well locations per plate, filling the top four rows of cells. We filled each well to the rim, but did not measure starting weights. The average starting weight for each individual well of diet from the 16 aquatic plates (μ = 0.420 g ± 0.0089 SD) was substituted as the approximate starting weight of each well of diet for the soil plates. We placed plates in mesh bags, secured with mini-binder clips, and buried the plates beneath 10-15 cm of soil under the most downstream tree at each deployment site along the Pysht and Little Hoko rivers. We did not complete the experiment in the Sekiu and Hoko rivers. Plates were retrieved after 29 days, washed gently to dislodge soil, weighed to the nearest centigram, and percent mass loss for each well was calculated. Replicate measures were incorporated into a nested random term of analysis of variance models, as described in detail below.

Statistical Analyses

We describe variation in 35 chemical compounds among 40 trees using a principal component analysis. Principal components were extracted using singular value decomposition of the correlation matrix to weight common and less common compounds equally (prcomp function, R Development Core Team, 2014). We tested whether ellagitannin content (via PC1 scores), diarylheptanoid content (via PC2 scores), and flavonoid content (via PC3 scores) were predicted by measured tree traits (including leaf % C, % N, % P, leaf thickness, and trunk diameter) using linear regression (Table 5.B.4). We tested what traits (including leaf % C, % N, % P, leaf thickness, trunk diameter, and scores for PC1, 2 and 3) best predicted decomposition rates in rivers using linear mixed-effects models with individual tree as the random effect. In addition to using PC scores as metrics of secondary metabolites, we also tested which specific compounds (either within the class of ellagitannins, or within diarylheptanoids) best predicted decomposition rates in rivers using linear mixed-effects models. We selected best fitting models by comparing AIC scores and for mixed-effect models report marginal R^2 values to describe variance explained by the fixed factors (Nakagawa and Schielzeth 2013). We tested whether differences in chemical classes (quantified as differences in scores along each principal component) among trees corresponded to geographic distance among trees using a Mantel test. Because ellagitannins can be quite complex in molecular structure (Karonen et al. 2010) and vary six-fold in their oxidative capacity, we estimated oxidative function of each ellagitannin using the following formula (Barbehenn et al. 2006, Moilanen and Salminen 2008):

$$OA = (15.5A + 6.6B + 4.9C + 4.5D + 3.6E + 1.9F + 1.1G) / W,$$

where A = number of valoneoyl groups, B = number of nonahydroxytriphenoyl groups, C = number of valoneoyl or sanguirsorboyl groups, D = number of xylose/lyxose groups, E = number of acyclic castalagin-type glucoses, F = number of hexahydroxydiphenoyl groups, and G = number acyclic vescalagin-type glucoses, and W is the molecular weight of the ellagitannin (g/mol). We then used these calculations to ask whether the ellagitannins selected by our model as the strongest predictors of decomposition in rivers also had relatively strong oxidative function.

For the diet experiments, we tested whether diets prepared from alder leaves sourced from different relative locations decomposed at different rates using a five group ANOVA. The diets were prepared from trees either growing 1. At the home site on the home river 2. Upstream on the home river 3. Downstream on the home river 4. Upstream on the away river 5. Or downstream on the away river. Our two fixed factors were this home/away variable and tree identity, and our two random factors were deployment location and a nested term of plate replicate nested within tree identity and deployment location. Because we had hypotheses based on prior results from reciprocal transplant leaf pack experiments in streams (Jackrel and Wootton 2014), we used our a-priori ordered predictions to calculate a directional five-group ANOVA using Spearman rank correlations (Rice and Gaines 1994). For the riparian soil data, we used a three-group ANOVA (home site, away site on the home river, or away river) because we did not have an a-priori expectation that upstream versus downstream sites on the home river would yield different results in a terrestrial system.

To test whether alder trees growing in geographic proximity were more similar in chemical composition than distant neighbors, we constructed a chromatogram distance matrix among trees (with elements S_{ij}) by calculating pairwise Euclidean distances between tree pairs:

$$S_{ij} = \sqrt{\sum_{k=1}^{35} (C_{ik} - C_{jk})^2}$$

where C_{ij} is the log BPC of chemical compound k in tree i. We log transformed data because relative ratios of chemical compounds are often essential for conferring information (Christensen et al. 1989). We tested whether this chromatogram distance matrix was significantly correlated with a geographic distance matrix (using GPS coordinates for each tree) using a Mantel test. We determined whether a model including chromatogram data alone could predict tree growing location in nature with a discriminant function analysis (DFA) (SPSS IBM Corp. 2013). Using the DFA, we identify which chemical compounds differ most among riparian sites. To maximize statistical power and identify a more parsimonious model, we entered all 35 chemical compounds into the model and iteratively removed variables one-by-one by selecting the variable with the smallest standardized coefficient on DF1 until any additional removal reduced cross-validation reclassification accuracy. We report these results with and without leave-one-out cross-validation because our experimental design required an unusually large removal (20%) of the original data set (1 of the 5 trees per riparian site).

RESULTS

Each red alder tree contained a mixture of 35 compounds that were eluted within the first 45 minutes of each chromatography column run (Fig 5.1). We characterized 13 ellagitannins (Fig 5.A.1), 3 flavonoids, and 10 diarylheptanoids (Fig 5.A.2) (Table 5.A.1 provides references for each characterization). Ellagitannin elution order has been clearly modeled (Moilanen et al. 2013), which facilitates mass spectrometry characterization. We characterized each compound, molecular mass and formulae of parent molecules, fragmentation patterns, and corresponding peak numbers, as illustrated (Fig 5.1). The ellagitannin di-HHDP-glucose (consistent with pedunculagin α), diarylheptanoid oregonin, and flavonoid quercetin glucuronide were generally observed at the highest levels in each tree chromatogram (Table 5.A.1). We found two potentially novel diarylheptanoids with mass spectra not yet reported in the literature, and though definitive identification will require future investigations via NMR, both contain glucose rather than xylose and elute prior to previously studied compounds, as expected given the increased polarity of the glucoside (Table 5.A.1, Fig 5.A.2).

Principal components analysis independently separated the chemical signatures of individual trees primarily along the three compound families (ellagitannins, diarylheptanoids, and flavonoids, Table 5.D.1, Fig 5.2). The first axis is loaded most strongly by nine ellagitannins, the second axis is loaded with eight diarylheptanoids, and the third axis contains the three flavonoids (Table 5.D.1). Trees varied considerably in secondary metabolite composition: some ellagitannin relative abundances varied over twelve-fold (#15 di-HHDP-galloyl-glucose β, consistent with casuarictin) and some diarylheptanoids varied over three hundred-fold (#23

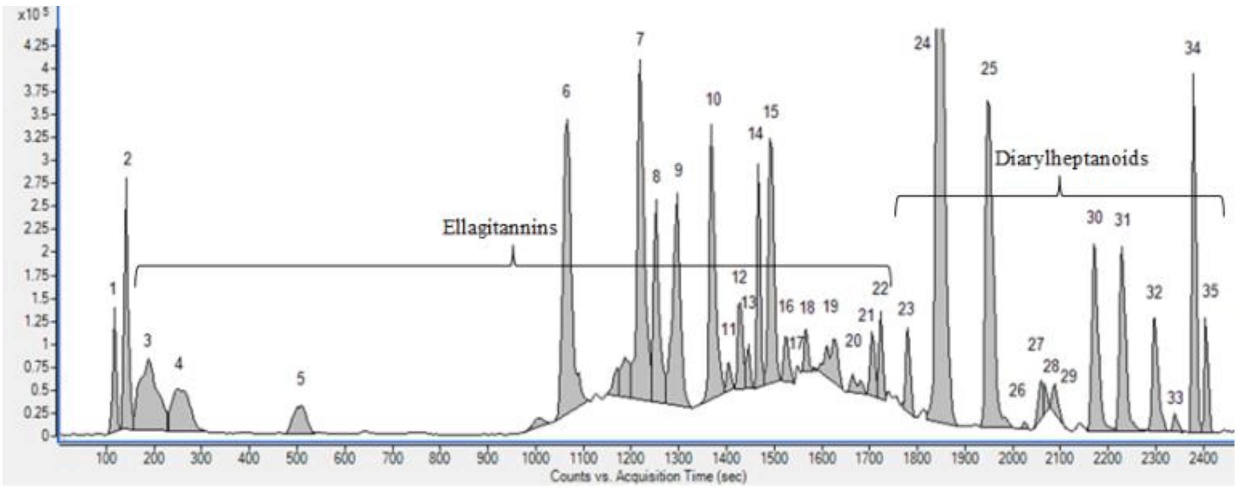

Figure 5.1: Example chromatogram from a red alder tree growing in the riparian zone of the Pysht River (ELK 4). Gray shading indicates the area of each peak after baseline correction. Note peak 24 (oregonin) is cutoff to provide a better view of less relatively abundant compounds.

HOG). We then asked if this variation in defensive compounds corresponded with ecologically important traits, most of which showed substantial variation within the population: % N content ranged two-fold (mean 2.89 ± 0.42% SD), % P content ranged three-fold (0.16 ± 0.047%), leaf thickness ranged four-fold (0.007 ± 0.002 g/unit^2), tree diameter ranged forty-six fold (55.8 ± 24.1 cm), and $^{15}N/^{14}N$ ranged three-fold (-1.48 ± 0.27 ‰), whereas $^{13}C/^{12}C$ was fairly constant (-32.00 ± 0.97 ‰). Stepwise regression showed that trees with leaves containing a high relative abundance of ellagitannins, as measured by PC 1, tended to contain less nitrogen and relatively less phosphorus (i.e. elevated N:P) ($F_{2,37} = 13.84$, $p < 0.001$, Table 5.B.1, Table 5.D.1, Fig 5.3a). Trees with leaves containing high relative abundances of diarylheptanoids, as measured by PC 2, tended to have thinner leaves, reduced C:P and elevated C:N and N:P than leaves lower in diarylheptanoids ($F_{4,35} = 10.42$, $p < 0.001$, Table 5.D.1, Table 5.B.2). Leaf flavonoids (PC 3) exhibited a weak inverse correlation with $^{15}N/^{14}N$ (Table 5.B.2).

We then found that leaf decomposition in streams is best predicted by both chemistry and mechanical traits. Based on our leaf pack experiments across four rivers, ellagitannin content (as represented by PC1) and leaf thickness were the best predictors of leaf decomposition rate in streams (marginal $R^2 = 0.48$, n = 148 leaf packs, Table 5.B.4), exceeding all other measured variables including all of our nutrient variables, tree diameter, diarylheptanoid content (as represented by PC2), and flavonoid content (as represented by PC3). Ellagitannin content alone explained 18% of the variance in decomposition rate (Fig 5.3b), and we found that disparity among pairs of red alder trees along this ellagitannin axis (via pairwise distances between PC1 scores) corresponded with geographic distance between them (Mantel test, $p = 0.014$). Among the thirteen compounds largely contributing to that ellagitannin axis of PC1 (Table 5.D.1), HHDP-galloyl-glucose (consistent with isostrictinin) and di-HHDP-galloyl-glucose β (consistent

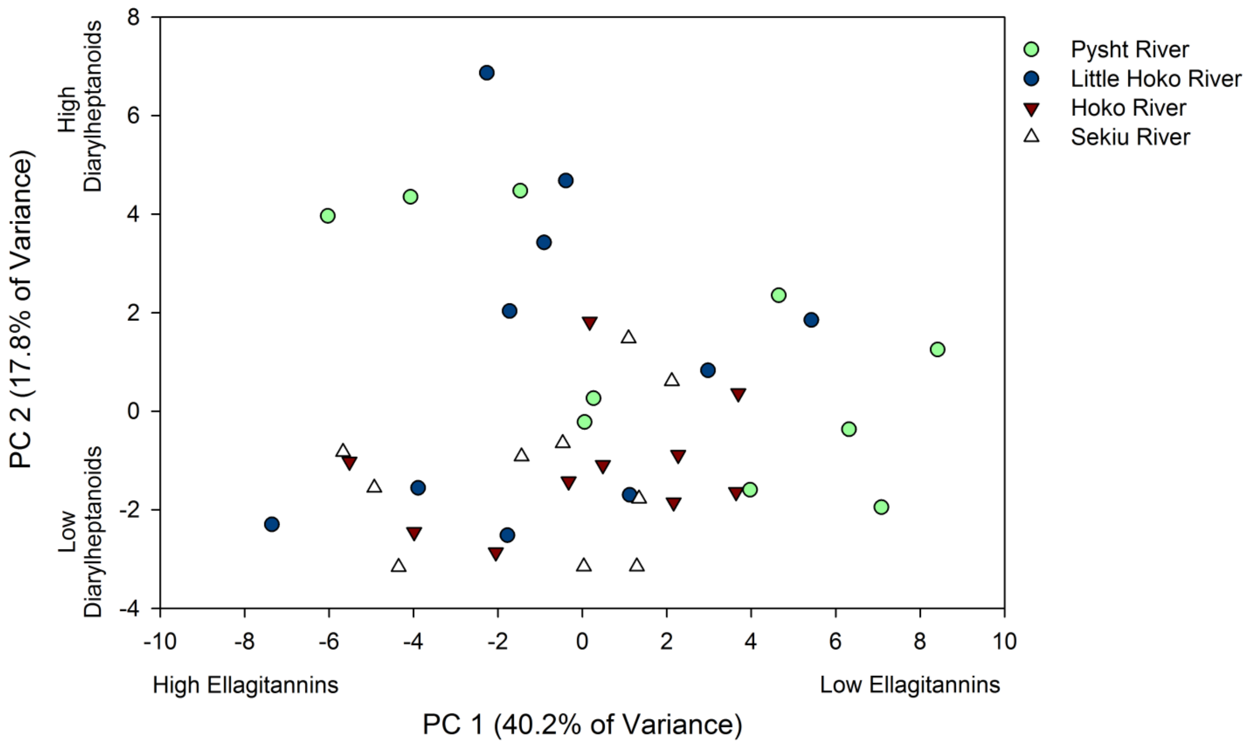

Figure 5.2: Individual red alder trees growing in the riparian zones of four rivers vary in leaf chemistry along a largely ellagitannin axis and of secondary importance, a diarylheptanoid axis via a principle component analysis. The analysis includes 35 variables, one for the size of each of the 35 peaks as shown in Figure 1. See Table 5.D.1 for PC loadings.

with casuarictin) appeared to be the strongest inhibitors of aquatic decomposition (linear mixed-effects model: marginal R^2 = 0.30, HHDP-galloyl-glucose, t_{37} = 3.0, p = 0.0048, di-HHDP-galloyl-glucose β, t_{37} = -4.7, p < 0.001). When we used molecular structure to calculate approximate oxidation rate for ellagitannins we characterized in red alder, these two compounds had among the highest oxidation rates (4.1 and 4.9 abs/s/mM, Table 5.A.1).

Relative abundance of several diarylheptanoids also predicted substantial variation in aquatic decomposition rate (linear mixed-effects model: marginal R^2 = 0.155, methylhirsutanonol t_{35} = 2.11, p = 0.043, oregonin t_{35} = -1.73, p = 0.093, platyphylanolanol-xyloside t_{35} = -2.10, p = 0.043, alnuside A t_{35} = 1.77, p = 0.086). Additionally, these compounds were fairly variable in the population (mean relative abundance ± 1 SD of each compound is reported in Table 5.A.1), but unlike ellagitannins, this variation did not correspond with the scale of geographic distances our study explored: pairwise distances between PC2 scores were not correlated with geographic distance between red alder trees (Mantel test, p = 0.15).

We constructed a chromatogram distance matrix to consider the relative abundances of all 35 chemical compounds, and we again found that red alder trees growing in geographic proximity shared more similar secondary metabolite chemistry than more distant neighbors (Mantel test, p = 0.0035). Entering all 35 compounds in a discriminant function, across the eight riparian sites (Wilk's λ < 0.001, χ_{189}^2 = 288.9, p < 0.0001), illustrates the strong effects of geography on the chemical profiles of these trees. The first discriminant function accounted for 93.9% of the variation and was such a strong predictor of geographic location that 100% of the 40 trees were classified to the correct site on the correct river (compared to 12.5% correct classification by chance) (Fig 5.4). Even when removing 20% of the original data to enable

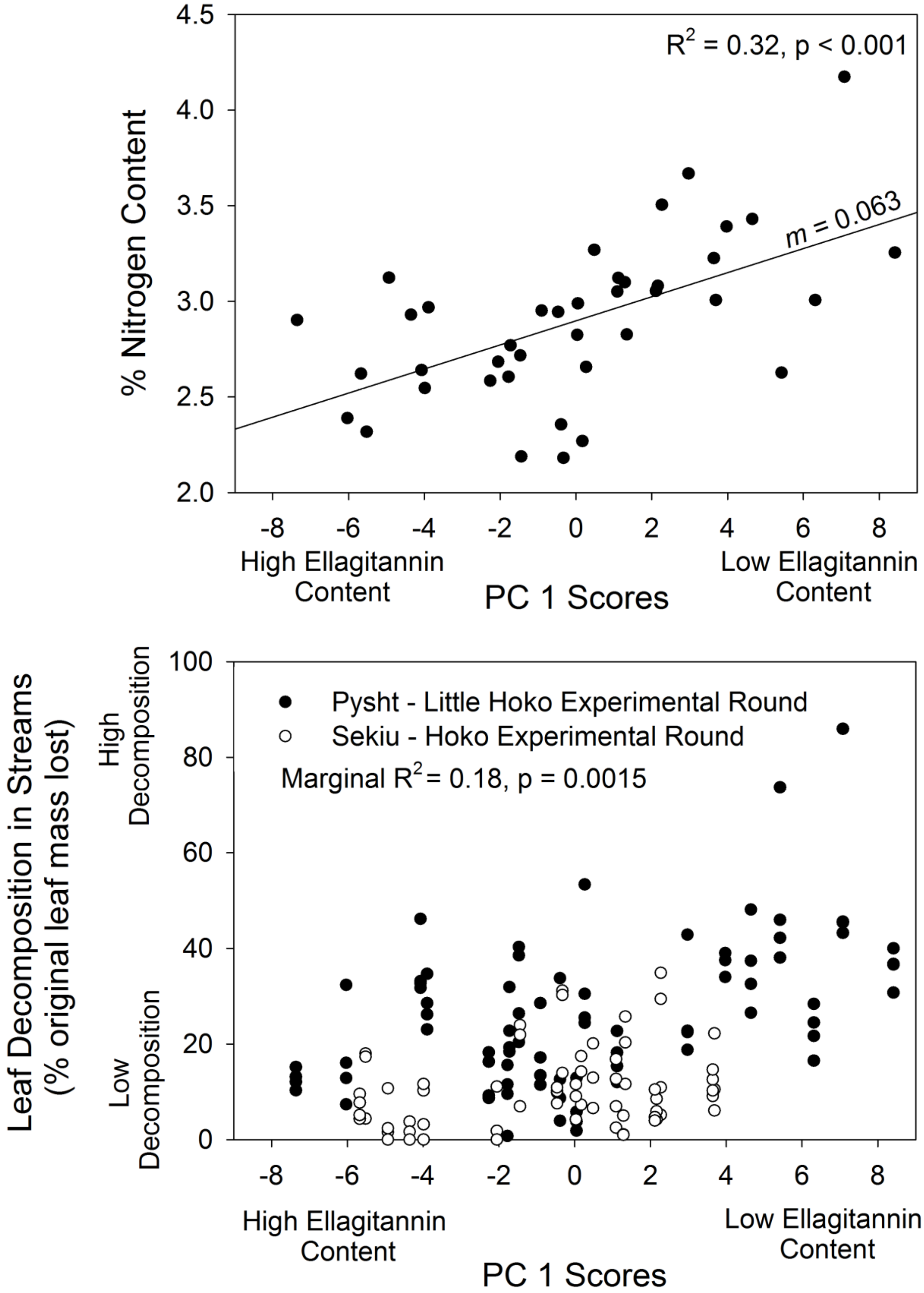

Figure 5.3: Variation in ellagitannins (as shown by PC 1 of Table S4) predicts (*a*) % Nitrogen content of leaves from individual red alder trees and (*b*) aquatic decomposition rate of leaves in streams.

cross-validation, reclassification was correct in 45% of the trees, which is 3.5-fold more trees than expected by chance. The first discriminant function is a complex compilation of twenty-seven compounds (Table 5.E.1), including at least thirteen ellagitannins, which as we showed above are generally strong predictors of aquatic decomposition.

We found that this spatial structuring of ellagitannins, diarylheptanoids and flavonoids in riparian trees drove local decomposer responses both in the terrestrial and riparian environment. To separate chemistry from structural leaf properties, we prepared 40 diets containing tree extracts (prepared in the same way as extracts loaded onto the mass spectrometer) for *in situ* feeding experiments. We found aquatic communities consumed diets prepared with local red alder extracts 24.7% more than diets prepared with red alder growing along a different river. We also found this same pattern of local matching at the within-river scale. Our *a priori* prediction was that communities are most efficient at consuming chemical components that are present in leaves supplied to that particular location. Due to our experimental design, our away sites on the home river represent one of two scenarios: at downstream sites, leaves from the upstream site wash downstream and represent a natural food resource, but at upstream sites, leaves from the downstream sites wash further downstream and represent a novel food resource. In the first scenario, we found that aquatic communities consumed 11.2% less diet prepared from alder trees growing at an upstream site on the same river compared to trees growing at that deployment site, but in the second scenario, aquatic communities consumed 19.9% less diet prepared from alder trees growing at a downstream site on the same river (Fig 5.5a, Table 5.1, $p < 0.025$, ordered heterogeneity test). This result emphasizes that regular exposure, rather than distance alone, appears to contribute to local adaptation. We regularly observed *Psychoglypha* and *Dicosmoecus* caddisflies feeding on aquatic plates and assume them to be important consumers.

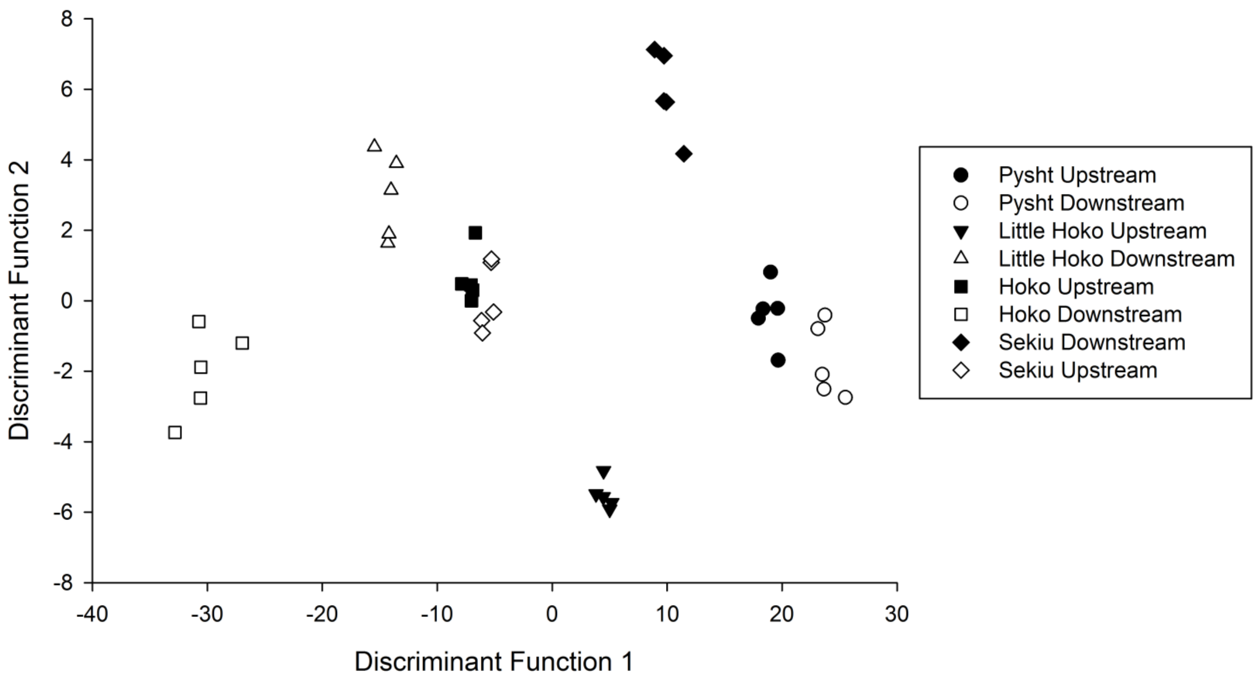

Figure 5.4: Secondary metabolite composition of 40 riparian alder trees groups trees into actual growing locations in nature via discriminant function analysis.

We found a similar pattern of local adaptation in riparian soils: the soil community consumed diets prepared from local red alder diets 11.3% more than diets prepared from red alder growing elsewhere along the same river, and 25.4% more than diets prepared from red alder growing next to different rivers (Fig 5.5b, $p < 0.025$, ordered heterogeneity test).

DISCUSSION

Variation in food resource quality affects consumer movement patterns, metamorphic and reproductive decisions, and plastic and genetic changes in physiology (Hunter and McNeil 1997, Awmack and Leather 2002). We show that variation within species in one ecosystem can alter key processes in another ecosystem through fluxes across boundaries. By pairing mass spectrometry data with reciprocal transplant experiments in the field, we show that intraspecific variation in plant chemistry drives an ecosystem function in streams and causes local terrestrial and aquatic communities to adjust to local leaf chemistry. Geographic variation among complex mixtures of secondary metabolites, notably ellagitannins, seems to drive these local matching patterns, which are evident at large (across-river) and small (within-river) scales. Within rivers, diets containing secondary metabolite extracts from upstream trees decompose quickly at downstream locations relative to diets from downstream trees at upstream locations, further suggesting that it is the exposure to leaves from local trees that is driving this process among aquatic decomposer communities. These results demonstrate that terrestrial processes shaping the chemical composition of ecosystem subsidies from donor habitats drives locally adaptive changes in recipient communities.

Red alder trees were highly variable in two classes of secondary metabolites: ellagitannins and diarylheptanoids. Both classes of compounds have only just begun to receive ecological consideration (Salminen and Karonen 2011), primarily for technical reasons. We

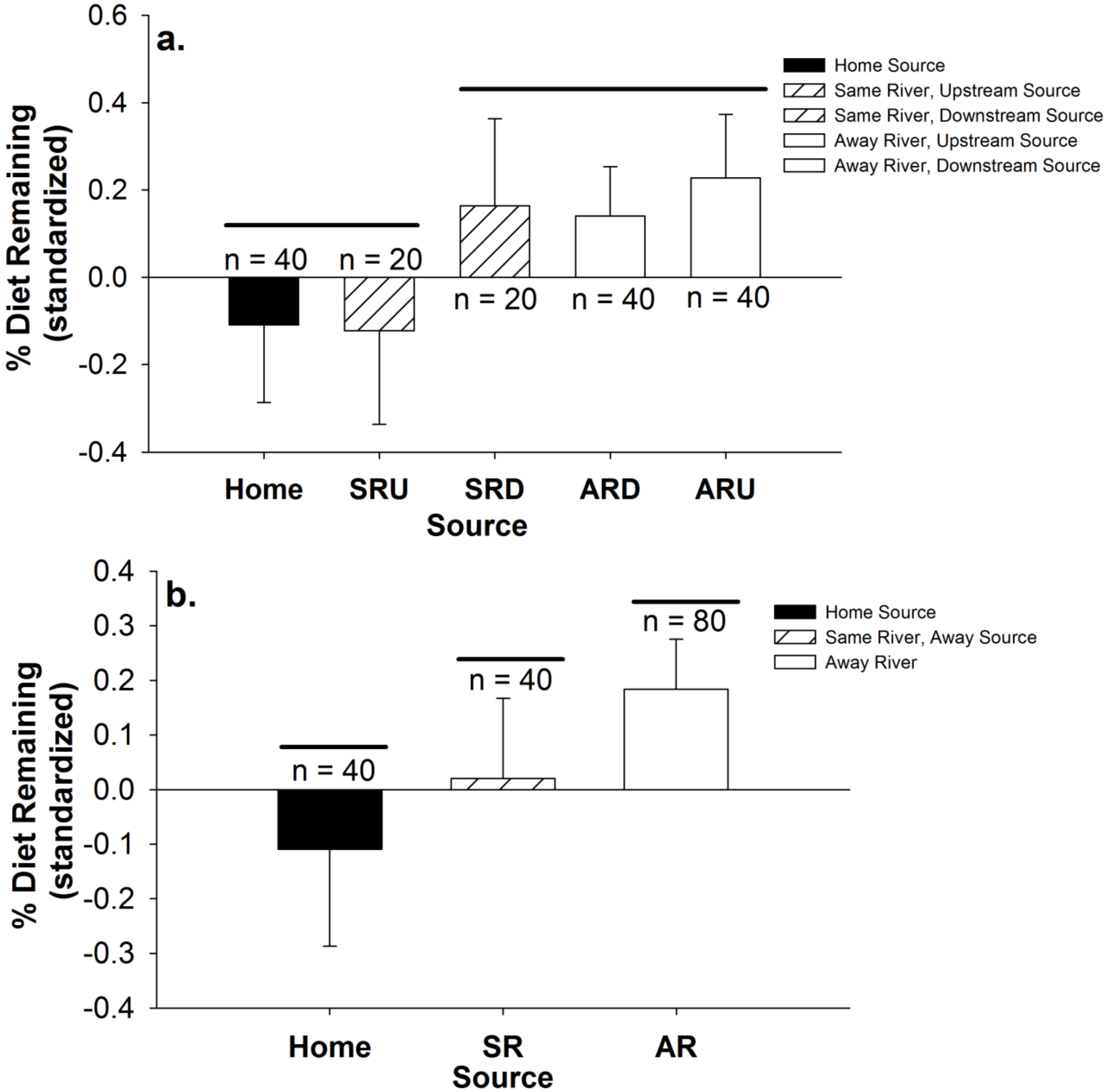

Figure 5.5: Average decomposition (± SE) in (*a*) streams and (*b*) soils of forty commercial diets prepared containing added leaf extracts from individual red alder trees.

show how frequent drivers of consumer population ecology, such as leaf nutrients and thickness, are correlated with these secondary metabolites. Further, we show that ellagitannin variation plays a key role in affecting rates of decomposition in streams. To estimate tannin content, studies have used functional metrics to measure important anti-herbivory properties, such as protein-precipitation capacity. Condensed tannin content correlates well with this measurement, but ellagitannins are poor protein precipitators and are consequently underestimated in these assays, and more generally have been underestimated in their ecological importance. Ellagitannins, however, are strong oxidants, a chemical property associated with increased metabolic costs in alkaline guts of herbivores, such as those of terrestrial lepidopterans and aquatic Chironomidae and Tipulidae insects (Clark 1999, Barbehenn et al. 2009, Salminen and Karonen 2011). Our finding that aquatic decomposition was best estimated by relative abundances of ellagitannins with relatively high oxidative measures, suggests that oxidative function may be important in aquatic systems. Therefore, we need additional studies that consider the role of ellagitannins in plant defense, insect metabolism, and decomposition by microbes and hyphomycetes.

Diarylheptanoids are found in substantial diversity in alder species (Sati et al. 2011), including at least six in the bark of red alder (González-Laredo et al. 1998, Chen et al. 2000). Our results show they are present in leaves, and are thus of relevance to folivores. Ecological studies on diarylheptanoids are limited, but biomedical research (Farrand et al. 2014) and traditional medicine records (McCutcheon et al. 1994) have noted anti-microbial and anti-oxidant properties, suggesting these compounds likely play substantial ecological roles. Interestingly, given their noted toxicity, we found that several diarylheptanoids appear to inhibit

Table 5.1: Analysis of variance comparing aquatic decomposition rates of diets containing red alder leaf extracts from individual riparian trees that were each deployed at four sites: the home site immediately downstream of the focal tree, the same river at a different site either upstream or downstream of the focal tree, and at two sites on a different river.

Source	Df	SS	MS	*F*	P**
Leaf Source	4	0.056	0.014	1.371	
Home river vs. away river	1	0.032	0.032	3.171	< 0.025
Local vs. non-local*	1	0.051	0.051	5.100	< 0.025
Tree Identity	38	0.539	0.014	1.382	
Error	160	6.99	0.044		

Notes: Indented lines are planned a-priori comparisons. * Local indicates diets made using extracts from red alder trees growing at the deployment site (Home in Fig 5a) or a same river site upstream (SRU in Fig 5a). Non-local indicates diets were made using extracts from trees growing downstream of the deployment site, or a different river entirely (indicated SRD, ARD, ARU in Fig5a). **Reported p-values include a-prior ordered heterogeneity corrections (Rice and Gaines, 1994).

decomposition. However, given their limited geographic variation at the scales we studied, they seem unlikely to explain the local adaptation patterns of decomposition in this system.

In our previous work, we have shown that induced plant defense to herbivory stress suppressed detrital energy capture in streams (Jackrel and Wootton 2015a). We found that red alder trees given an herbivory stress showed a marked decline in leaf nitrogen content, and thus aquatic decomposers preference for nitrogen-rich leaves seemed to be driving the observed effect on aquatic ecosystem function. Here, in a non-experimental setting, we found that ellagitannins are a stronger predictor of aquatic decomposition than % N (Table 5.B.4), but there is a negative correlation between ellagitannin and nitrogen content ($r^2 = 0.32$). Soil nitrogen additions are not known to effect ellagitannin content (estimated as ellagic acid equivalents) in non-nitrogen fixing trees including poplar, maple and oak (Kinney et al. 1997), but condensed tannins from poplar can inhibit nitrogen fixation in thinleaf alder (Schimel et al. 1998). Further study may clarify the interactive effects among induced defense responses to herbivory, ellagitannin production, and nitrogen fixation and allocation.

We found ellagitannin, diarylheptanoid and flavonoid variation were all correlated with leaf traits, such as thickness and nutrients that are well-known to affect consumers (Coley 1980, Mattson 1980a, Jackrel and Wootton 2015a). But our results from both leaf pack and diet experiments suggest ellagitannin content is a greater predictor of ecosystem processes than nutrients (Table 5.B.4), and therefore warrants further study into plant production pathways of these compounds and the ecological implications of relative nutrient vs. defense compound content in red alder and other plants.

The importance of intraspecific diversity has only recently been recognized in a community ecology context (Violle et al. 2012). We show that spatially variable factors such as genetics, environmental resources, or ecological interactions caused tree conspecifics growing a distance apart to produce more divergent leaf chemistry traits than nearby neighbors. Different genetic constraints may lead to variation in chemistry under similar environmental pressures, as in the genetically controlled variation of condensed tannins in cottonwoods (Schweitzer et al. 2004). Alternatively, divergent chemistry could be caused by environmental gradients in soil nutrients or variation in plant-insect interactions due to spatial changes in terrestrial herbivore composition or densities (Bryant et al. 1987b, Lankau 2007). Determining the relative contributions of and interaction between genetic and environmental factors in spatial variation of plant subsidies is an important future direction for predicting how natural and anthropogenic changes to the terrestrial environment will affect stream systems.

To predict the extent of such interactions in nature, we need to investigate the evolutionary development of these complex cross-ecosystem interactions. To do this, we need to understand the mechanisms of aquatic and terrestrial decomposers matching to these local subsidies. Accelerated decomposition efficiency may be arising from shifts in community composition (such as shifting aquatic invertebrates along gradients in stream size, (Vannote et al. 1980)) or phenotypically plastic or genetic shifts in individuals. Comparing stream and riparian decomposer communities in this system provides an ideal opportunity to compare evolutionary trajectories to local adaptation in the presence and absence of feedback interactions of decomposition processes on host trees. These insights may suggest the time-scale needed for these processes to occur, and therefore their potential generality in other ecosystems.

ACKNOWLEDGMENTS

We thank J. Bergelson, G. Dwyer, C.A. Pfister and T.D. Price for constructive comments and discussion on this work. This work was supported by the NSF GRFP, the DOE GAANN, NSF DDIG DEB-1311293, ARCS® (Achievement Rewards for College Scientists) Foundation, Inc.'s Scholar Illinois Chapter [2014 and 2015], and University of Chicago Hinds Fund grants to SLJ; an Olympic Natural Resources Grant and NSF grant DEB 09-19420 to JTW; and NSF grant OCE-0928232 to C.A. Pfister. We thank A. Colman, A. Mine, G. Olack and the Colman Isotope Lab at University of Chicago for assistance with nitrogen, carbon and phosphorus analyses. We thank Merrill & Ring Inc., J. Murray, M. Hurd, D. Hurd, Hoko River State Park, and the Washington State Department of Natural Resources for providing facilities and facilitating research on their lands.

Appendix 5A: Summary of chemical characterizations and structure drawings for thirty-five secondary metabolites.

Figure 5.A.1: Structures of ellagitannins with five side chains, R1 - R5, including a hydrogen atom (H), galloyl group (G) or hexahydroxydiphenoyl (HHDP) attached to the core glucose molecule. Side chain assignments are the most probable, but not definitive, positions.

HHDP

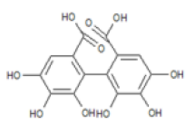

G (galloyl)

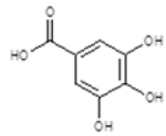

Glucose

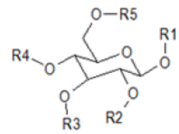

Peak	Compound	R1	R2	R3	R4	R5	Notes
3	HHDP-glucose	H	HHDP		H	H	
4	HHDP-glucose	H	H	H	HHDP		
5	galloyl-glucose						Multiple possible locations of galloyl
6	di-HHDP-glucose	H	HHDP		HHDP		Consistent with Pedunculagin β hydroxy
7	di-HHDP-glucose	H	HHDP		HHDP		Consistent with Pedunculagin α hydroxy
8	HHDP-galloyl-glucose	G	HHDP		H	H	Consistent with Isostrictinin
9	di-galloyl-HHDP-glucose	H	G	G	HHDP		Consistent with Tellimagrandin I β hydroxy
10	HHDP-galloyl-glucose	G	H	H	HHDP		Consistent with Corilagin
12	di-galloyl-HHDP-glucose	H	G	G	HHDP		Consistent with Tellimagrandin I α hydroxy
15	di-HHDP-galloyl-glucose	G	HHDP		HHDP		Consistent with Casuarictin
16	di-HHDP-galloyl-glucose	G	HHDP		HHDP		
18	tri-O-galloyl-HHDP-glucose	G	HHDP		G	G	Possibly β galloyl
22	tri-O-galloyl-HHDP-glucose	G	G	G	HHDP		Possibly α galloyl

Figure 5.A.2: Structures of diarylheptanoids with three side chains, R1-R3, including a hydrogen atom (H), hydroxyl group (OH) or other side chains attached to the core molecule.

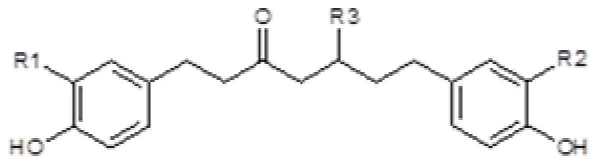

Peak	Compound	R1	R2	R3
23	Hirstunanonol-glycoside	OH	OH	O-β-D-glucopyranoside
24	Oregonin	OH	OH	O-β-D-xyloside
24	Related to Alnuside A	H	OH	O-β-D-glucoside
26	Alnuside A	H	OH	O-β-D-xyloside
27	Alnuside B	OH	H	O-β-D-xyloside
30	Methylhirsutanonol	OH	OH	O-CH3
31	Platyphylanonol-xyloside	H	H	O-β-D-xyloside
32	Hirsutanone	OH	OH	H
34	Related to Alnuside C	OH	OH	O-2-butenoyl-β-D-glucopyranoside
35	Alnuside C	OH	OH	O-2-butenoyl-β-D-xylopyranoside

Table 5.A.1: Compound characterizations (including tentative identifications where possible), retention time, exact mass, diagnostic ions, metabolomics confidence score, references, and mean fraction (± 1 SD) base peak chromatogram ion counts per milligram of red alder leaves of thirty-five secondary metabolites found in a population of forty trees in NW Washington.

Peak	RT (secs)	TIC % Area	M-H (%)	Exact Mass	Diff (ppm)	Diagnostic ions/TIC% first	second	third	fourth	Refs	Annotation Level[6]	Chemical ID, formula (MH-) and (oxidation activity abs/s/mM)
1	115	1.7 ± 1.2				122.92/100	206.88/50				4	
2	140	5.7 ± 2.6				191.05/100	267.15/20	405.09			4	
3	200	2.0 ± 1.5	481.0612 (25)	481.0624	-1.18	300.9976/100				1,2	3	HHDP-Glucose, $C_{20}H_{17}O_{14}$ (3)
4	270	1.2 ± 0.80	481.0632 (25)	481.0624	+0.82	300.9998/100				1,2	3	HHDP-Glucose, $C_{20}H_{17}O_{14}$ (3)
5	510	0.28 ± 0.21	331.0636 (100)	331.0612	-3.47	169.0119/60				1,2	3	galloyl glucose, $C_{13}H_{15}O_{10}$ (0)
6	1100	7.4 ± 3.3	783.0726 (80)	783.0668	+3.95	300.99/100	481.0658	301.0015	169.0147	1,2	3	di-HHDP-glucose, (Pedunculagin β), $C_{34}H_{23}O_{22}$ (5)
7	1190	9.8 ± 2.5	783.0699 (80)	783.0668	+1.25	300.99/100	481.0632	301	169.0147	1,2	3	di-HHDP-glucose (Pedunculagin α), $C_{34}H_{23}O_{22}$ (5)
8	1250	3.1 ± 0.61	633.0739 (25)	633.0733	+0.56	300.9908/100	275.01/20			1,2	3	HHDP-galloyl-glucose (Isostrictinin), $C_{27}H_{21}O_{18}$ (4.9)
9	1295	5.0 ± 0.73	785.0797 (80)	785.0843	-4.60	300.99/100	275.0213/25	829.07/10		1,2	3	di-galloyl-HHDP-glucose(Tellimagrandin Iβ),$C_{34}H_{25}O_{22}$ (3.3)
10	1370	4.8 ± 1.4	633.0726 (25)	633.0733	-0.74	300.9908/100	275.01/20			1,2	3	HHDP-galloyl-glucose (Corilagin), $C_{27}H_{21}O_{18}$ (3)
11	1401	1.4 ± 0.51	965.0825 (4)			124.0154/100	183.029/15	300.9998/13	783.0692		4	too small, but major galloyl in +
12	1427	3.7 ± 1.2	785.0882 (86)	785.0855	+3.90	300.9978/100	483.0692/2	481.0516/0.3	169.01285/12	1,2	3	di-galloyl-HHDP-glucose(Tellimagrandin Iα),$C_{34}H_{25}O_{22}$ (3.3)
13	1445	1.5 ± 0.31	965.0748 (2)			300.99/100	169.0136/35	483.0728/27	635.0744/3		4	
14	1467	2.0 ± 2.2				191.0529/100	375.0607/14	633.0561/1	729.1375/1		4	
15	1491	4.9 ± 0.94	935.0857 (57)	935.0737	-1.8	300.99/100	785.0676/2	633.0622/14	169.01/3	1,2	3	di-HHDP-galloyl-glucose β (Casuarictin), $C_{41}H_{27}O_{26}$ (4.1)
16	1525	1.7 ± 0.43	935.0789 (21)	935.0737	0.7	300.99/100	785.0723/2	633.0656/10	169.0128/4	1,2	3	di-HHDP-galloyl-glucose α, $C_{41}H_{27}O_{26}$ (4.1)
17	1550	1.3 ± 0.24				300.99/100	169.013/55	635.0781/8	465.0605/12		4	
18	1570	3.1 ± 1.3	937.0929 (39)	937.0952	-2.35	300.99/100	767.0562/2	465.0658/9	169.0141/20	1,2	3	tri-O-galloyl-HHDP-glucose (β?), $C_{41}H_{29}O_{26}$ (2)
19	1610	3.0 ± 1.0	1025.07 (2)			300.99/100	191/15	169/6			4	
20	1675	1.3 ± 0.52				300.99/100					4	
21	1705	1.7 ± 0.28	997.08 (4)			300.99/100	617.06/4	757.077/8	169.01/10		4	
22	1740	1.7 ± 0.64	937.0961 (17)	937.0952	+0.85	300.99/100	785.0707/2	465.0562/3	169.0152/12	1,2	3	tri-O-galloyl-HHDP-glucose (α?), $C_{41}H_{29}O_{26}$ (2)
23	1780	1.1 ± 0.89	507.1871 (17)	507.1872	-0.09	205.0874/100	327.1249/34	121.02/90		3	2	HOG*, $C_{25}H_{31}O_{11}$
24	1840	7.8 ± 3.4	477.1751 (45)	477.1766	-1.52	205.0874/60	121.02/100	327.1249/53		3	1	Oregonin**, $C_{24}H_{29}O_{10}$
	1915		491.1925 (4)	491.1922	+0.23	121.0284/100	311.12/41	205.083/56	189.087/38	3,4	2	Related to Alnuside A with glucose, $C_{25}H_{30}O_{10}$
25	1960	7.6 ± 2.5	477.0666 (55)	477.0675	-0.86	301.0273/100	150.9997/24	255.0212/4	178.9932/8	5	2	Quercitin-glucuronide, $C_{21}H_{17}O_{13}$
	1971		463.0899 (100)	463.0882	+1.70	271.0226/89	300.024/88	301.029/51	255.0267/35	5	2	Quercitin-glucoside, $C_{21}H_{19}O_{12}$
26	2025	0.25 ± 0.29	461.1858(2)	461.1817	+4.19	311.1322	121.0308/62	205.0901/18	189.0943/6	3	2	Alnuside A, $C_{24}H_{29}O_9$
27	2060	1.3 ± 0.65	461.1837 (2)	461.1817	+1.99	311.1309	121.0303/62	205.0887/18		3	2	Alnuside B, $C_{24}H_{29}O_9$
28	2090	1.3 ± 0.65	483.012 (15)			300.99	299.9957/13				4	
29	2170	5.7 ± 2.0	447.0964 (100)	447.0933	+3.12	301.0372/61	178.9975/3	151.0024/3	283.0394/6	5	2	Quercitin-rhamnoside, $C_{21}H_{19}O_{11}$
30	2230	1.5 ± 0.98	359.1517 (1)	359.1500	+1.69	121.028/100	205.08/3	327.116/2		3	2	Methylhirsutanonol, $C_{20}H_{23}O_6$
31	2250	0.63 ± 1.1	445.1866 (1)	445.1868	-0.19	295.1349/100	189.0928/45	121.0297/10	169.0136/1	3	2	platyphylanolanol-xyloside, $C_{24}H_{30}O_8$
32	2298	1.0 ± 0.68	327.1232 (13)	327.1238	-0.60	121.031/100	205.0896/8	109.028/11		3	2	Hirsutanone, $C_{19}H_{19}O_5$
33	2310	0.26 ± 0.18	485 (0)			255.026/100	227.03/66	121.027/11	327.127/6		4	
34	2380	2.7 ± 2.0	591.2442 (4)	591.2447	-0.50	205.086/100	327.1282/44	121.02/34		4	3	novel diarylheptanoid***, $C_{30}H_{39}O_{12}$
35	2405	0.45 ± 0.62	561.2274(7)	561.2341	-1.44	205.0897/100	121/48	327.1274/32	109.029/9	4	2	Alnuside C, $C_{29}H_{37}O_{11}$

References: 1: (Moilanen et al. 2013), 2: (Gu et al. 2013), 3: (Novakavic et al. 2014), 4: (Lv and Shea 2010), 5. (Falcao et al. 2012) 6. (Sumner et al. 2007)

*HOG: 1,7-bis(3,4-dihydroxyphenyl)-5-β-D-xylopyranosyl-3-heptanone

**Oregonin: 1,7-bis(3,4-dihydroxyphenyl)-5-β-D-glycopyranosyl-3-heptanone

*** Novel diarylheptanoid: 1,7-bis-(3,4-dihydroxy-phenyl)-5-hydroxy-3-heptanone-5-0-[2-(2-methylbutenoyl)]-β-D-glucopyranoside

References

Moilanen J, Sinkkonen J, Salminen J-P. Characterization of bioactive plant ellagitannins by chromatographic, spectroscopic and mass spectrometric methods. Chemoecology. 2013;23(3): 165-79.

Gu D, Yang Y, Bakri M, Chen Q, Xin X, Aisa HA. A LC/QTOF–MS/MS application to investigate chemical compositions in a fraction with protein tyrosine phosphatase 1B inhibitory activity from *Rosa rugosa* flowers. Phytochemical Analysis. 2013;24(6): 661-70.

Novaković M, Pešić M, Trifunović S, Vučković I, Todorović N, Podolski-Renić A, et al. Diarylheptanoids from the bark of black alder inhibit the growth of sensitive and multi-drug resistant non-small cell lung carcinoma cells. Phytochemistry. 2014;97: 46-54.

Lv H, She G. Naturally occurring diarylheptanoids. Natural Product Communications. 2010;5(10): 1687-708.

Falcão SI, Vale N, Gomes P, Domingues MRM, Freire C, Cardoso SM, et al. Phenolic profiling of Portuguese propolis by LC–MS spectrometry: Uncommon propolis rich in flavonoid glycosides. Phytochemical Analysis. 2013;24(4): 309-18.

Sumner L, Amberg A, Barrett D, Beale M, Beger R, Daykin C, et al. Proposed minimum reporting standards for chemical analysis. Metabolomics. 2007;3(3): 211-21.

Appendix 5B: Leaf traits correlated with ellagitannin, diarylheptanoid and flavonoid content.

Table 5.B.1: Standardized coefficients from type III linear regression ($F_{2,37} = 13.84$, $p < 0.001$), showing the association of various leaf traits on Principal Component 1 (i.e. ellagitannin content, but see Table 5.D.1). Variables excluded from the model were tree diameter, leaf thickness, %C, %P, C:N, C:P, $^{15}N/^{14}N$, and $^{13}C/^{12}C$.

Source	Estimated	t value	Pr(>|t|)
% Nitrogen	2.377	4.995	< 0.0001
Nitrogen: Phosphorus	-1.243	-2.612	0.0129

Table 5.B.2: Standardized coefficients from type III linear regression ($F_{4,35} = 10.42$, $p < 0.001$), showing leaf thickness and nutrient level is associated with Principal Component 2 (i.e. diarylheptanoid content, but see Table 5.D.1). Variables excluded from the model were tree diameter, %N, %C, %P, $^{15}N/^{14}N$, and $^{13}C/^{12}C$.

Source	Estimated	t value	Pr(>|t|)
Leaf thickness	-1.167	-3.431	0.00156
Carbon: Nitrogen	4.687	3.201	0.00291
Carbon: Phosphorus	-6.983	-2.813	0.00799
Nitrogen: Phosphorus	5.741	2.537	0.0158

Table 5.B.3: Standardized coefficients from type III linear regression ($F_{3,36} = 3.46$, $p < 0.026$), showing the association of various leaf traits on Principal Component 3 (i.e. flavonoid content, but see Table 5.D.1). Variables excluded from the model were tree diameter, C:N, N:P, C:P, %N, %P, and $^{13}C/^{12}C$.

Source	Estimated	t value	Pr(>|t|)
$^{15}N/^{14}N$	0.545	2.232	0.032
Leaf Thickness	-0.415	-1.709	0.096
% Carbon	-0.332	-1.372	0.18

Table 5.B.4: Standardized coefficients from best fitting stepwise linear mixed model (marginal $R^2 = 0.48$), showing ellagitannin-depleted and thin leaves are correlated with high rates of aquatic leaf decomposition in the Pysht, Little Hoko, Hoko and Sekiu Rivers. Variables excluded from the model were PC2, PC3, tree diameter, % N, % C, % P, C:N, C:P, N:P, $^{13}C/^{12}C$ and $^{15}N/^{14}N$.

Source	Estimated	t value	Pr(>|t|)
PC1 (ellagitannin content)	0.057	3.086	0.0038
Leaf thickness	-0.119	-6.543	> 0.001

Appendix 5C: Illustration of experimental design for reciprocal transplant experiments.

Figure 5.C.1: Five red alder trees from each of four sites, two from each river, were used to construct twenty diets. These diets were used to make diet plates containing all twenty diets. All aquatic diet plates and all riparian soil diet plates were constructed identically, but were deployed in each of the four different sites in the experimental run. Therefore, at each aquatic deployment site, there were twenty diet options made from leaves collected from twenty alder trees. For example, incubating in the water at Site 1 of the Little Hoko River were 5 diets from 5 trees growing along Site 1 of the Little Hoko, 5 diets from trees growing along Site 2 of the Little Hoko, and 10 diets from the 10 trees growing along the Pysht River. This diagram includes arrows for only one tree of five per site and for only two of the four sites, one per river, as a partial example of the complete design.

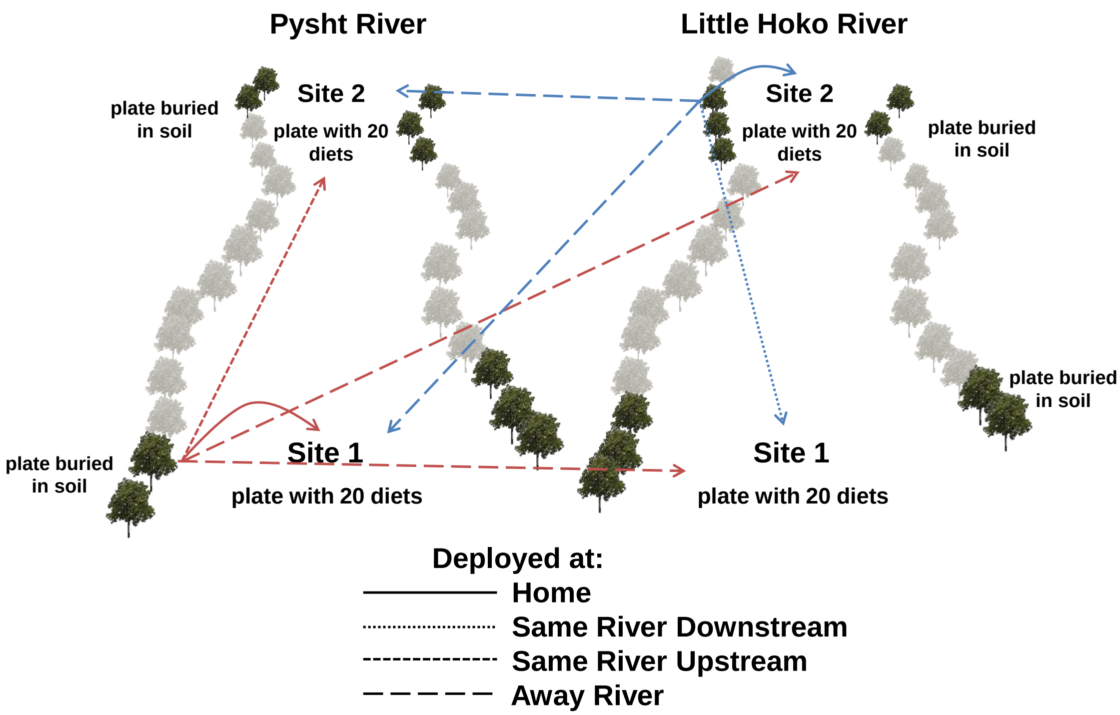

Figure 5.C.2: Twenty diets containing different red alder tree extracts deployed underwater in a 96 well plate on a stream bed.

Figure 5.C.3: Caddisflies feeding on a diet plate deployed on a stream bed.

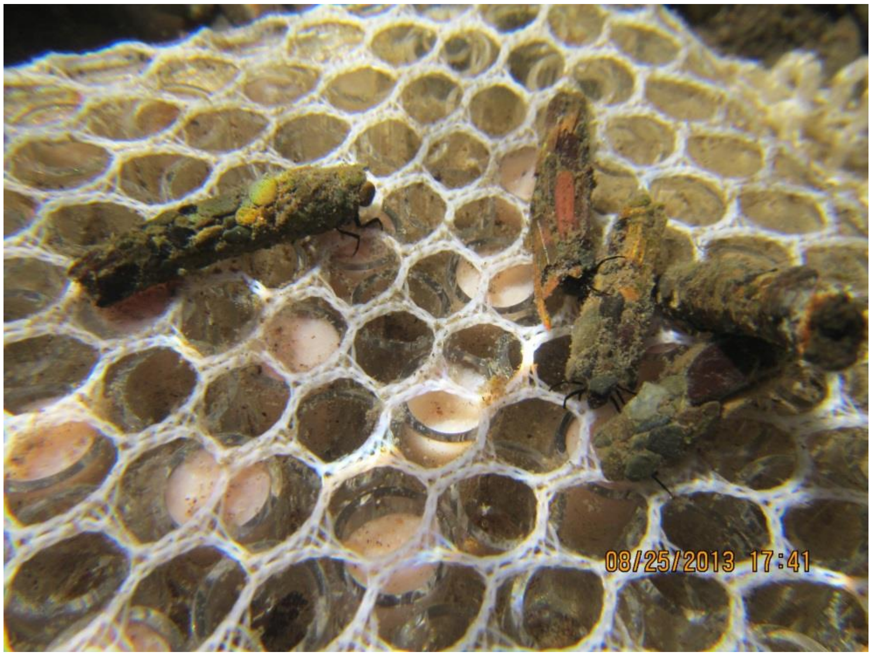

Appendix 5D: Loadings for principal component analysis.

Table 5.D.1: Variation in chromatograms of secondary metabolites in leaves of a red alder population explained by differences in relative quantities of ellagitannins (PC1), relative quantities of diarylheptanoids (PC2), and relative quantities of flavonoids (PC3) using a principal component analysis. Largest PC loadings (≥ |0.20|) and listed for each component.

PC1 Cumulative % of Variance: 40.2		PC2 Cumulative % of Variance: 58.0		PC3 Cumulative % of Variance: 65.5	
HHDP-galloyl-glucose (# 10)	-0.249	HOG (#23)	0.364	quercetin-rhamnose (#29)	-0.381
# 17	-0.249	methylhirsutanonol (# 30)	0.363	# 33	-0.335
di-HHDP-galloyl-glucose α (# 16)	-0.249	hirsutanone (# 32)	0.357	HHDP-glucose (# 4)	-0.332
di-HHDP-galloyl-glucose β (# 15)	-0.248	alnuside C (glucose replaces xylose) # 34	0.345	# 1	0.332
di-galloyl-HHDP-glucose (# 9)	-0.246	alnuside C (# 35)	0.297	quercetin-glucuronide and quercetin-glucoside (# 25)	-0.315
# 13	-0.243	oregonin (# 24)	0.265	HHDP-glucose (# 3)	0.241
# 21	-0.234	platyphylanol-xylose (# 31)	0.223	# 14	-0.206
di-HHDP-glucose (# 7)	-0.228	alnuside A (# 26)	0.205		
di-galloyl-HHDP-glucose (# 12)	-0.227	# 14	0.204		
HHDP-galloyl-glucose (# 8)	-0.217				
tri-O-galloyl-HHDP-glucose (β) (# 18)	-0.209				
di-HHDP-glucose (#6)	-0.207				
# 28	-0.200				

Appendix 5E: Canonical correlation coefficients and structure matrix for discriminant function analysis.

Table 5.E.1: Importance of ellagitannins, diarylheptanoids and flavonoids with DF1 (shown in Fig. 5.4). Numbering corresponds with chromatogram peaks described in Fig 5.1. Bold/italics highlights four compounds that most strongly influence discriminant scores.

Chemical Compound	Standardized Canonical Coefficients	Structure Matrix
1 (unknown)	18.744	0.017
4 (HHDP-Glucose)	11.559	-0.008
5 (galloyl-glucose)	***-28.468***	0
6 (di-HHDP-glucose)	1.911	-0.011
8 (HHDP-galloyl-glucose)	-8.305	0.002
9 (di-galloyl-HHDP-glucose)	12.228	-0.009
10 (HHDP-galloyl-glucose)	***26.767***	-0.007
11 (unknown ellagitannin)	-3.514	-0.013
12 (di-galloyl-HHDP-glucose)	-12.943	-0.01
14 (unknown)	9.135	0.001
15 (di-HHDP-galloyl-glucose β)	-3.043	-0.012
16 (di-HHDP-galloyl-glucose α)	-15.62	-0.01
17 (unknown)	11.823	-0.009
18 (tri-O-galloyl-HHDP-glucose β)	19.123	-0.015
19 (unknown ellagitannin)	16.65	-0.004
20 (unknown)	-7.769	-0.004
21 (unknown)	-7.916	-0.009
22 (tri-O-galloyl-HHDP-glucose α)	***-21.657***	-0.035
23 (HOG)	***23.527***	0.012
24 (Oregonin)	14.145	0.007
26 (Alnuside A)	8.119	0.013
27 (Alnuside B)	13.512	0.01
28 (unknown)	-8.181	0
29 (Quercitin-rhamnose)	-2.437	-0.018
30 (methylhirsutanonol)	-9.896	0.018
33 (unknown diarylheptanoid)	7.007	-0.011
34 (1,7-bis-(3,4-dihydroxy-phenyl)-5-hydroxy-3-heptanone-5-0-[2-(2-methylbutenoyl)]-β-D-glucopyranoside)	-8.687	0.013

Appendix 5F: Detailed mass spectrometry data.

Figure 5.F.1a-x: Mass spectrometry data for twenty-five ellagitannins, diarylheptanoids and flavonoids.

Figure 5.F.1a:

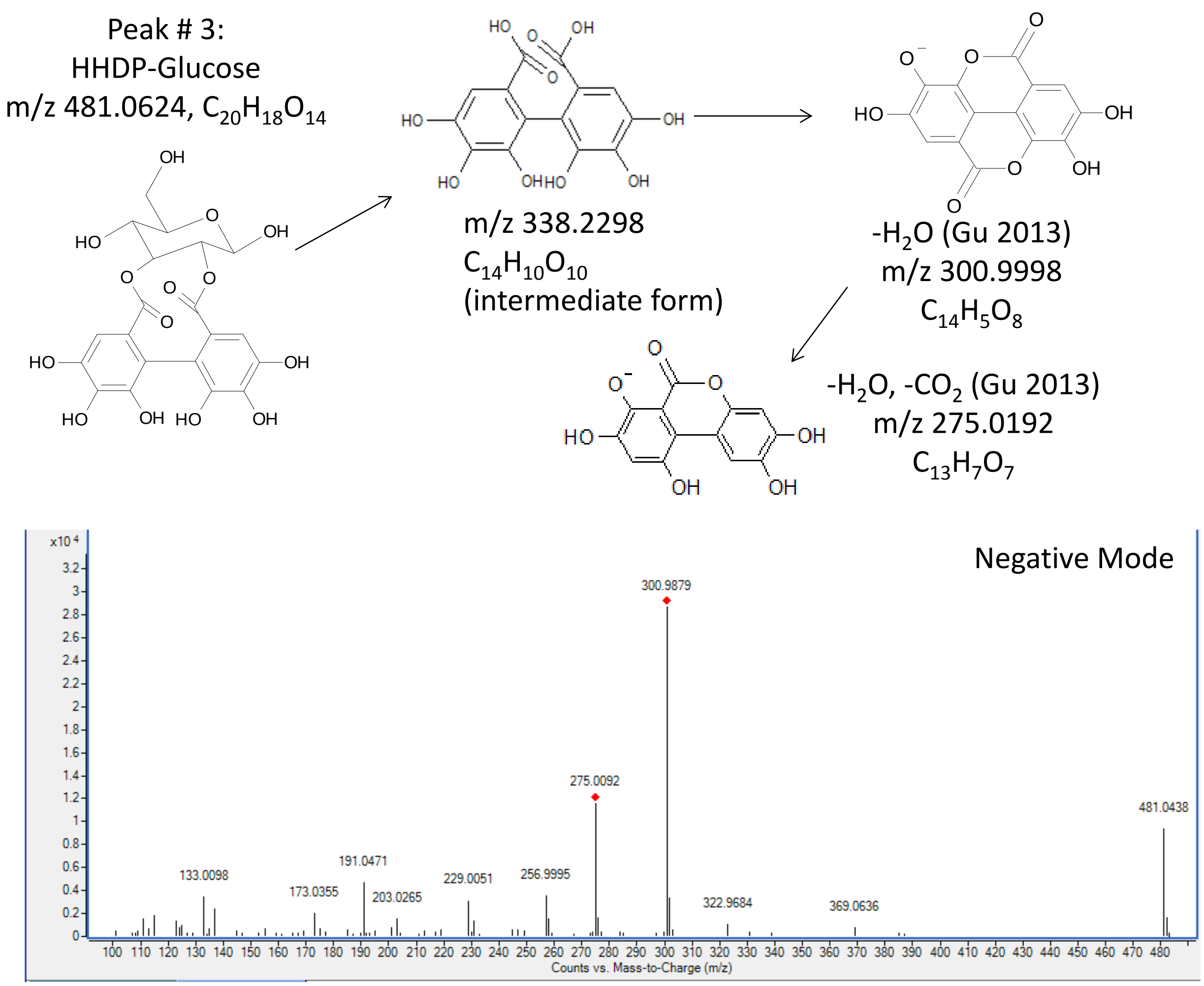

Figure 5.F.1a-x, continued:

Figure 5.F.1b:

Peak # 4:
HHDP-Glucose
m/z 481.0624, $C_{20}H_{18}O_{14}$

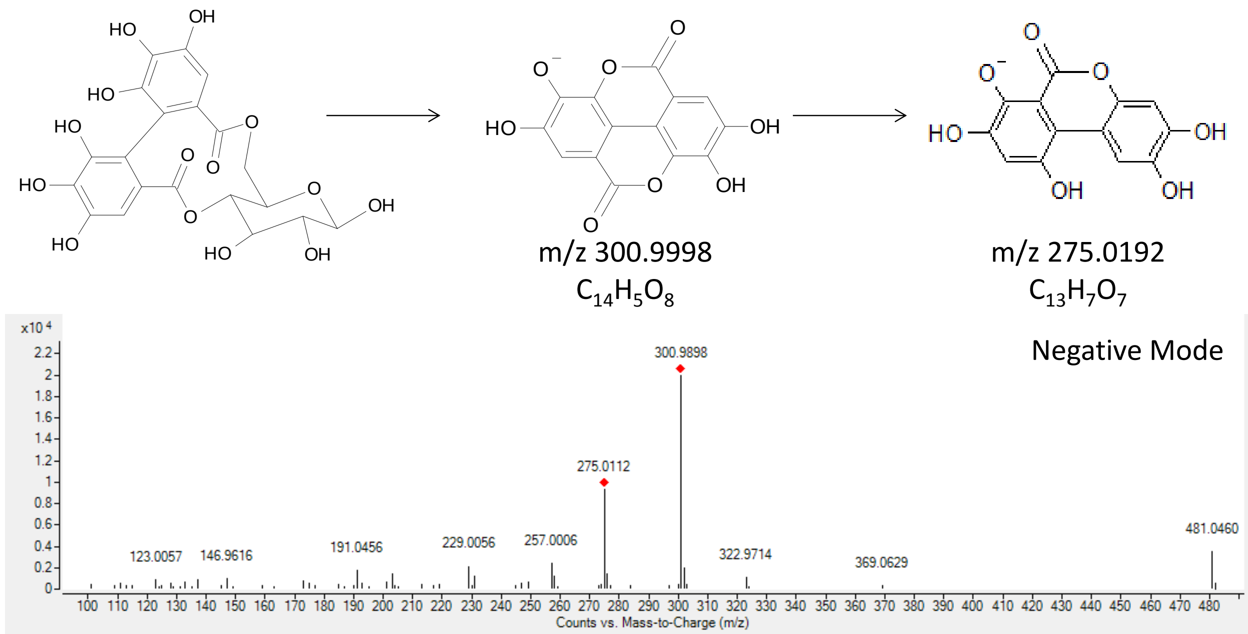

Figure 5.F.1a-x, continued:

Figure 5.F.1c:

Peak # 5:
Glucose + 3G
m/z = 331.0743, $C_{13}H_{16}O_{10}$

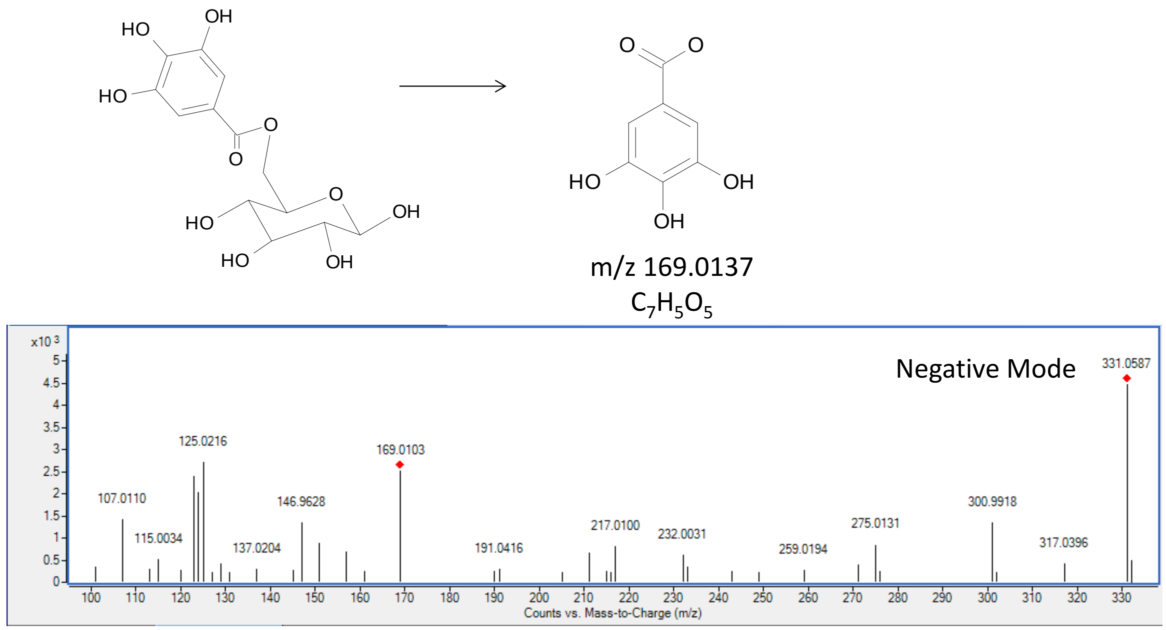

Figure 5.F.1a-x, continued:

Figure 5.F.1d:

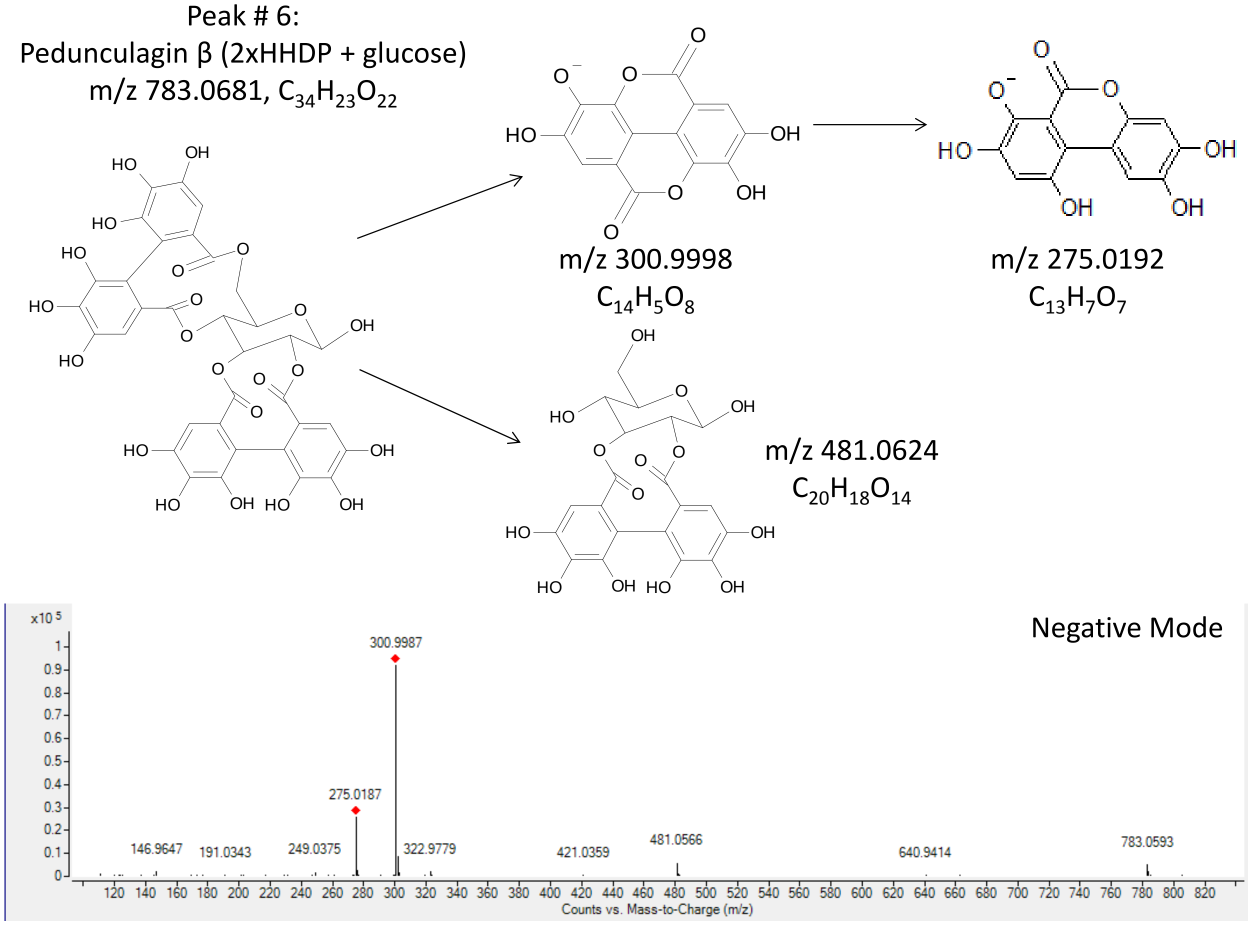

Figure 5.F.1a-x, continued:

Figure 5.F.1e:

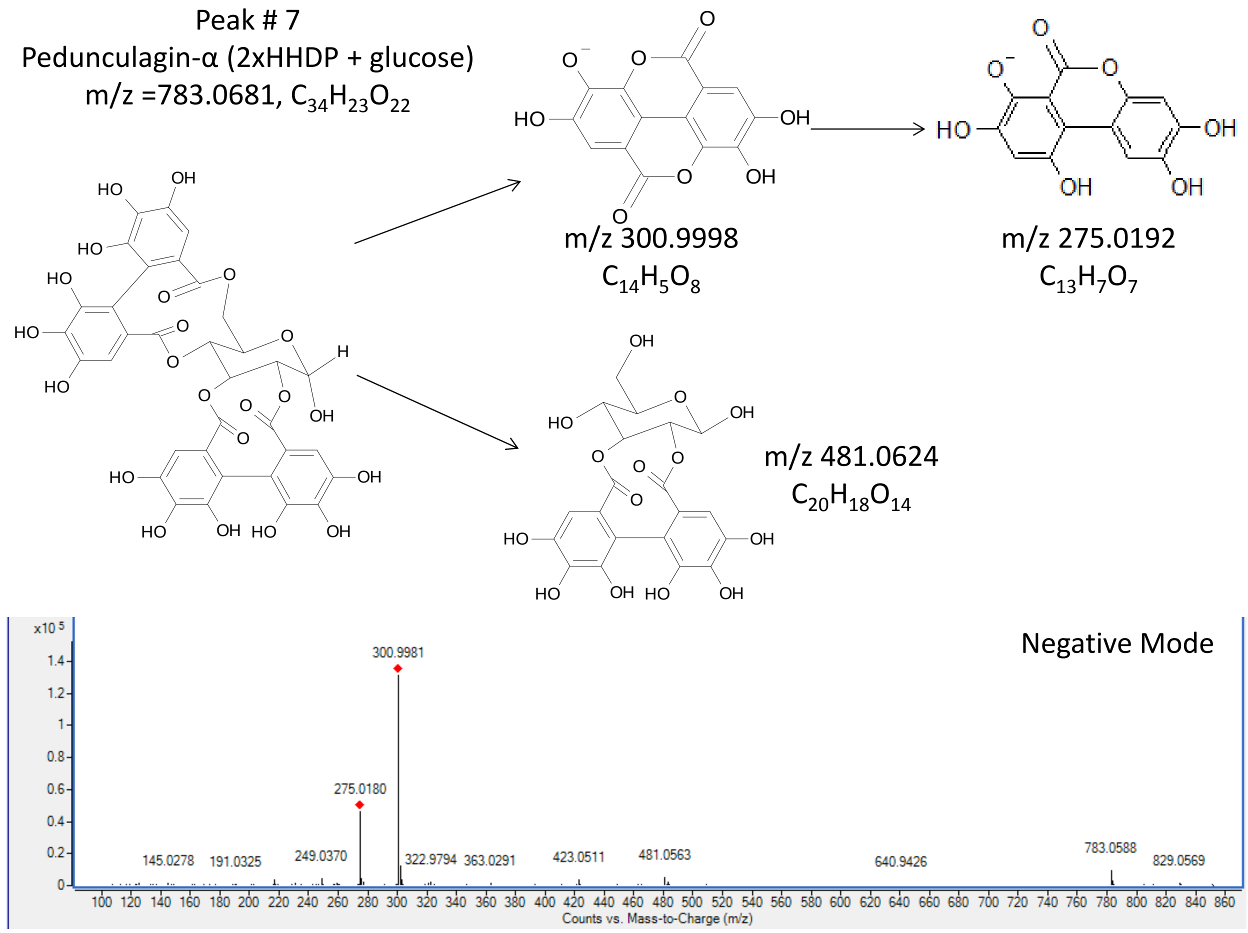

Figure 5.F.1a-x, continued:

Figure 5.F.1f:

Peak # 8:
Isostrictinin (1G+HHDP+glucose)
m/z 633.0733373, $C_{27}H_{22}O_{18}$

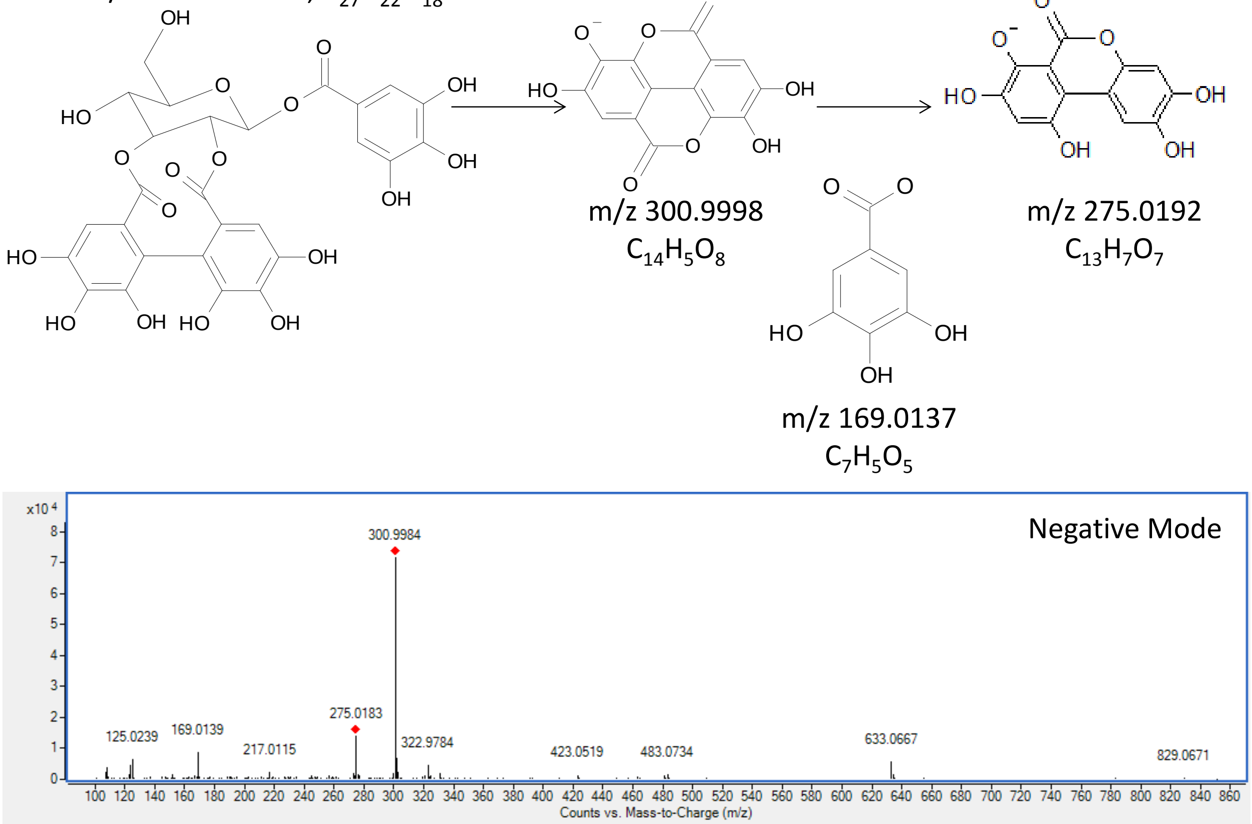

Figure 5.F.1a-x, continued:

Figure 5.F.1g:

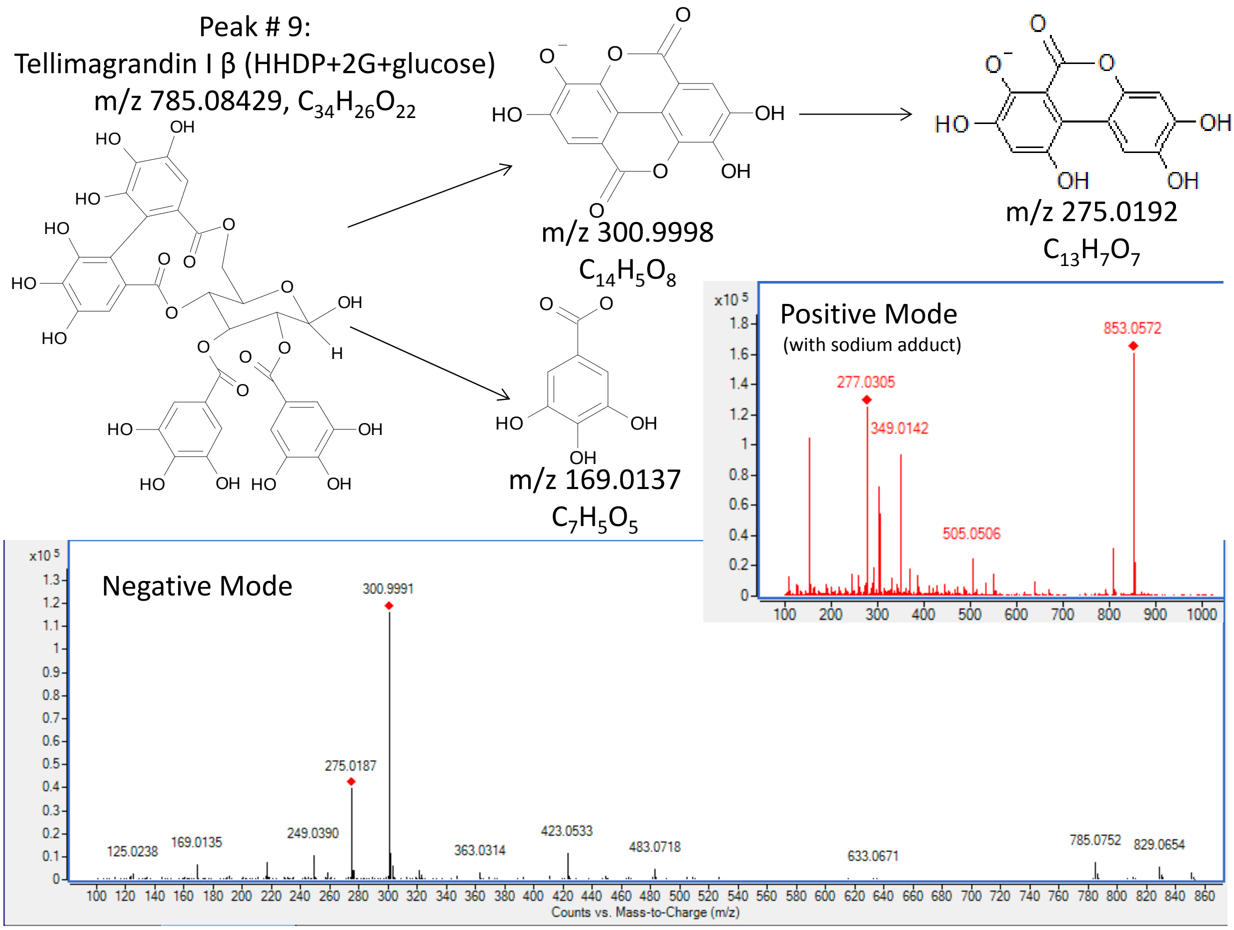

Figure 5.F.1a-x, continued:

Figure 5.F.1h:

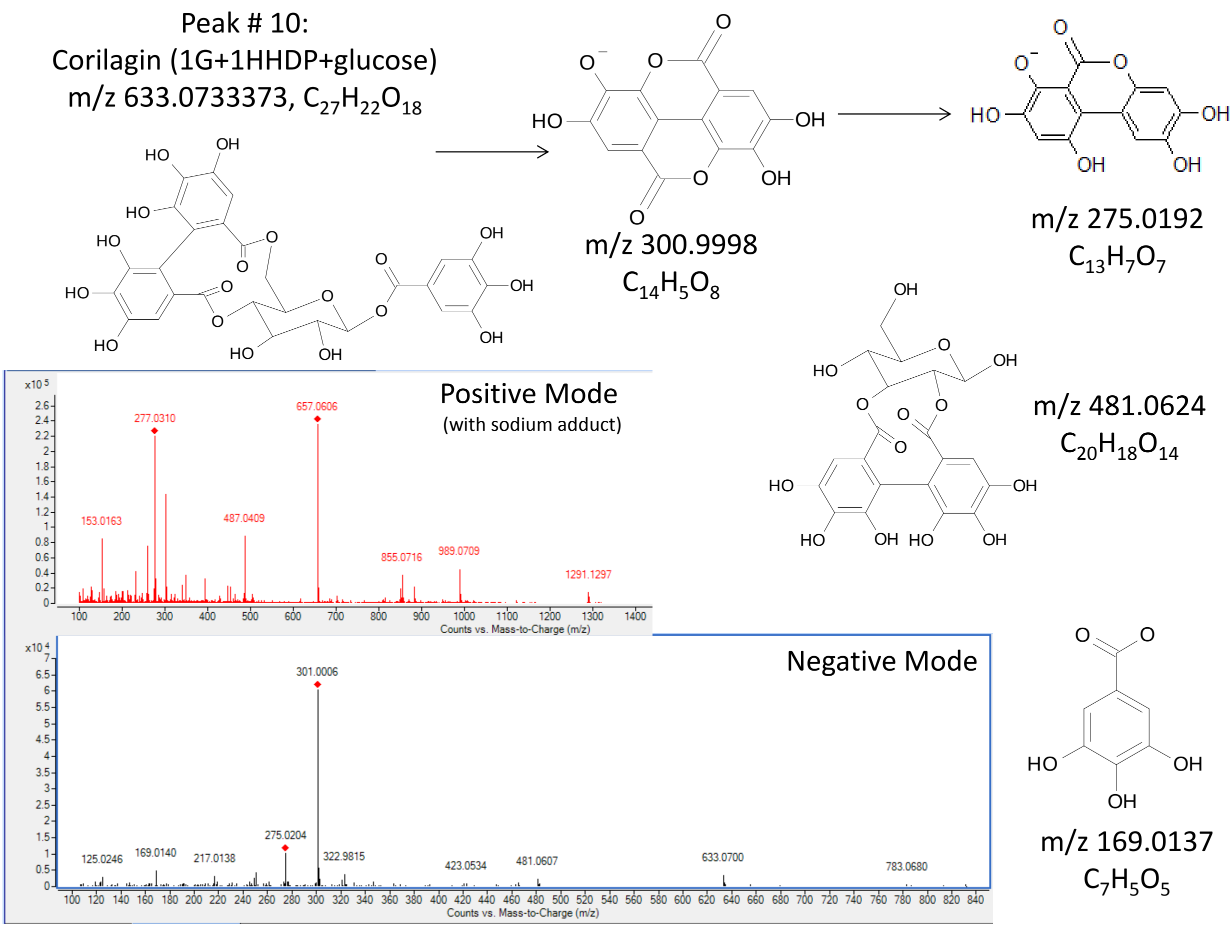

Figure 5.F.1a-x, continued:

Figure 5.F.1i:

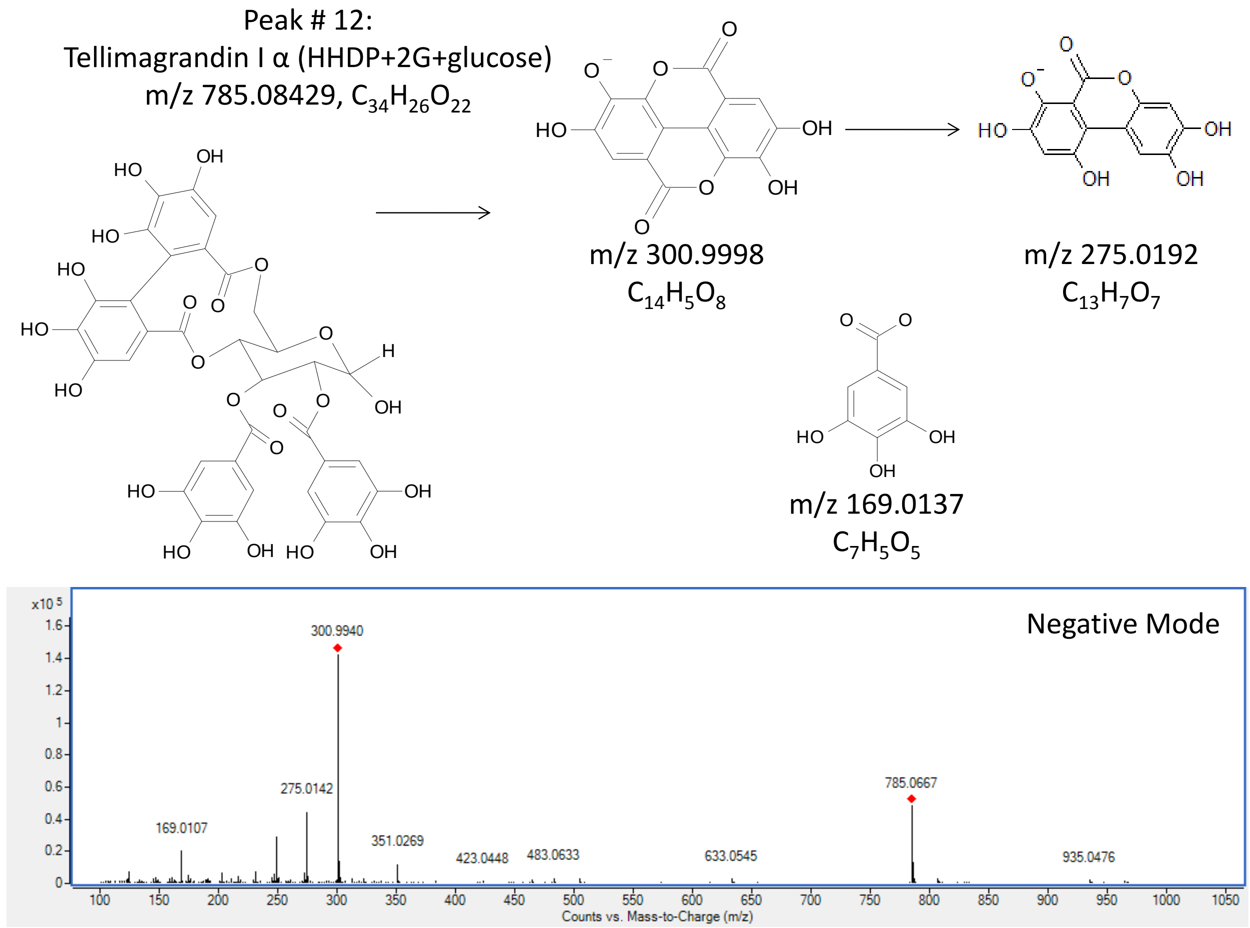

Figure 5.F.1a-x, continued:

Figure 5.F.1j:

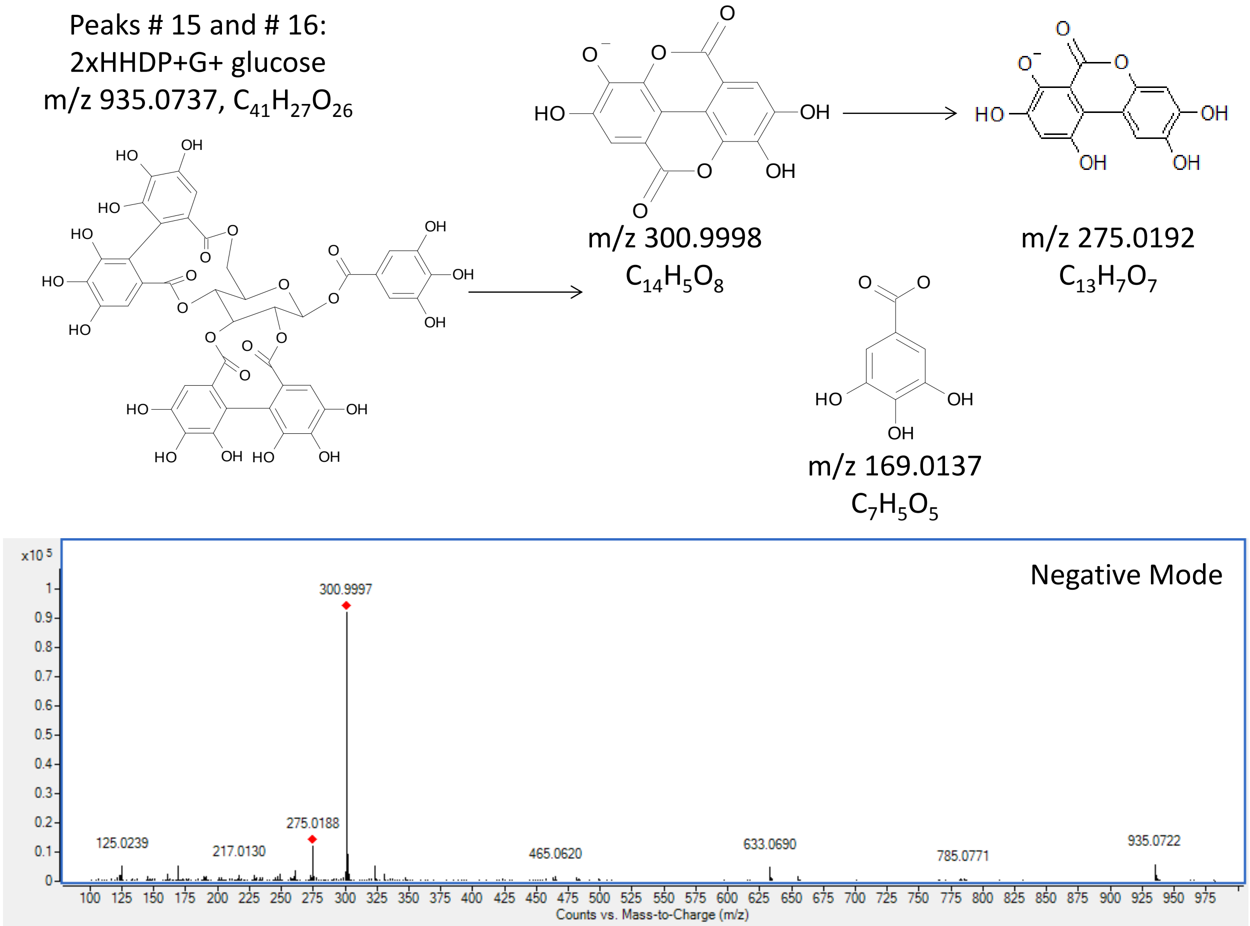

Figure 5.F.1a-x, continued:

Figure 5.F.1k:

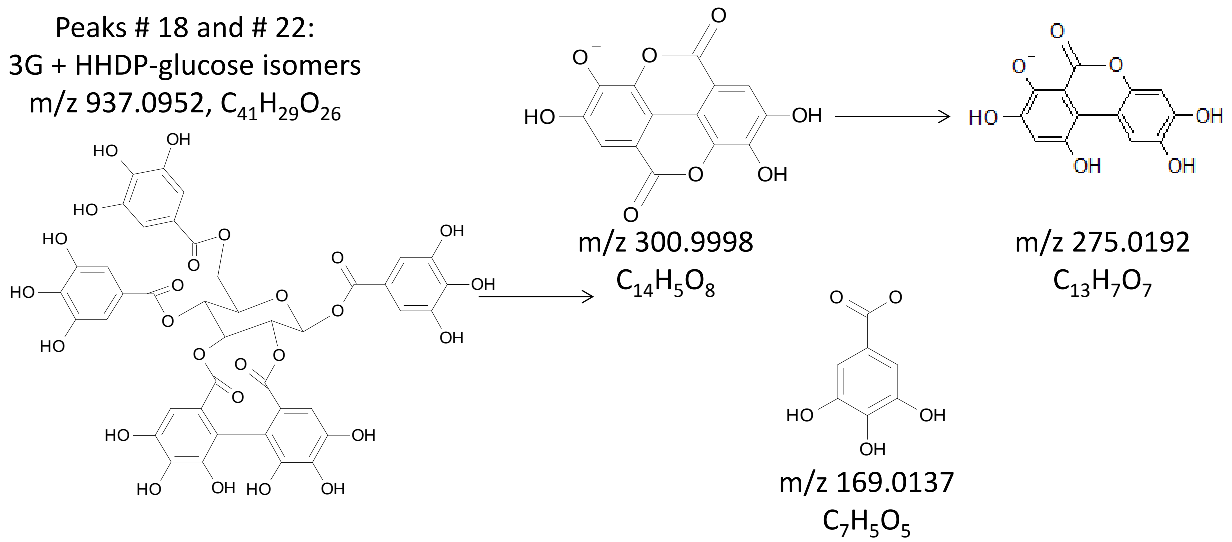

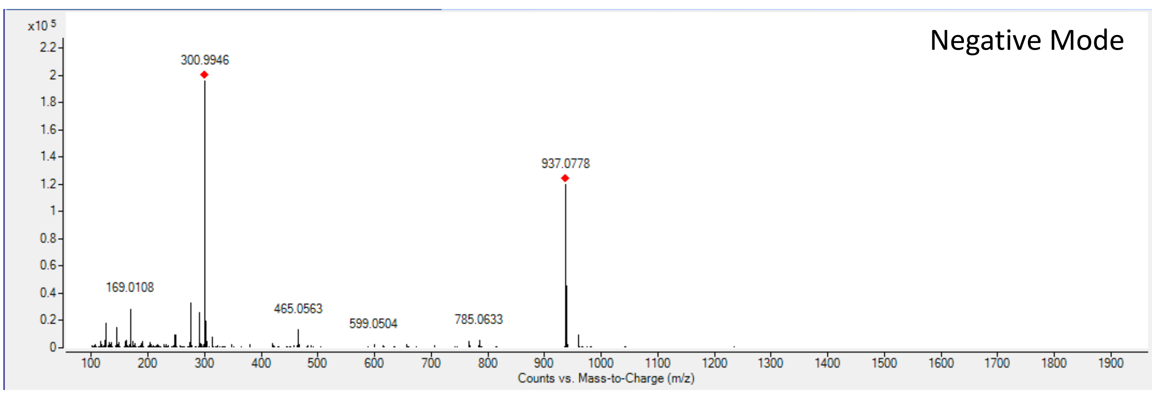

Figure 5.F.1a-x, continued:

Figure 5.F.1l:

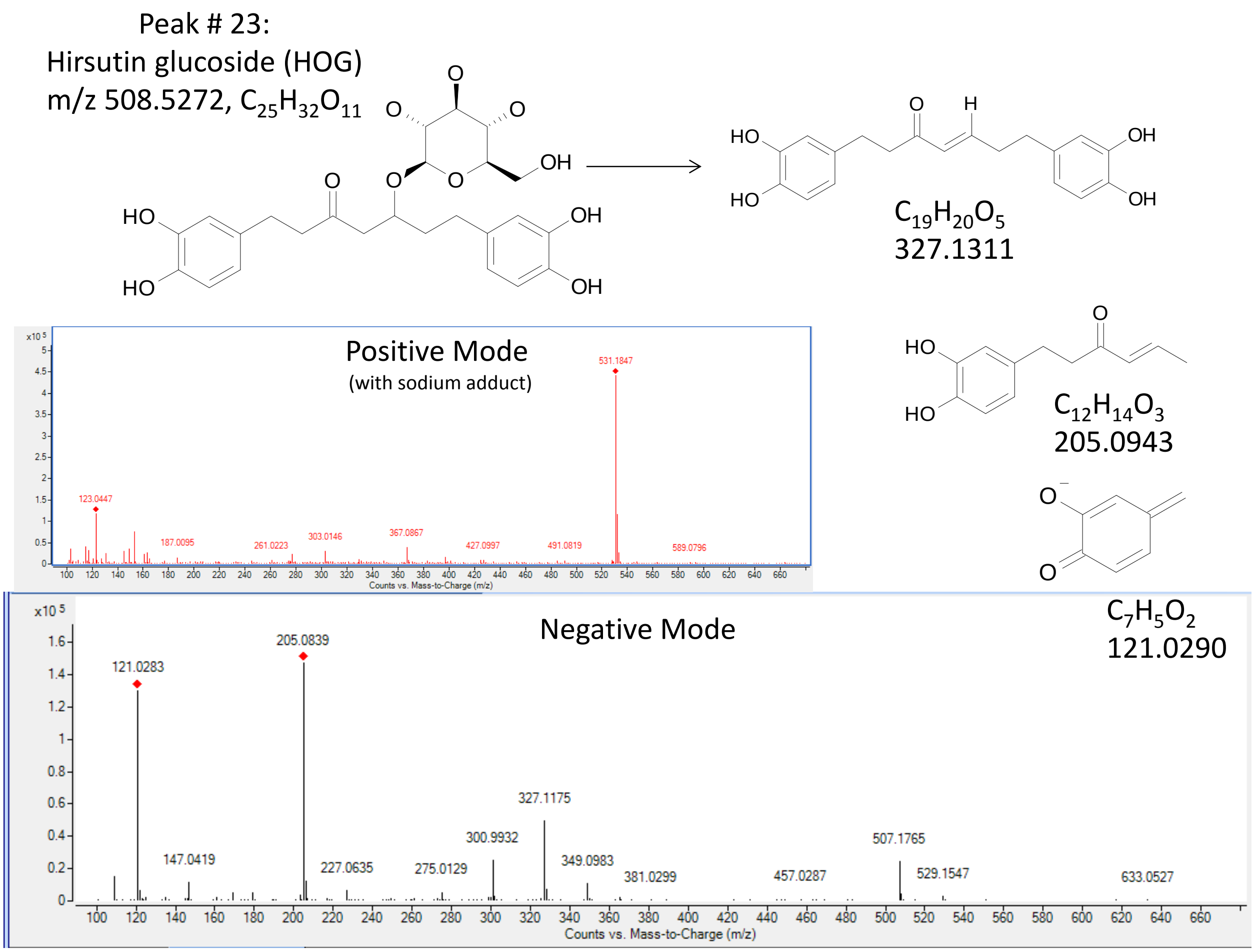

Figure 5.F.1a-x, continued:

Figure 5.F.1m:

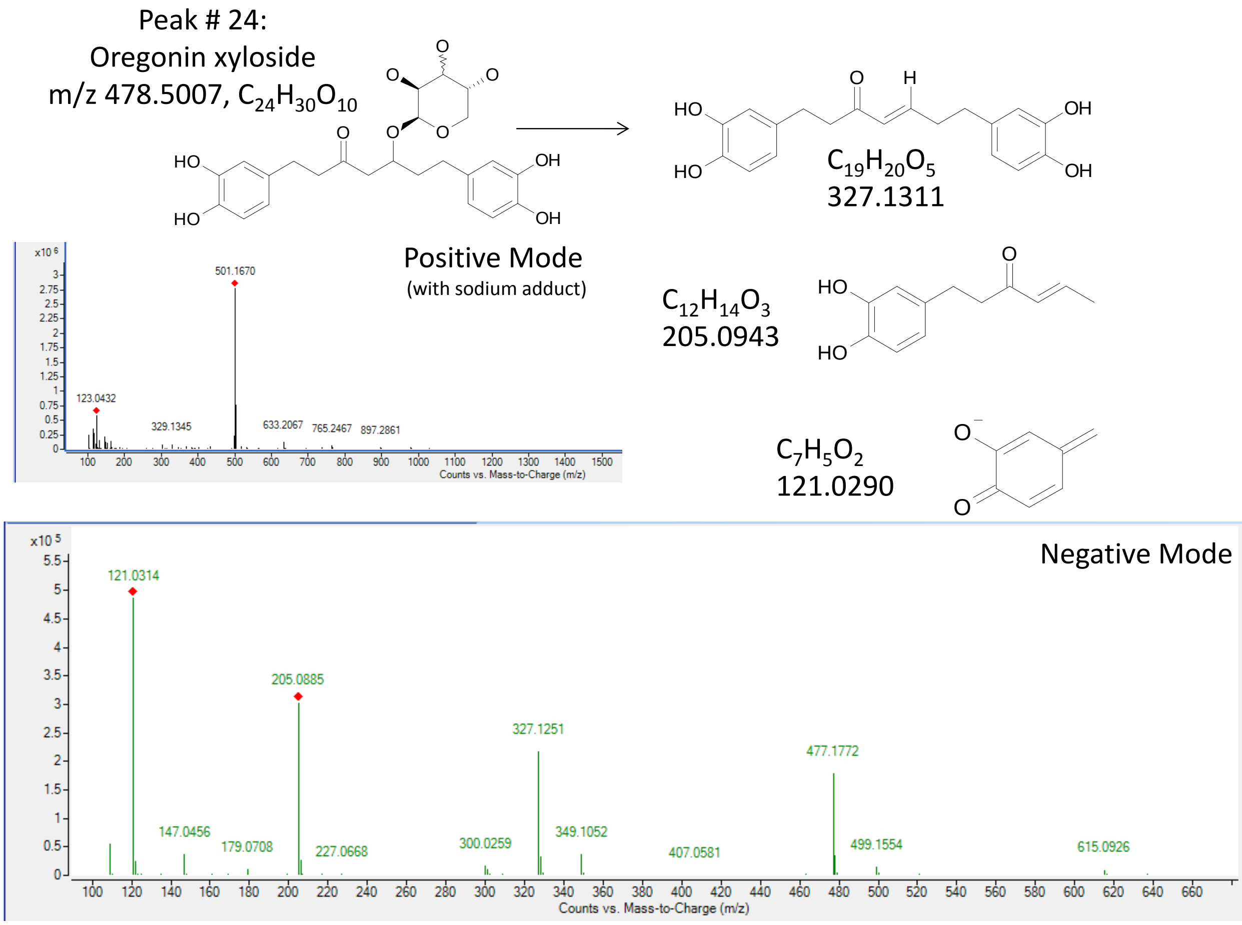

Figure 5.F.1a-x, continued:

Figure 5.F.1n:

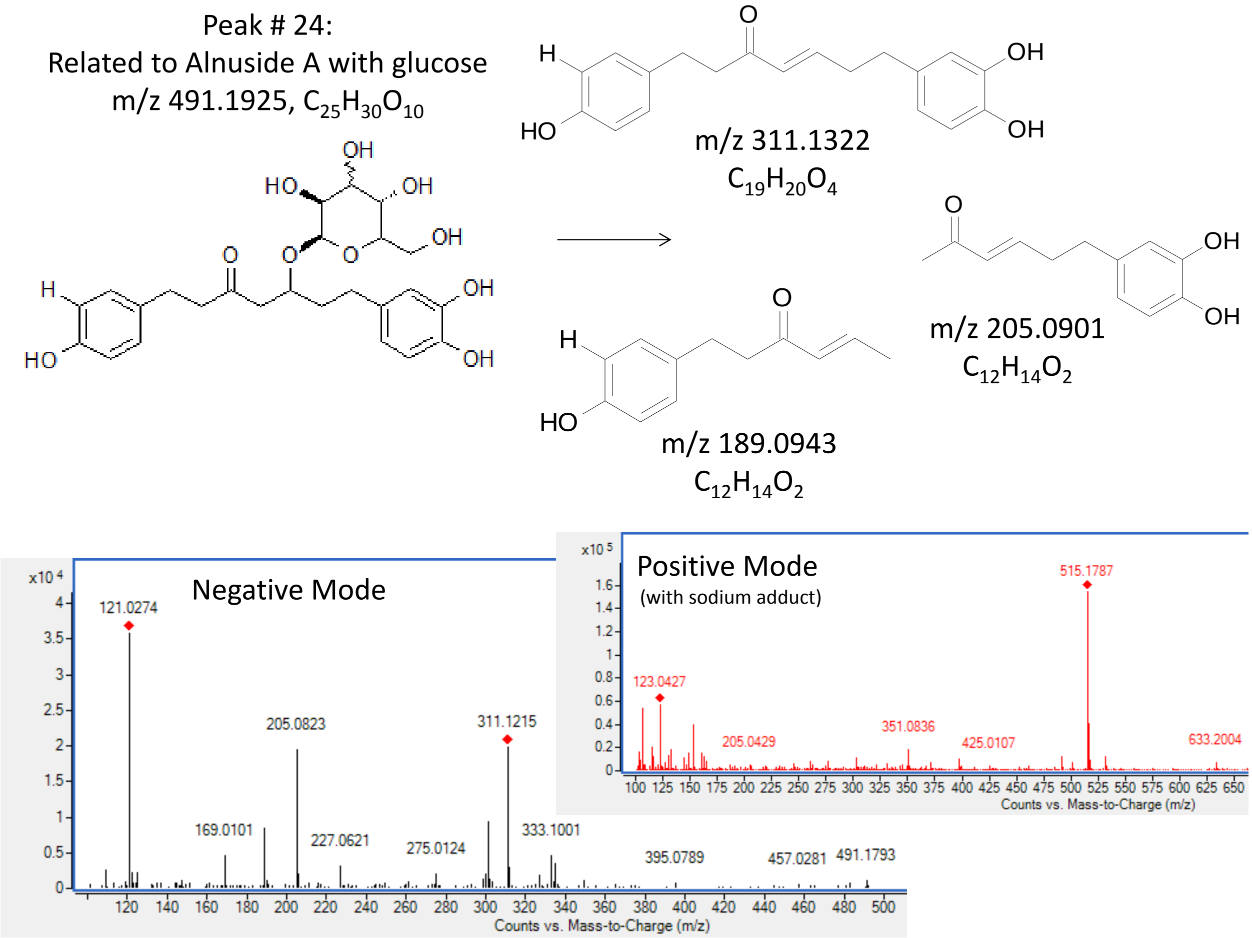

Figure 5.F.1a-x, continued:

Figure 5.F.1o:

Peak # 25:
Quercitin glucuronide
m/z 477.0675, $C_{21}H_{18}O_{13}$

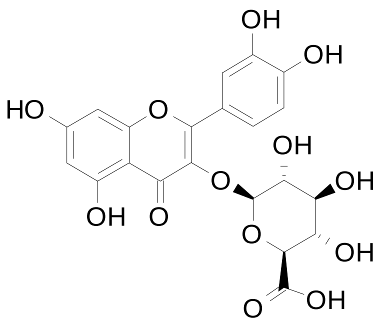

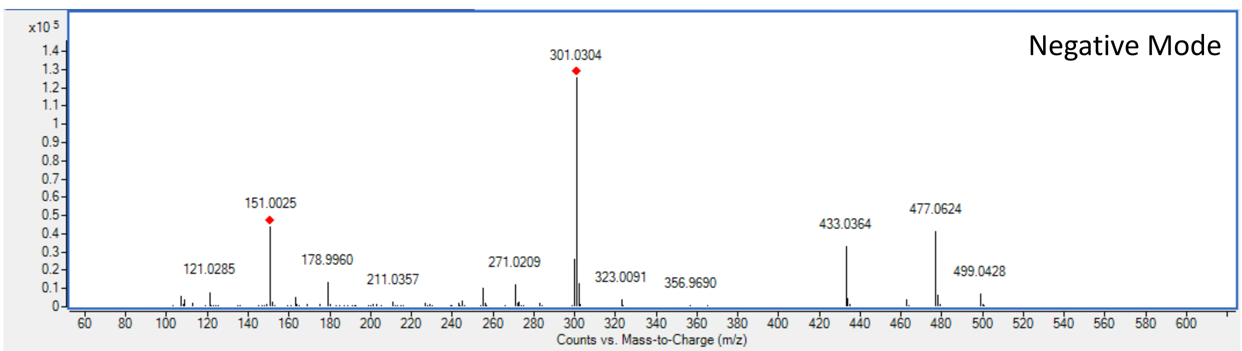

Figure 5.F.1a-x, continued:

Figure 5.F.1p:

Peak # 25:
Quercetin3-O-glucoside
m/z 463.0882, $C_{21}H_{20}O_{12}$

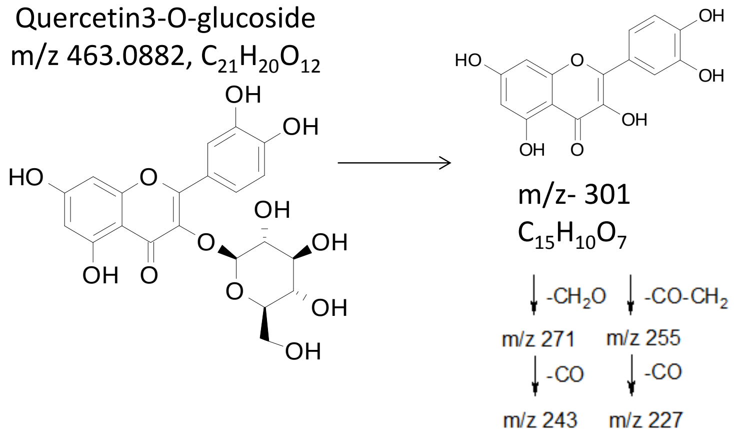

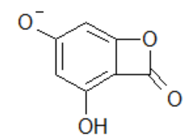

m/z 151
$C_7H_{30}O_4$

Xaio-qin et al 2009 Investigation of the chemical constituents and variation of the flower buds of Lonicera species by UPLC-ESI-MS/MS and principle component analysis. Act. Pharm Sin 44:895-904.

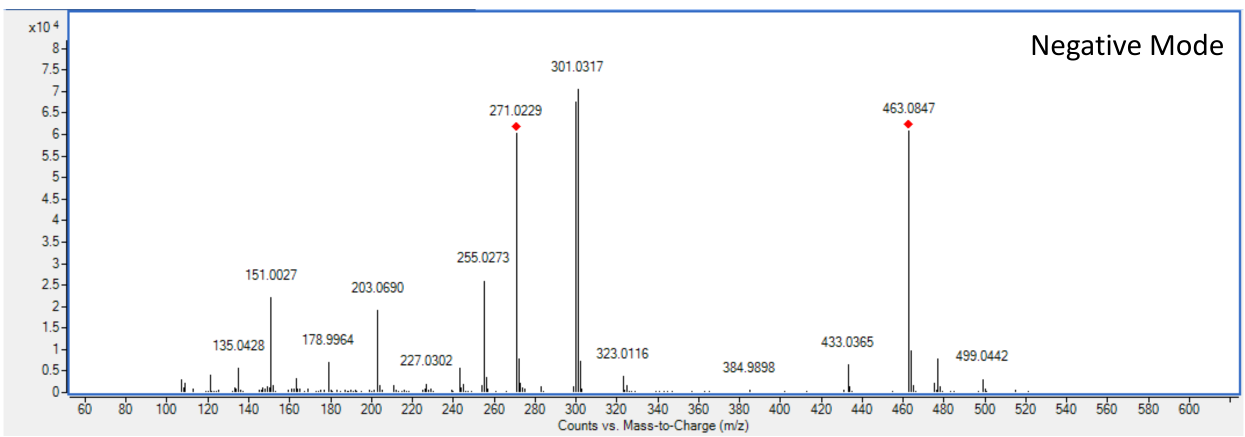

Figure 5.F.1a-x, continued:

Figure 5.F.1q:

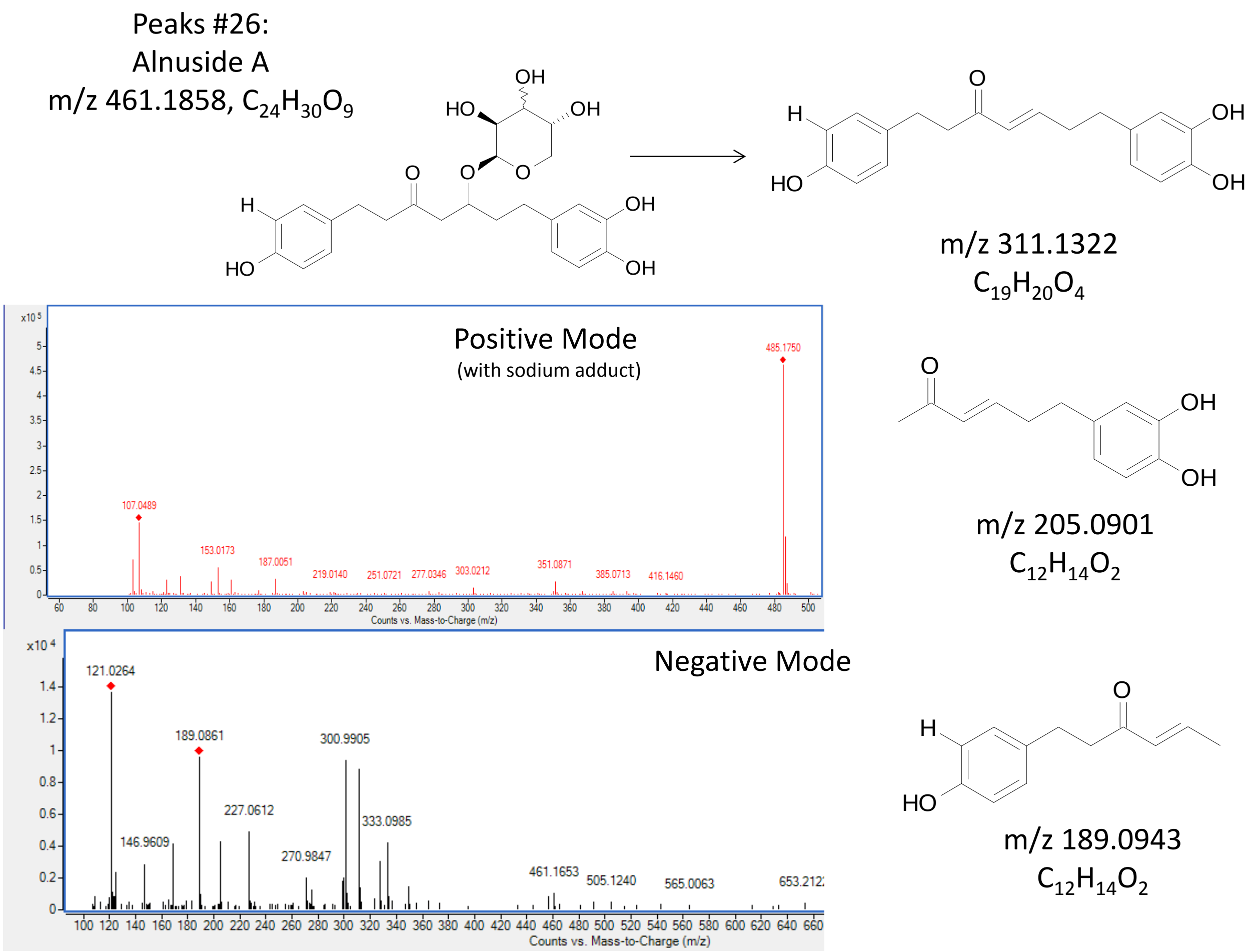

Figure 5.F.1a-x, continued:

Figure 5.F.1r:

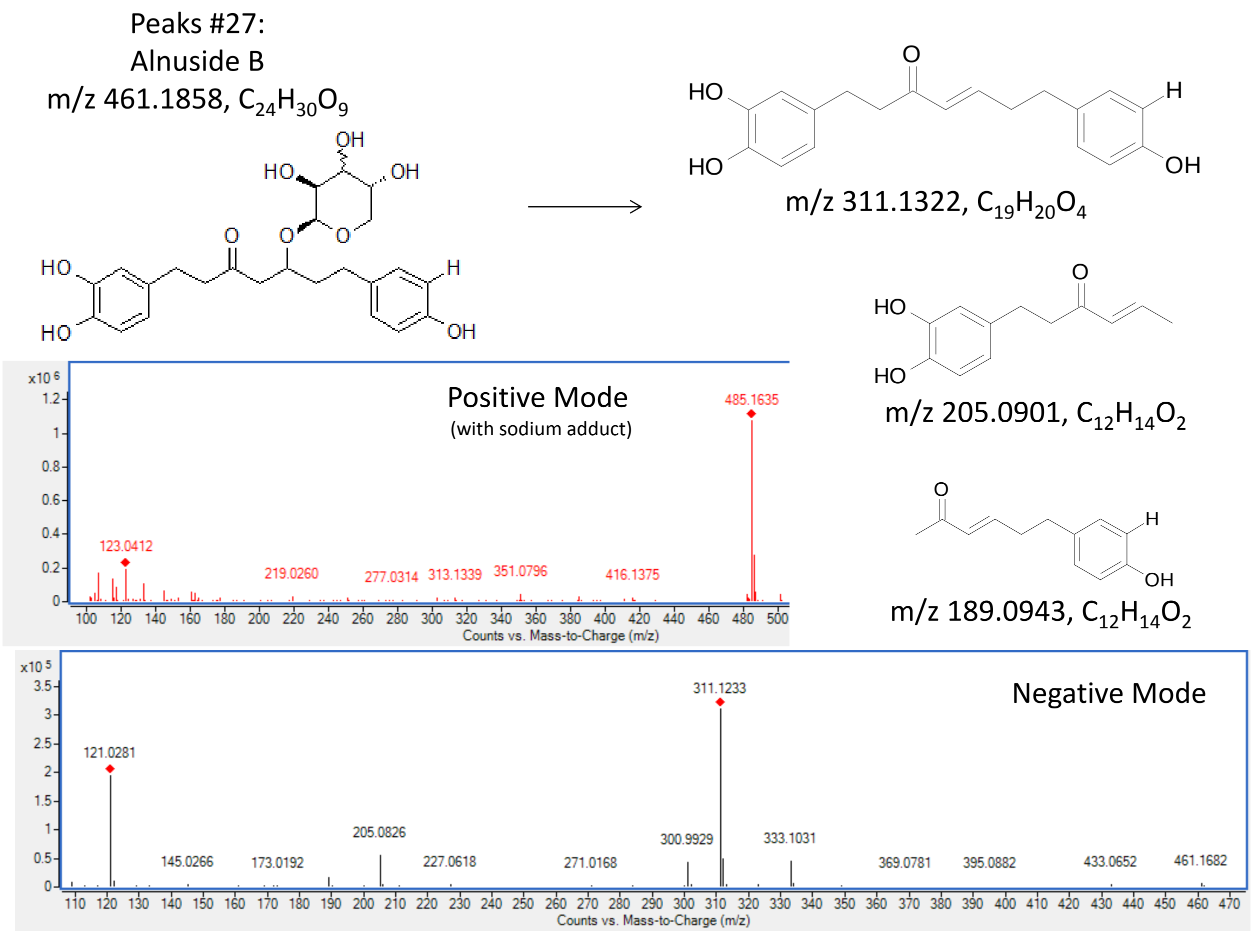

Figure 5.F.1a-x, continued:

Figure 5.F.1s:

Peak # 29:
Quercitin rhamnoside
m/z 447.0964, $C_{21}H_{19}O_{11}$

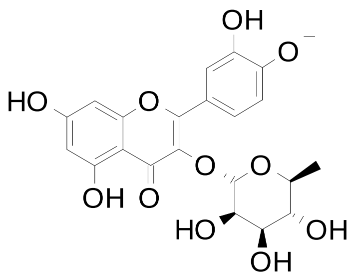

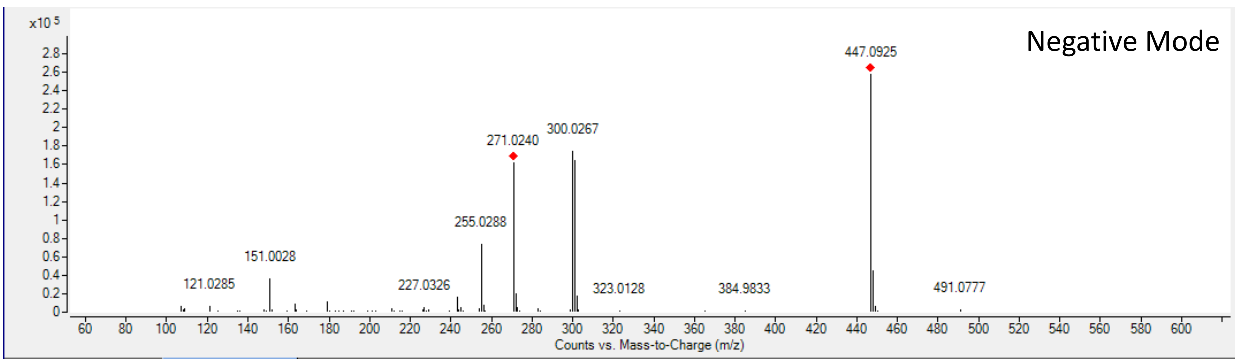

Figure 5.F.1a-x, continued:

Figure 5.F.1t:

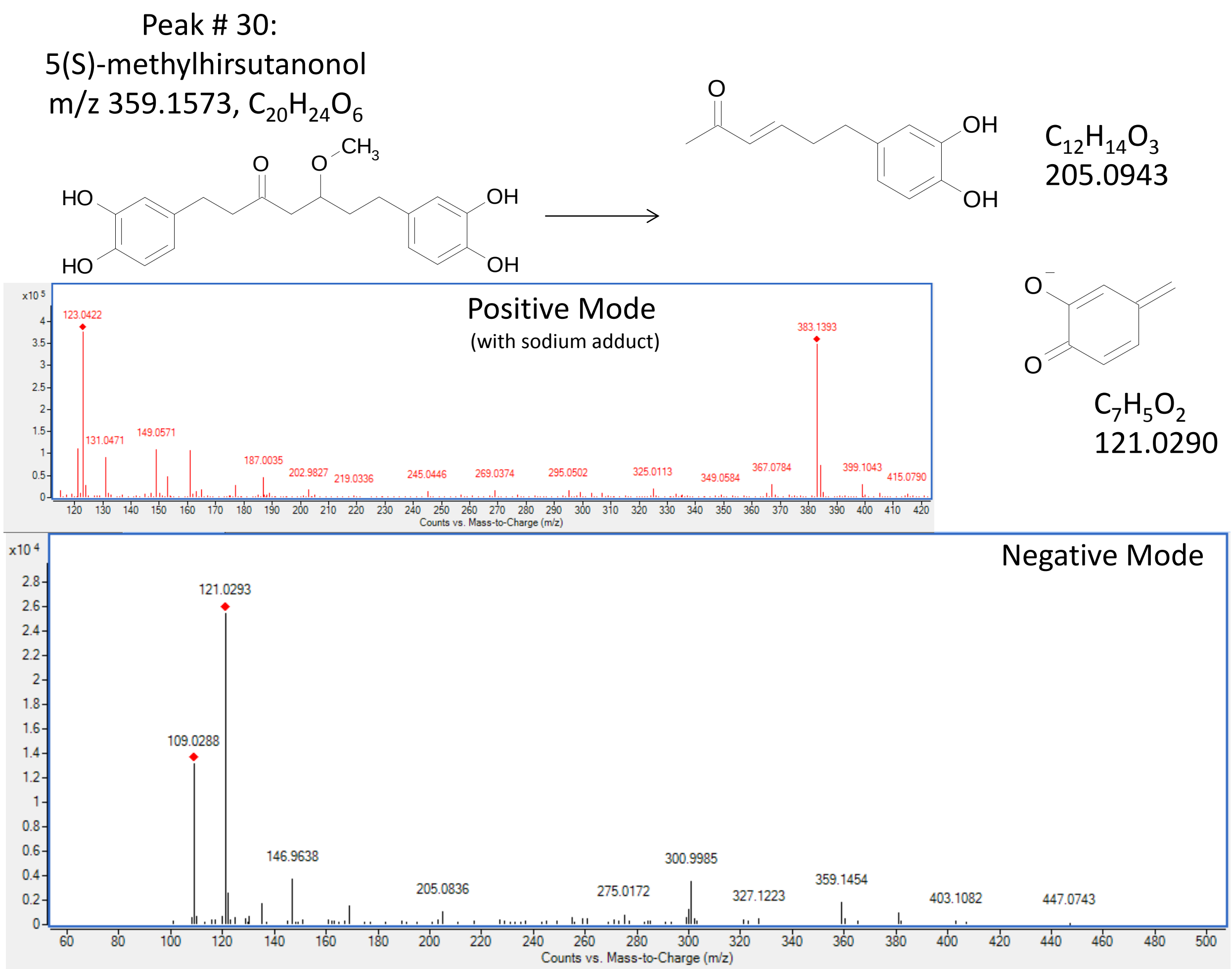

Figure 5.F.1a-x, continued:

Figure 5.F.1u:

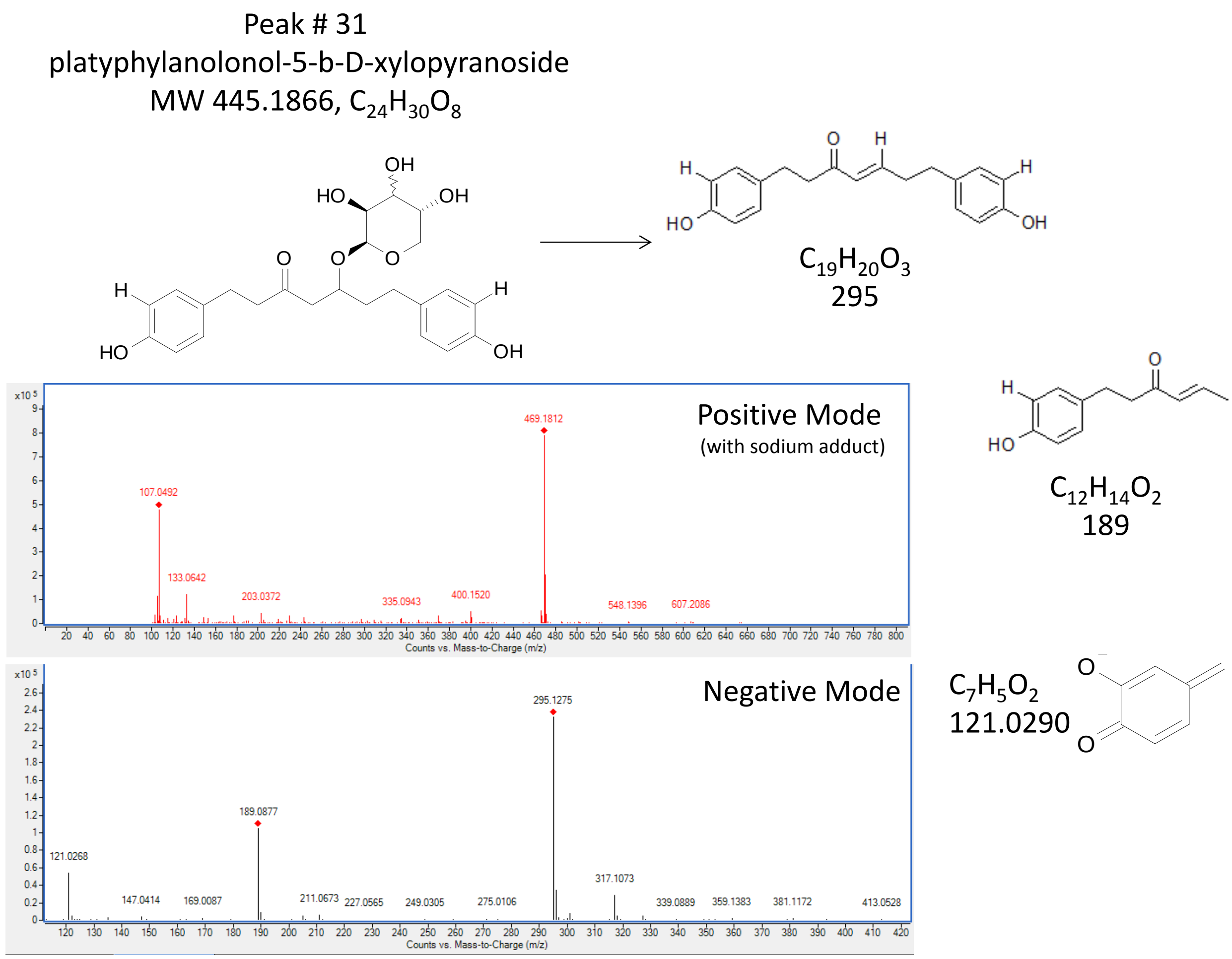

Figure 5.F.1a-x, continued:

Figure 5.F.1v:

Peak # 32:
Hirsutanone
M-H 327.12379, $C_{19}H_{19}O_5$

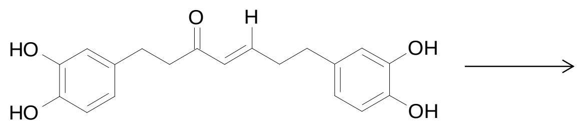

$C_{19}H_{20}O_5$
327.1311

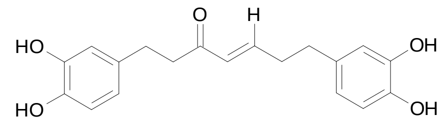

$C_{12}H_{14}O_3$
205.0943

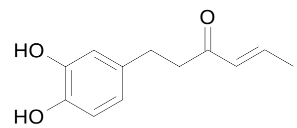

$C_7H_5O_2$
121.0290

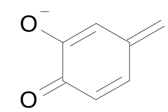

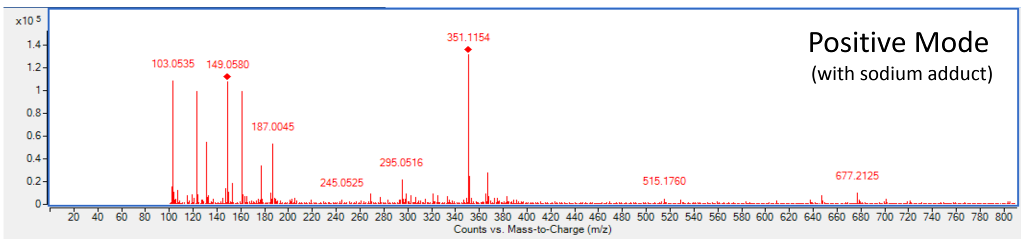

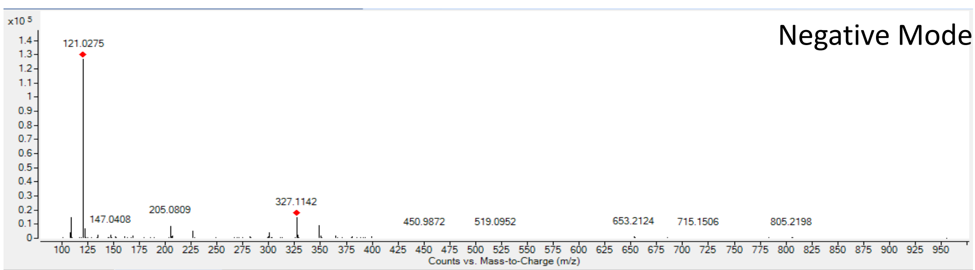

Figure 5.F.1a-x, continued:

Figure 5.F.1w:

Peak # 34:
derivative of Alnuside C with glucose replacing xylose
m/z 591.2520, $C_{30}H_{40}O_{12}$

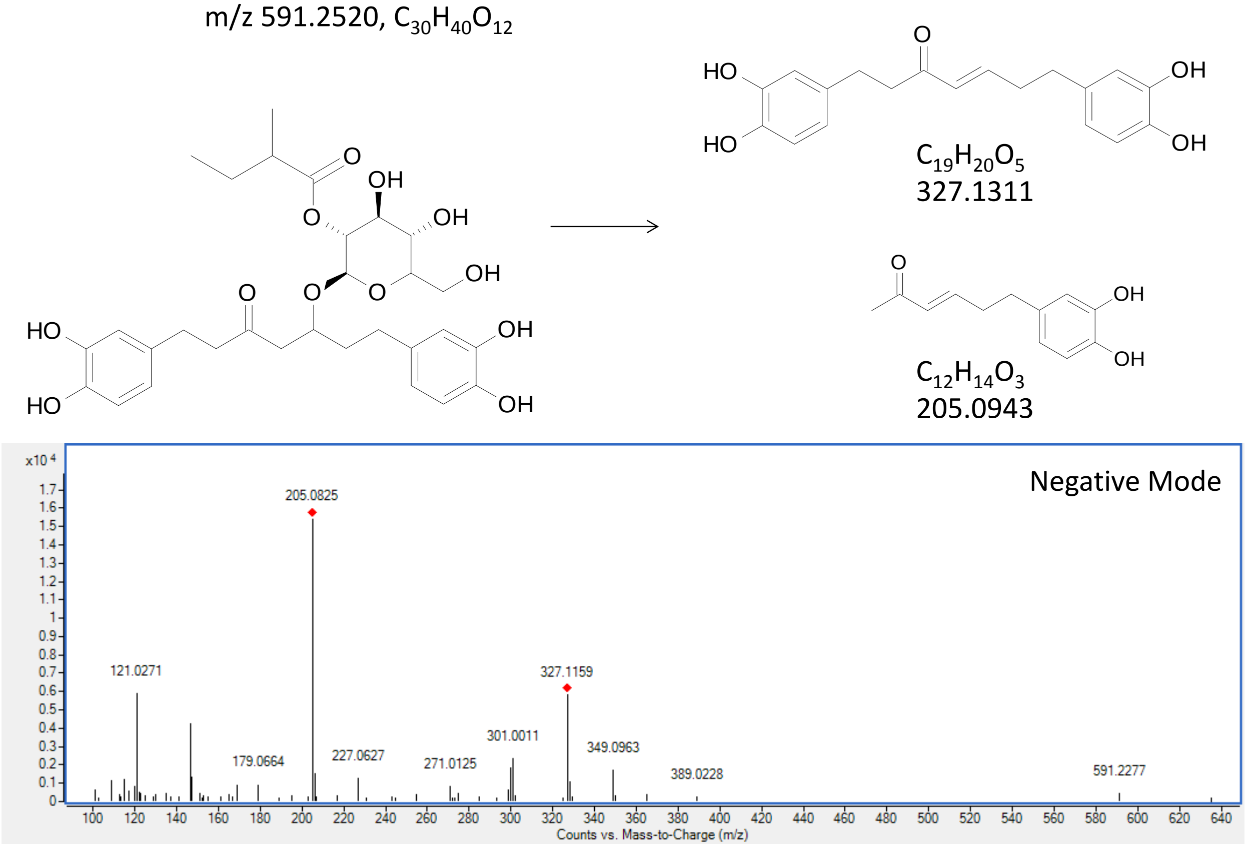

Figure 5.F.1a-x, continued:

Figure 5.F.1x:

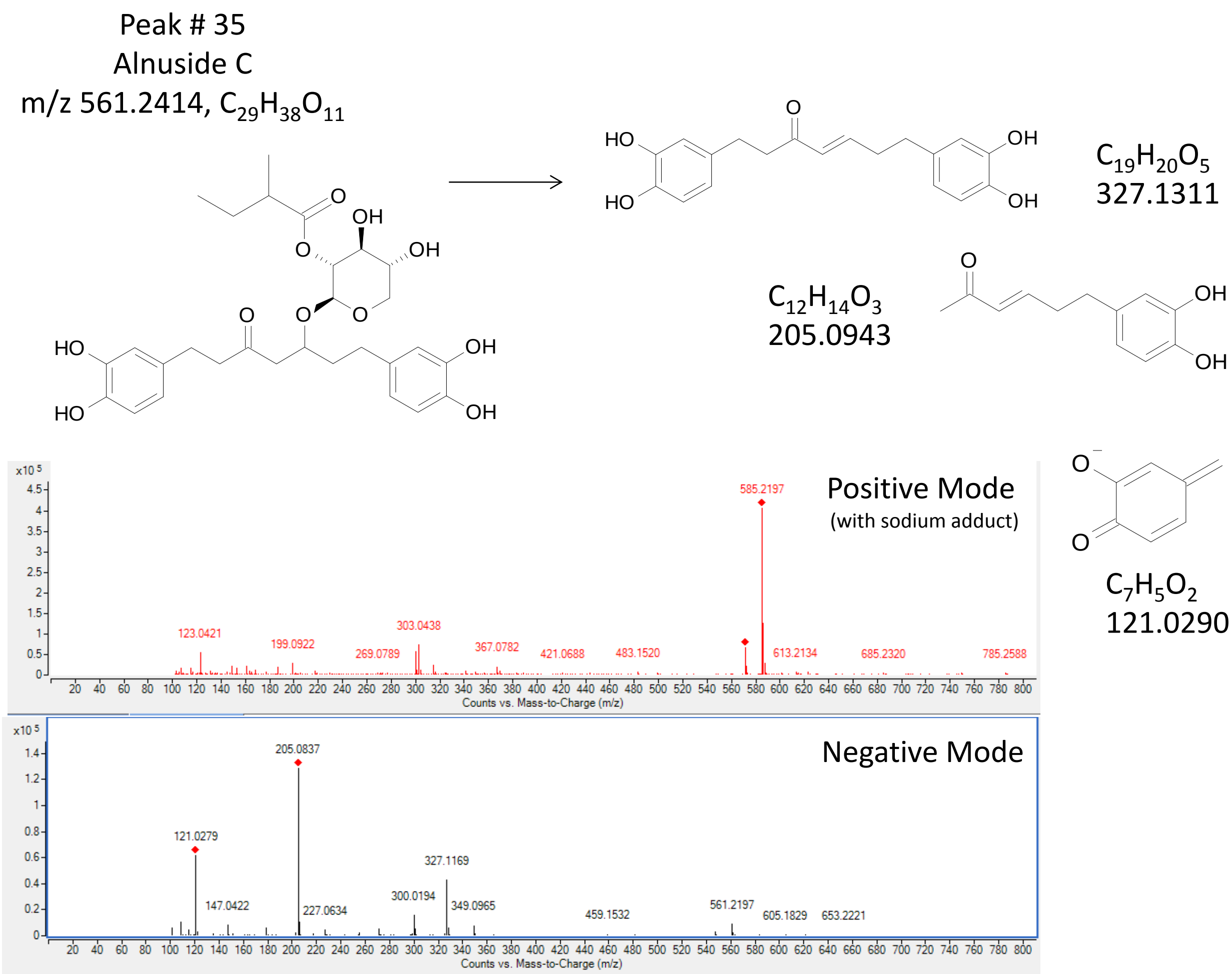

CHAPTER VI

HERBIVORE STRESS AND NUTRIENT ADDITIONS ALTER SECONDARY METABOLITE CHEMISTRY

A major driver of phenotypic diversity in plants involves plant defense methods aimed at minimizing damage inflicted by terrestrial consumers. These defense methods vary from mechanical deterrents such as spines and trichomes to chemical toxins such as tannins, cardenolides, and glucosinolates. Plant methods can further range from release of chemical volatiles to attract predatory insects towards an infestation, chemically signaling to nearby plants of impending attack, mimicry of insect eggs to deter oviposition, and reallocation of valuable nutrients from leaves to inaccessibly storage organs such as the roots and stem. Induced plant defenses also vary by the means of herbivore damage. Studies contrasting the use of actual herbivores to inflict damage, mimicked physical damage treatments, and chemical treatments (using plant signaling hormones with known involvement in herbivore and/or pathogen defense) find that different treatments can elicit different plant responses. Indeed there is evidence that plants respond differently depending on the attacker (such as using signals in the saliva of generalist versus specialist herbivores to elicit different responses).

In chapter III, we show that induced plant defenses to herbivory can have cascading effects on aquatic systems, suppressing decomposition by as much as 60% compared to trees receiving ambient levels of herbivory. We show in this chapter that much of this reduction in decomposition could be explained by the sharp decline in leaf nitrogen. While this indeed appears to be one very important component of a red alder tree's defense response, we now investigate the role plant secondary metabolites. Here we present high-resolution chemistry data of a tree's response to an herbivory treatment with and without supplemental fertilizer. We incorporate these data with our previously reported leaf nutrient data to elucidate the relative importance of leaf traits in driving ecosystem function.

We characterized relative abundance of 62 compounds, consisting largely of ellagitannins and diarylheptanoids, in a population of 84 red alder trees. Ellagitannins are an understudied group of tannins that have recently been the focus of several natural selection studies and we have found previous evidence that they are strongly predictive of intrinsic red alder leaf quality to aquatic decomposer communities. Diarylheptanoids have been the recent focus of biomedical research, and have been investigated for their potential role in cancer treatments. The ecological literature however remains to find a strong role of these compounds in plant defense against consumers.

The same compounds were typical found in trees across all four treatments, but at different relative abundances. We are coarsely classifying peaks # 1 – 2 as chlorogenic acid derivatives, peaks # 3 – 41 as ellagitannins, and peaks # 42 - 63 as diarylheptanoids (Fig 6.A.1). Prior to implementing the experimental treatments, we found that secondary metabolite chemistry was similar across treatment groups (Fig 6.1). Immediately after experimental treatments, the group of trees given both the phosphorus fertilizer and simulated herbivory treatment diverged significantly from all other treatment groups (Fig 6.1: discriminant function 2: Wilk's $\lambda = 0.510$, $\chi_{152}^2 = 92.9$, $p = 0.004$, 82% correct reclassification and 61% classified correctly with cross validation; paired t-test of discriminant scores $t = 5.24$, $p < 0.001$). The model retained a complex set of 21 ellagitannins and diarylheptanoids weighting these two discriminant functions (see Table 6.A.1).

To further illustrate this shift in secondary metabolite composition, we ran a separate model using only the post-treatment data points (Fig 6.2: Wilk's λ = 0.015, p = 0.001, 96% correct reclassification and 45% classified correctly with cross validation, Appendix 6.A.2). As we reported previously (Jackrel and Wootton 2015a), leaf decomposition rates in streams were lowest among the tree group given the experimental herbivory and fertilizer treatments. Here, we illustrate that this treatment group differs in secondary metabolite chemistry, and further that the group centroids for each treatment group along the first discriminant function are ordered from the group that decomposed the most (fertilized group) to the group that decomposed the least (fertilized + herbivory group) (Fig 6.2). This divergence in secondary metabolite chemistry significantly predicts leaf decomposition in streams (Fig 6.3a, 6.3b) but not soils (Fig 6.3c).

In addition to an overall shift in secondary metabolites, we observe a similar pattern when considering only ellagitannins. We found a significant model retaining 21 ellagitannins again distinctly separated the fertilizer and herbivory group (Figure 6.A.2: discriminant function 2: Wilk's λ = 0.558, χ_{152}^{2} = 80.46, p = 0.040). We did not however find a significant model using only diarylheptanoids (Appendix 6A). We then completed further analyses on the fertilized group of trees because the effect of the simulated herbivory treatment appeared particularly strong when paired with fertilizer. Among the fertilized group of trees, we find that trees that had shared similar secondary metabolite composition diverged significantly along an axis of 22 ellagitannins and diarylheptanoids (Figure 6.A.4), as well an ellagitannin-only model (Fig. 6.4, Figure 6.A.3). We highlight eight of these compounds that shift significantly among the fertilizer-herbivory treatment group but not among the fertilizer-only treatment group (paired t-tests, # 4: t_{18} = 4.39, p < 0.001; # 11: t_{18} = 3.31, p = 0.004; # 12: t_{18} = -2.14, p = 0.046; #16 t = -

2.65, $p = 0.016$; # 42: $t_{18} = -3.76$, $p = 0.0014$; # 45: $t_{18} = -2.52$, $p = 0.021$, # 52: $t_{18} = -2.31$, $p = 0.033$; # 61: $t_{18} = 2.87$, $p = 0.010$, Fig. 6.5).

In addition to these shifts in secondary metabolites, trees across all four treatment groups tended to decline in Nitrogen (from $\mu = 2.78\% \pm 0.45$ S.D. or 17.38 C:N ± 3.03 to $\mu = 2.44\% \pm 0.54$ or 20.97 C:N ± 5.73). However the fertilizer and herbivory treatment group, which showed the strong shift in secondary metabolite composition, also declined most sharply in Nitrogen (to an average of 2.24%, or 24.02 C:N, paired t-test $t = -4.27$, $p < 0.001$) (Fig 6.1). Lastly, using this subset of fertilized trees that demonstrated the most clear shift in secondary metabolite composition, we found that both leaf secondary metabolite composition and C:N strongly predicted leaf decomposition rate in streams (C:N $t_{11,27} = -3.83$, $p = 0.0028$; secondary metabolites $t_{11,27} = 3.99$, $p = 0.0021$, Table 6.B.1).

We conclude that red alder trees allocate excess nutrients (via phosphorus fertilizer) towards shifting secondary metabolite composition of their leaves. This synergistic interaction of an altered phenolic profile combined with nutrient suppression evidently leads to reduced consumption by aquatic decomposers.

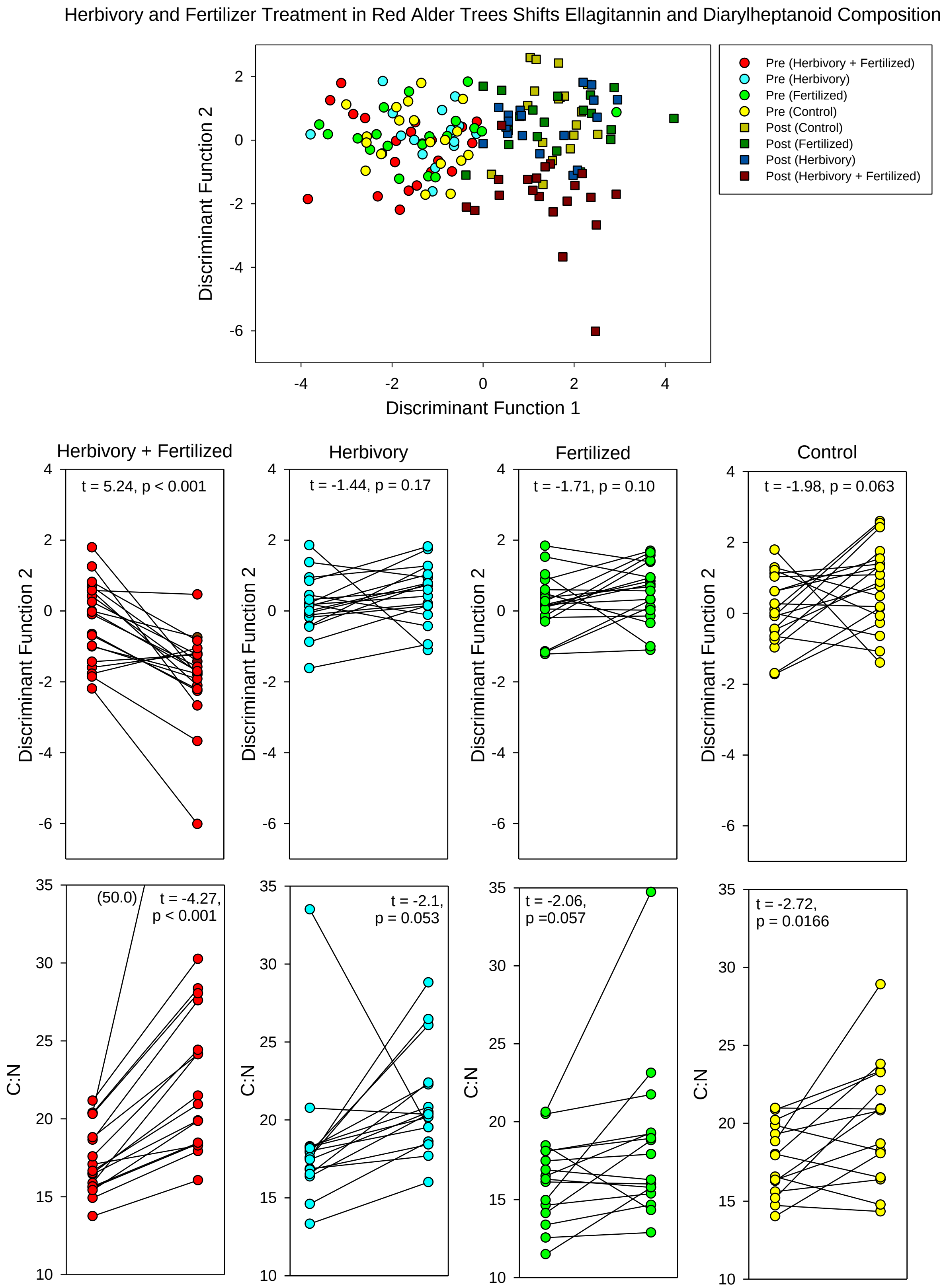

Figure 6.1: Red alder trees given an herbivory and fertilizer treatment shift significantly in leaf ellagitannin and diarylheptanoid composition (see variables most strongly weighting discriminant functions in Table 6.A.1. Similarly, trees given the herbivory and fertilizer treatment also decline sharply in Nitrogen (as previously reported).

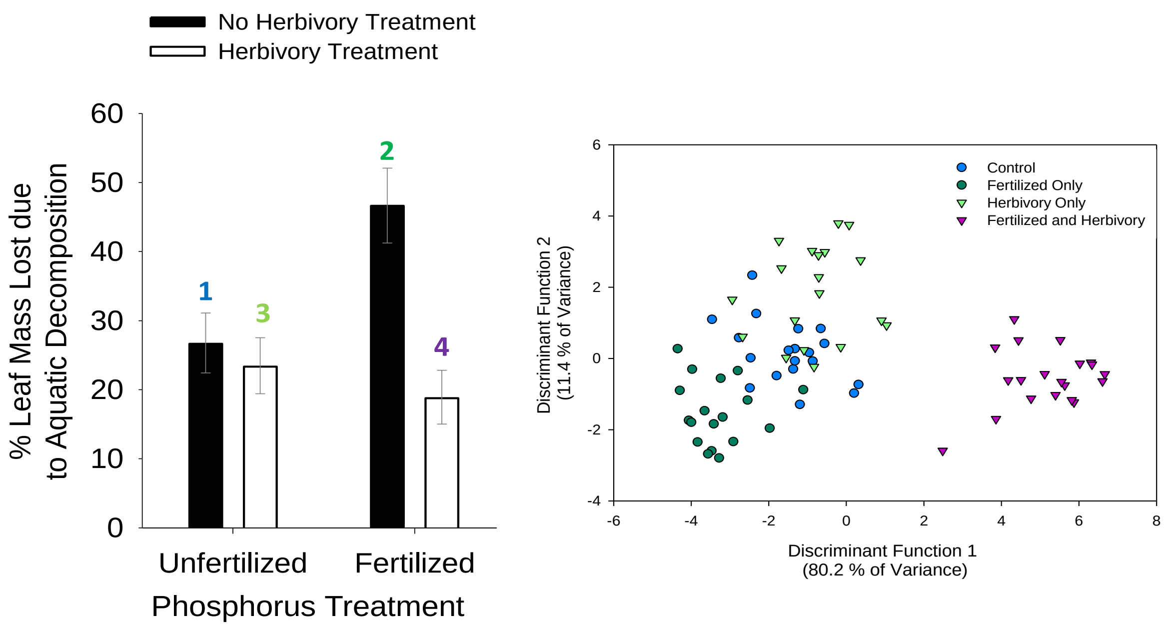

Figure 6.2: (*a*) Reprinted figure from (Jackrel and Wootton, 2015) showing residual effect (mean ± s.e.) of herbivory and fertilizer treatments on aquatic decomposition of red alder from analysis of variance after factoring out deployment location. (*b*) Divergence of secondary metabolite composition of 78 riparian alder trees after fertilizer and herbivory treatments.

.

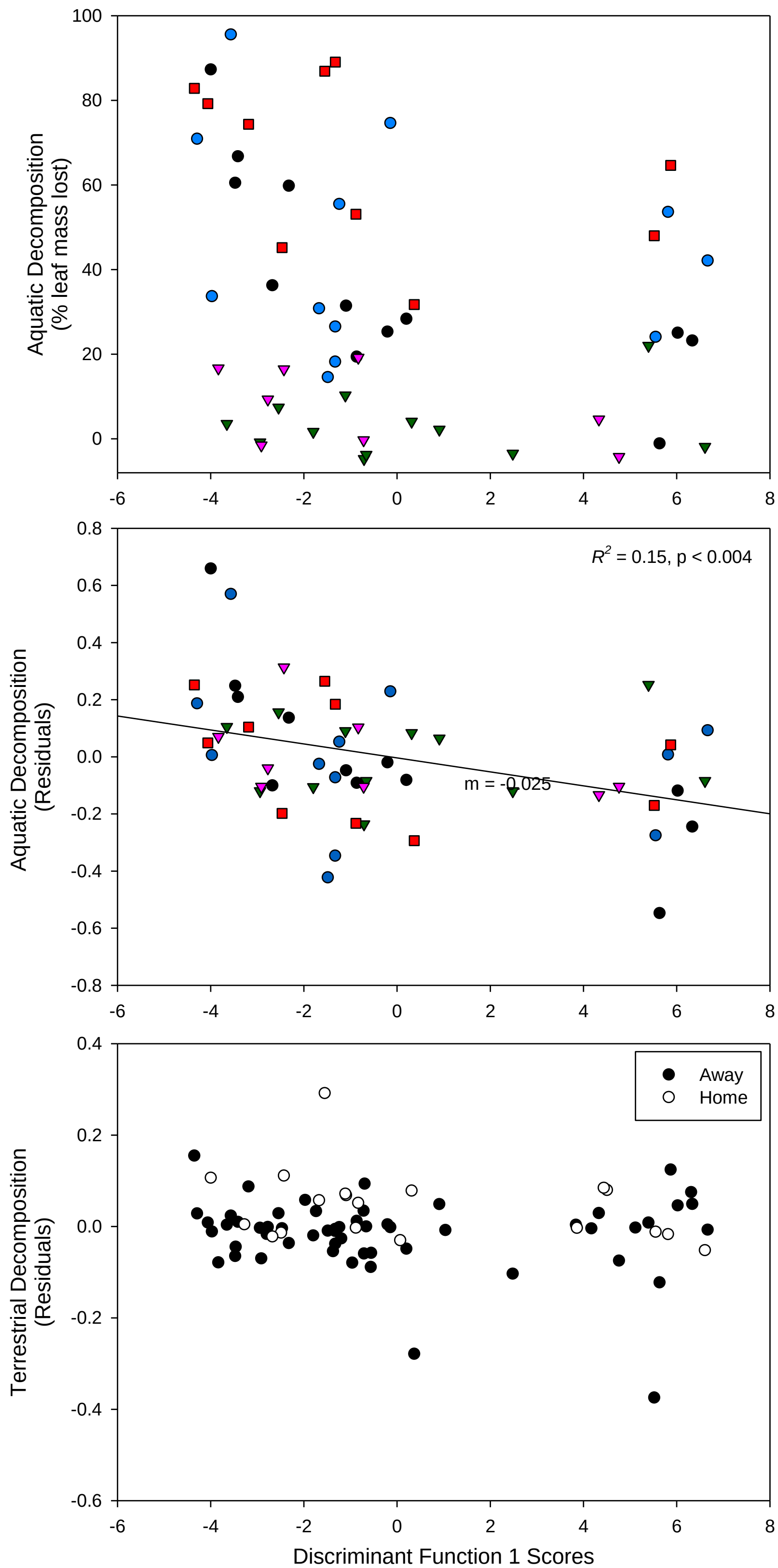

Figure 6.3: (*a*) Secondary metabolite composition as indicated by discriminant function 1 scores predicts aquatic leaf decomposition in streams. (*b*) Regression analysis illustrating predictive power of discriminant scores in predicting aquatic leaf decomposition rate in streams ($F_{1,52} = 9.217$, $p = 0.0037$). Note regression standardizes across multiple rounds of experiments (round indicated by color) by extracting residuals of aquatic decomposition after factoring out deployment location and tree block. (*c*) In contrast, secondary metabolite composition did not predict rate of leaf decomposition in soil. Regression is used to standardize across multiple rounds of experiments by extracting residuals of terrestrial decomposition after factoring out tree block. Also note that as previously reported (Jackrel and Wootton, 2015), the immediately local tree to the deployment location showed significant higher decomposition rates than other nearby trees in the block (suggesting a local preference).

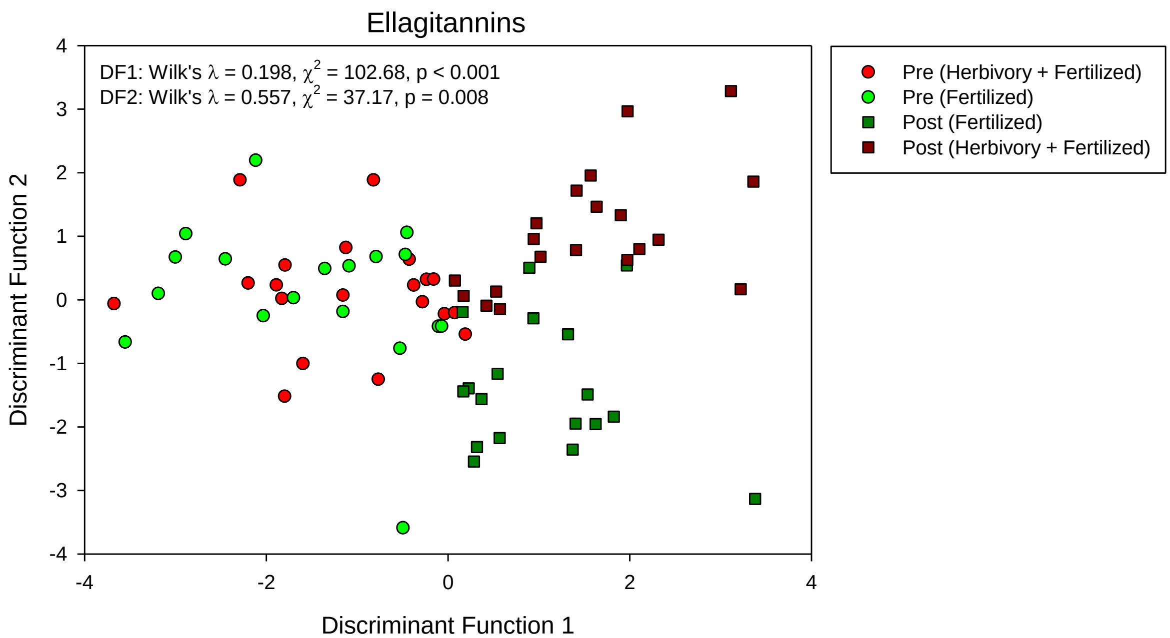

Figure 6.4: Among trees receiving the fertilizer treatment, those trees receiving versus not receiving the herbivory treatment diverged significantly in ellagitannin composition. Compounds most strongly influencing this separation are reported in Appendix 6.A.3.

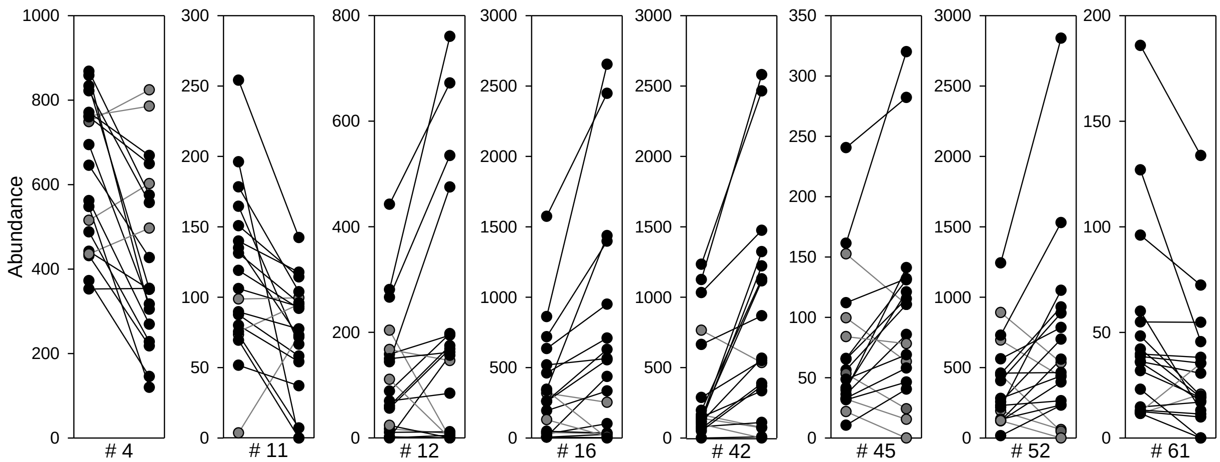

Figure 6.5: Eight compounds that changed significantly in relative concentration following a fertilizer and herbivory treatment, but did not change in the fertilizer only group. All shown are significant paired t-tests with the pre-treatment concentration on the left connected to the post-treatment concentration on the right. Gray shading emphasizes the few trees showing opposing shifts in concentration. Numbering corresponds to Figure 6.A.1.

Appendix 6A: Detailed secondary metabolite data.

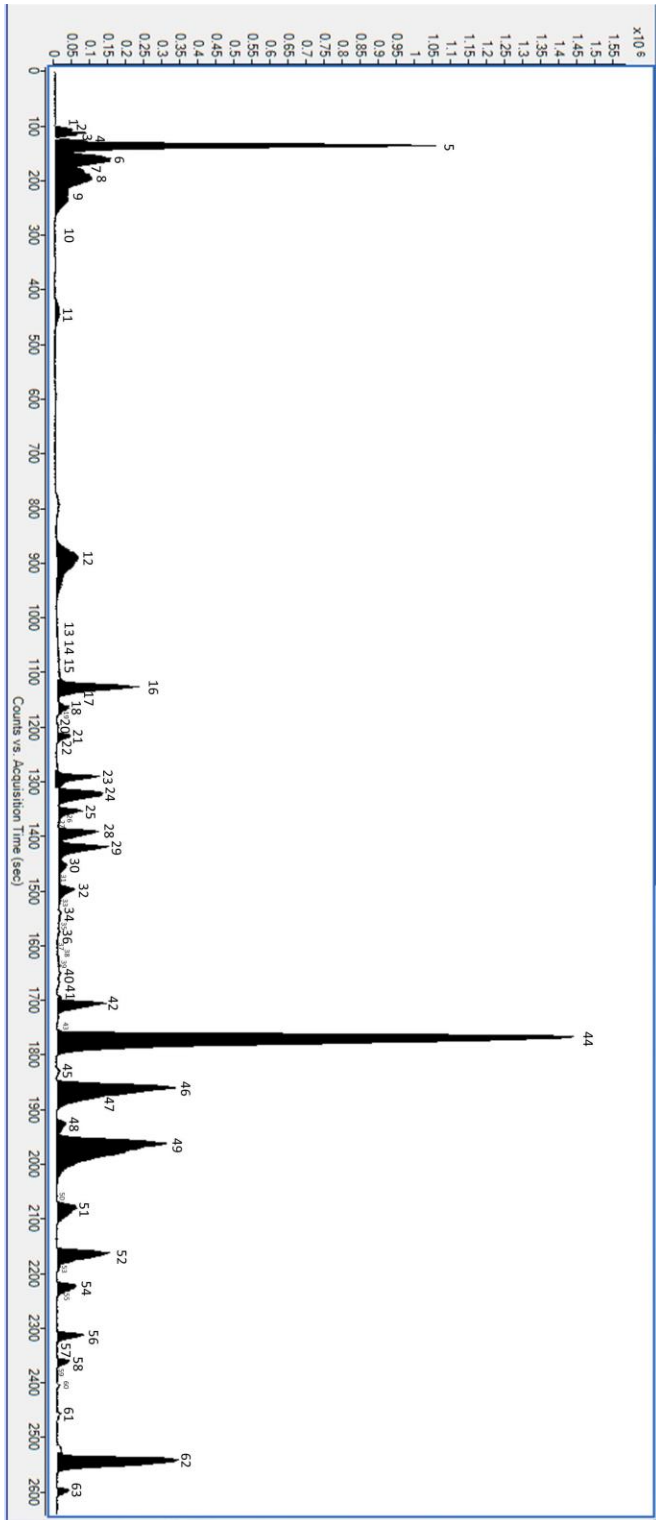

Figure 6.A.1: Example chromatogram from a red alder tree that was given both the fertilizer and herbivory treatments.

Table 6.A.1: Trees receiving both the fertilizer and herbivory treatment shifted significantly in ellagitannin and diarylheptanoid composition. Bolding in the table below highlights those compounds that most strongly influence separation along discriminant function 2.

Variable	DF1 Standard Coefficient	DF2 Standard Coefficient
# 11	-0.576	0.484
# 12	0.425	-1.005
# 14	0.174	0.426
# 16	-0.444	0.512
# 18	-0.177	-0.922
# 19	0.618	1.414
# 20	-0.74	-0.902
# 21	0.151	-0.584
# 22	0.055	-0.406
# 27	0.8	0.45
# 34	-0.169	-0.519
# 36	-0.129	0.642
# 40	-0.486	0.383
# 41	-0.049	-0.616
# 44	0.726	0.666
# 49	0.103	0.652
# 54	0.299	0.831
# 56	0.164	-0.497
# 58	-0.56	-0.804
# 60	0.085	-1.433
# 61	-0.065	1.533

Table 6.A.2: Trees that had received the four treatment groups diverged significantly in their secondary metabolite composition (Fig 6.2b of the main text). Bolding in the table below highlights those compounds that most strongly influence separation along discriminant function 1.

Variable	DF1 Standard Coefficients	DF2 Standard Coefficients
# 3	-1.065	-0.142
# 4	3.137	-0.077
# 5	-2.309	0.07
# 7	-3.356	0.281
# 8	**7.072**	-0.323
# 10	1.84	1.059
# 11	-3.392	0.558
# 12	0.844	0.056
# 13	3.343	1.281
# 15	-1.557	-0.255
# 16	1.903	-0.755
# 18	3.162	-4.087
# 19	-3.233	2.645
# 20	4.531	-0.475
# 21	5.351	0.697
# 22	5.923	-0.579
# 23	-5.595	-0.427
# 24	-4.334	-0.164
# 25	-4.378	-1.038
# 26	**6.244**	-0.734
# 27	-2.466	0.36
# 29	**8.276**	3.417
# 30	**-11.968**	-0.155
# 31	-2.842	-2.561
# 32	1.185	0.169
# 34	1.476	0.842
# 36	-3.251	-0.114
# 37	1.258	-0.301
# 38	1.674	-0.241
# 39	-1.273	0.535
# 41	3.407	1.147
# 42	0.877	3.274
# 45	-4.867	-1.398
# 47	-2.744	-0.358
# 48	3.082	1.83
# 49	-3.489	1.543
# 50	2.914	-0.66
# 51	-1.007	-0.587
# 52	2.894	-2.134
# 53	-3.816	0.786
# 54	-2.373	-0.631
# 56	1.461	-1.247
# 59	4.46	-0.1
# 60	2.514	-2.545
# 61	-2.357	2.547
# 62	-1.995	-0.477

Figure 6.A.2: Trees receiving both the fertilizer and herbivory treatment shifted significantly in ellagitannin composition. Bolding in the table below highlights those compounds that most strongly influence separation along discriminant function 2. In contrast to this ellagitannin-only model and the combined model in Figure 1, we found no significant model separating any of the post-treatment groups using only diarylheptanoids (data from non-significant model not shown).

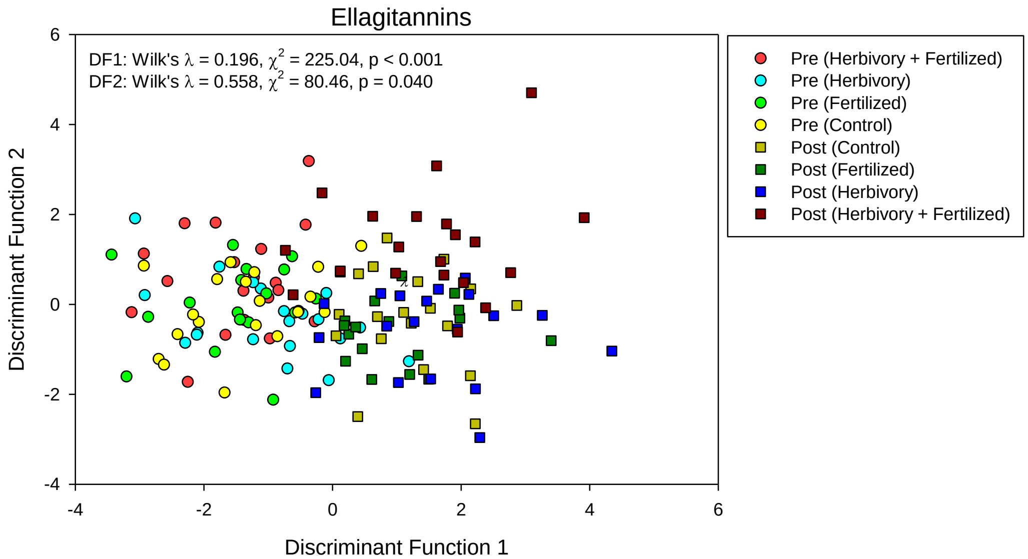

Variable	DF1 Standard Coefficients	DF2 Standard Coefficients
# 1	0.218	-0.331
# 9	0.243	0.292
# 11	-0.498	**-0.699**
# 12	0.358	**1.117**
# 15	-0.021	0.291
# 16	-0.277	**-0.503**
# 18	0.121	0.51
# 19	0.585	**-1.105**
# 20	-0.637	**0.877**
# 24	-0.261	**-0.607**
# 26	-0.623	0.335
# 27	0.687	-0.363
# 29	-0.578	**0.588**
# 30	0.469	**-0.612**
# 31	0.095	-0.6
# 32	-0.048	0.405
# 34	-0.021	0.484
# 36	-0.075	-0.256
# 37	0.01	**0.699**
# 41	0.288	**0.764**
# 42	0.426	-0.452

Figure 6.A.3: Among trees receiving the fertilizer treatment, those trees receiving the herbivory treatment versus not receiving the herbivory treatment diverged significantly in ellagitannin composition (Fig 6.3 of main text). Bolding in the table below highlights those compounds that most strongly influence separation along discriminant function 2.

Variable	DF1 Standard Coefficients	DF2 Standard Coefficients
# 7	-0.122	**2.115**
# 8	-0.609	-0.592
# 9	0.548	-0.578
# 11	-0.481	-0.275
# 16	0.409	**1.073**
# 17	-0.093	-0.817
# 19	0.678	**-1.337**
# 20	-0.464	**1.655**
# 22	-0.266	0.52
# 23	0.842	**-1.647**
# 26	-1.246	0.995
# 29	-0.913	**-1.097**
# 30	1.203	-0.963
# 31	0.211	-0.92
# 32	-0.835	**2.613**
# 34	0.294	0.387
# 35	-0.25	0.612
# 36	-0.162	**-1.277**
# 41	0.955	-0.472
# 42	0.347	0.25

Figure 6.A.4: Among trees receiving the fertilizer treatment, those trees receiving the herbivory treatment and those trees not receiving the herbivory treatment diverged significantly in ellagitannin and diarylheptanoid composition. Bolding in the table below highlights those compounds that most strongly influence separation along discriminant function 2 in the combined model. We did not however find a significant diarylheptanoid-only model (data from non-significant model not shown).

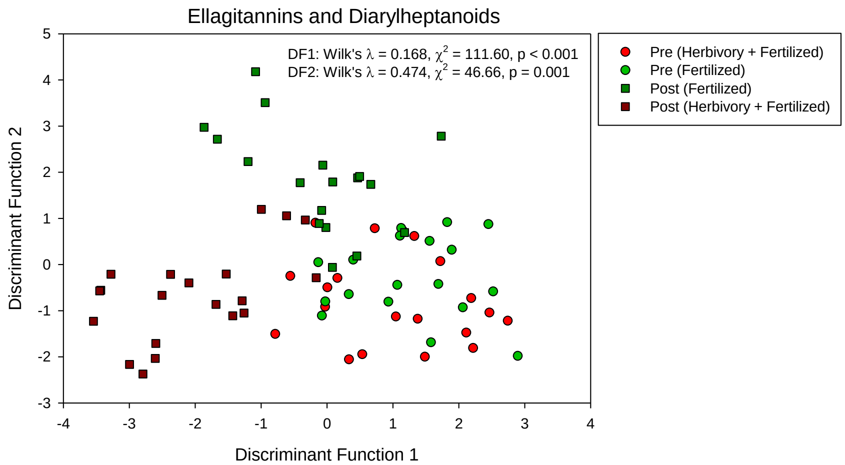

Variable	DF1 Standard Coefficients	DF2 Standard Coefficients
# 7	-1.624	-0.741
# 8	1.744	0.727
# 14	0.284	0.632
# 17	0.768	0.174
# 20	-1.06	-1.811
# 22	-0.27	-1.066
# 24	1.38	0.44
# 25	-1.13	-0.124
# 29	0.169	2.602
# 30	0.324	0.709
# 31	1.116	0.433
# 32	-0.3	-3.281
# 36	0.489	0.474
# 38	-0.421	-0.641
# 41	-0.93	1.025
# 42	-1.518	-1.905
# 44	-0.836	0.848
# 46	-0.215	-0.365
# 52	1.208	1.259
# 54	0.572	1.369
# 58	0.297	-0.788
# 60	0.313	0.372

Figure 6.A.5: Among the unfertilized groups, trees receiving an herbivory treatment diverged significantly in ellagitannin content compared to control trees. Bolding in the table below highlights those compounds that most strongly influence separation along discriminant function 2.

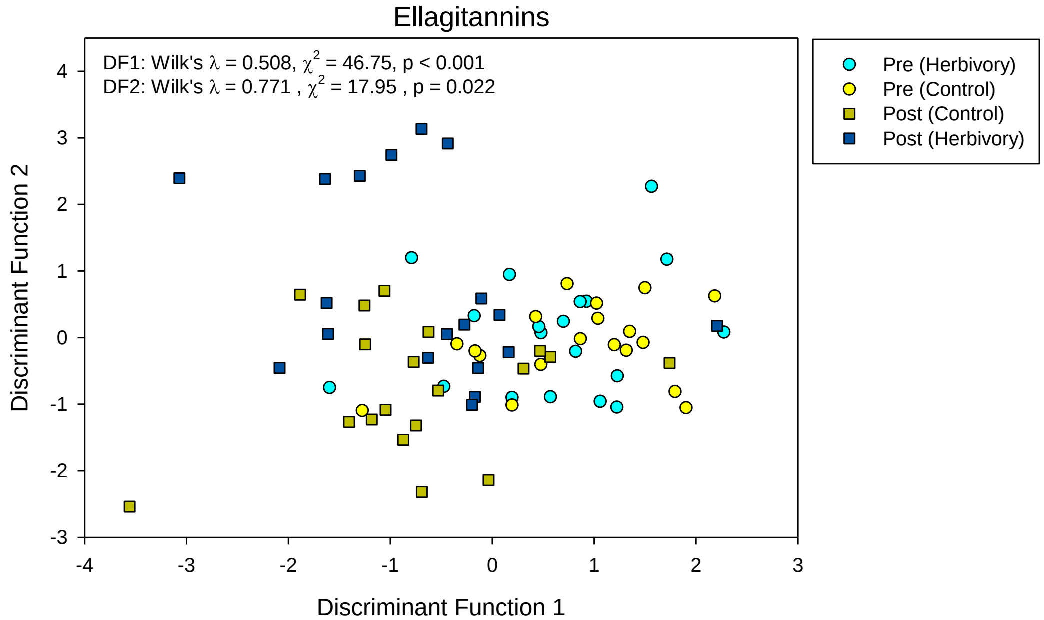

	DF1 Standard Coefficients	DF2 Standard Coefficients
# 6	1.146	0.287
# 9	-0.422	-0.64
# 10	-0.04	0.704
# 12	0.025	**1.068**
# 18	-0.071	-0.83
# 28	-0.714	-0.364
# 35	0.029	**0.907**
# 36	0.409	**-1.013**
# 41	0.135	0.722

Figure 6.A.6: Among the unfertilized groups, the group of trees receiving the herbivory treatment diverged significantly in ellagitannin and diarylheptanoid content compared to the control group of trees. Bolding in the table below highlights those compounds that most strongly influence separation along discriminant function 2. We did not however find a significant diarylheptanoid-only model (data from non-significant model not shown).

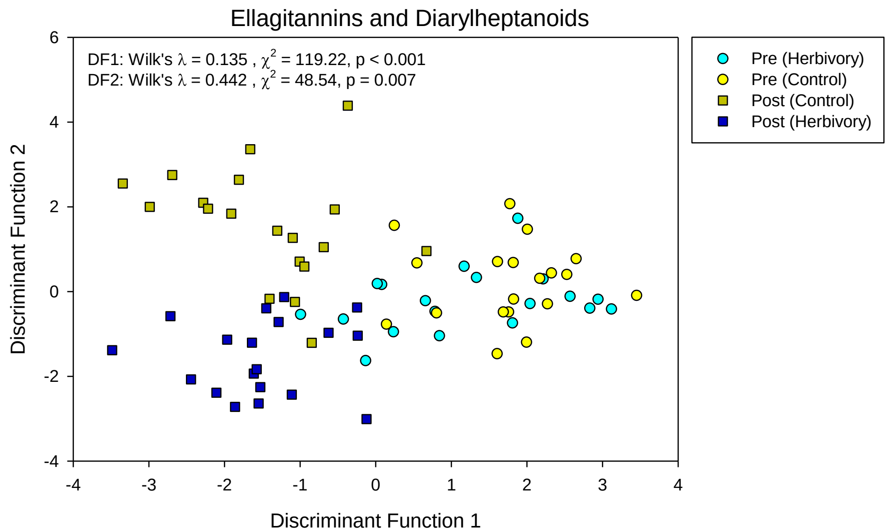

Variable	DF1 Standard Coefficients	DF2 Standard Coefficients
# 5	1.216	0.875
# 7	0.235	**1.848**
# 10	-0.867	-0.758
# 16	0.555	**-1.792**
# 18	0.253	**1.843**
# 19	-0.225	**-1.082**
# 20	1.628	**-1.167**
# 21	-1.567	0.768
# 22	-0.166	-0.691
# 23	-0.337	-0.932
# 29	-0.631	0.876
# 32	0.188	0.903
# 35	0.514	**-1.247**
# 36	0.45	0.73
# 38	-0.233	**-1.252**
# 39	0.464	-0.518
# 44	-0.459	0.56
# 45	1.123	**-4.191**
# 46	0.344	1.42
# 48	-1.591	**4.917**
# 50	-0.51	0.951
# 51	0.022	-0.717
# 53	0.319	**-1.622**
# 54	0.193	-0.775
# 56	0.358	**-1.758**
# 57	-0.253	**1.408**
# 58	0.024	0.671
# 63	-0.091	**1.525**

Appendix 6B: Variables predicting aquatic leaf decomposition.

Table 6.B.1: Among trees receiving the fertilizer treatment, C:N and secondary metabolite composition strongly predict aquatic leaf decomposition (stepwise mixed-effects linear regression, marginal $R^2 = 0.35$). Secondary metabolite composition was entered in the model via discriminant function scores (see Appendix 6A). Variables not retained in the model were % N, % P, % C, C:P, $N^{15}N^{14}$, $C^{13}C^{12}$.

Source	Estimated	t value	Pr(>|t|)
C:N	-0.144	-3.83	0.0028
Secondary Metabolites	0.137	3.99	0.0021

CHAPTER VII

IDENTIFYING THE PLANT ASSOCIATED MICROBIOME ACROSS AQUATIC AND TERRESTRIAL ENVIRONMENTS: THE EFFECTS OF PRIMER TYPE ON TAXA DISCOVERY

ABSTRACT

Plants in terrestrial and aquatic environments contain a diverse microbiome. Yet, the chloroplast and mitochondria organelles of the plant eukaryotic cell originate from free living cyanobacteria and Rickettsiales. This represents a challenge for sequencing the microbiome of plant tissue with universal primers, as ~99% of 16S rRNA sequences may consist of chloroplast and mitochondrial sequences. Peptide nucleic acid primers offer a potential solution by blocking the amplification of these host-associated sequences. We assessed the efficacy of chloroplast and mitochondria-blocking primers against a range of microbial taxa from soil, freshwater, and marine environments. While we found that the mitochondrial blocking primer appears to be a robust method for assessing animal-associated microbiota, Proteobacterial 16S rRNA binds to the chloroplast blocking primer, resulting in a strong sequencing bias against this group. We attribute this bias to a conserved 14 base pair sequence in the Proteobacteria that matches the 17 base pair chloroplast blocking primer. By scanning the Greengenes Database, we provide a reference list of the nearly 1500 microbial taxa that contain this 14 base pair sequence, including 48 families such as the Rhodobacteraceae, Phyllobaceriaceae, Rhizobiaceae, Kiloniellaceae, and Caulobacteraceae. To determine where these taxa are found in nature, we mapped this taxa reference list against the Earth Microbiome Project database. These taxa are abundant in a diversity of environments, particularly aquatic and semi-aquatic freshwater and marine habitats. While these primers may remain a feasible option for primarily terrestrial-based studies focused

on certain microbial taxa, we recommend caution for any studies using these methods for assessing relative abundance of diverse microbial phyla across multiple environments.

INTRODUCTION

Natural ecosystems contain an incredible diversity of microbiota, which remains largely undescribed. Recent advances in sequencing technologies have facilitated the description of this diversity throughout a range of terrestrial and aquatic biomes from the semi-natural environments of agricultural soils to the extreme environments of the deep sea (Caporaso et al. 2010, Gilbert et al. 2014). We are discovering the tremendous importance of free-living and organismal-associated microbiota to both ecosystem and organismal health and functioning (Zak et al. 2003, Smith et al. 2015). Continued advancement in this field demands increasingly sophisticated studies that contrast the microbiomes across habitats and trace the source-sink dynamics of these microbial communities. Vital to this aim is use of a common methodology that enables comparisons across environments and microbial taxa. Ribosomal RNA genes are the typical targets for amplicon sequencing because they are conserved across microbial taxa, yet sufficiently polymorphic for taxonomic assignment.

Plant chloroplast and mitochondrial organelles are evolutionarily derived from free-living Cyanobacteria and Rickettsiales (Margulis 1981). Sequencing the internal or external plant microbiome thus represents a particular challenge because these organelles retain the microbial rRNA of their ancestors. Sequencing plant tissue typically yields upwards of 99% chloroplast and mitochondrial sequences (Lundberg et al. 2012, Zarraonaindia et al. 2015). Intensive sequencing, where only the remaining 1% of sequences is analyzed after filtering out chloroplast, is rarely an economically feasible option. Instead, a new method that blocks the amplification of these organelles using peptide nucleic acid PCR clamps, thus sequencing only the remaining microbes, has been proposed (Lundberg et al. 2013). These synthetic oligomers physically block amplification of a contaminant by binding tightly and specifically to the unique contaminant sequence (von Wintzingerode, et al. 2000). Although use of these organelle blockers may help reveal rare taxa of a microbiome in the presence of eukaryotic plant material, it might also bias discovery rates if applied across habitats, such as aquatic systems that often contain many free-living Cyanobacteria and Rickettsiales, by blocking amplification of nucleic acids of taxa closely related to organelles.

In our study, we aim to describe the benefits and drawback of using universal Earth Microbiome Project primers versus organelle-blocking clamps for studies across a range of environments and microbial taxa. By sequencing identical samples from terrestrial, marine and freshwater habitats we find that organelle-blocking clamps are strongly biased against many taxa, particularly the Proteobacteria (including 48 families such as the Rhodobacteraceae, Phyllobaceriaceae, Rhizobiaceae, Kiloniellaceae, and Caulobacteraceae).

We trace this bias to a 14 base pair conserved region that matches the chloroplast-blocking primer. We provide a scan of the Greengenes Database for other taxa containing this conserved region, and using the Earth Microbiome Project Database, demonstrate that these particular taxa are abundant in many aquatic, terrestrial, and animal-associated environments. We conclude that use of these organelle blocking clamps poses a considerable bias for any studies aiming to eventually compare a plant-associated microbiome with a diversity of other environments.

METHODS

Field collections

Our field samples were collected for a number of different studies and are considered here only for comparing amplification methods. The majority of samples were from an experiment designed to test for the direct versus indirect effects of individual variation within red alder tree leaf litter on microbial colonization in streams. The experiment was conducted in 2013 on the Hoko and Sekiu Rivers on the Olympic Peninsula of Washington (48° 15′29.58 N, 124° 21′8.59 W). We carried out a reciprocal transplant design in which fresh green leaves from individual trees growing along rivers were enclosed in mesh leaf packs and were either placed in the adjacent river or in a different river (4.5 km away). Our reciprocal transplant design is described in detail elsewhere (Jackrel and Wootton 2014, Jackrel et al. 2016). We sequenced the microbiome of a subset of these samples for primer comparison. From each red alder tree, we constructed leaf packs containing 16 leaves each. Four leaves from each of these leaf packs were removed after 5, 10, 15, and 20 days of incubation, sealed in WhirlPak bags, and frozen.

At each of these four time points, we also sampled the freshwater microbiota immediately upstream of each leaf pack deployment location. Six liters of river water were pumped through Sterivex™ filters (EMD Millipore, Darmstadt, Germany) using a peristaltic pump. Immediately before and after the 20 day experiment, we collected both soil samples beneath each source tree and fresh leaves from each tree. All samples were kept cool and frozen at -20°C upon returning from the field locations, and then stored at -80°C at Argonne National Labs until processing.

Seawater samples were collected using the same method described above for freshwater samples. Collections occurred on the outer coast of Washington State both immediately from the shore by standing on rocky bench Tatoosh Island, 48.39° N, 124.74° W and offshore at 48.432 N, 124.738 W and 48.439 N, 124.831 W at approximately 70 m and 340 m total depth, respectively. The offshore samples were taken in July and August of 2011 and 2012 at both surface depths in the photic zone as well as depths below the photic zone (100, 125, 140, 300, 325 m) where 16S rRNA sequences from phototrophs would be minimal. Offshore samples were collected from the R/V Clifford Barnes with casts from a 12-sample CTD array (Seabird Electronics, Bellevue, Washington, USA) with 10-L Niskin bottles (General Oceanics, Miami, Florida, USA). Environmental variables associated with this collection are reported in Pfister et al. 2014 and online (http://www.bco-dmo.org/dataset/489045/data).

We extracted DNA from all samples using PowerSoil DNA Isolation Kits (MO BIO Laboratories, Carlsbad, California, USA). For water samples, Sterivex casings were cut with PVC cutters and half of the filter paper was removed, then ground and extracted as a solid sample. After extraction, we amplified the 254bp length V4 region using the Earth Microbiome Project universal primers (515F primer and 806 GoLay-barcoded reverse primers) (Caporaso et al. 2012) with and without the mitochondrial and chloroplast blocking PNA clamps. The mPNA sequence to block mitochondria contamination is GGCAAGTGTTCTTCGGA and the pPNA sequence to block chloroplast contamination is GGCTCAACCCTGGACAG (PNABio, Thousand Oaks, California, USA). We pooled PCR product and cleaned products using an UltraClean®PCR Clean-Up Kit (MO BIO Laboratories, Carlsbad, California, USA). We sequenced DNA fragments in a MiSeq 2x150bp run at the Next Generation Sequencing Core at Argonne National Laboratory following the procedures of Caparaso et al. (2012).

Analysis

We performed all sequence quality analyses and microbial community difference metrics among samples using the QIIME pipeline (Caporaso et al. 2010). We classified operational taxonomic units (OTUs) from the Illumina reads at the 97% similarity level using open reference-based clustering with uclust. We assigned a taxonomy using the RDP taxonomic assignment comparing the OTUs sequences against the Greengenes database (version 13_8). We generated all rarefaction, alpha diversity, principal coordinate and Procrustes analyses following the QIIME pipeline (Caporaso et al. 2010). We used Procrustes analysis to statistically compare the shapes of two sets of corresponding points. To minimize the distance between the two set of points, the second matrix is superimposed on the first matrix after translating, scaling and rotation (Gower 1975). In our study, our matrices are β-diversity outputs comparing samples amplified with EMP primers versus the same samples amplified with PNA primers. We also identified the taxa significantly enriched and therefore responsible for the differences observed via paired t-tests and corrected for multiple comparisons via Benjamini-Hochberg False Discovery Rate (R Development Core Team, 2014, (Benjamini and Hochberg 1995, Shogan et al. 2014, De Filippis et al. 2016). We then scanned each OTU sequence in our dataset for complete or partial matches (including all 12-mer, 13-mer, and 14-mers) to the mPNA and pPNA sequences (Geneious version 9.0.5). We found no complete matches, but we did find a subset of OTUs with a partial 14 of 17 base pairs match (***GGCTCAACCCTGGA***CAG) to the pPNA chloroplast-blocking sequence. We then scanned the entire Greengenes database for other OTUs not represented in our dataset that contained this same 14 base pair sequence.

Metanalysis

Our new data described above draws comparisons across samples that were analyzed identically throughout OTU picking and all downstream analyses. In our metanalyses, we instead drew comparisons using existing BIOM tables for all studies in the Earth Microbiome Project Database (we excluded studies from lab systems or the built environment) (QIITA, https://qiita.ucsd.edu/) (Appendix 7D). Samples included in this database may have used varied OTU picking methods, while our new dataset controls for these potential contributing sources of variation. For the datasets included in the metanalysis, we removed all chloroplast and mitochondria sequences, and rarefied all samples to 5000 sequences. Some datasets were excluded because they contained only samples with less than 5000 sequences (see Appendix 7D). We scanned the remaining samples for all OTUs containing the 14 base pair match to the pPNA clamp (see this reference list of OTUs in the Supplementary Tables). Those samples containing at least 50 sequences of OTUs in this reference list (i.e., at least 1%) were assembled into Table 7.1, and we describe the environmental sample type using the metadata made available by the authors in the EMP Database.

RESULTS

Our dataset generated using the EMP method generally contained greater percentages of chloroplast and mitochondrial sequences than the dataset generated from the identical samples amplified using the PNA method. For example, after rarefaction to even sampling depth, the proportion of remaining sequences in our fresh red alder leaf samples that were of chloroplast and mitochondrial origin was reduced from 77.4 ± 17.0% (mean ± 1 S.D.) chloroplast and 1.25 ± 0.47% mitochondria of all sequences using the EMP method to 4.84 ± 3.17% chloroplast and

4.29 ± 6.06% mitochondria using the PNA method. Similarly red alder leaves decomposing in river water contained 11.6 ± 7.03% chloroplast and 1.05 ± 0.51% mitochondria with the EMP method, and only 0.21 ± 0.33% and 1.25 ± 0.67% with the PNA method. Seawater, freshwater, and soils contained similar percentages of chloroplast and mitochondria regardless of method (Seawater: 5.54 ± 11.7% chloroplast and 0.02 ± 0.058% mitochondria with EMP vs. 6.38 ± 12.5% chloroplast and 0.045 ± 0.125% mitochondria with PNA; Freshwater: 0.208 ± 0.229% chloroplast and 0.0056 ± 0.01% mitochondria with EMP vs. 0.189 ± 0.14% chloroplast and 0.0132 ± 0.0121% mitochondria with PNA; Soils: 0.236 ± 0.20% chloroplast and 0.0165 ± 0.0155% mitochondria with EMP vs. 0.498 ± 0.227% chloroplast and 0.043 ± 0.036% mitochondria with PNA.

Beyond this targeted reduction in chloroplast and mitochondrial amplification, sequencing identical samples across a range of aquatic and terrestrial environments demonstrated that the EMP versus PNA methods yielded substantial discontinuities. The Proteobacteria phylum contained a number of taxa amplified at significantly different relative abundances in the EMP versus PNA-EMP sequence data. We illustrate that samples particularly enriched in Alphaproteobacteria, such as seawater, show sharp discrepancies when amplified with EMP versus PNA primers (Fig 7.1a). In particular, the Rhodobacterales (including Octadecabacter, Pseudoruegeria, Loktanella, and Sulfitobacter species), Rhizobiales (include the Phyllobacteriaceae and Hyphomicrobiacea families), and Kiloniellales (family Kiloniellaceae) were all lower in relative abundance in seawater when amplified with PNA primers (all $p < 0.01$ with false discovery rate correction, Table 7.C.4). Pairwise differences for all freshwater, submerged alder leaves, fresh alder leaves, and soil samples are illustrated in Appendix 7C. In addition to these results in seawater, we again found particular taxa to be of lower abundance in most of these samples when amplified with PNA primers (Fig 7.C.1 – Fig 7.C.3). In submerged alder leaf samples, Alphaproteobacteria (including Rhodobacterales and Caulobacterales), Deltaproteobacteria (Bdellovibrionales), Spartobacteria (Chthoniobacterales), and other taxa were amplified at lower abundances with PNA primers (Table 7.C.3, all $p < 0.05$ with false discovery rate correction). Further, while our freshwater and soil results were not significant after false discovery rate correction, the same patterns were observed: in freshwater samples, Alphaproteobacteria (including Rhodobacterales, Rhizobiales, and Rickettsiales), Betaproteobacteria (including Methylophilales and Burkholderiales), Deltaproteobacteria (Myxococcales), Flavobacteria, Actinobacteria, and other taxa (Table 7.C.1) were amplified at lower abundances with PNA primers (all $p < 0.05$ prior to correction for false discovery rate, Table 7.C.1). In soil samples, we found PNA primers amplified a number of rare taxa at lower abundances, including the Alphaproteobacteria (Rhodobacterales, Caulobacterales, and Sphingomonadales), Betaproteobacteria (Burkholderiales), Deltaproteobacteria (Myxococcales), Spartobacteria (Chthoniobacterales) and other taxa (Table 7.C.2, all $p < 0.02$ prior to correction for false discovery rate). Lastly, our fresh alder leaf samples were highly variable, and although we did not find significant trends in this group, those samples containing a high abundance of Actinobacteria and Alphaproteobacteria when amplified with EMP primers showed sharp declines in these groups when amplified with PNA primers.

We found that nearly all of these taxa amplified at lower abundances across these samples have a common conserved 14 base pair sequence that matches most of the 17 base pair pPNA chloroplast blocking primer (***GGCTCAACCCTGGA***CAG). We provide a full list of OTUs that contain this conserved 14 base pair sequence in the Supplementary Tables. We found that 1,405

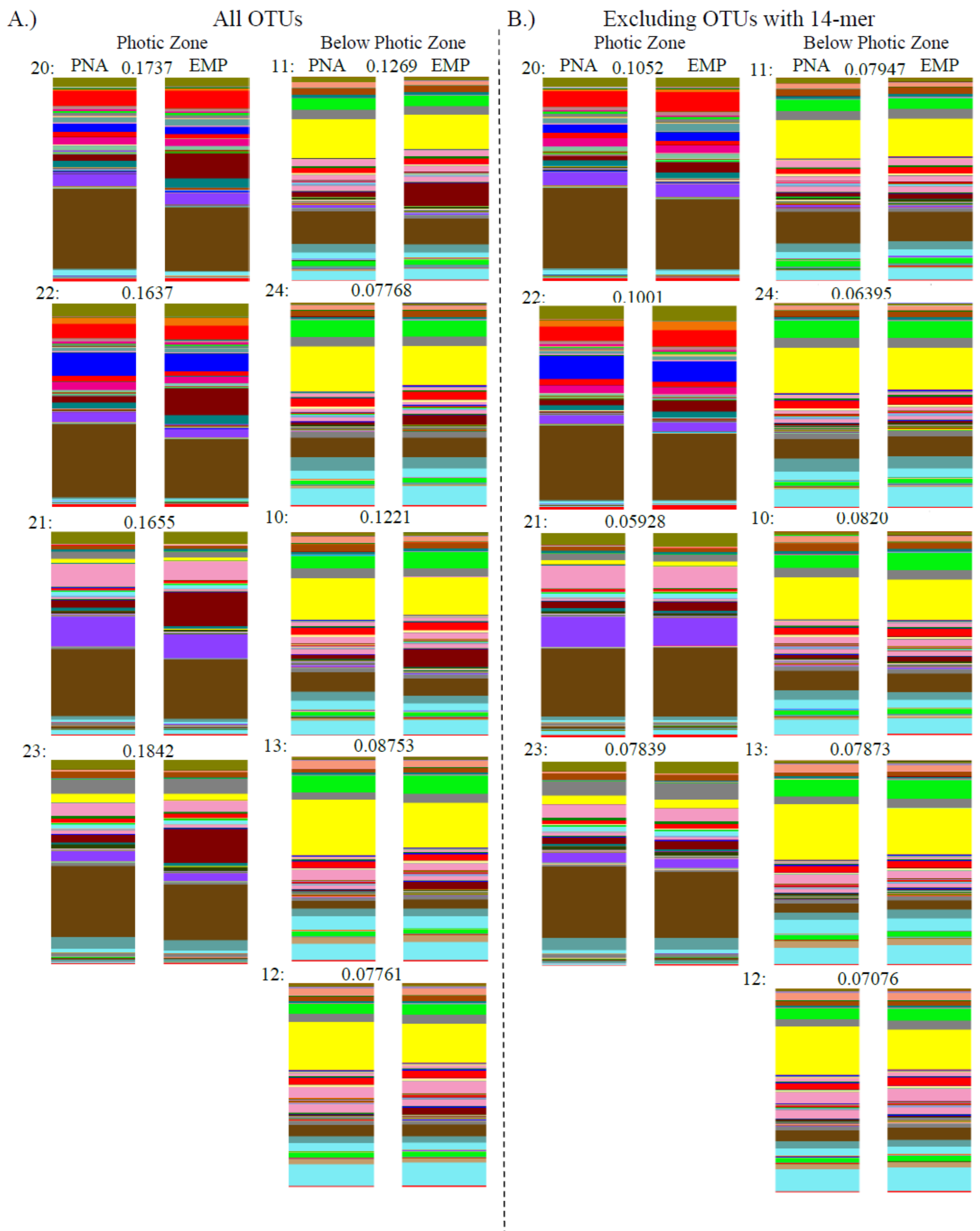

Figure 7.1: Seawater samples from Tatoosh Island, Washington, including onshore surface (#20, #22), offshore surface (#21, #23), 100 m deep (#11), 125 m deep (#24) 140 m deep (#10), 300 m deep (#13) and 325 m deep (#12). Relative abundance of microbial taxa at the family level depicted via color. (A) Includes all OTUs after filtering out chloroplast and mitochondria, and (B) excludes all chloroplast, mitochondria and OTUs listed in the Supplementary Tables. Weighted UniFrac distances listed adjacent to each sample number quantify the similarity of the microbial community amplified with each primer method. [See appendices for all habitat results].

OTUs in the Greengenes Database match this 14 base pair sequence, and therefore likely bind to the pPNA primer. Proteobacteria comprised 76% of these Greengenes OTUs. Our dataset also contains OTUs not yet included in the database, and 6,391 of these OTUs unique to our dataset match this 14 base pair sequence as well. When we filtered out this 7,796 OTU list and repeated our pairwise comparisons across seawater, freshwater, leaf and soil samples, we found greater community similarity between replicate samples amplified with the two methods via weighted UniFrac distances (seawater comparisons: paired t-test, $t_8 = 4.01$, $p < 0.01$, Fig 7.1b; and Appendix 7C for other sample comparisons). Many other OTUs in the Greengenes Database contained subsets of the 14-mer described above. A total of 1,887 OTUs contained the 13-mer (***GGCTCAACCCTGG***ACAG) and 2,381 OTUs contained the 12-mer section (***GGCTCAACCCTG***GACAG). The discrepancies between our replicate samples that remain even after filtering out taxa listed in the Supplementary Tables may be due to such taxa with similar sequences that may also bind to the pPNA primer. In contrast, when we scanned the Greengenes Database for all 12-mer subsections of the mPNA primer, we found no matches and therefore conclude that this clamp likely remains broadly useful for eukaryotes, including animal-associated studies.

We next aimed to compare these amplification methods by specifically contrasting communities where the abundance of photosynthetic organisms differed. Using our Tatoosh seawater samples that were collected at varying depths, we compare these two amplification methods for surface samples (which should contain phototrophic communities) versus samples 100m and deeper (which in contrast should be dominated by chemolithotrophic communities). Weighted UniFrac distances between replicated samples were used to quantify community similarity (see Fig 7.1 for the distance metric for each pairwise comparison). Amplification

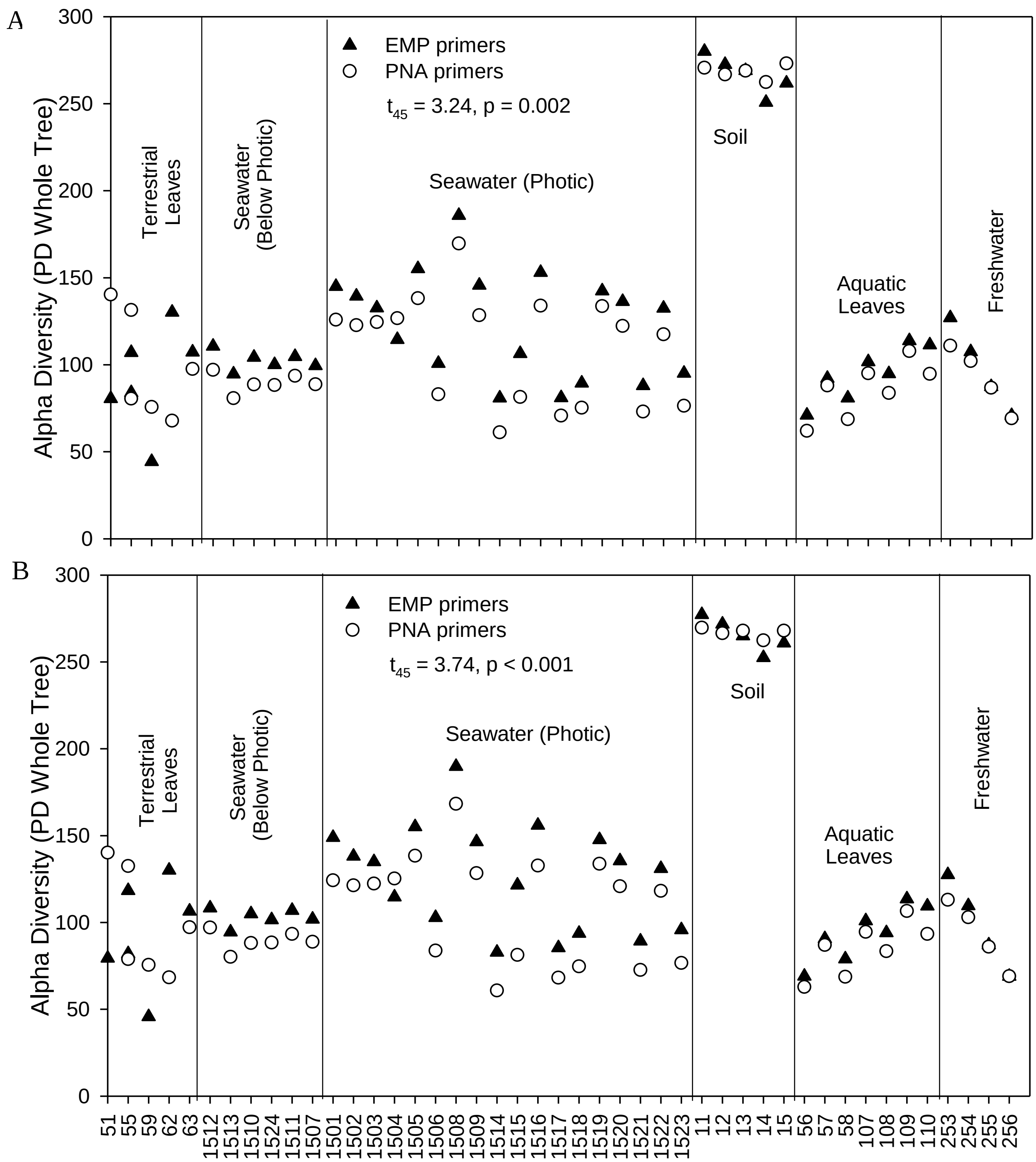

Figure 7.2: Alpha diversity is consistently higher with EMP primers than PNA primers both when (*a*) filtering out chloroplast and mitochondrial sequences and when (*b*) filtering out chloroplast, mitochondrial sequences, and OTUs in the Supplementary Tables.

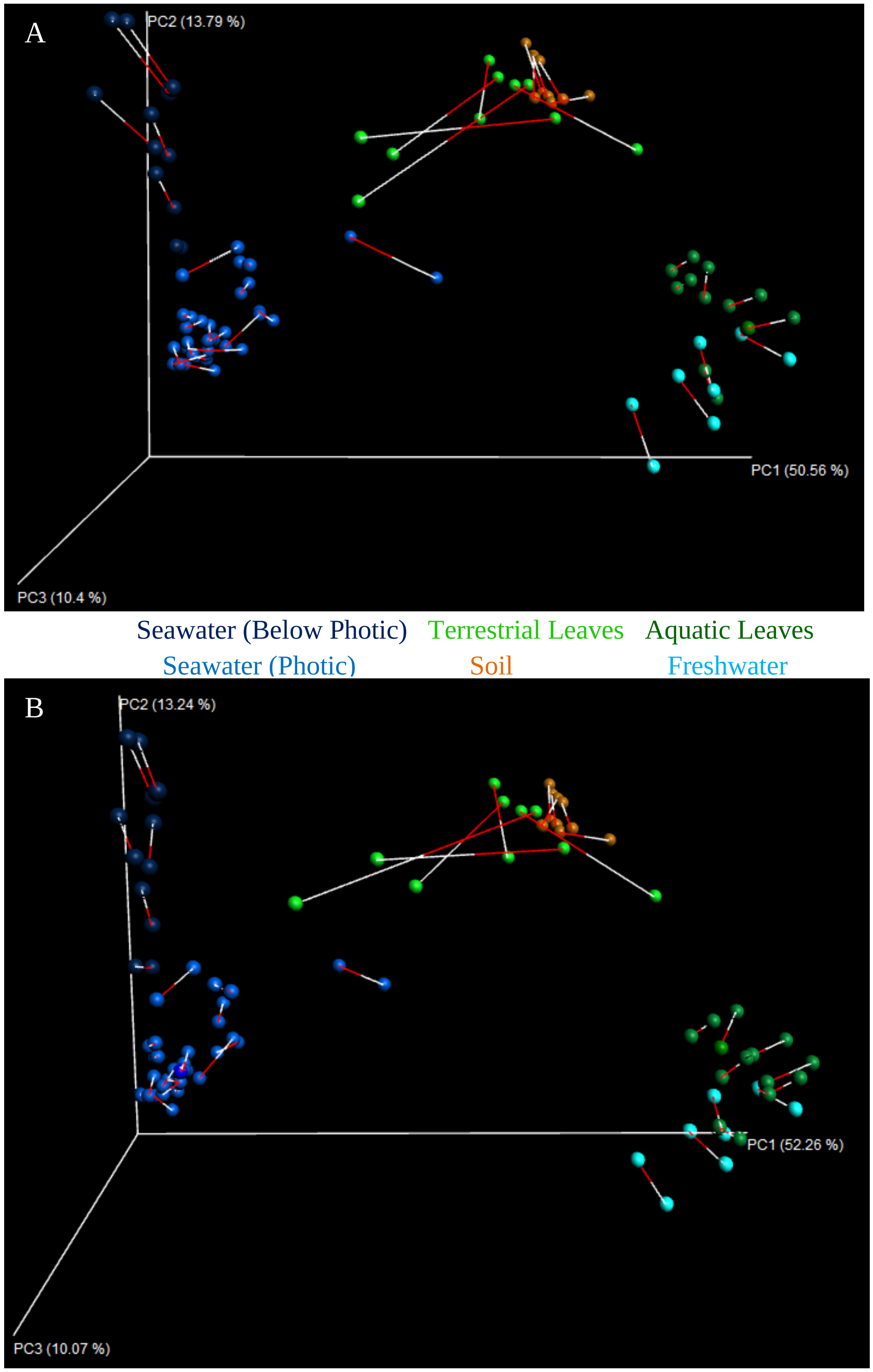

Figure 7.3: Larger scale trends remain evident regardless of PNA versus EMP primer method, illustrated as a Procrustes analysis. (*a*) Samples are shown after filtering out chloroplast and mitochondria, and (*b*) chloroplast, mitochondria, and OTUs in the Supplementary Tables.

method bias was significantly stronger among phototrophic communities than deeper water assemblages that are likely chemolithotrophic (t-test: $t_7 = 5.66$, $p < 0.001$). This increased bias was likely due to the greater natural abundance in these phototrophic communities of the Rhodobacterales, which contain the 14-mer conserved region that likely binds to the pPNA primer. After filtering out all OTUs containing this 14-mer (i.e., OTUs listed in the Supplementary Tables), phototrophic and chemolithotrophic communities showed a similar degree of bias by amplification method (t-test: $t_7 = 1.07$, $p = 0.32$).

Overall α-diversity measured as phylogenetic diversity was higher in samples amplified with EMP primers than PNA primers (Fig 7.2a, paired t-test: $t_{45} = 3.24$, $p < 0.01$) (see Appendix 7B for similar results using OTU #, Chao's α-diversity, and rarefaction curves). Even after filtering out taxa that contain the 14-mer conserved region, there remained higher diversity in the EMP amplified samples (Fig 7.1b, $t_{45} = 3.74$, $p < 0.01$). While we observed significant amplification differences when using these two methods that resulted in different α-diversity levels and relative abundances of particular taxa, we found that each method still generated the same general trends across sample types. Each environmental sample type is depicted in distinct clusters regardless of method (Procrustes Analysis, $p < 0.001$, $M^2 = 0.091$, Fig 7.3a when filtering out only chloroplast and mitochondria, and Figure 3B when filtering for chloroplast, mitochondria, and OTUs in the Supplementary Tables). Generally, analysis on each environmental sample type independently also showed similar trends regardless of amplification method (such as a geographic gradient with soil samples, freshwater samples, and aquatic leaf samples, as well as a depth gradient within seawater samples; see Fig 7.A.1 – Fig 7.A.5).

Lastly, in our survey of the Earth Microbiome Project database, we found that the OTUs containing the conserved 14 base pair sequence were abundant throughout a diversity of environments. All except two of the 113 datasets that we surveyed contained taxa listed in the Supplementary Tables. Ninety-five of these datasets contained at least one sample that was comprised of at least 1% of these taxa (Table 7.1). Seaweeds, seawater, freshwater, and aquatic sediments contained the highest abundance of these taxa (Table 7.1). Fish, reptile, amphibian, mammal, and avian-associated samples also contained high abundances of these taxa. These percentages are also likely conservative estimates because in our dataset, over 90% of the OTUs that matched this conserved sequence were from our open reference clustering of environmental samples. The percentages we report in our metanalysis only scan for those taxa remaining in the closed reference sequences that map to an OTU in the Greengenes database.

DISCUSSION

Comparative microbial ecology studies across environments are becoming increasingly common. A significant part of the discovery of microbes across ecosystems is the demonstration that microbes live in association with animals (Muegge et al. 2011, Sullam et al. 2012, Bolnick et al. 2014, Kwong and Moran 2016) and phototrophs including seaweeds (Egan et al. 2013, Campbell et al. 2015, Singh and Reddy 2015), terrestrial angiosperms (Berendsen et al. 2012, Badri et al. 2013) and more. These plant and animal-associated microbial communities are proving essential for elucidating the dynamic ecology of both the organisms and the ecosystems in which they reside (Zak et al. 2003, Kardol et al. 2007). As plants dominate many global environments, unbiased comparative analytical tools to characterize the associated microbial ecology require a degree of universality that until now has not been assessed. We found that the use of PNA blocking primers can strongly bias the characterization of nearly 1,500 microbial OTUs inhabiting a diversity of environments, particularly in aquatic samples containing high relative abundances of Alphaproteobacteria. Chloroplast-blocking pPNA primers appear to

Table 7.1: Subset of datasets from the EMP Database containing samples with 1% or more of their sequences matching taxa containing the conserved 14 base pair sequence, listed in the Supplementary Tables.

Dataset	# of Samples	Range (%)	Description of Samples
659	7	1.02 – 1.64	Agricultural Soils, New Zealand
1721	174	1 - 38.52	Agricultural Soils, Australia
1642	25	1 - 1.64	Rice Agricultural Soil sand Rhizosphere, Japan
1717	47	1.06 - 3.14	Agricultural Soils, Kenya
1711	51	1 – 3.54	Agricultural and Forest Soils, Kenya
846	13	1.2 – 3.84	Agricultural Soil, Italy
805	8	1 – 2.3	Agricultural Soils, Scotland
1001	20	1.04 – 3.66	Agricultural soils, Cannabis, USA
1792	63	1.02 – 10.8	Agricultural soil, maize, USA
1674	135	1.04 - 5.78	Rooftop Soils, New York City
2104	632	1 - 7.54	Soils, Central Park, New York City
10180	36	1 – 1.84	Agricultural soil, sugarcane, Brazil
1715	18	1 – 1.4	Agricultural Soils, coffee, Nicaragua
829	2	2.30 – 2.58	Semi-arid soil, Thar Desert, India
864	48	1 – 2.38	Montane Grassland Soils, Mongolia
990	29	1 – 2.62	Grassland soils, USA
1043	6	1 – 1.24	Grassland soils, USA
1526	82	1.02 – 7.3	Soils, Glens Canyon, USA
1579	43	1 – 4.38	Volcanic Soil, Hawaii
10278	29	1 – 2.92	Peat bog soils, Whales
1713	10	1.28 – 2.8	Forest Soils, Malaysia
1714	10	1 – 2.14	Forest Soils, Malaysia
1716	4	1 – 1.54	Forest Soils, Panama
808	11	1.00 – 1.70	Forest soils, Florida
1031	3	1.06 – 1.60	Forest soils, USA
1038	14	1 – 3.72	Forest soils, USA
10363	55	1.16 – 4.40	Coniferous Forest Soils, USA
1030	123	1 – 4.44	Soils, Boreal Forest, Alaska
1036	14	1 – 3.74	Permafrost soils, USA
1530	85	1.14 – 13.12	Soils, Alaska
1578	7	1.04 – 3.08	Soils, Alaska
10246	58	1.02 - 9.02	Tundra Soils, Alaska
1692	26	1.04 – 6.67	Soils and Biofilms, Alaska
1037	2	1.02 – 3.90	Soils, Canada
632	3	1.10 – 1.34	Soils, Canada
1034	9	1 – 4.32	Soils, Arctic
1702	17	1.02 – 2.74	Montane Shrub land Soils, China
1035	9	1 - 13.82	Sand, Antarctic
1033	3	1.06 – 10.32	Soils, Antarctic
776	2	1.46 – 1.58	Soil, Antarctica
10245	7	1 – 2.22	Leaf litter, Peru
807	43	1.02 – 2.96	Riverbed Sediments, USA
809	13	1.14 - 3.92	Lakebed Sediments, Canada
925	9	1 – 5.18	Hot springs Microbial Mats, Yellowstone
1622	35	1 - 15.88	Freshwater Pond Sediment, USA
1627	6	1.28 – 5.74	Freshwater Sediment, Tibetan Plateau
10156	47	1 – 4.8	Wetland Soils, USA
638	58	1.10 - 64.56	Freshwater Lakes, Antarctic
945	320	1 – 68.4	Freshwater Lakes, Germany
1041	43	1.04 - 5.14	Freshwater, Great Lakes, USA
1242	11	1 – 5.68	Freshwater, Lake Mendota, USA
1288	397	1 – 15.82	Freshwater, Temperate Bog, USA
1818	52	1 – 16.96	Wastewater, Florida
1883	794	1 – 16.52	Lake water, Seawater, Lake Epithilion, Alaska
861	8	1.86 - 24.78	Karst Sinkholes, Mexico
940	32	1 – 5.6	Freshwater Fish (Fecal, and Surface Mucus), USA
2259	5	1.12 - 3.94	Stickleback gut, USA
10308	172	1 – 36.34	Freshwater Fish (Mucosal Surface), USA
10272	31	1.24 – 10.92	Amphibian Skin Swabs, USA
10196	2	1.82 – 2.04	Panamanian Golden Frog, captive, skin swab

Table 7.1, continued.

1064	4	1.06 – 2.02	Bee, Puerto Rico
10324	1	1.68	Lone Star Tick, USA
1845	8	1.1 – 5.24	Deer Tick, USA
1632	37	1 – 6.98	Bird Eggshells, Spain
1694	114	1 - 97.62	Starling Eggshells
1773	76	1.04 - 19.16	Passerine Bird (Intestine), Venezuela
963	6	1 – 2.28	Iguana feces
1747	22	1.1 – 6.48	Komodo Dragon saliva, captive, USA
2338	6	1.08 – 4.56	Frugivorous bat feces, Costa Rica
1734	8	1.12 – 58.76	Phyllostomid bat feces, Belize
1056	14	1.06 – 7.72	Fecal, Ant-eating Mammals
1736	1	1.12	Cape Buffalo feces, South Africa
894	85	1 – 24.92	Marsupial Feces, Australia
1665	30	1.16 – 17.14	Skin Surface, Marine Mammals
910	1	1.54	Coral/algae tissue, Curacao Island
804	56	1.06 – 32.2	Hydrothermal Vent Chimney Biofilms
10273	23	1.2 – 10.26	Coral Mucus Swabs, USA
10346	285	1 – 41.96	Seawater and Sponges, Spain, Madagascar
1740	282	1 – 42.22	Seawater and Sponges, Australia, Spain, Madagascar
2229	1271	1 – 74.18	Seaweeds (Surface Swab), Australia
933	321	1.36 - 51.38	Kelp Forest, Australia
1197	101	1.12 – 36.14	Contaminated Ocean Sediment, Deepwater Horizon, USA
1198	57	1.94 - 15.92	Marine Sediment, Argentina and Antarctica
678	204	1 – 5.34	Marine Sediments, England
905	38	1.04 – 11.86	Marine Sediments, Scandinavia
1039	8	1.76 – 9.2	Marine Sediment and Seawater, Brazil
1580	8	1.18 – 5.94	Saline Freshwater and Seawater, USA
2080	26	1.08 – 9.66	Seawater, North Atlantic Ocean
10145	86	2.4 – 28.76	Seawater, British Columbia
1222	71	18.02 - 58.26	Seawater, Scandinavia
1235	256	1.02 – 18.88	Seawater, Scandinavia
1240	140	1.02 – 53.76	Seawater, English Channel
662	42	1.04 - 54.1	Seawater, Pacific Northwest
723	64	1.02 – 9.12	Seawater, Arctic
889	7	1.04 – 1.74	Seawater, Italy

adhere to similar sequences, including those containing 14 of the 17 base pairs, but may also be binding to even less conserved sequences. Many of the discrepancies between our replicate samples that remain even after filtering out taxa listed in the Supplementary Tables may be due to a number of these other taxa with similar sequences, such as those 2,381 OTUs containing a 12-mer subsection of the 14-mer, that may also bind to the pPNA primer.

We found that these taxa are abundant in a diversity of ecosystems, and would likely be under sampled with pPNA primers. Our metanalysis showing the ubiquity of these taxa illustrates the potential biases of studies contrasting the microbiome of multiple ecosystems. For example, studies that could use the chloroplast pPNA clamps to assess microbes associated with agricultural crops may mask the presence of certain taxa that are relatively abundant in agricultural soils. In contrast, mitochondrial mPNA clamps did not appear biased, and so these primers may remain useful for animal-only studies. However, studies comparing animal and plant microbiomes, such as diet studies, should use these clamps with caution. Given that we found a number of herbivorous reptiles, birds, and mammals contained these biased taxa in their gut and feces, use of pPNA clamps to assess the plant microbiome and compare that with an herbivorous animal microbiome may yield biased results. However, aquatic plants themselves pose one of the largest biases for using the pPNA primers due to the clear utility of chloroplast-blocking clamps and the abundance of particular taxa, such as the typically surface-associated Rhodobacterales that are abundant in seawater and on the surface of seaweeds (Gilbert et al. 2012, Fu et al. 2013, Taylor et al. 2014).

We highlighted our results from such marine systems by comparing surface phototrophic against deeper chemolithotrophic communities, which contrast strongly in community membership. We found that phototrophic communities tend to contain a far greater proportion of taxa containing the 14-mer oligonucleotide. Due to these natural differences in community membership, the PNA amplification method yielded substantially more biased results in the photic zone, where indeed the use of these pPNA clamps would otherwise be particularly useful for studying plant-associated microbiomes. While the pPNA amplification method may remain a technically viable option below the photic zone because of the apparent lack of taxa containing the 14-mer oligonucleotide, we do not expect these primers to be particularly useful in such ecosystems with few photosynthetic organisms and therefore minimal contaminating chloroplast.

Further, we used our marine samples to ask whether these amplification methods are biased in the detection of cyanobacteria. As the free-living predecessors to chloroplast, we tested whether a chloroplast blocking technique would inhibit their amplification. We found that both methods yield quite robust results for cyanobacteria. Of the 774 non-chloroplast cyanobacteria OTUs in our dataset and the 1389 non-chloroplast cyanobacteria OTUs in Greengenes, only 7 OTUs in our dataset and 21 OTUs in Greengenes contain the 14-mer oligonucleotide that matches the pPNA primer. None of these OTUs, or indeed any cyanobacteria, were amplified at significantly different levels with the two methods. With suitable sequencing depth, either method should yield satisfactory results for studying cyanobacteria. However, using the EMP primers and simply screening out chloroplast reads will give equivalent results for cyanobacteria without the issue of reduced Alphaproteobacteria and similar taxa (listed in the Supplementary Tables).

Lundberg et al. (2013) found that both amplification methods yielded similar relative abundances of all tested microbial OTUs (including 75 OTUs in plant roots and 1,010 OTUs in soil samples). They found when amplifying replicate soil samples, their PNA method excluded 31 OTUs compared to the EMP method (Lundberg et al. 2013). Although in our scan of the

Greengenes database, we found a 14-mer match to 1405 OTUs to the pPNA primer, Lundberg et al. scanned 9-mer through 13-mer oligonucleotides of the their pPNA and mPNA sequences against the Greengenes database and did not find matches. The reason for this discrepancy is unclear.

We also note our terrestrial leaf samples, which were each obtained from a different individual red alder tree, yielded highly variable microbial communities (see Fig 7. C.4). Though the cause of this variability cannot be determined with our current data, there are a number of possible explanations related to the inherent variation in leaves. While the phyllosphere is conclusively not sterile (Lindow and Brandl 2003, Lundberg et al. 2013), living plant material may be somewhat protected by antimicrobial compounds and is noticeably less diverse than many other types of habitats, such as soils (Badri et al. 2013). Further, the leaves from our study were taken from the lower branches of riparian trees that experience higher levels of anti-microbial solar radiation than the lower branches of trees inhabiting interior forest. This variability may also be due to natural cross-contamination of microbes from freshwater and soil environments, perhaps due to wildlife activity.

Despite the constraints of organelle-blocking primers, this amplification method did not obscure general trends in our datasets. We were able to clearly observe differences across soil, freshwater, seawater and plant samples. Geographic gradients within each of these sample categories remained consistent regardless of amplification method. These methods may therefore remain suitable for more targeted studies focusing on particular taxa that do not contain the conserved region. We did not find any taxa that matched either the entire pPNA or mPNA primer sequence. Future studies could aim to optimize these organelle clamps by modifying the

PCR technique to select for higher specificity, such as through modifying the temperature protocol or perhaps lengthening the primer sequence (Mullis et al. 1989).

ACKNOWLEDGMENTS

We thank J.T. Wootton, J. Bergelson, G. Dwyer, and T.D. Price for constructive comments and discussion on this work. This work was supported by the NSF GRFP, the DOE GAANN, NSF DDIG DEB-1311293, ARCS® (Achievement Rewards for College Scientists) Foundation, Inc.'s Scholar Illinois Chapter [2014 and 2015], and University of Chicago Hinds Fund grants to SLJ; and the NSF-OCE 09-28232 to CAP. We thank Capt. R. McQuin and the crew of the R/V C. Barnes, especially J. Postels, and seawater sampling help from S. Betcher, N. Bian, C. Kanichy, L. Harris, B. He, S. Pather, C. Stepien, and P. Zaykoski. We also thank N. Sangwan, M. D'Souza, S.M. Gibbons, J. Hampton-Marcell, A. Frazier, N. Gottel, S. Lax and the Gilbert Lab at University of Chicago and Argonne National Labs for assistance with sequencing and analyses. We thank the Makah Tribal Nation, Merrill & Ring Inc., J. Murray, Hoko River State Park, and the Washington State Department of Natural Resources for facilitating research on their lands.

Appendix 7A: Procrustes analyses for each environmental sample type.

Figure 7.A.1. Procrustes analysis illustrating distance in principal coordinate space among microbial communities of each soil sample. Distance between replicate samples amplified with EMP versus PNA primers shown with connecting lines. Sample # 11 is from beneath a tree growing furthest downstream on the Hoko River (48° 15′29.58 N, 124° 21′8.59 W). Sample numbers increase for trees growing further upstream.

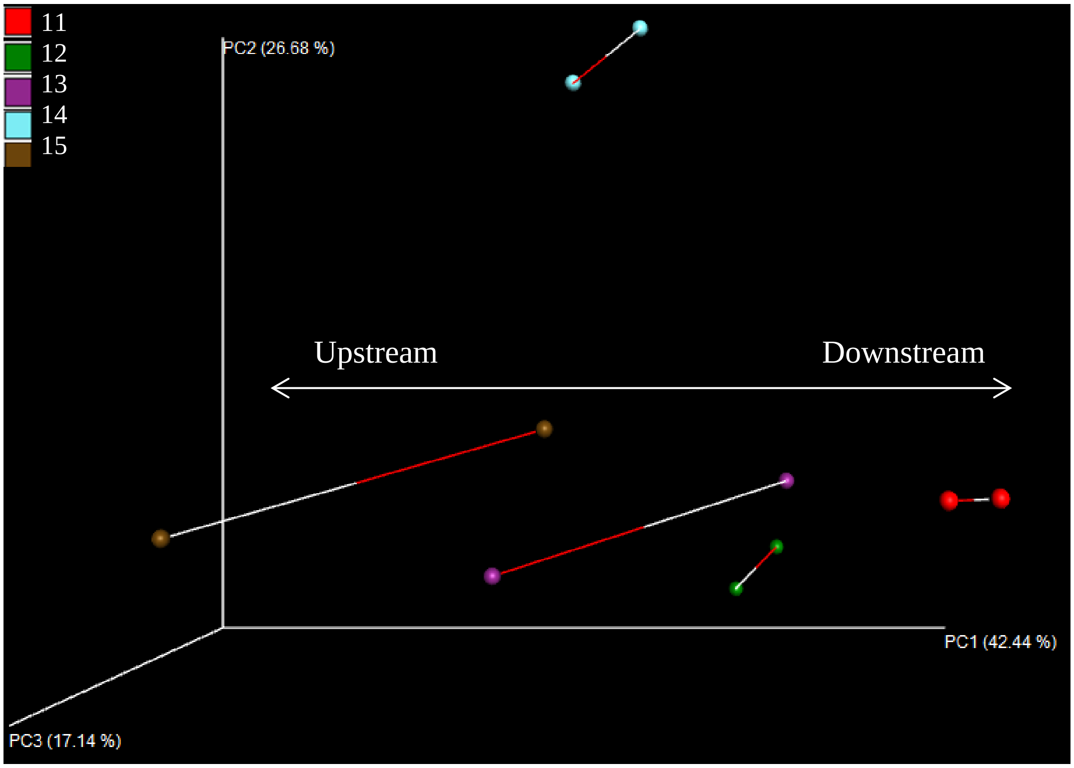

Figure 7.A.2: Procrustes analysis illustrating distance in PC space among microbial communities of each freshwater sample. Distance between replicate samples amplified with EMP versus PNA primers shown with connecting lines. Samples were collected upstream of two deployment sites on the Hoko River and two deployment sites on the Sekiu River.

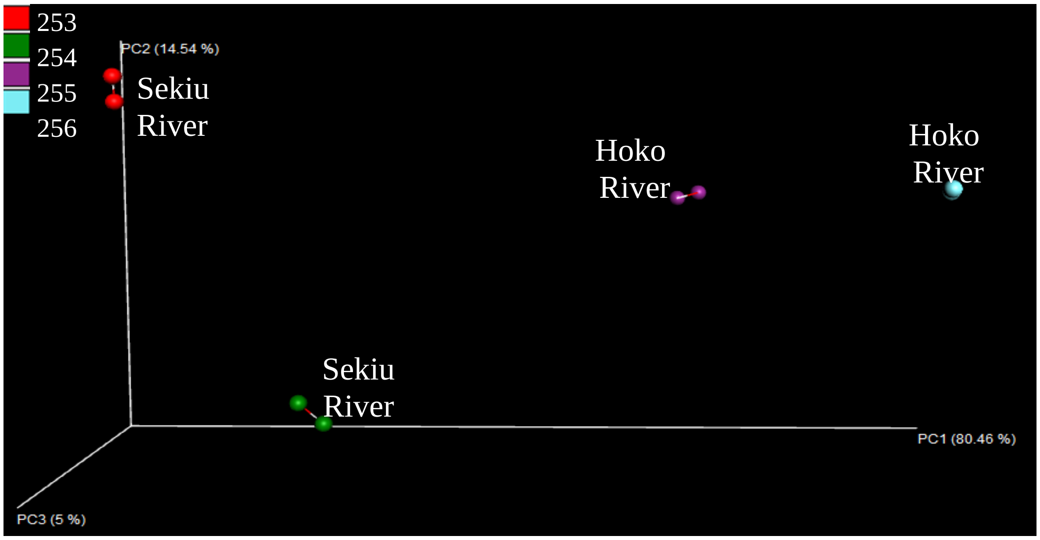

Figure 7.A.3: Procrustes analysis illustrating distance in PC space among microbial communities of each seawater sample. Distance between replicate samples amplified with EMP versus PNA primers shown with connecting lines. Sample #1501 – 1509 and #1514 – 1519 are surface samples at Slip Point, WA (48.26° N, 124.25° W); #1520 – 1523 are surface samples at Tatoosh Island, WA (48.39° N, 124.74° W), #1511 is at 100 m deep, #1524 is at 125 m deep, #1510 is at 140 m deep, #1512 is at 325 m deep, and #1513 is at 300 m deep

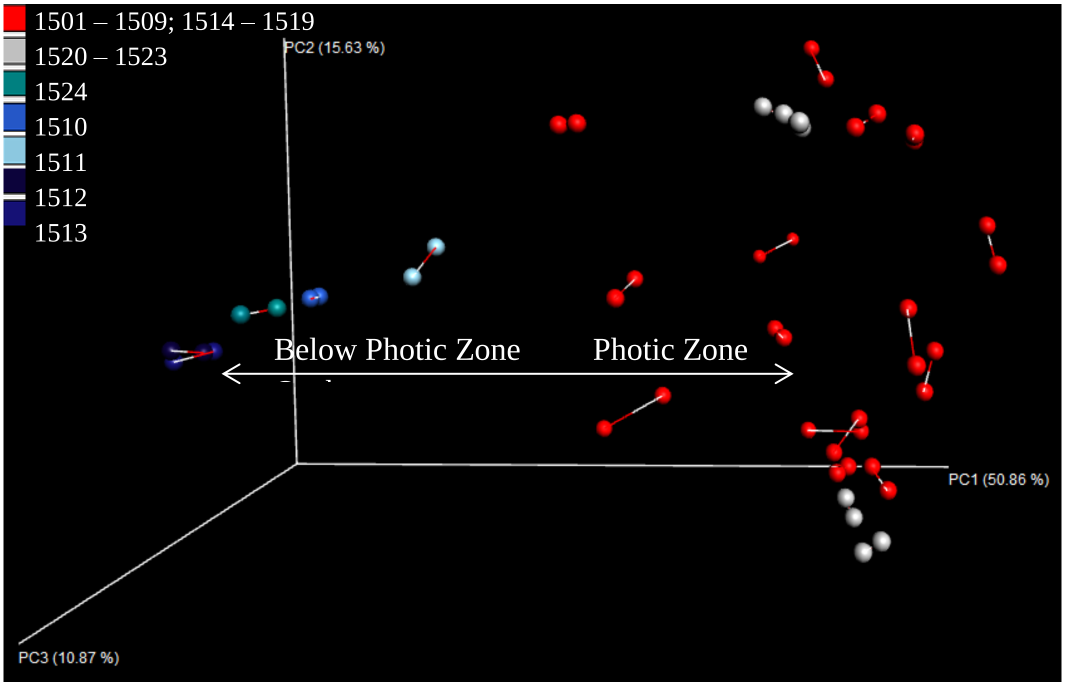

Figure 7.A.4: Procrustes analysis illustrating distance in PC space among microbial communities of each aquatic leaf sample. Distance between replicate samples amplified with EMP versus PNA primers shown with connecting lines. Sample #55 – 58 are leaves taken from the same red alder tree alongside the Sekiu River, but deployed in different locations. Sample #107 – 110 are leaves take from the same red alder tree growing alongside the Hoko River, but deployed in different locations.

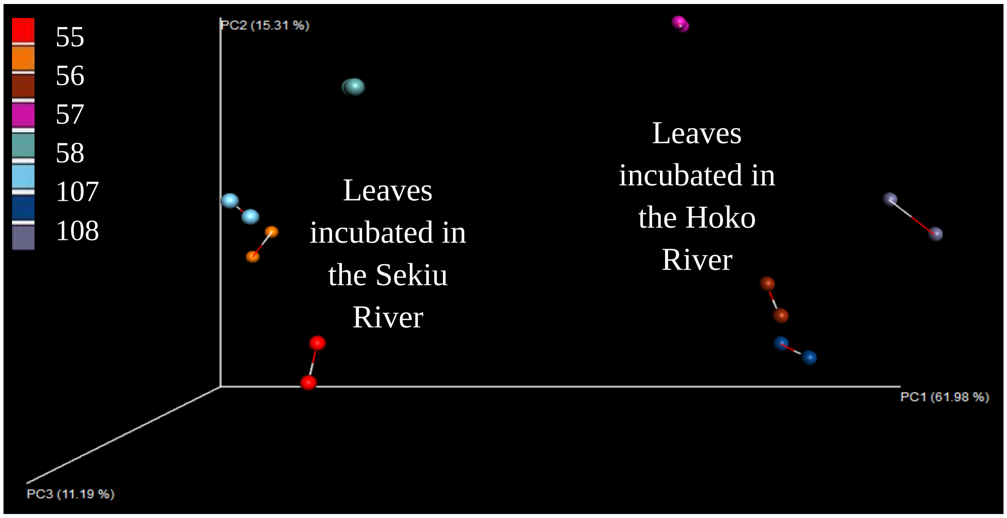

Figure 7.A.5: Procrustes analysis illustrating distance in PC space among microbial communities of each terrestrial leaf sample. Distance between replicate samples amplified with EMP versus PNA primers shown with connecting lines. Each sample consisted of one leaf from an individual red alder tree. Increasing sample number indicates that the parent tree was growing further upstream alongside the Hoko River.

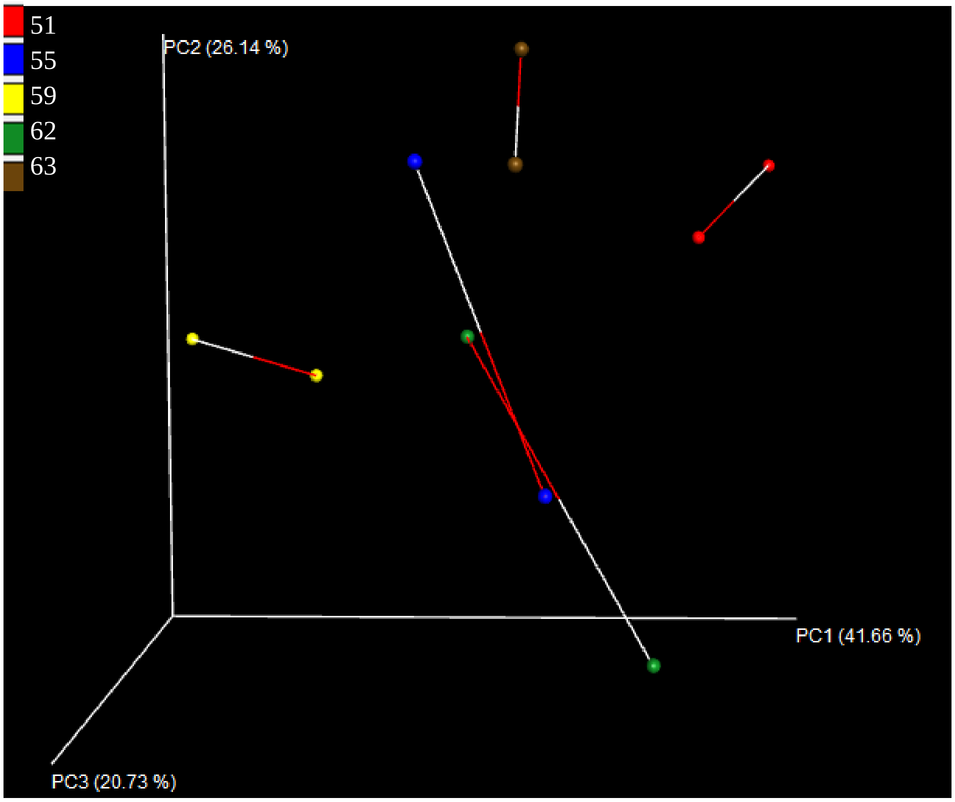

Appendix 7B: Diversity metrics and rarefaction curves.

Figure 7.B.1: OTU #, Phylogenetic, and Chao's alpha diversity metrics (mean + SE) of all samples by environment type (terrestrial leaves, aquatic leaves, freshwater, seawater, or soil samples) amplified with EMP vs PNA primers. (B) indicates filtering out only chloroplast and mitochondria. (A) indicates filtering out chloroplast, mitochondria, and OTUs in the Supplementary Tables.

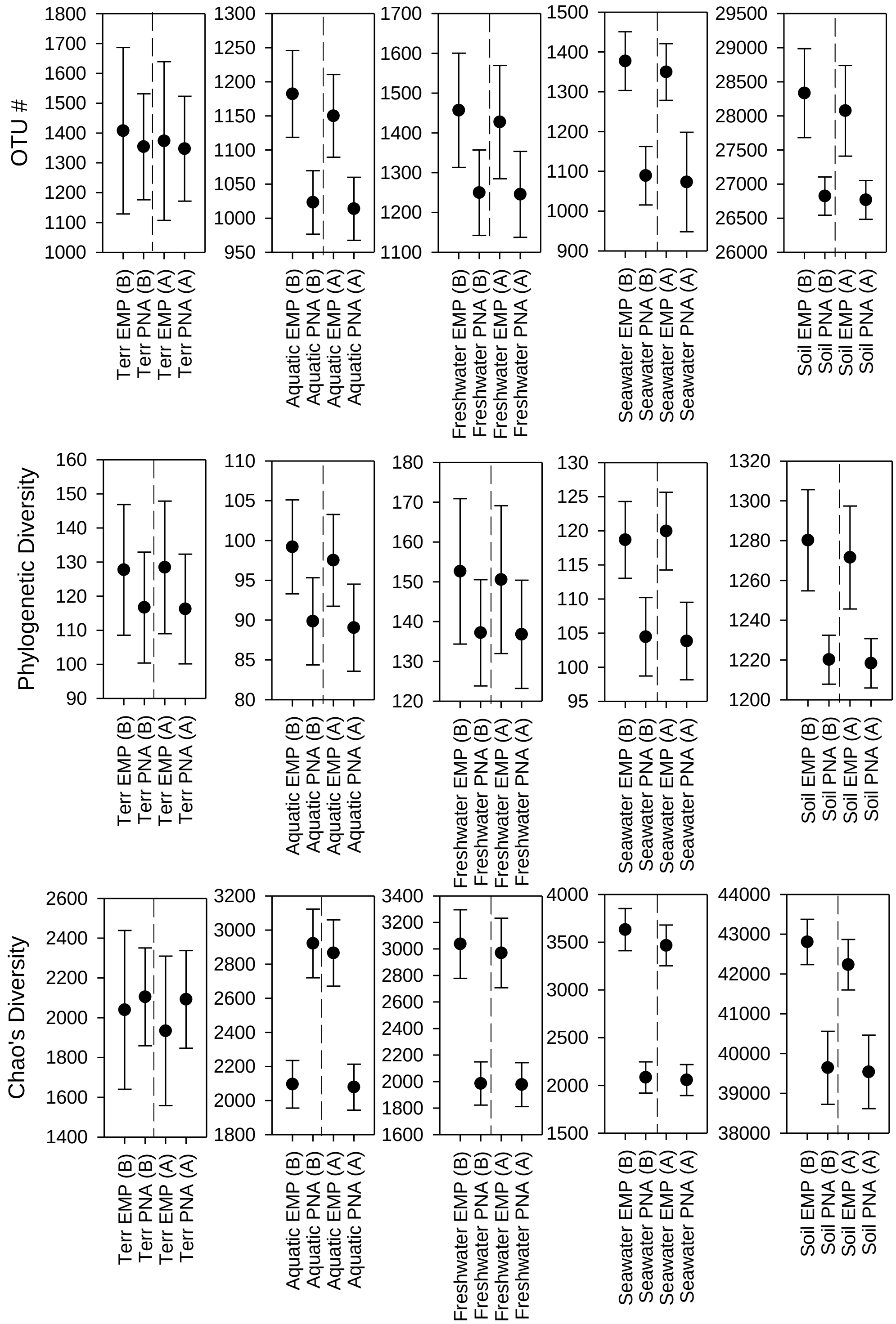

Figure 7.B.2: Rarefaction curves illustrating alpha diversity of microbial taxa via number of OTUs in aquatic leaves (*a*), freshwater (*b*), seawater (*c*), soil (*d*), and terrestrial leaf (*e*) samples sequenced with either chloroplast and mitochondria-blocking PNA primers (Blue) or universal EMP primers (Red). Filtering out only chloroplast and mitochondria (not OTUs in the Supplementary Tables).

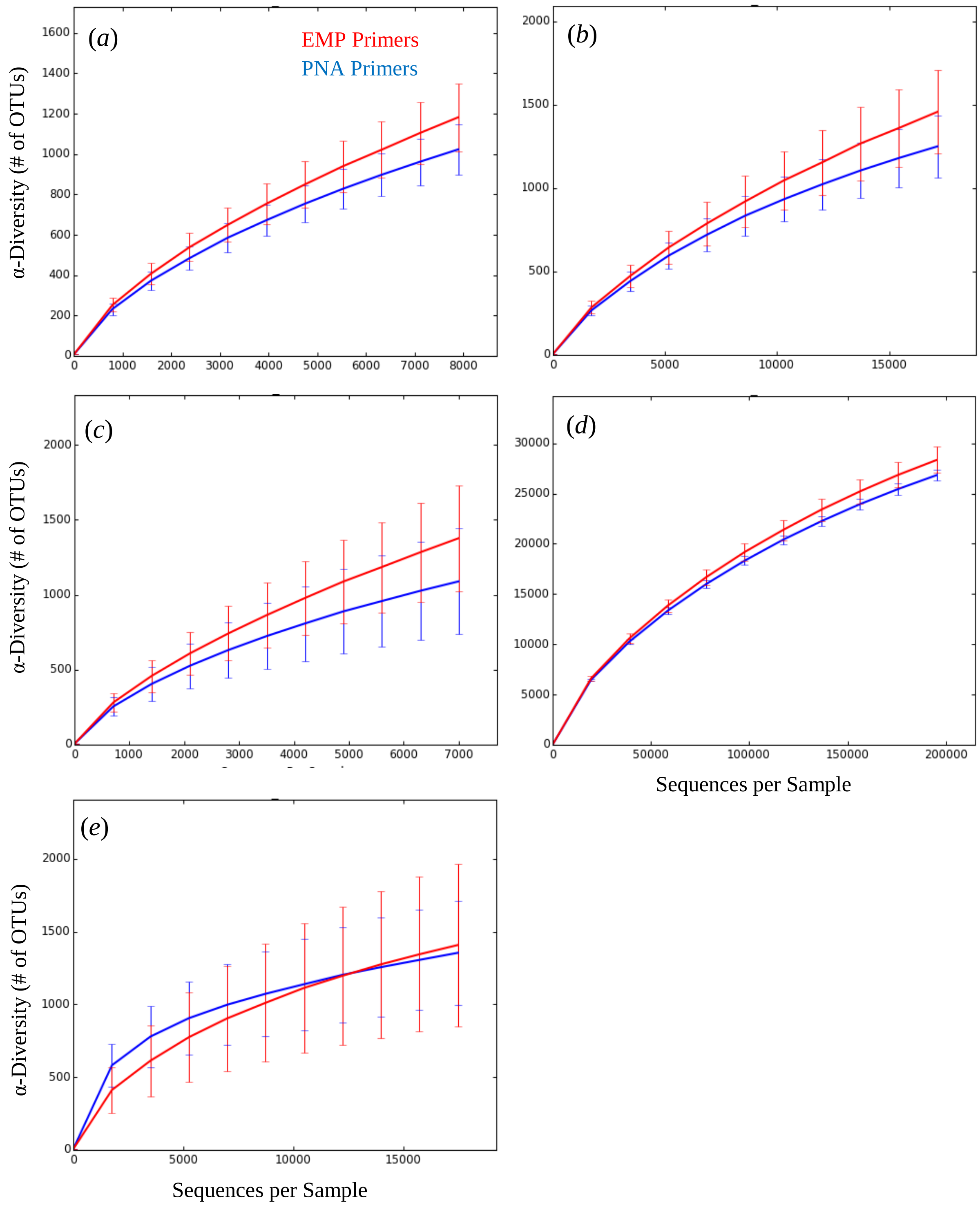

Figure 7.B.3: Rarefaction curves illustrating alpha diversity of microbial taxa via number of OTUs in aquatic leaves (*a*), freshwater (*b*), seawater (*c*), soil (*d*), and terrestrial leaf (*e*) samples sequenced with either chloroplast and mitochondria-blocking PNA primers (Blue) or universal EMP primers (Red). Filtering out chloroplast, mitochondria, and OTUs in the Supplementary Tables.

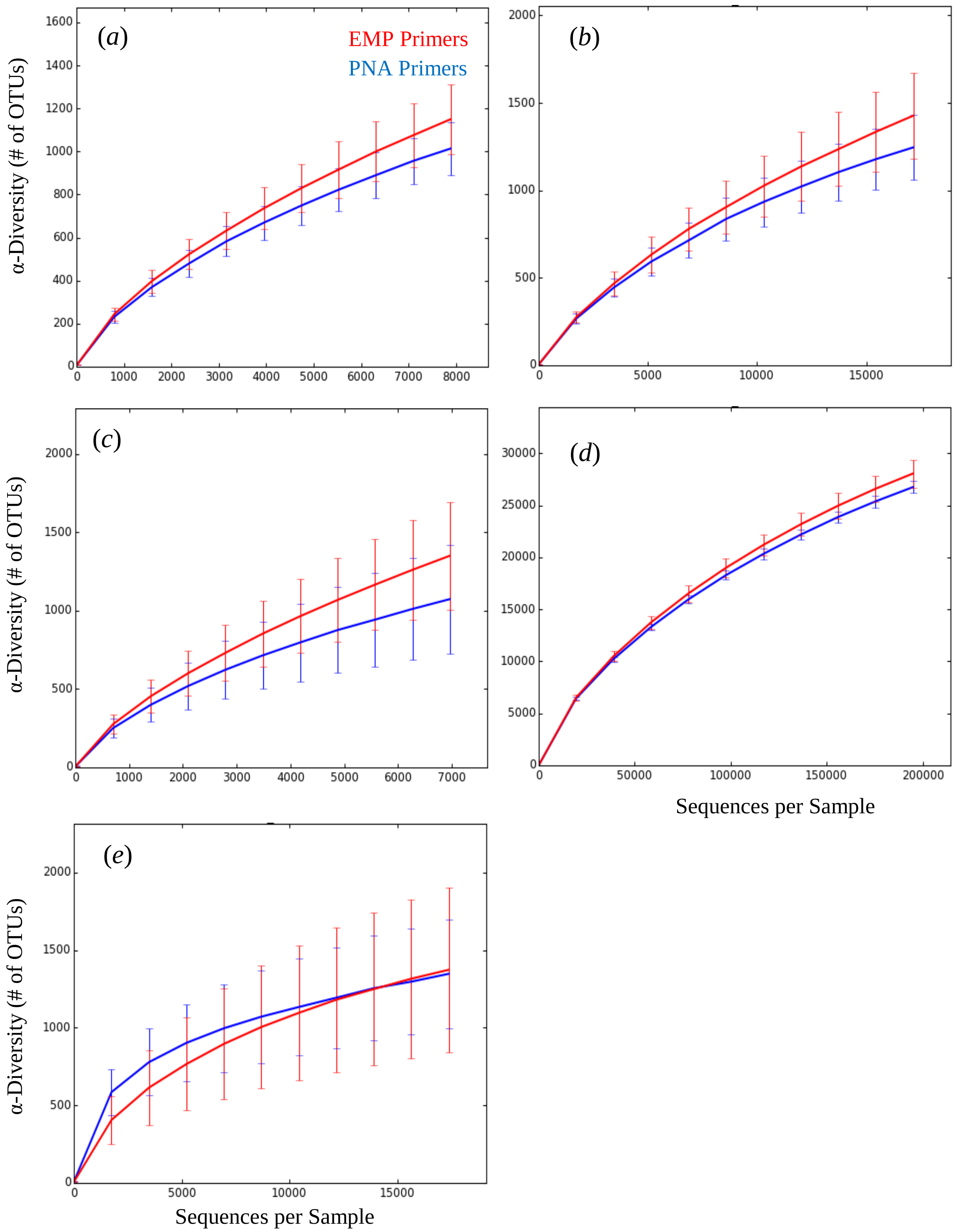

Appendix 7C: Microbial communities vary depending on primer amplification method.

Figure 7.C.1: Paired comparisons of freshwater samples sequenced with either universal EMP primers or organelle-blocking PNA primers. Relative abundance of microbial taxa at the family level depicted via color. ‘Before’ samples depict communities after filtering out chloroplast and mitochondrial sequences. ‘After’ samples depict communities after additionally filtering out OTUs in Supplementary Tables. Weighted UniFrac distances between replication samples quantify community similarity as a measure of discontinuity by amplification method.

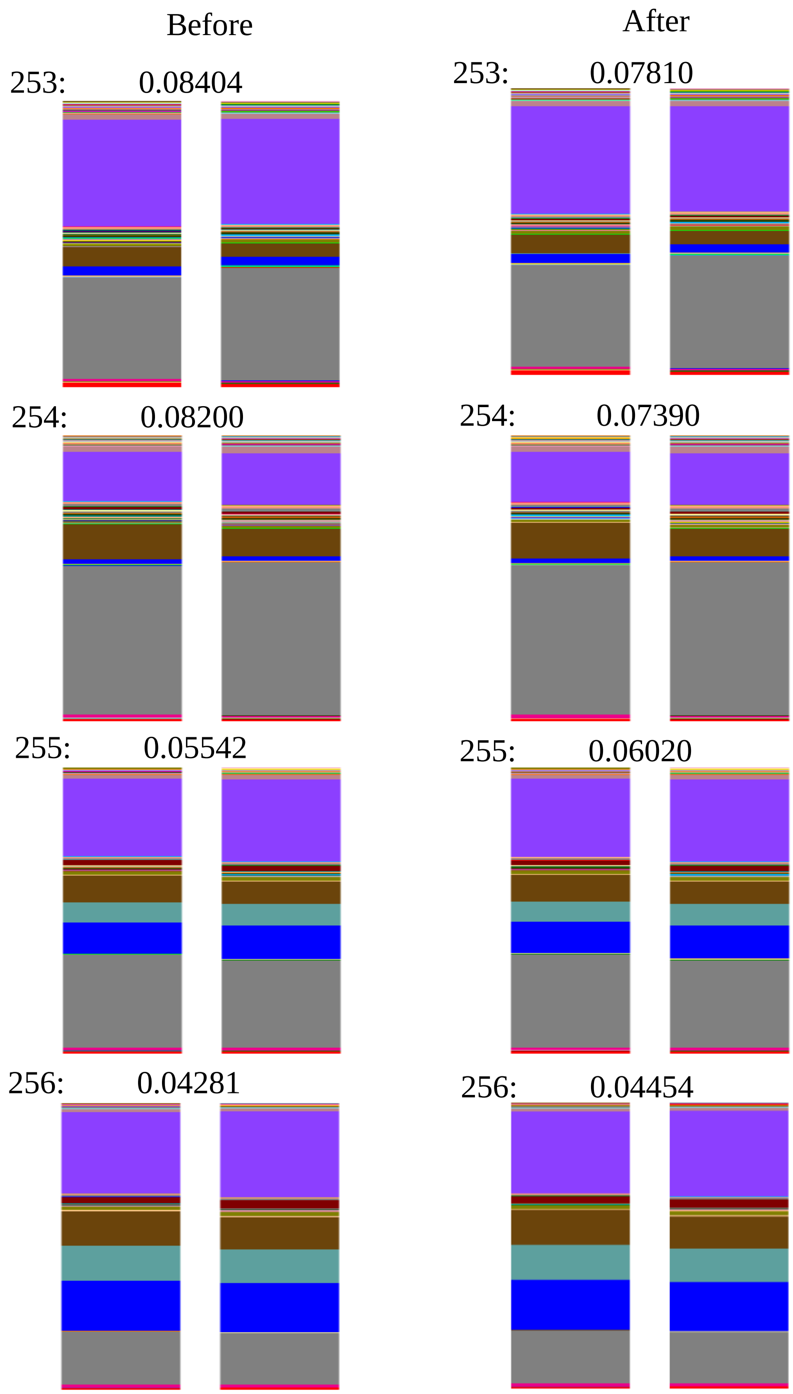

Table 7.C.1: Microbial taxa at lower relative abundance in freshwater samples when sequenced with PNA primers versus EMP primers. The first column lists rank order abundance of each taxa in the entire freshwater sample set. Reported p-values are from paired t-tests with and without false discovery rate correction..

Abundance	P-value	FDR	Taxonomic Classification
# 306	0.0039	1	Proteobacteria;c_Betaproteobacteria;o_**Methylophilales**;f_;g_
# 7	0.014	1	Actinobacteria;c_Actinobacteria;o_**Actinomycetales**;f_Microbacteriaceae;g_Candidatus Rhodoluna
# 62	0.016	1	OD1;c_ZB2;o_;f_;g_
# 4	0.020	1	Bacteroidetes;c_Flavobacteriia;o_**Flavobacteriales**;f_Flavobacteriaceae;g_Flavobacterium
# 328	0.023	1	Proteobacteria;c_Alphaproteobacteria;o_**Rhizobiales**;f_Hyphomicrobiaceae;g_Pedomicrobium
# 259	0.027	1	Proteobacteria;c_Betaproteobacteria;o_**Burkholderiales**;f_Comamonadaceae;g_Acidovorax
# 202	0.031	1	Actinobacteria;c_Rubrobacteria;o_Rubrobacterales;f_Rubrobacteraceae;g_Rubrobacter
# 53	0.031	1	Proteobacteria;c_Alphaproteobacteria;o_**Rhodobacterales**;f_Rhodobacteraceae;g_
# 89	0.032	1	Proteobacteria;c_Alphaproteobacteria;o_**Rhizobiales**;f_Phyllobacteriaceae;g_
# 30	0.036	1	Proteobacteria;c_Alphaproteobacteria;o_**Rickettsiales**;f_;g_
# 35	0.034	1	Proteobacteria;c_Deltaproteobacteria;o_**Myxococcales**;f_;g_
# 33	0.037	1	Proteobacteria;c_Alphaproteobacteria;o_**Rhodobacterales**;f_Hyphomonadaceae;g_
# 153	0.038	1	Parvarchaeota;c_[Parvarchaea];o_YLA114;f_;g_

Figure 7.C.2: Paired comparisons of soil samples sequenced with either universal EMP primers or organelle-blocking PNA primers. Relative abundance of microbial taxa at the family level depicted via color. 'Before' samples depict communities after filtering out chloroplast and mitochondrial sequences. 'After' samples depict communities after additionally filtering out OTUs in the Supplementary Tables. Weighted UniFrac distances between replication samples quantify community similarity as a measure of discontinuity by amplification method.

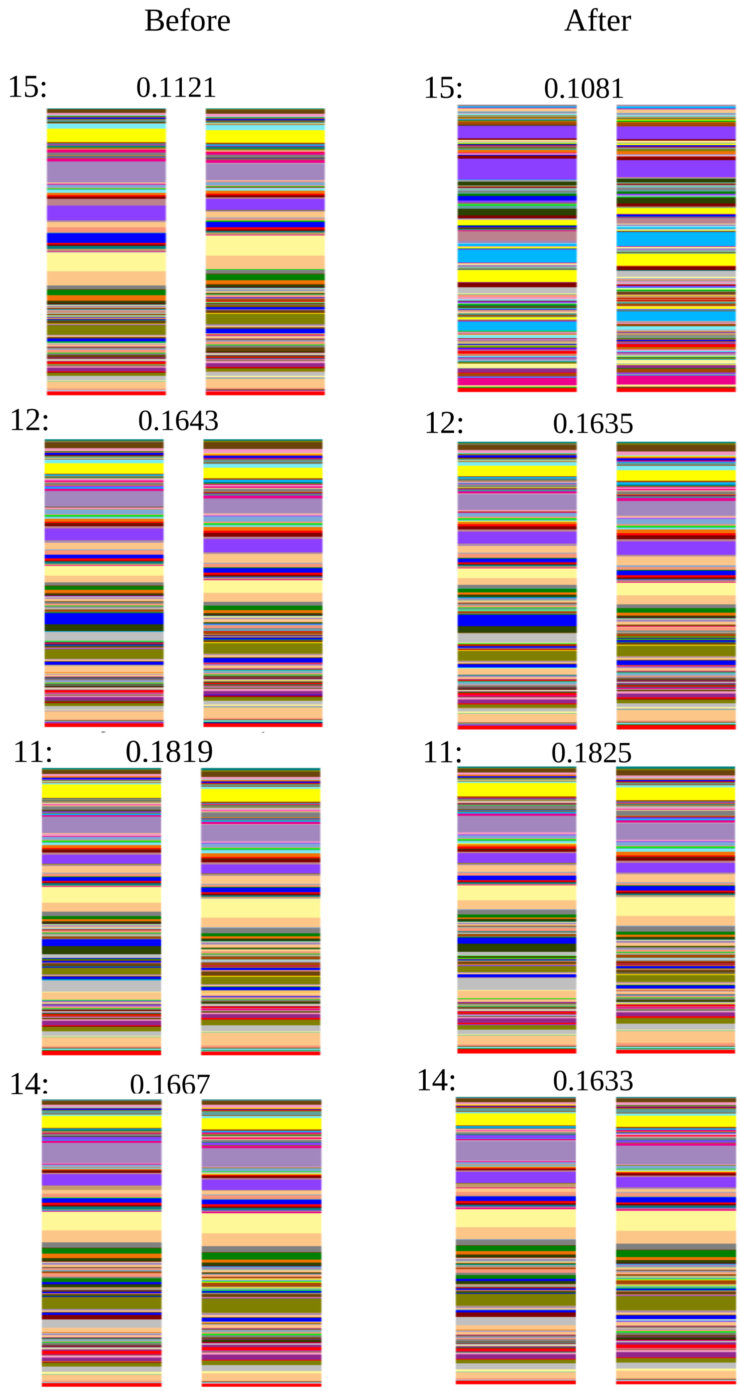

Table 7.C.2: Microbial taxa at lower relative abundance in soil samples when sequenced with PNA primers versus EMP primers. The first column lists rank order abundance of each taxa in the entire soil sample set. Reported p-values are from paired t-tests with and without false discovery rate correction.

Abund.	**P-value**	**FDR**	**Taxonomic Classification**
# 1167	0.0011	0.24	Verrucomicrobia;c_Spartobacteria;o_**Chthoniobacterales**;f_Chthoniobacteraceae
# 684	0.0036	0.24	Planctomycetes;c_C6;o_d113
# 672	0.0089	0.24	OP3;c_koll11
# 785	0.010	0.25	Proteobacteria;c_Alphaproteobacteria;o_**Rhodobacterales**;f_Rhodobacteraceae;g_Amaricoccus
# 866	0.011	0.25	Proteobacteria;c_Betaproteobacteria;o_**Burkholderiales**;f_Comamonadaceae;g_Rhodoferax
# 624	0.011	0.50	GN02;c_BB34
# 730	0.013	0.24	Proteobacteria;c_Alphaproteobacteria;o_**Caulobacterales**;f_Caulobacteraceae;Other
# 824	0.014	0.28	Proteobacteria;c_Alphaproteobacteria;o_**Sphingomonadales**;f_Sphingomonadaceae;g_Novosphingobium
# 783	0.015	0.35	Proteobacteria;c_Alphaproteobacteria;o_**Rhodobacterales**;f_Hyphomonadaceae;g_
# 100	0.016	0.24	Actinobacteria;c_Actinobacteria;o_**Actinomycetales**;f_ACK-M1;g_
# 768	0.017	0.25	Proteobacteria;c_Alphaproteobacteria;o_**Rhizobiales**;f_Phyllobacteriaceae;Other
# 978	0.019	0.25	Proteobacteria;c_Deltaproteobacteria;o_**Myxococcales**;f_OM27;g_
# 792	0.019	0.25	Proteobacteria;c_Alphaproteobacteria;o_**Rhodobacterales**;f_Rhodobacteraceae;Other

Figure 7.C.3: Paired comparisons of aquatic leaf samples sequenced with either universal EMP primers or organelle-blocking PNA primers. Relative abundance of microbial taxa at the family level depicted via color. 'Before' samples depict communities after filtering out chloroplast and mitochondrial sequences. 'After' samples depict communities after additionally filtering out OTUs in the Supplementary Tables. Weighted UniFrac distances between replication samples quantify community similarity as a measure of discontinuity by amplification method.

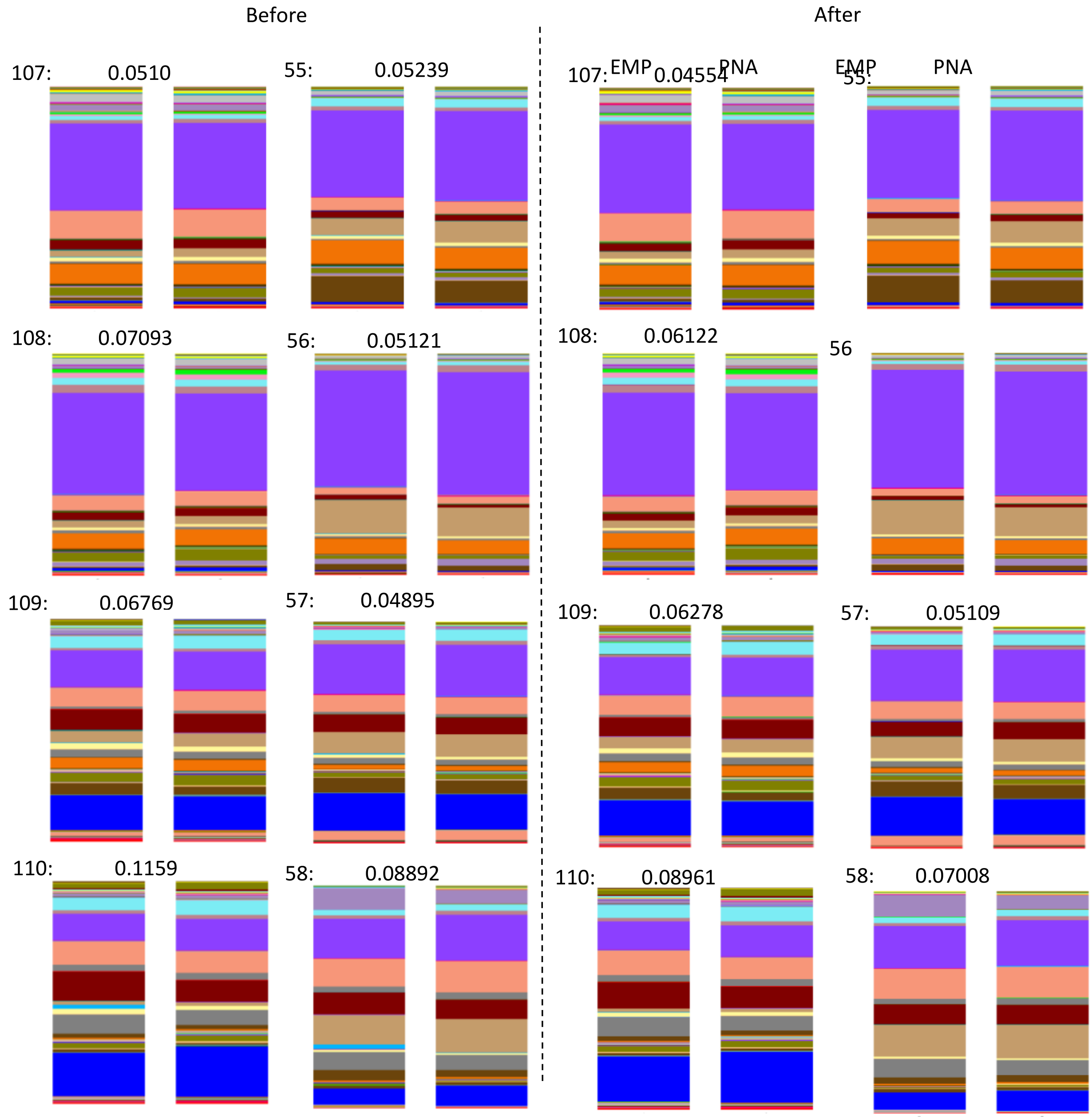

Table 7.C.3: Microbial taxa at lower relative abundance in aquatic leaf pack samples when sequenced with PNA primers versus EMP primers. The first column lists rank order abundance of each taxa in the entire aquatic leaf pack sample set. Reported p-values are from paired t-tests with and without false discovery rate correction.

Abund.	P-value	FDR	Taxonomic Classification
# 221	0.00029	0.048	Crenarchaeota;c_Thaumarchaeota;o_Nitrososphaerales;f_Nitrososphaeraceae;g_Candidatus Nitrososphaera
# 222	0.00052	0.048	Actinobacteria;c_Rubrobacteria;o_Rubrobacterales;f_Rubrobacteraceae;g_Rubrobacter
# 79	0.00071	0.048	Proteobacteria;c_Deltaproteobacteria;o_**Bdellovibrionales**;f_Bdellovibrionaceae;g_Bdellovibrio
# 168	0.00089	0.048	Verrucomicrobia;c_Spartobacteria;o_**Chthoniobacterales**;f_Chthoniobacteraceae;g_DA101
# 27	0.00097	0.048	Unassigned;Other;Other;Other;Other;Other
# 66	0.0011	0.048	Proteobacteria;c_Alphaproteobacteria;o_**Rhodobacterales**;f_Hyphomonadaceae
# 28	0.0013	0.048	Proteobacteria;c_Alphaproteobacteria;o_**Rhodobacterales**;f_Rhodobacteraceae
# 109	0.0023	0.050	Proteobacteria;c_Alphaproteobacteria;o_**Caulobacterales**;f_Caulobacteraceae;g_Phenylobacterium
# 173	0.0060	0.075	Proteobacteria;c_Gammaproteobacteria;o_Methylococcales;f_Crenotrichaceae;g_Crenothrix
# 20	0.0091	0.134	Proteobacteria;c_Alphaproteobacteria;o_**Rhizobiales**;f_Hyphomicrobiaceae;g_Devosia

Figure 7.C.4: Paired comparisons of terrestrial leaf samples sequenced with either universal EMP primers or organelle-blocking PNA primers. Relative abundance of microbial taxa at the family level depicted via color. 'Before' samples depict communities after filtering out chloroplast and mitochondrial sequences. 'After' samples depict communities after additionally filtering out OTUs in Appendix7.A. Weighted UniFrac distances between replication samples quantify community similarity as a measure of discontinuity by amplification method.

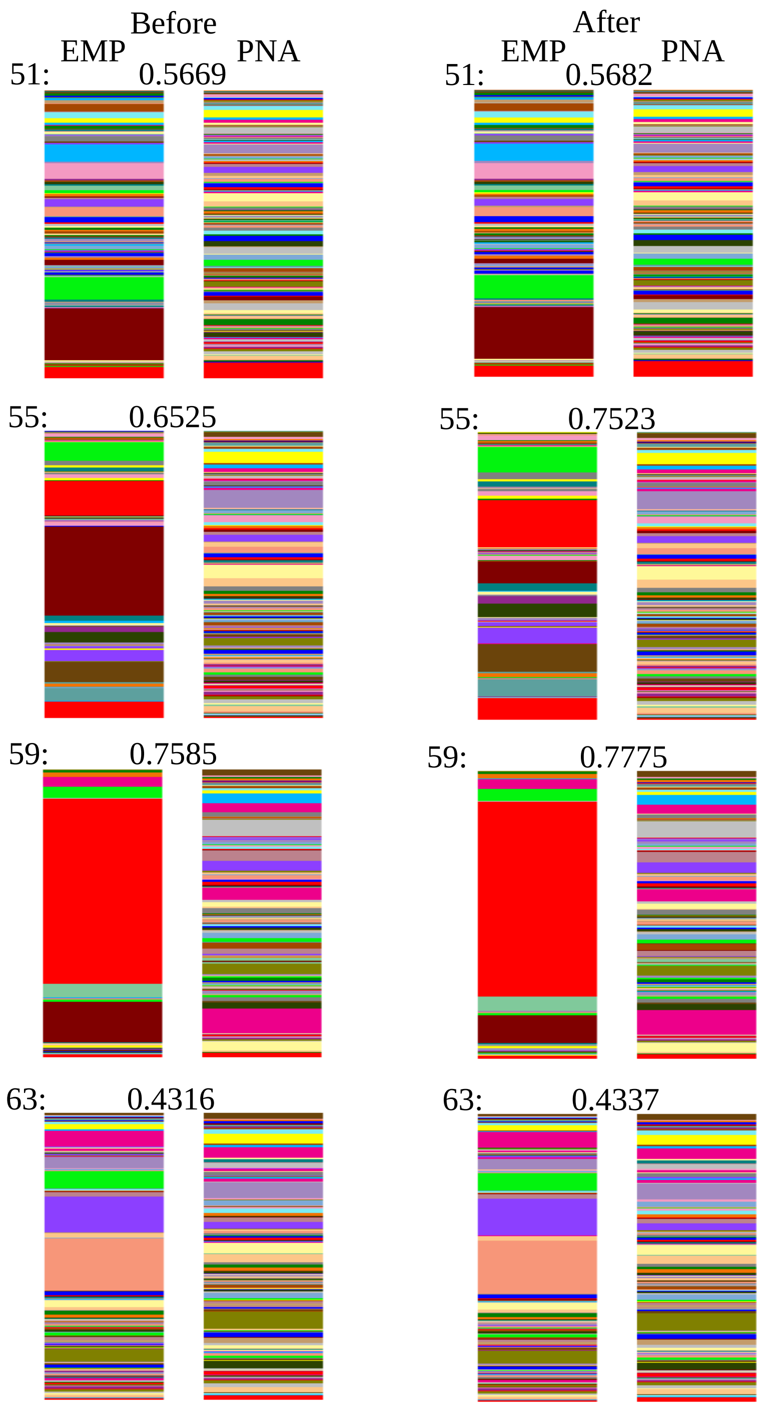

Figure 7.C.5: Seawater samples from Split Point, Washington (48.26° N, 124.25° W). Relative abundance of microbial taxa at the family level depicted via color. (*a*) Includes all OTUs after filtering out chloroplast and mitochondria, and (*b*) excludes all chloroplast, mitochondria and OTUs listed in the Supplementary Tables. Weighted UniFrac distances between replication samples quantify community similarity.

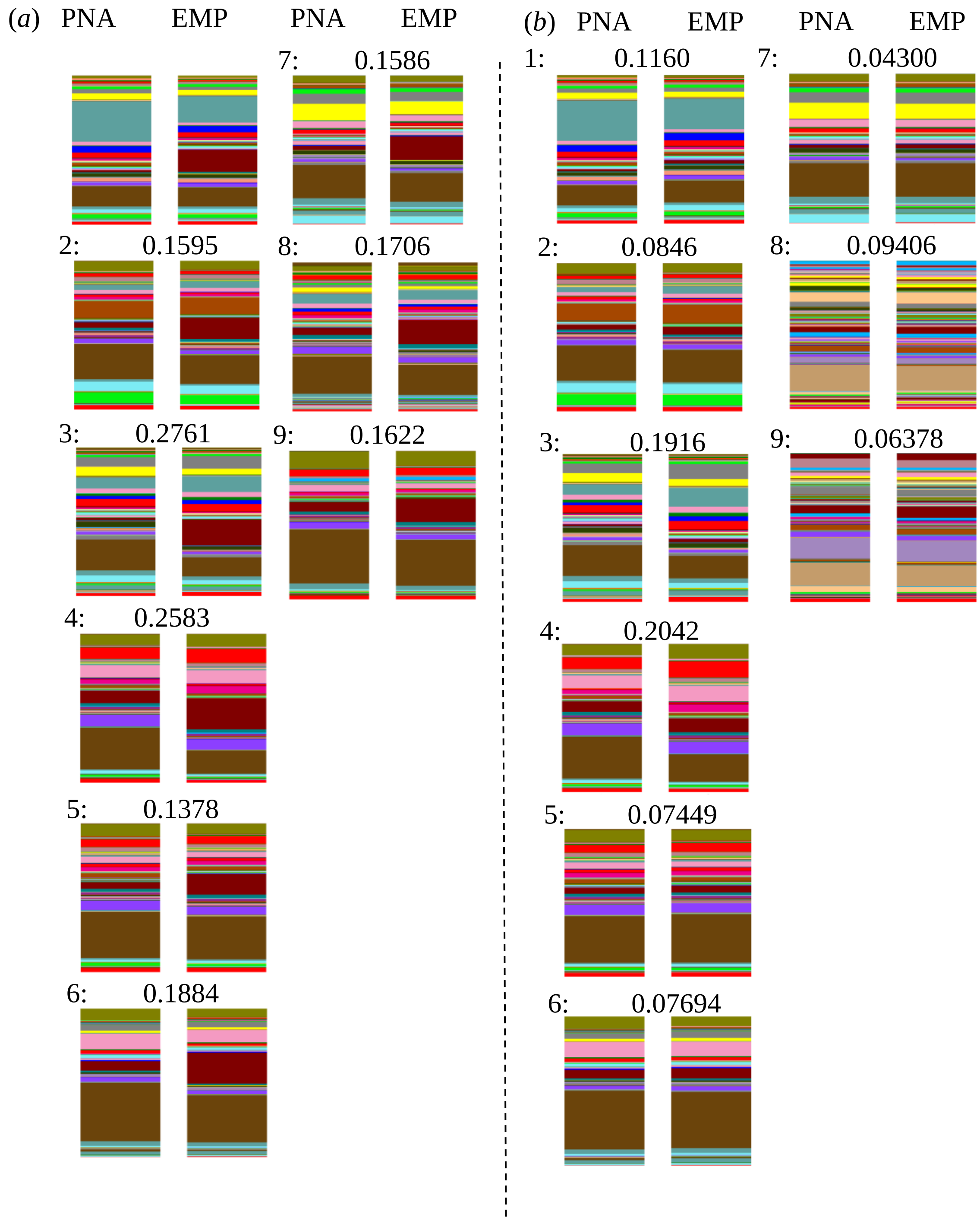

Figure 7.C.6: Seawater samples from Split Point, Washington (48.26° N, 124.25° W). Relative abundance of microbial taxa at the family level depicted via color. (*a*) Includes all OTUs after filtering out chloroplast and mitochondria, and (*b*) excludes all chloroplast, mitochondria and OTUs listed in the Supplementary Tables. Weighted UniFrac distances between replication samples quantify community similarity.

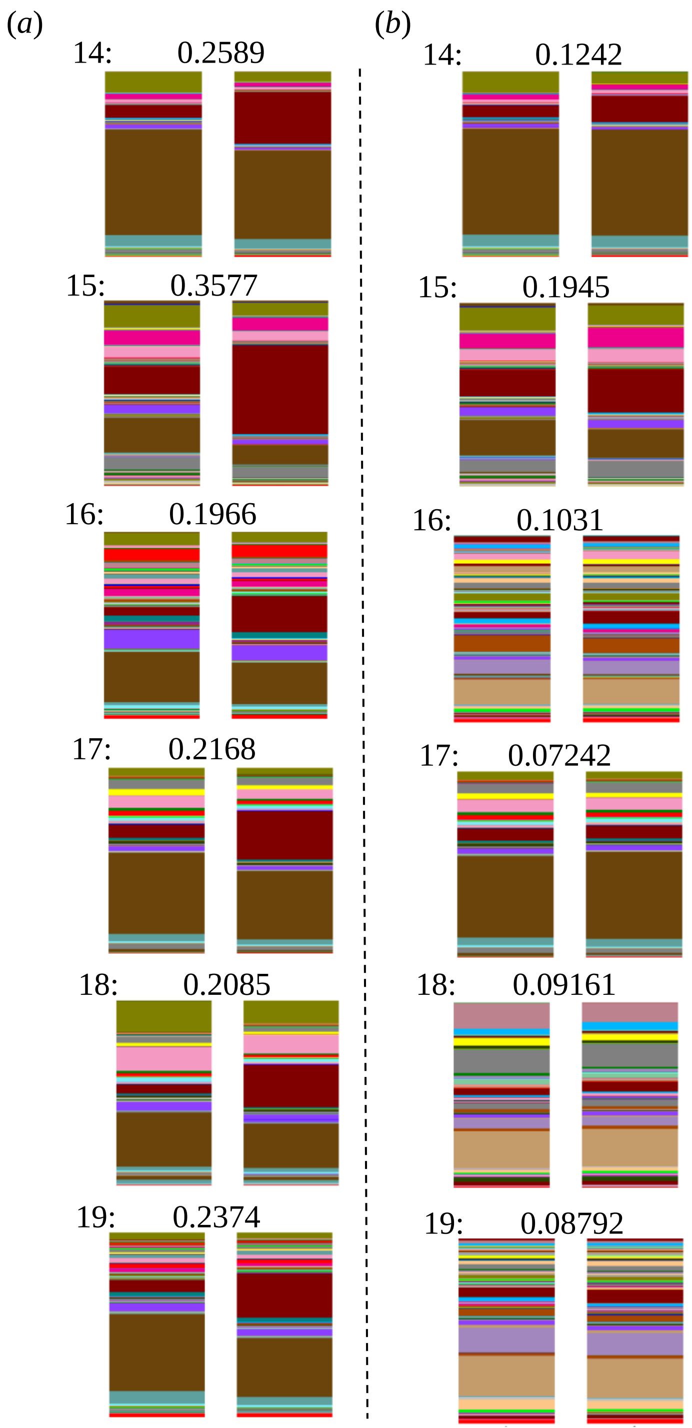

Table 7.C.4: Microbial taxa at lower relative abundance in seawater samples when sequenced with PNA primers versus EMP primers. The first column lists rank order abundance of each taxa in the entire seawater sample set. Reported p-values are from paired t-tests with and without false discovery rate correction.

Abund.	P-value	FDR	Taxonomic Classification
# 2	3.12^{-08}	2.21^{-04}	Proteobacteria;c_Alphaproteobacteria;o_**Rhodobacterales**;f_Rhodobacteraceae;g_
# 11	1.25^{-06}	1.54^{-03}	Proteobacteria;c_Alphaproteobacteria;o_**Rhodobacterales**;f_Rhodobacteraceae;g_Octadecabacter
# 50	3.78^{-06}	1.66^{-05}	Proteobacteria;c_Alphaproteobacteria;o_**Rhodobacterales**;f_Rhodobacteraceae;g_Pseudoruegeria
# 79	1.76^{-05}	5.01^{-04}	Proteobacteria;c_Alphaproteobacteria;o_**Rhodobacterales**;f_Rhodobacteraceae;Other
# 393	1.82^{-04}	2.57^{-03}	Proteobacteria;c_Alphaproteobacteria;o_**Rhizobiales**;f_Phyllobacteriaceae;Other
# 112	3.75^{-04}	2.63^{-03}	Proteobacteria;c_Alphaproteobacteria;o_**Kiloniellales**;f_Kiloniellaceae;g_
# 699	6.71^{-04}	2.76^{-03}	Proteobacteria;c_Gammaproteobacteria;o_34P16;f_;g_
# 66	0.0010	3.49^{-03}	Proteobacteria;c_Alphaproteobacteria;o_BD7-3;f_;g_
# 187	0.0013	7.66^{-04}	Proteobacteria;c_Alphaproteobacteria;o_**Rhizobiales**;f_Hyphomicrobiaceae;g_
# 175	0.0016	1.98^{-04}	Actinobacteria;c_Acidimicrobiia;o_**Acidimicrobiales**;f_TK06;g_
# 83	0.0019	7.90^{-03}	Proteobacteria;c_Alphaproteobacteria;o_**Rhodobacterales**;f_Rhodobacteraceae;g_Loktanella
# 457	0.0033	8.07^{-03}	Proteobacteria;c_Alphaproteobacteria;o_**Rhodobacterales**;f_Rhodobacteraceae;g_Sulfitobacter
# 70	0.0036	1.07^{-02}	Proteobacteria;c_Alphaproteobacteria;o_**Rhizobiales**;f_Phyllobacteriaceae;g_
# 167	0.0039	1.32^{-02}	Planctomycetes;c_OM190;o_CL500-15;f_;g_
# 478	0.0074	1.34^{-02}	Proteobacteria;c_Gammaproteobacteria;o_**Thiotrichales**;f_Piscirickettsiaceae;g_Methylophaga
# 759	0.0078	1.44^{-02}	Chlamydiae;c_Chlamydiia;o_**Chlamydiales**;f_Parachlamydiaceae;Other
# 286	0.0082	1.71^{-02}	Bacteroidetes;c_Bacteroidia;o_**Bacteroidales**;f_Porphyromonadaceae;g_Paludibacter
# 265	0.0090	1.73^{-02}	Proteobacteria;c_Gammaproteobacteria;o_**Alteromonadales**;f_Alteromonadaceae;g_nsmpVI18

Appendix 7D: Earth Microbiome Project database scan.

Table 7.D.1: Datasets scanned from the Earth Microbiome Project database. Samples were first filtered for low sequence number. Samples with at least 5000 sequences were filtered again for only those taxa listed in the Supplementary Tables that contain a 14 of 17 bp match to the pPNA primer. The last column lists the number of samples in each of these datasets that contain at least 1% of these taxa when amplified with EMP primers, suggesting that these types of environmental samples may lead to biased results if sequenced with pPNA primers. See Table 1 of the main text for a summary of the datasets containing samples in the last column.

Study #	Study Name	Total Samples	Samples w/ at least 5000 sequences	Samples w/ taxa in Supplementary Tables	# Samples in Table 1
94	Soil bacterial and fungal communities across a pH gradient in an arable soil.	26	0	N/A	N/A
103	Pyrosequencing-based assessment of soil pH as a predictor of soil bacterial community structure at the continental scale.	89	0	N/A	N/A
104	Soil bacterial diversity in the Arctic is not fundamentally different from that found in other biomes.	52	0	N/A	N/A
213	Shifts in bacterial community structure associated with inputs of low molecular weight carbon compounds to soil.	48	1	1	0
214	Microbial consumption and production of volatile organic compounds at the soil-litter interface.	12	0	N/A	N/A
231	Preliminary study of barn swallow microbiome.	83	0	N/A	N/A
314	Characterization of airborne microbial communities at a high-elevation site and their potential to act as atmospheric ice nuclei.	11	0	N/A	N/A
316	Population genetic structure of the prairie dog flea and plague vector, Oropsylla hirsute.	251	0	N/A	N/A
353	Effect of storage conditions on the assessment of bacterial community structure in soil and human-associated samples.	144	0	N/A	N/A
391	Postprandial remodeling of the gut microbiota in Burmese pythons.	130	0	N/A	N/A
396	The ecology of the phyllosphere: geographic and phylogenetic variability in the distribution of bacteria on tree leaves.	107	1	1	0
619	Neon soils.	337	0	N/A	N/A
632	Canadian metamicrobiome initiative.	13	11	11	3
638	Protist diversity in a permanently ice-covered Antarctic Lake during the polar night transition.	89	89	89	58
659	New Zealand free air carbon dioxide enrichment, agroresearch.	24	23	23	7
662	Intertidal microbes 16s for 2009 and 2010	46	46	46	42
678	Bioturbating shrimp alter the structure and diversity of bacterial communities in coastal marine sediments.	275	257	257	204
713	Diversity of carbonate deposits and basement rocks in continental and marine serpentine seeps.	51	1	1	0
723	Catlin arctic survey 2010 l3.	97	84	84	64
776	Jurelivicius Antarctic cleanup.	30	29	29	2
804	Brazelton LostCity chimney biofilm.	93	78	74	56
805	Effect of soil pH on soil metagenome.	14	14	14	8
807	Gibbons tongue river 16S.	44	44	44	43
808	NEON soils EMP Pilot.	15	13	13	11
809	NEON soils EMP Pilot.	21	19	19	13
810	Ocean Drilling Program Leg 201.	7	3	2	0

Table 7.D.1, continued.

829	Environmental metagenomic interrogation of Thar desert microbial communities.	2	2	2	2
846	Influence of tillage practices on soil microbial diversity and activity in a long-term corn experimental field under continuous maize production.	48	48	48	13
861	Comparison of groundwater samples from karst sinkholes (cenotes) from the Yucatan Peninsula, Mexico.	21	21	20	8
864	Magnificent Mongolian microbes.	230	228	228	48
889	Rees Volcano island MedSea.	8	8	8	7
894	Catchment sources of microbes.	1994	1920	1655	375
905	Hulth Gullmarsfjord sediments.	52	52	52	38
910	Viral communities associated with algal/coral interactions.	59	56	24	1
925	Yellowstone gradients.	412	356	136	32
926	Seasonal restructuring of the ground squirrel gut microbiota over the annual hibernation cycle.	46	0	N/A	N/A
929	Bacterial communities associated with the lichen symbiosis.	16	0	N/A	N/A
933	Latitudinal surveys of algal-associated microorganisms.	335	321	321	321
940	Song Colorado freshwater fish.	275	209	174	32
945	Routine samples of German Lakes.	1142	1089	1012	320
963	Green Iguana hindgut microbiome.	100	90	82	6
990	Fermilab spatial study.	708	697	697	29
1001	Cannabis soil microbiome.	26	23	23	20
1024	The soil microbiome influences grapevine-associated microbiota.	348	100	96	36
1030	Impact of fire on active layer and permafrost microbial communities and metagenomes in an upland Alaskan boreal forest.	150	147	147	123
1031	Myrold alder fir.	12	11	11	3
1033	Myrold alder fir.	12	5	5	3
1034	CryoCARB permafrost soil microbiome.	90	90	89	45
1035	New Zealand Terrestrial Antarctic Biocomplexity survey (NZTABS).	121	117	117	88
1036	Geochemical landscapes.	68	66	66	14
1037	Long term soil productivity project.	24	24	24	19
1038	Myrold Oregon transect.	21	21	21	14
1039	Rio de Janeiro coastline.	25	23	23	8
1041	Great Lake microbiome.	49	49	49	43
1043	Laboratory directed research and development biological carbon sequestration.	56	54	54	6
1056	Comparison of microbial flora in ant-eating mammals.	93	92	79	14
1064	Bee microbiome.	387	271	72	4
1197	Metagenome, metatranscriptome and single-cell sequencing reveal microbial response to Deepwater Horizon oil spill.	106	103	103	101
1198	Polluted polar coastal sediments.	61	57	57	57
1222	Bergen Ocean acidification mesocosms.	72	71	71	71
1235	EPOCA Svalbard 2010.	268	258	258	256
1240	L4 Time Series 2009-2010.	145	140	140	140
1242	Mendota Lake Eleven year time series.	96	91	90	11
1288	Temperate bog lakes.	1505	1350	1342	397
1289	Temple TX native exotic precipitation study.	65	64	64	49
1364	Temporal dynamics in bacterial community of hydra polyps after hatching	39	3	2	0
1453	Metcalf San Diego Zoo folivorus primate.	316	292	133	0
1485	Predator-prey interactions 18S.	60	58	0	N/A

Table 7.D.1, continued.

1526	Recovery of biological soil crust-like microbial communities in previously submerged soils of Glen canyon.	95	95	95	82
1530	Impact of fire on active layer and permafrost microbial communities and metagenomes in an upland Alaskan boreal forest.	98	94	94	85
1552	Lake microbial communities are resilient after a whole-ecosystem disturbance.	18	0	N/A	N/A
1578	Ice wedge polygon.	35	35	33	7
1579	Hawaii Kohana volcanic soils.	128	125	117	43
1580	Saline environments that may harbor novel lignocellulolytic activities tolerant of ionic liquids.	26	25	23	8
1621	Saline environments that may harbor novel lignocellulolytic activities tolerant of ionic liquids.	192	188	153	0
1622	Biodiversity and functional patterns of microbial assemblages in postglacial pond sediment profiles.	353	345	245	35
1627	Chu Tibetan plateau lake sediments.	18	18	18	6
1632	Bird egg shells from Spain.	604	527	278	37
1642	Microbial community of the bulk soil and rhizosphere of rice plants over its lifecycle.	644	623	623	25
1665	Marine mammal skin microbiomes.	186	114	86	30
1671	Bacterial communities associated with the surfaces of fresh fruits and vegetables.	214	0	N/A	N/A
1673	Mission Bay sediment viromes.	26	22	14	4
1674	Green roofs as biodiversity corridors in New York City.	151	146	146	135
1692	Friedman Alaska peat soils.	89	75	75	26
1694	Peralta starlings.	562	443	339	114
1696	Comparison of gut flora foliverous primates.	160	157	136	0
1702	Chu Changbai mountain soil.	22	22	22	17
1711	McGuire Kakamenga Kenya soils.	77	71	71	51
1713	Malaysia Lambir Soils.	34	34	34	10
1714	Malaysia Pasoh Land use logged forest.	25	23	23	10
1715	McGuire Nicaragua coffee soil.	61	60	60	18
1716	Panama precipitation grad soil.	43	41	41	4
1717	McGuire SW Kenya soils.	56	54	54	47
1721	Thomas soil agricultural enhancement.	292	260	246	174
1734	Gut microbiota of Phyllostomid bats that span a breadth of diets.	94	63	39	8
1736	Ezenwa Cape Buffalo.	614	500	468	1
1740	The global sponge microbiome: diversity and structure of symbiont communities across the phylum Porifera.	1403	1206	1098	282
1747	Development of the oral microbiota in captive Komodo dragons (Varanus komodoensis)	210	178	166	22
1773	Garcia bird gut microbiome	122	116	116	76
1792	Diversity and heritability of the maize rhizosphere microbiome under field conditions.	463	213	212	63
1818	Florida decay wastewater study.	198	186	167	52
1845	Variation in the microbiota of Ixodes ticks with geography, species and sex Illumina.	124	91	56	8
1883	Crump Arctic LTREB main.	3153	2415	2368	794
1885	Variation in the Microbiota of Ixodes ticks with geography, species and sex.	139	16	10	0
2019	Microbial biogeography of wine grapes is conditioned by cultivar, vintage, and climate.	272	81	60	0
2020	Study 2020.	98	0	N/A	N/A
2080	Seyler North Atlantic water column.	54	53	53	26
2104	Biogeographic patterns in below-ground diversity in New York City's Central Park are similar to those observed globally 16S.	1160	1160	1160	632

Table 7.D.1, continued.

2182	Hale folivorous primates.	167	162	78	4
2229	Thomas CMB Australian seaweed.	1378	1285	1285	1270
2259	Individual's diet diversity influences gut microbial diversity in two freshwater fish (threespine stickleback and Eurasian perch).	62	46	31	5
2300	Gut microbiome of hibernating bears.	96	68	16	0
2338	Song whitehead bats.	192	102	30	6
2382	The soil microbiome influences grapevine-associated microbiota HiSeq.	401	315	309	106
10119	Microbial biogeography of grapes predicts regional metabolite patterns in wine.	47	0	N/A	N/A
10141	Metcalf microbial community assembly and metabolic function during mammalian corpse decomposition mouse exp.	68	0	N/A	N/A
10142	Metcalf microbial community assembly and metabolic function during mammalian corpse decomposition SHSU winter.	104	0	N/A	N/A
10143	Metcalf microbial community assembly and metabolic function during mammalian corpse decomposition SHSU April 2012 exp.	927	796	0	N/A
10145	Beach sand microbiome from Calvert Island Canada.	114	91	91	86
10156	The effect of wetland age and restoration methodology on long term development and ecosystem functions of restored wetlands.	192	179	178	47
10180	Metagenome of microbial communities involved in the nitrogen cycle in sugarcane soils in Brazil.	128	112	110	36
10196	Composition of symbiotic bacteria as a predictor of survival in Panamanian golden frogs infected with Batrachochytrium dendrobatidis.	37	37	36	2
10245	Diversity, host affinity and ecology of foliar endophytic microbes in Amazonian Peru.	120	103	61	7
10246	The North American Arctic Transect, NAAT and the Eurasian Arctic Transect, EAT.	112	70	70	58
10272	Most of the dominant members of amphibian skin bacterial communities can be readily cultured.	64	64	59	31
10273	SM April WHOI SeaWater	67	45	45	23
10278	Identifying the microbial cohorts associated with drought-driven carbon release from peatland ecosystems.	216	215	215	29
10308	Whitehead fish.	1208	938	697	172
10311	Ecological succession reveals signatures of marine–terrestrial transition in salt marsh fungal communities.	58	0	N/A	N/A
10324	Diversity of Rickettsiales in the microbiome of the Lone Star Tick, Amblyomma americanum.	87	1	1	1
10346	The global sponge microbiome: diversity and structure of symbiont communities across the phylum Porifera – final.	1390	1194	1068	285
10363	Investigating the rhizosphere microbiome as influenced by soil selenium, plant species, plant selenium accumulation and geographic proximity.	64	58	58	55
10369	Obligate biotroph pathogens defend their niche against competing microbes by keeping host defense at a functional level.	9	0	N/A	N/A
10376	Muegge mammals.	22	22	17	0

LITERATURE CITED

Agrawal, A. A. 1998. Induced responses to herbivory and increased plant performance. Science **279**:1201-1202.

Agrawal, A. A. 2007. Macroevolution of plant defense strategies. Trends in Ecology and Evolution **22**:103-109.

Agrawal, A. A., A. P. Hastings, M. T. J. Johnson, J. L. Maron, and J.-P. Salminen. 2012. Insect herbivores drive real-time ecological and evolutionary change in plant populations. Science **338**:113-116.

Allmann, S., and I. T. Baldwin. 2010. Insects betray themselves in nature to predators by rapid isomerization of green leaf volatiles. Science **329**:1075-1078.

Awmack, C. S., and S. R. Leather. 2002. Host plant quality and fecundity in herbivorous insects. Annual Review of Entomology **47**:817-844.

Badri, D. V., J. M. Chaparro, R. Zhang, Q. Shen, and J. M. Vivanco. 2013. Application of natural blends of phytochemicals derived from the root exudates of arabidopsis to the soil reveal that phenolic-related compounds predominantly modulate the soil microbiome. Journal of Biological Chemistry **288**:4502-4512.

Baldwin, I. T. 1998. Jasmonate-induced responses are costly but benefit plants under attack in native populations. Proceedings of the National Academy of Sciences USA **95**:8113-8118.

Barbehenn, R., C. Jones, A. Hagerman, M. Karonen, and J.-P. Salminen. 2006. Ellagitannins have greater oxidative activities than condensed tannins and galloyl glucoses at high pH: Potential impact on caterpillars. Journal of Chemical Ecology **32**:2253-2267.

Barbehenn, R. V., A. Jaros, G. Lee, C. Mozola, Q. Weir, and J.-P. Salminen. 2009. Hydrolyzable tannins as "quantitative defenses": Limited impact against *Lymantria dispar* caterpillars on hybrid poplar. Journal of Insect Physiology **55**:297-304.

Bassar, R. D., M. C. Marshall, A. López-Sepulcre, E. Zandonà, S. K. Auer, J. Travis, C. M. Pringle, A. S. Flecker, S. A. Thomas, and D. F. Fraser. 2010. Local adaptation in Trinidadian guppies alters ecosystem processes. Proceedings of the National Academy of Sciences **107**:3616-3621.

Behmer, S. T., and A. Joern. 1993. Diet choice by a grass-feeding grasshopper based on the need for a limiting nutrient. Functional Ecology **7**:522-527.

Benjamini, Y., and Y. Hochberg. 1995. Controlling the false discovery rate: A practical and powerful approach to multiple testing. Journal of the Royal Statistical Society. Series B (Methodological) **57**:289-300.

Benner, R., M. L. Fogel, E. K. Sprague, and R. E. Hodson. 1987. Depletion of ^{13}C in lignin and its implications for stable carbon isotope studies. Nature **329**:708-710.

Berendsen, R. L., C. M. J. Pieterse, and P. A. H. M. Bakker. 2012. The rhizosphere microbiome and plant health. Trends in Plant Science **17**:478-486.

Berge, G., I. Nordal, and G. Hestmark. 1998. The effect of breeding systems and pollination vectors on the genetic variation of small plant populations within an agricultural landscape. Oikos **81**:17-29.

Boege, K., and R. J. Marquis. Facing herbivory as you grow up: The ontogeny of resistance in plants. Trends in Ecology & Evolution **20**:441-448.

Bolnick, D. I., P. Amarasekare, M. S. Araújo, R. Bürger, J. M. Levine, M. Novak, V. H. W. Rudolf, S. J. Schreiber, M. C. Urban, and D. A. Vasseur. 2011. Why intraspecific trait variation matters in community ecology. Trends in Ecology and Evolution **26**:183-192.

Bolnick, D. I., L. K. Snowberg, P. E. Hirsch, C. L. Lauber, E. Org, B. Parks, A. J. Lusis, R. Knight, J. G. Caporaso, and R. Svanbäck. 2014. Individual diet has sex-dependent effects on vertebrate gut microbiota. Nature Communication **5**.

Bormann, B. T., and D. S. DeBell. 1981. Nitrogen content and other soil properties related to age of red alder stands. Soil Science Society of America Journal **45**:428–432.

Breedlove, D. E., and P. R. Ehrlich. 1968. Plant-herbivore coevolution: Lupines and lycaenids. Science **162**:671-672.

Brown, K. R., and P. J. Courtin. 2003. Effects of phosphorus fertilization and liming on growth, mineral nutrition, and gas exchange of *Alnus rubra* seedlings grown in soils from mature alluvial *Alnus* stands. Canadian Journal of Forest Research **33**:2089-2096.

Brown, K. R., P. J. Courtin, and R. W. Negrave. 2011. Growth, foliar nutrition and $\delta^{13}C$ responses of red alder (*Alnus rubra*) to phosphorus additions soon after planting on moist sites. Forest Ecology and Management **262**:791-802.

Bruin, J., M. W. Sabelis, and M. Dicke. 1995. Do plants tap SOS signals from their infested neighbours? Trends in Ecology and Evolution **10**:167-170.

Bruno, J. F., and M. I. O'Connor. 2005. Cascading effects of predator diversity and omnivory in a marine food web. Ecology Letters **8**:1048-1056.

Bryant, J. P., F. S. Chapin, III, and D. R. Klein. 1983. Carbon/nutrient balance of boreal plants in relation to vertebrate herbivory. Oikos **40**:357-368.

Bryant, J. P., F. S. Chapin, III, P. B. Reichardt, and T. P. Clausen. 1987a. Response of winter chemical defense in Alaska paper birch and green alder to manipulation of plant carbon/nutrient balance. Oecologia **72**:510-514.

Bryant, J. P., T. P. Clausen, P. B. Reichardt, M. C. McCarthy, and R. A. Werner. 1987b. Effect of nitrogen fertilization upon the secondary chemistry and nutritional value of quaking aspen (*Populus tremuloides Michx.*) leaves for the large aspen tortrix (*Choristoneura conflictana* (Walker)). Oecologia **73**:513-517.

Campbell, A. H., E. M. Marzinelli, J. Gelber, and P. D. Steinberg. 2015. Spatial variability of microbial assemblages associated with a dominant habitat-forming seaweed. Frontiers in Microbiology **6**:230.

Caporaso, J. G., J. Kuczynski, J. Stombaugh, K. Bittinger, F. D. Bushman, E. K. Costello, N. Fierer, A. G. Pena, J. K. Goodrich, J. I. Gordon, G. A. Huttley, S. T. Kelley, D. Knights, J. E. Koenig, R. E. Ley, C. A. Lozupone, D. McDonald, B. D. Muegge, M. Pirrung, J. Reeder, J. R. Sevinsky, P. J. Turnbaugh, W. A. Walters, J. Widmann, T. Yatsunenko, J. Zaneveld, and R. Knight. 2010. QIIME allows analysis of high-throughput community sequencing data. Nature Methods **7**:335-336.

Caporaso, J. G., C. L. Lauber, W. A. Walters, D. Berg-Lyons, J. Huntley, N. Fierer, S. M. Owens, J. Betley, L. Fraser, M. Bauer, N. Gormley, J. A. Gilbert, G. Smith, and R. Knight. 2012. Ultra-high-throughput microbial community analysis on the Illumina HiSeq and MiSeq platforms. ISME J:1621-1624.

Cardinale, B. J., D. S. Srivastava, J. E. Duffy, J. P. Wright, A. L. Downing, M. Sankaran, and C. Jouseau. 2006a. Effects of biodiversity on the functioning of trophic groups and ecosystems. Nature **443**:989-992.

Cardinale, B. J., D. S. Srivastava, J. Emmett Duffy, J. P. Wright, A. L. Downing, M. Sankaran, and C. Jouseau. 2006b. Effects of biodiversity on the functioning of trophic groups and ecosystems. Nature **443**:989-992.

Cebrian, J. 1999. Patterns in the fate of production in plant communities. American Naturalist **154**:449-468.

Chen, J., R. F. Gonzalez-Laredo, and J. J. Karchesy. 2000. Minor diarylheptanoid glycosides of *Alnus rubra* bark. Phytochemistry **53**:971-973.

Choudhury, D. 1988. Herbivore induced changes in leaf-litter resource quality: a neglected aspect of herbivory in ecosystem nutrient dynamics. Oikos **51**:389-393.

Christensen, T. A., H. Mustaparta, and J. G. Hilderbrand. 1989. Discrimination of sex pheromone blends in the olfactory system of the moth. Chemical Senses **14**:463-477.

Cipollini, D., and J. Bergelson. 2001. Plant density and nutrient availability constrain constitutive and wound-induced expression of trypsin inhibitors in *Brassica napus*. Journal of Chemical Ecology **27**:593-610.

Clark, T. 1999. Evolution and adaptive significance of larval midgut alkalinization in the insect superorder *Mecopterida*. Journal of Chemical Ecology **25**:1945-1960.

Coley, P. D. 1980. Effects of leaf age and plant life history patterns on herbivory. Nature **284**:2.

Coley, P. D. 1983. Herbivory and defensive characteristics of tree species in a lowland tropical forest. Ecological Monographs **53**:209-234.

Coley, P. D., J. P. Bryant, and F. S. Chapin III. 1985. Resource availability and plant antiherbivore defense. Science **230**:895-899.

Crutsinger, G. M., M. D. Collins, J. A. Fordyce, Z. Gompert, C. C. Nice, and N. J. Sanders. 2006. Plant genotypic diversity predicts community structure and governs an ecosystem process. Science **313**:966-968.

Crutsinger, G. M., L. Souza, and N. J. Sanders. 2008. Intraspecific diversity and dominant genotypes resist plant invasions. Ecology Letters **11**:16-23.

Cyr, H., and M. L. F. Face. 1993. Magnitude and patterns of herbivory in aquatic and terrestrial ecosystems. Nature **361**:148-150.

Dai, G.-Z., J.-L. Shang, and B.-S. Qiu. 2012. Ammonia may play an important role in the succession of cyanobacterial blooms and the distribution of common algal species in shallow freshwater lakes. Global Change Biology **18**:1571-1581.

De Filippis, F., A. Genovese, P. Ferranti, J. A. Gilbert, and D. Ercolini. 2016. Metatranscriptomics reveals temperature-driven functional changes in microbiome impacting cheese maturation rate. Scientific Reports **6**:21871.

DeBell, D. S., and M. A. Radwan. 1984. Foliar chemical concentrations in red alder stands of various ages. Plant and Soil **77**:391-394.

Dolch, R., and T. Tscharntke. 2000. Defoliation of alders (*Alnus glutinosa*) affects herbivory by leaf beetles on undamaged neighbours. Oecologia **125**:504-511.

Driebe, E. M., and T. G. Whitham. 2000. Cottonwood hybridization affects tannin and nitrogen content of leaf litter and alters decomposition. Oecologia **123**:99-107.

Egan, S., T. Harder, C. Burke, P. Steinberg, S. Kjelleberg, and T. Thomas. 2013. The seaweed holobiont: Understanding seaweed–bacteria interactions. FEMS Microbiology Reviews **37**:462-476.

Elderd, B. D., B. J. Rehill, K. J. Haynes, and G. Dwyer. 2013. Induced plant defenses, host–pathogen interactions, and forest insect outbreaks. Proceedings of the National Academy of Sciences USA **110**:14978-14983.

Elser, J. J., M. E. S. Bracken, E. E. Cleland, D. S. Gruner, W. S. Harpole, H. Hillebrand, J. T. Ngai, E. W. Seabloom, J. B. Shurin, and J. E. Smith. 2007. Global analysis of nitrogen and phosphorus limitation of primary producers in freshwater, marine and terrestrial ecosystems. Ecology Letters **10**:1135-1142.

Farmer, E. E., and C. A. Ryan. 1990. Interplant communication: Airborne methyl jasmonate induces synthesis of proteinase inhibitors in plant leaves. Proceedings of the National Academy of Sciences USA **87**:7713-7716.

Farrand, L., J. Y. Kim, S. Byun, A. Im-aram, J. Lee, J. Y. Suh, K. W. Lee, H. J. Lee, and B. K. Tsang. 2014. The diarylheptanoid hirsutenone sensitizes chemoresistant ovarian cancer cells to cisplatin via modulation of apoptosis-inducing factor and X-linked inhibitor of apoptosis. Journal of Biological Chemistry:1723-1731.

Fonte, S. J., and T. D. Schowalter. 2004. Decomposition of greenfall vs. senescent foliage in a tropical forest ecosystem in Puerto Rico. Biotropica **36**:474-482.

Foré, S. A., R. J. Hickey, J. L. Vankat, S. I. Guttman, and R. L. Schaefer. 1992. Genetic structure after forest fragmentation: A landscape ecology perspective on *Acer saccharum*. Canadian Journal of Botany **70**:1659-1668.

Fu, Y., K. F. Keats, R. B. Rivkin, and A. S. Lang. 2013. Water mass and depth determine the distribution and diversity of *Rhodobacterales* in an Arctic marine system. FEMS Microbiology Ecology **84**:564-576.

Fukui, D., M. Murakami, S. Nakano, and T. Aoi. 2006. Effect of emergent aquatic insects on bat foraging in a riparian forest. Journal of Animal Ecology **75**:1252-1258.

Gartner, T. B., and Z. G. Cardon. 2004. Decomposition dynamics in mixed-species leaf litter. Oikos **104**:230-246.

Gessner, M. O. 1991. Differences in processing dynamics of fresh and dried leaf litter in a stream ecosystem. Freshwater Biology **26**:12.

Gessner, M. O., C. M. Swan, C. K. Dang, B. G. McKie, R. D. Bardgett, D. H. Wall, and S. Hättenschwiler. 2010. Diversity meets decomposition. Trends in Ecology & Evolution **25**:372-380.

Gilbert, J. A., J. K. Jansson, and R. Knight. 2014. The Earth Microbiome project: Successes and aspirations. BMC Biology **12**:1-4.

Gilbert, J. A., J. A. Steele, J. G. Caporaso, L. Steinbruck, J. Reeder, B. Temperton, S. Huse, A. C. McHardy, R. Knight, I. Joint, P. Somerfield, J. A. Fuhrman, and D. Field. 2012. Defining seasonal marine microbial community dynamics. Pages 298-308 ISME J:298-308.

González-Hernández, M. P., E. E. Starkey, and J. Karchesy. 2000. Seasonal variation in concentrations of fiber, crude protein, and phenolic compounds in leaves of red alder (*Alnus Rubra*): Nutritional implications for cervids. Journal of Chemical Ecology **26**:293-301.

González-Laredo, R. F., R. F. Helm, J. Chen, and J. J. Karchesy. 1998. Two acylated diarylheptanoid glycosides from red alder bark. Journal of Natural Products **61**:1292-1294.

Gower, J. C. 1975. Generalized procrustes analysis. Psychometrika **40**:33-51.

Gundlach, H., M. J. Müller, T. M. Kutchan, and M. H. Zenk. 1992. Jasmonic acid is a signal transducer in elicitor-induced plant cell cultures. Proceedings of the National Academy of Sciences USA **89**:2389-2393.

Gómez, S., R. A. Ferrieri, M. Schueller, and C. M. Orians. 2010. Methyl jasmonate elicits rapid changes in carbon and nitrogen dynamics in tomato. New Phytologist **188**:835-844.

Gökkaya, K., T. M. Hurd, and D. J. Raynal. 2006. Symbiont nitrogenase, alder growth, and soil nitrate response to phosphorus addition in alder (*Alnus incana* ssp. *rugosa*) wetlands of the Adirondack Mountains, New York State, USA. Environmental and Experimental Botany **55**:97-109.

Horner, J. D., J. R. Gosz, and R. G. Cates. 1988. The role of carbon-based plant secondary metabolites in decomposition in terrestrial ecosystems. American Naturalist **132**:869-883.

Howe, G. A., and G. Jander. 2008. Plant immunity to insect herbivores. Annual Review of Plant Biology **59**:41-66.

Hunter, M. D., and J. N. McNeil. 1997. Host-plant quality influences diapause and voltinism in a polyphagous insect herbivore. Ecology **78**:977-986.

Hunter, M. D., and J. C. Schultz. 1995. Fertilization mitigates chemical induction and herbivore responses within damaged oak trees. Ecology **76**:1226-1232.

Hutchens, J. J., and E. F. Benfield. 2000. Effects of forest defoliation by the gypsy moth on detritus processing in southern appalachian streams. The American Midland Naturalist **143**:397-404.

Hättenschwiler, S., and P. M. Vitousek. 2000. The role of polyphenols in terrestrial ecosystem nutrient cycling. Trends in Ecology and Evolution **15**:238-243.

Irons Iii, J. G., J. P. Bryant, and M. W. Oswood. 1991. Effects of moose browsing on decomposition rates of birch leaf litter in a subarctic stream. Canadian Journal of Fisheries and Aquatic Sciences **48**:442-444.

Ives, A. R., and S. R. Carpenter. 2007. Stability and diversity of ecosystems. Science **317**:58-62.

Jackrel, S. L., T. C. Morton, and J. T. Wootton. 2016. Intraspecific leaf chemistry drives locally accelerated ecosystem function in aquatic and terrestrial communities. Ecology:n/a-n/a.

Jackrel, S. L., and J. T. Wootton. 2014. Local adaptation of stream communities to intraspecific variation in a terrestrial ecosystem subsidy. Ecology **95**:37-43.

Jackrel, S. L., and J. T. Wootton. 2015a. Cascading effects of induced terrestrial plant defences on aquatic and terrestrial ecosystem function. Proceedings of the Royal Society of London B: Biological Sciences **282**.

Jackrel, S. L., and J. T. Wootton. 2015b. Diversity of riparian plants among and within species shapes river communities. PLoS ONE **10**:e0142362.

Kardol, P., N. J. Cornips, M. M. L. van Kempen, J. M. T. Bakx-Schotman, and W. H. van der Putten. 2007. Microbe-mediated plant-soil feedback causes historical contigency effects in plant community assembly. Ecological Monographs **77**:147-162.

Karonen, M., J. Parker, A. Agrawal, and J.-P. Salminen. 2010. First evidence of hexameric and heptameric ellagitannins in plants detected by liquid chromatography/electrospray ionisation mass spectrometry. Rapid Communications in Mass Spectrometry **24**:3151-3156.

Kato, C., T. Iwata, S. Nakano, and D. Kishi. 2003. Dynamics of aquatic insect flux affects distribution of riparian web-building spiders. Oikos **103**:113-120.

Kayranli, B., M. Scholz, A. Mustafa, and Å. Hedmark. 2009. Carbon storage and fluxes within freshwater wetlands: A critical review. Wetlands **30**:111-124.

Kind, T., and O. Fiehn. 2007. Seven Golden Rules for heuristic filtering of molecular formulas obtained by accurate mass spectrometry. BMC Bioinformatics: 105.

Kinney, K. K., R. L. Lindroth, S. M. Jung, and E. V. Nordheim. 1997. Effects of CO_2 and NO_3^- availability on deciduous trees: Phytochemistry and insect performance. Ecology **78**:215-230.

Knight, T. M., M. W. McCoy, J. M. Chase, K. A. McCoy, and R. D. Holt. 2005. Trophic cascades across ecosystems. Nature **437**:880-883.

Kominoski, J. S., L. B. Marczak, and J. S. Richardson. 2011. Riparian forest composition affects stream litter decomposition despite similar microbial and invertebrate communities. Ecology **92**:151-159.

Kotilainen, T., J. Haimi, R. Tegelberg, R. Julkunen-Tiitto, E. Vapaavuori, and P. J. Aphalo. 2009. Solar ultraviolet radiation alters alder and birch litter chemistry that in turn affects decomposers and soil respiration. Oecologia **161**:719-728.

Kuiters, A. T. 1990. Role of phenolic substances from decomposing forest litter in plant-soil interactions. Acta Botanica Neerlandica **39**:329-348.

Kwong, W. K., and N. A. Moran. 2016. Gut microbial communities of social bees. Nature Reviews Microbiology **14**:374-384.

Lankau, R. A. 2007. Specialist and generalist herbivores exert opposing selection on a chemical defense. New Phytologist **175**:176-184.

Lecerf, A., and E. Chauvet. 2008. Intraspecific variability in leaf traits strongly affects alder leaf decomposition in a stream. Basic and Applied Ecology **9**:598-605.

Lecerf, A., M. Dobson, C. Dang, and E. Chauvet. 2005. Riparian plant species loss alters trophic dynamics in detritus-based stream ecosystems. Oecologia **146**:432-442.

Lecerf, A., G. Marie, J. S. Kominoski, C. J. LeRoy, C. Bernadet, and C. M. Swan. 2011. Incubation time, functional litter diversity, and habitat characteristics predict litter-mixing effects on decomposition. Ecology **92**:160-169.

LeRoy, C. J., T. G. Whitham, S. C. Wooley, and J. C. Marks. 2007. Within-species variation in foliar chemistry influences leaf-litter decomposition in a Utah river. Journal of the North American Benthological Society **26**:426-438.

Lindow, S. E., and M. T. Brandl. 2003. Microbiology of the phyllosphere. Applied and Environmental Microbiology **69**:1875-1883.

Luken, J. O., and R. W. Fonda. 1983. Nitrogen accumulation in a chronosequence of red alder communities along the Hoh River, Olympic National Park, Washington. Canadian Journal of Forest Research **13**:1228-1237.

Lundberg, D. S., S. L. Lebeis, S. H. Paredes, S. Yourstone, J. Gehring, S. Malfatti, J. Tremblay, A. Engelbrektson, V. Kunin, T. G. d. Rio, R. C. Edgar, T. Eickhorst, R. E. Ley, P. Hugenholtz, S. G. Tringe, and J. L. Dangl. 2012. Defining the core *Arabidopsis thaliana* root microbiome. Nature **488**:86-90.

Lundberg, D. S., S. Yourstone, P. Mieczkowski, C. D. Jones, and J. L. Dangl. 2013. Practical innovations for high-throughput amplicon sequencing. Nature Methods **10**:999-1002.

Magurran, A. E. 1988. Ecological diversity and its measurement. Chapman & Hall.

Margulis, L. 1981. Symbiosis in cell evolution: Life and its environment on the early earth.

Martin, D. M., J. Gershenzon, and J. Bohlmann. 2003. Induction of volatile terpene biosynthesis and diurnal emission by methyl jasmonate in foliage of Norway spruce. Plant Physiology **132**:1586-1599.

Mason, C., K. Rubert-Nason, R. Lindroth, and K. Raffa. 2015. Aspen defense chemicals influence midgut bacterial community composition of gypsy moth. Journal of Chemical Ecology **41**:75-84.

Mattson, W. J. 1980a. Herbivory in relation to plant nitrogen content. Annual Review of Ecology and Systematics **11**:119-161.

Mattson, W. J. 1980b. Herbivory in relation to plant nitrogen content. Annual Review of Ecology and Systematics **11**:42.

McCutcheon, A. R., S. M. Ellis, R. E. W. Hancock, and G. H. N. Towers. 1994. Antifungal screening of medicinal plants of British Columbian native peoples. Journal of Ethnopharmacology **44**:157-169.

Merritt, R. W., K. W. Cummins, and M. B. Berg. 2008. An Introduction to the Aquatic Insects of North America. Kendall/Hunt Publishing Co., Dubuque, Iowa.

Mithöfer, A., G. Wanner, and W. Boland. 2005. Effects of feeding *Spodoptera littoralis* on lima bean leaves. II. Continuous mechanical wounding resembling insect feeding is sufficient to elicit herbivory-related volatile emission. Plant Physiology **137**:1160-1168.

Moilanen, J., and J.-P. Salminen. 2008. Ecologically neglected tannins and their biologically relevant activity: Chemical structures of plant ellagitannins reveal their in vitro oxidative activity at high pH. Chemoecology **18**:73-83.

Moilanen, J., J. Sinkkonen, and J.-P. Salminen. 2013. Characterization of bioactive plant ellagitannins by chromatographic, spectroscopic and mass spectrometric methods. Chemoecology **23**:165-179.

Motomori, K., H. Mitsuhashi, and S. Nakano. 2001. Influence of leaf litter quality on the colonization and consumption of stream invertebrate shredders. Ecological Research **16**:173-182.

Muegge, B. D., J. Kuczynski, D. Knights, J. C. Clemente, A. González, L. Fontana, B. Henrissat, R. Knight, and J. I. Gordon. 2011. Diet drives convergence in gut microbiome functions across mammalian phylogeny and within humans. Science **332**:970-974.

Muilenburg, V. L., P. L. Phelan, P. Bonello, and D. A. Herms. 2011. Inter- and intra-specific variation in stem phloem phenolics of paper birch (*Betula papyrifera*) and European white birch (*Betula pendula*). Journal of Chemical Ecology **37**:1193-1202.

Mullis, K. B., H. A. Erlich, N. Arnheim, G. T. Horn, R. K. Saiki, and S. J. Scharf. 1989. Process for amplifying, detecting, and/or cloning nucleic acid sequences. Google Patents.

Murakami, N., and S. Nakano. 2002 Indirect effect of aquatic insect emergence on a terrestrial insect population through predation by birds. Ecology Letters **5**:5.

Nakagawa, S., and H. Schielzeth. 2013. A general and simple method for obtaining R^2 from generalized linear mixed-effects models. Methods in Ecology and Evolution **4**:133-142.

Nakano, S., and M. Murakami. 2001. Reciprocal subsidies: Dynamic interdependence between terrestrial and aquatic food webs. Proceedings of the National Academy of Sciences USA **98**:166-170.

Oleksyn, J., P. Karolewski, M. J. Giertych, R. Zytkowiak, P. B. Reich, and M. G. Tjoelker. 1998. Primary and secondary host plants differ in leaf-level photosynthetic response to herbivory: Evidence from *Alnus* and *Betula* grazed by the alder beetle, *Agelastica alni*. New Phytologist **140**:239-249.

Posch, T., O. Koster, M. M. Salcher, and J. Pernthaler. 2012. Harmful filamentous cyanobacteria favoured by reduced water turnover with lake warming. Nature Climate Change **2**:809-813.

Reymond, P., H. Weber, M. Damond, and E. E. Farmer. 2000. Differential gene expression in response to mechanical wounding and insect feeding in *Arabidopsis*. Plant Cell **12**:707-720.

Rice, W. R., and S. D. Gaines. 1994. The ordered-heterogeneity family of tests. Biometrics **50**:746-752.

Rothermel, B. B., and R. D. Semlitsch. 2002. An experimental investigation of landscape resistance of forest versus old-field habitats to emigrating juvenile amphibians. Conservation Biology **16**:1324-1332.

Sabo, J. L., and M. E. Power. 2002. River-watershed exchange: Effects of riverine subsidies on riparian lizards and their terrestrial prey. Ecology **83**:10.

Salminen, J.-P., and M. Karonen. 2011. Chemical ecology of tannins and other phenolics: we need a change in approach. Functional Ecology **25**:325-338.

Sati, S. C., N. Sati, and O. P. Sati. 2011. Bioactive constituents and medicinal importance of genus *Alnus*. Pharmacognosy Reviews **5**:174-183.

Schimel, J., R. Cates, and R. Ruess. 1998. The role of balsam poplar secondary chemicals in controlling soil nutrient dynamics through succession in the Alaskan taiga. Biogeochemistry **42**:221-234.

Schindler, D. W. 1977. Evolution of phosphorus limitation in lakes. Science **195**:260-262.

Schindler, M. H., and M. O. Gessner. 2009. Functional leaf traits and biodiversity effects on litter decomposition in a stream. Ecology **90**:1641-1649.

Schweitzer, J., M. Madritch, J. Bailey, C. LeRoy, D. Fischer, B. Rehill, R. Lindroth, A. Hagerman, S. Wooley, S. Hart, and T. Whitham. 2008. From genes to ecosystems: The genetic basis of condensed tannins and their role in nutrient regulation in a *Populus* model system. Ecosystems **11**:1005-1020.

Schweitzer, J. A., J. K. Bailey, B. J. Rehill, G. D. Martinsen, S. C. Hart, R. L. Lindroth, P. Keim, and T. G. Whitham. 2004. Genetically based trait in a dominant tree affects ecosystem processes. Ecology Letters **7**:127-134.

Shogan, B. D., D. P. Smith, S. Christley, J. A. Gilbert, O. Zaborina, and J. C. Alverdy. 2014. Intestinal anastomotic injury alters spatially defined microbiome composition and function. Microbiome **2**:1-10.

Singh, R. P., and C. R. K. Reddy. 2015. Unraveling the functions of the macroalgal microbiome. Frontiers in Microbiology **6**:1488.

Smith, C. C. R., L. K. Snowberg, J. Gregory Caporaso, R. Knight, and D. I. Bolnick. 2015. Dietary input of microbes and host genetic variation shape among-population differences in stickleback gut microbiota. ISME J **9**:2515-2526.

Stevens, M., A. Gusse, and R. Lindroth. 2014. Root chemistry in populus tremuloides: Effects of soil nutrients, defoliation, and genotype. Journal of Chemical Ecology **40**:31-38.

Stout, R., W. Taft, and R. Merrit. 1985. Patterns of macroinvertebrate colonization on fresh and senescent alder leaves in two Michigan streams. Freshwater Biology **15**:7.

Sullam, K. E., S. D. Essinger, C. A. Lozupone, M. P. O'Connor, G. L. Rosen, R. O. B. Knight, S. S. Kilham, and J. A. Russell. 2012. Environmental and ecological factors that shape the gut bacterial communities of fish: A meta-analysis. Molecular Ecology **21**:3363-3378.

Sun, J., V. Cardoza, D. M. Mitchell, L. Bright, G. Oldroyd, and J. M. Harris. 2006. Crosstalk between jasmonic acid, ethylene and Nod factor signaling allows integration of diverse inputs for regulation of nodulation. The Plant Journal **46**:961-970.

Sunnerheim, K., and K. Bratt. 2004. Identification of centrolobol as the platyphylloside metabolite responsible for the observed effect on in vitro digestibility of hay. Journal of Agricultural and Food Chemistry **52**:5869-5872.

Swan, C. M., M. A. Gluth, and C. L. Horne. 2009. Leaf litter species evenness influences nonadditive breakdown in a headwater stream. Ecology **90**:1650-1658.

Taylor, J. D., S. D. Cottingham, J. Billinge, and M. Cunliffe. 2014. Seasonal microbial community dynamics correlate with phytoplankton-derived polysaccharides in surface coastal waters. ISME J **8**:245-248.

Teece, M. A., and M. L. Fogel. 2007. Stable carbon isotope biogeochemistry of monosaccharides in aquatic organisms and terrestrial plants. Organic Geochemistry **38**:458-473.

Thompson, J. N. 2005. The geographic mosaic of coevolution. University of Chicago press, Chicago, Illinois, USA.

Triska, F. J., and J. R. Sedell. 1976. Decomposition of four species of leaf litter in response to nitrate manipulation. Ecology **57**:783-792.

Tscharntke, T., S. Thiessen, R. Dolch, and W. Boland. 2001. Herbivory, induced resistance, and interplant signal transfer in *Alnus glutinosa*. Biochemical Systematics and Ecology **29**:1025-1047.

Tylianakis, J. M., R. K. Didham, J. Bascompte, and D. A. Wardle. 2008. Global change and species interactions in terrestrial ecosystems. Ecology Letters **11**:1351-1363.

Valentine, H., W. Wallner, and P. Wargo. 1983. Nutritional changes in host foliage during and after defoliation, and their relation to the weight of gypsy moth pupae. Oecologia **57**:298-302.

Vannote, R. L., G. W. Minshall, K. W. Cummins, J. R. Sedell, and C. E. Cushing. 1980. The river continuum concept. Canadian Journal of Fisheries and Aquatic Sciences **37**:8.

Violle, C., B. J. Enquist, B. J. McGill, L. Jiang, C. H. Albert, C. Hulshof, V. Jung, and J. Messier. 2012. The return of the variance: intraspecific variability in community ecology. Trends in Ecology & Evolution **27**:244-252.

Vitousek, P. M., and R. W. Howarth. 1991. Nitrogen limitation on land and in the sea: How can it occur? Biogeochemistry **13**:87-115.

Vitousek, P. M., H. A. Mooney, J. Lubchenco, and J. M. Melillo. 1997. Human domination of Earth's ecosystems. Science **277**:494-499.

Ward, G. M., and K. W. Cummins. 1979. Effects of food quality on growth of a stream detritivore, *Paratendipes Albimanus* (Meigen) (Diptera: *Chironomidae*). Ecology **60**:57-64.

Whitham, T. G., J. K. Bailey, J. A. Schweitzer, S. M. Shuster, R. K. Bangert, C. J. LeRoy, E. V. Lonsdorf, G. J. Allan, S. P. DiFazio, B. M. Potts, D. G. Fischer, C. A. Gehring, R. L. Lindroth, J. C. Marks, S. C. Hart, G. M. Wimp, and S. C. Wooley. 2006. A framework for community and ecosystem genetics: From genes to ecosystems. Nature Reviews Genetics **7**:24.

Wootton, J. T. 2012a. Effects of timber harvest on river food webs: Physical, chemical and biological responses. PLoS ONE **7**:e43561.

Wootton, J. T. 2012b. River food web response to large-scale riparian zone manipulations. PLoS ONE **7**:e51839.

Worthington, N. P., F. A. Johnson, G. R. Staebler, and W. J. Lloyd. 1960. Normal yield tables for red alder. U.S. Dept. of Agriculture Forest Service, Pacific Northwest Forest and Range Experimental Station.

Wright, M. S., and A. P. Covich. 2005. Relative importance of bacteria and fungi in a tropical headwater stream: Leaf decomposition and invertebrate feeding preference. Microbial Ecology **49**:536-546.

Young, A. G., H. G. Merriam, and S. I. Warwick. 1993. The effects of forest fragmentation on genetic variation in *Acer saccharum* Marsh. (sugar maple) populations. Heredity **71**:277-289.

Zak, D. R., W. E. Holmes, D. C. White, A. D. Peacock, and D. Tilman. 2003. Plant diversity, soil microbial communities, and ecosystem function: Are there any links? Ecology **84**:2042-2050.

Zarraonaindia, I., S. M. Owens, P. Weisenhorn, K. West, J. Hampton-Marcell, S. Lax, N. A. Bokulich, D. A. Mills, G. Martin, S. Taghavi, D. van der Lelie, and J. A. Gilbert. 2015. The soil microbiome influences grapevine-associated microbiota. mBio **6**.

Zeneli, G., P. Krokene, E. Christiansen, T. Krekling, and J. Gershenzon. 2006. Methyl jasmonate treatment of mature Norway spruce (*Picea abies*) trees increases the accumulation of terpenoid resin components and protects against infection by *Ceratocystis polonica*, a bark beetle-associated fungus. Tree Physiology **26**:977-988.